PROCEEDINGS OF A WORKSHOP ON THE KITIMAT MARINE ENVIRONMENT

Edited by R.W. Macdonald

Institute of Ocean Sciences
Department of Fisheries and Oceans
Sidney, B.C., V8L 4B2

1983

CANADIAN TECHNICAL REPORT OF HYDROGRAPHY AND OCEAN SCIENCES NO. 18

Fisheries and Oceans / Pêches et Océans

Canada

Canadian Technical Report of Hydrography and Ocean Sciences

These reports contain scientific and technical information of a type that represents a contribution to existing knowledge but which is not normally found in the primary literature. The subject matter is generally related to programs and interests of the Ocean Science and Surveys (OSS) sector of the Department of Fisheries and Oceans.

Technical Reports may be cited as full publications. The correct citation appears above the abstract of each report. Each report will be abstracted in Aquatic Sciences and Fisheries Abstracts. Reports are also listed in the Department's annual index to scientific and technical publications.

Technical Reports are produced regionally but are numbered and indexed nationally. Requests for individual reports will be fulfilled by the issuing establishment listed on the front cover and title page. Out of stock reports will be supplied for a fee by commercial agents.

Regional and headquarters establishments of Ocean Science and Surveys ceased publication of their various report series as of December 1981. A complete listing of these publications and the last number issued under each title are published in the *Canadian Journal of Fisheries and Aquatic Sciences*, Volume 38: Index to Publications 1981. The current series began with Report Number 1 in January 1982.

Rapport technique canadien sur l'hydrographie et les sciences océaniques

Ces rapports contiennent des renseignements scientifiques et techniques qui constituent une contribution aux connaissances actuelles mais que l'on ne trouve pas normalement dans les revues scientifiques. Le sujet est généralement rattaché aux programmes et intérêts du service des Sciences et Levés océaniques (SLO) du ministère des Pêches et des Océans.

Les rapports techniques peuvent être considérés comme des publications à part entière. Le titre exact figure au-dessus du résumé du chaque rapport. Les résumés des rapports seront publiés dans la revue Résumés des sciences aquatiques et halieutiques et les titres figureront dans l'index annuel des publications scientifiques et techniques du Ministère.

Les rapports techniques sont produits à l'échelon régional mais sont numérotés et placés dans l'index à l'échelon national. Les demandes de rapports seront satisfaites par l'établissement auteur dont le nom figure sur la couverture et la page de titre. Les rapports épuisés seront fournis contre rétribution par des agents commerciaux.

Les établissements des Sciences et Levés océaniques dans les régions et à l'administration centrale ont cessé de publier leurs diverses séries de rapports depuis décembre 1981. Vous trouverez dans l'index des publications du volume 38 du *Journal canadien des sciences halieutiques et aquatiques*, la liste de ces publications ainsi que le dernier numéro paru dans chaque catégorie. La nouvelle série a commencé avec la publication du Rapport n° 1 en janvier 1982.

Canadian Technical Report of

Hydrography and Ocean Sciences

No. 18

1983

PROCEEDINGS OF A WORKSHOP ON THE KITIMAT MARINE ENVIRONMENT

edited by

R.W. Macdonald

Institute of Ocean Sciences

Department of Fisheries and Oceans

Sidney, B.C. V8L 4B2

Minister of Supply and Services Canada 1983
Cat. No. FS 97-18/18 ISSN 0711-6764

Correct citation for this publication:

Macdonald, R.W., 1983. Proceedings of a Workshop on the Kitimat Marine Environment. Can. Tech. Rep. Hydrogr. Ocean Sci. 18, 1-218.

TABLE OF CONTENTS

	PAGE NO.
Abstract/Résumé	IV
Acknowledgements	V
Special Credits	1
The Kitimat Fjord system: An Introduction *R.W. Macdonald, B.D. Bornhold and I. Webster*	2
The Baroclinicity of the Semi-diurnal Tidal Currents in Douglas Channel, B.C. *I. Webster*	14
Surface Currents in the Approaches to Kitimat *W. S. Huggett and S.O. Wigen*	34
Chemical Characteristics of Water in the Kitimat Fjord System *R.W. Macdonald, W.J. Cretney, C.S. Wong and P. Erickson*	66
Sedimentation in Douglas Channel and Kitimat Arm *B.D. Bornhold*	88
The Distribution and Dynamics of Suspended Particles in the Kitimat Fjord System *R.W. Macdonald*	116
Bottom Water Temperature Variations as Observed, and as Recorded in the Bottom Sediments, Alice Arm and Douglas Channel, British Columbia *T. Lewis*	138
Polycyclic Aromatic Hydrocarbons in Surface Sediments and Age-Dated Cores from Kitimat Arm, Douglas Channel and Adjoining Waterways *W.J. Cretney, C.S. Wong, R.W. Macdonald, P.E. Erickson, and B.R. Fowler*	162
Histopathological Evaluation of Bivalves from Kitimat Arm - Douglas Channel and Alberni Inlet, British Columbia *D.A. Brown, K.A. Thompson, W.A. Heath, P.E. Erickson, W.J. Cretney and C.S. Wong*	196

ABSTRACT

Macdonald, R.W., 1983. Proceedings of a Workshop on the Kitimat Marine Environment. Can. Tech. Rep. Hydrogr. Ocean Sci. 18, 1-218.

In September, 1980, a workshop was held on the Kitimat marine environment. The impetus to hold such a workshop was the result of recent data aquisitions collected by and consolidated at Ocean Sciences. The reports contained herein were presented at that workshop, and include such aspects as physics, chemistry, geology and biology. All of the reports have been subjected to peer review and consist of the following; 1. The Kitimat fjord system; an introduction, 2. The baroclinicity of the semi-diurnal tidal currents in Douglas Channel, B.C., 3. Surface currents in the approaches to Kitimat, 4. Chemical characteristics of water in the Kitimat fjord system, 5. Sedimentation in Douglas Channel and Kitimat Arm, 6. The distribution and dynamics of suspended particulates in the Kitimat fjord sytem, 7. Bottom water temperature variations as observed, and as recorded in the bottom sediments, Alice Arm and Douglas Channel, British Columbia, 8. Polycyclic aromatic hydrocarbons in surface sediments and age-dated cores from Kitimat Arm, Douglas Channel and adjoining waterways, 9. Histopathological evaluation of bivalves from Kitimat Arm-Douglas Channel and Alberni Inlet, British Columbia.

Key words: bathymetry, currents, histopathology, Kitimat nutrients, particulates, sedimentation, temperature, tides.

RÉSUMÉ

Macdonald, R.W., 1983. Proceedings of a Workshop on the Kitimat Marine Environment. Can. Tech. Rep. Hydrogr. Ocean Sci. 18, 1-218.

En september 1980, un atelier fût monté pour le milieu - marin du Kitimat. L'impulsion qui a fait naître cet atelier fût le résultat du data récemment aquis et consolider par les Sciences Océanographiques Ocean Sciences). Les démarches démontrent les rapports présentés à l'atelier même, en plus d'un rapport préliminaire, qui met en scène tout le plan physique, chémique, géologique, et biologique. Tout ces rapports ont été soumis pour la révision et consistent à ce qui suit: 1. Le système Kitimat Fjord - une introduction, 2. La baro-clinique semi-journalière des courants du Douglas Channel C.B., 3. Courants de surface en approche du Kitimat Arm, 4. Characteristiques-chimiques des eaux, pour le système Kitimat Fjord, 5. Déposition dans le Douglas Channel, 6. Distributions et dynamiques des particles en disponibilité dans le Kitimat Fjord, 7. La variation de la température du fond des eaux dûment observée et enrégistrée dans le fond des dépôts Alice Arm et Douglas Channel. C.B., 8. La concentration des nombreuses cycliques sélectionnées aromatiques d'hydrocarbure du Kitimat Arm, Douglas Channel et des eaux avaisinantes, 9. Evaluation histopatalogique des palourdes du Kitimat Arm et des eaux avaisinontes.

Mot-clés: bathometrie, courants, dépositions, éléments nutritifs, histo-pathology, Kitimat, marée, particulière, température.

ACKNOWLEDGEMENTS

I wish to thank the many people who assisted in the preparation of this collection of papers. L.S.C. Thomson advised on many aspects of the technical editing and helped us arrive at a mutually satisfactory format. Technigraphics prepared many of the illustrations and hydrographic services assisted with photographic reductions. I thank Alan Cornford for his generous monetary support and the long term commitment to provide that support. Lastly I would like to acknowledge the reviewers whose efforts remain anonymous but certainly not thankless, and the authors who showed remarkable patience during the interval between the workshop and this final product.

R.W. Macdonald

SPECIAL CREDITS

During the preparation of these proceedings, many revisions were required, papers had to be retyped to uniform style, and figures had to be reduced and inserted appropriately into the text. Julie Poulin took responsibility for these tasks and the final appearance of this report is, in large measure, a result of her efforts.

LE SYSTÈME KITIMAT FJORD: UNE INTRODUCTION

R.W. Macdonald
Institute of Ocean Sciences, Sidney, B.C.

B.D. Bornhold
Geological Survey of Canada
Pacific Geoscience Center, Sidney, B.C.

I. Webster
Department of Civil Engineering, The University of Western Australia
Nedlands, Western Australia 6009

RÉSUMÉ

Un apercu du système Kitimat Fjord est présenté. Ces faits de développement historiques, bathométrie, topographie, géographie, circulation d'eau, climat et décharge des eaux fraiches sont brièvement passer en revue.

Macdonald, R.W., B.D. Bornhold, and I. Webster. 1983. The Kitimat fjord system: An Introduction. Can. Tech. Rep. Hydrogr. Sci. 18, 2-13.

Mot-clés: bathométrie, climat, décharge des eaux fraiches, fjord, Kitimat, topographie.

THE KITIMAT FJORD SYSTEM: AN INTRODUCTION

R.W. Macdonald
Institute of Ocean Sciences, Sidney, B.C.

B.D. Bornhold
Geological Survey of Canada
Pacific Geoscience Center, Sidney, B.C.

I. Webster
Department of Civil Engineering, The University of Australia
Nedlands, Western Australia 6009

ABSTRACT

An overview of the Kitimat fjord system is presented. Such aspects as historical development, bathymetry, topography, geography, water circulation, climate and freshwater discharge are briefly reviewed.

Macdonald, R.W., B.D. Bornhold, and I. Webster. 1983. The Kitimat fjord system: An introduction. Can. Tech. Rep. Hydrogr. Ocean Sci. 18, 2-13.

Key Words: bathymetry, climate, fjord, freshwater discharge, Kitimat,

INTRODUCTION

The system of channels connecting Kitimat with British Columbia coastal waters will be referred to here as the Kitimat fjord system. It is located on the northern British Columbia mainland from about 53° to 54° N latitude and 128° to 129.5° longitude (Fig. 1), and communicates with coastal waters in Queen Charlotte Sound and Hecate Strait.

Man's impact began with the Native Indians who have utilized the area, according to legend, for perhaps 600 years (Bell and Kallman, 1976). The first survey by Vancouver was not until 1792-4 and the first recorded white settler engaged in land clearing operations about a century later. A logging operation towed logs to the Swanson Bay Pulp Mill between the years 1906-23 but the mill was closed and transferred to Ocean Falls at the end of that period (Holland et al, 1972). Modern industry started in 1954 when the Alcan smelter began aluminum production at a plant established on the west side at the head of Kitimat Arm. At that time the town of Kitimat was planned and built to house employees of Alcan and a supporting population. With the construction of a Kraft Pulp and Paper mill by Eurocan in the early 70's the town grew to 13,000 by 1976 (Bell and Kallman, 1976), a growth which may be expected to continue with the recent approval to build a methanol plant. In the mid 1970's Kitimat was proposed as an oil port (Kitimat Pipe Line Ltd., 1976) with Alaskan oil to be transported by tanker to Kitimat and thence by pipeline to Edmonton. Although this plan was publicly condemned by the federal government it appears still to be a distant possiblity. The present harbour facilities on the west side of the Kitimat delta are adequate for the two operating industries but would require expansion to support oil tanker traffic.

Understanding how the Kitimat system works is fundamental for the avoidance of conflict of use. For example some of the more obvious impacts of industrialization include emission of polynuclear aromatics (PAH)

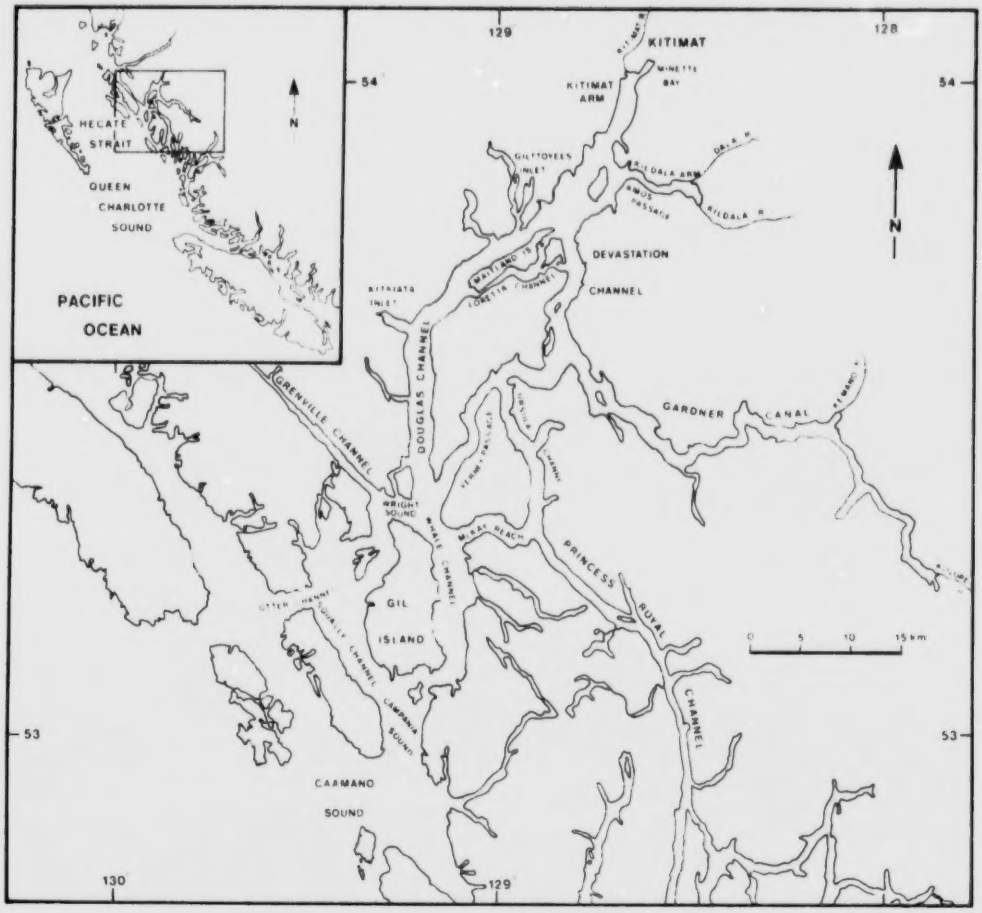

Fig. 1. The Kitimat fjord system.

fluorides and sulphur dioxide from the Alcan plant, discharge of treated pulpmill effluent by Eurocan, ocean dumping of dredgeate, alteration of the flow on the Kemano River due to power development, alteration of land runoff characteristics by logging or land clearing and the discharge of treated municipal sewage. Oceanographic interest in the Kitimat fjord system began in the early fifties, but it cannot be said that an adequate marine data base has preceded industrial growth. The status of oceanographic information has been reviewed by Bell and Kallman (1976) who note that eight oceanographic surveys of Douglas Channel and Kitimat Arm were carried out from 1951 to 1975. Within the last three years a number of oceanographic surveys investigating the physics, chemistry, biology and geology have been performed whose synthesis should greatly assist intelligent resource utilization where it affects the marine environment.

GEOGRAPHY

The Kitimat fjord system lies within the Kitimat Ranges, a physiographic sub-province of the British Columbia Coast Mountains, with peaks as high as 2700 m but generally between 2000-2200 m in elevation. These peaks are composed of massive granitic rocks many of which have been glaciated in the past. Presently there is a relative scarcity of glaciers compared to ranges to the north or south, but remnants of glaciers and permanent snow fields are still to be found on the higher peaks and ridges.

The fjord system is complex topographically but its shape appears to be controlled by the large scale lineaments which characterize the Kitimat Ranges (Holland, 1976). These take the form of long straight valleys and channels; one set trending north-westerly and the other north to north easterly. Structural control appears to be fundamental to both sets but they have been extensively modified by Pleistocene glaciation as well as by fluvial processes. The fjord channels and adjacent sub-aerial valleys contain thick sequences of glacial, glaciomarine, marine deltaic and fluvial sediments and many of the inlet basins continue to fill through progradation of fjord head deltas. The present extent of dynamic factors including eustatic changes, isostatic rebound and sedimentation, and some of the more important dimensions are given in Table 1. The geometry within the Kitimat system is complicated by the presence of numerous islands and side channels, Gardner Canal which is 90 km long being the most important example of the latter.

BATHYMETRY

Although topographically complex in plan, the fjords of the Kitimat system possess a typical morphology with steep bedrock walls and relatively smooth sediment-floored basins separated by sills of rugged relief (Figs. 2 and 3). These sills divide the fjord system into 3 major marine basins. The innermost basin here referred to as "Gardner Basin" includes all of Gardner Canal and is defined by a sill at a depth of 100 m just north of where Gardner Canal and Devastation Channel join (Fig. 2c.). The greatest depths of about 500 m are attained in the inner section of Gardner Canal (Fig. 2b).

A sill at 211 m which crosses Douglas Channel at the Southward bend just south of Kitkiata Inlet defines the second basin here called "Maitland Basin". It includes the northern half of Douglas Channel, Kitimat Arm and Devastation

Table 1. Physical dimensions of the Kitimat fjord system.

Region	Length of Shoreline (km)	Surface Area (km^2)	Water Volume (km^3)
Kitimat Arm, Douglas Channel, Loretta Channel	326	380	89
Kildala Arm, Amos Passage	60	59	9
Gardner Canal	202	207	37
Devastation Channel, Verney Passage	132	165	30
Ursula Channel, Princess Royal Channel* McKay Reach	208	185	50
Wright Sound, Whale Channel, Squally Channel, Campania Sound	260	604	250
Grenville Channel*	87	43	5
Total fjord system	1275	1643	470

* Dimensions calculated only as far as the sill.

Channel as far south as the 100 m deep sill which crosses it at its confluence with Gardner Canal. Maitland Basin is further separated into two sub-basins by a minor sill which rises approximately 50 m above the adjacent sea floor between northern Maitland Island and the entrance to Gilttoyees Inlet. Maitland Basin attains its maximum depth, 420 m, in the more southerly sub-basin while the greatest depths of 380 m in the northerly sub-basin are found in the broad depression which connects Devastation and Douglas Channels to Kitimat Arm. Kildala Arm, a short inlet branching off Kitimat Arm contains a small perched basin with a maximum depth of 210 m and a sill depth of 165 m in Amos Passage. The floor of Maitland Basin rises gently towards the north until about 6 km south of the sub-aerial edge of the Kitimat Delta where in 210 m of water the hummocky deltaic sediments are encountered. Minette Bay, a small semi-enclosed basin 30 m deep forms a short 5 km extension at the north-east corner of Kitimat Arm and appears destined ultimately to be pinched off from the marine environment by the accreting delta.

The third or outer basin referred to here as "Gil Basin" is separated from Queen Charlotte Sound by a 200 m deep sill at Otter Channel and a broader 170 m sill at the entrance to Caamano Sound. It is the most complex basin in plan view and includes all the channels surrounding Gil Island. Of particular note are an 80 m sill crossing Grenville Channel, a sill at 150 m crossing

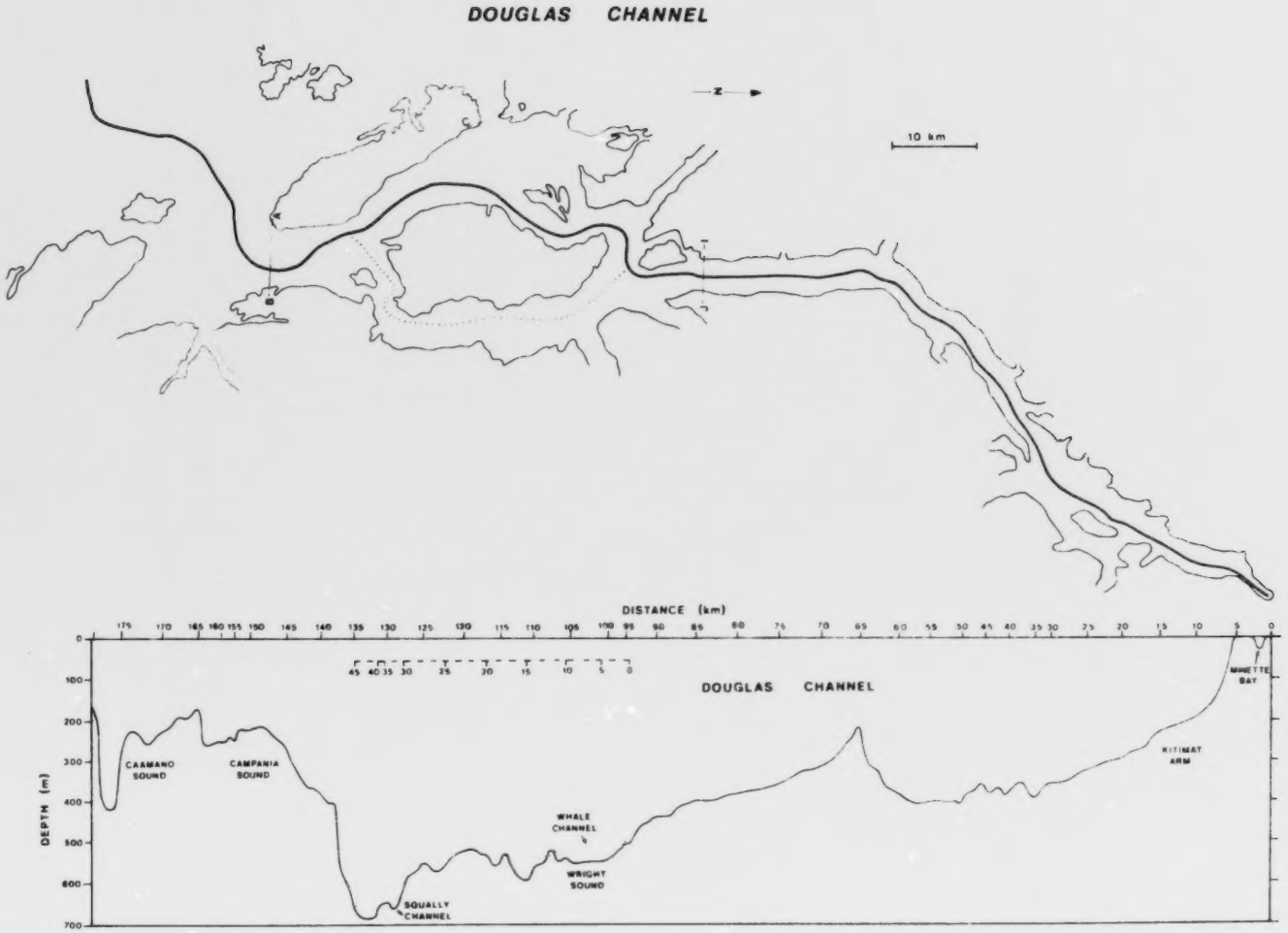

Fig. 2a. Longitudinal section of Douglas Channel.

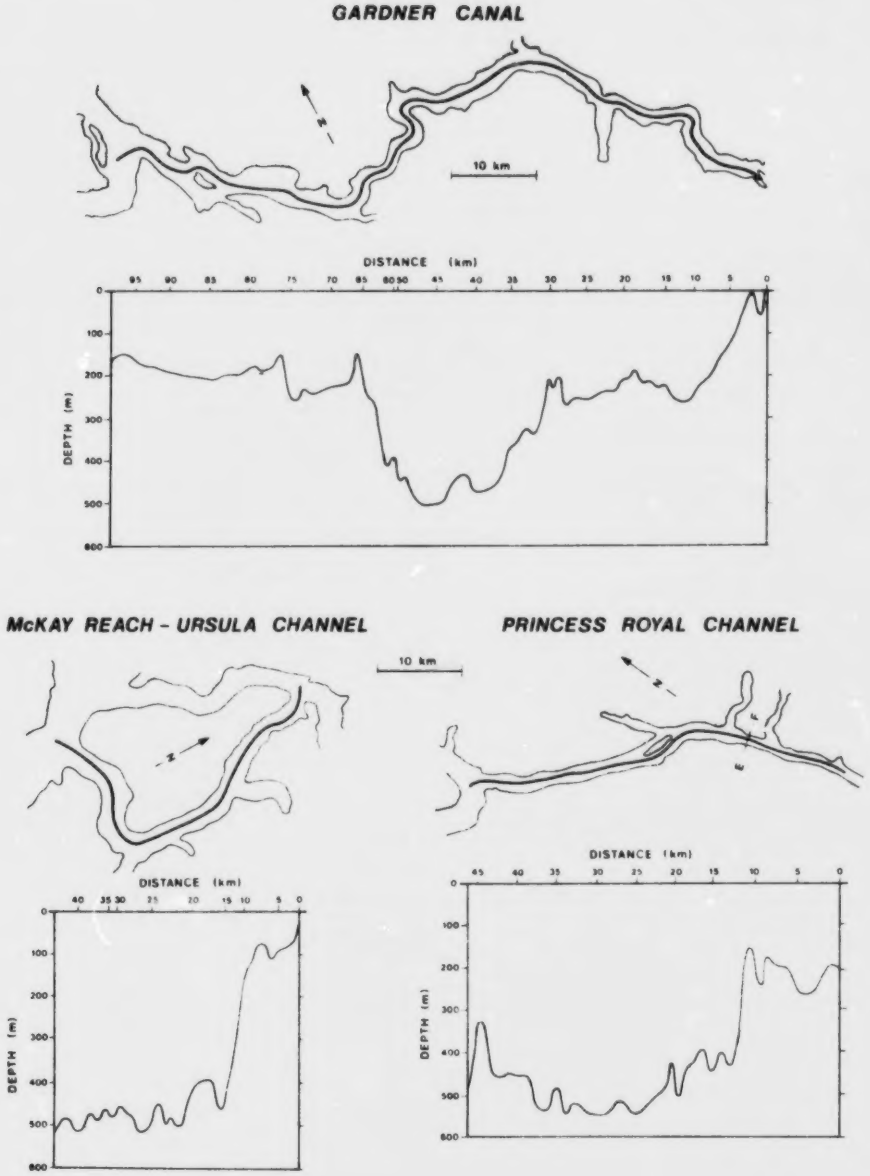

Fig. 2b. Longitudinal sections of Gardner Canal, McKay Reach and Princess Royal Channel.

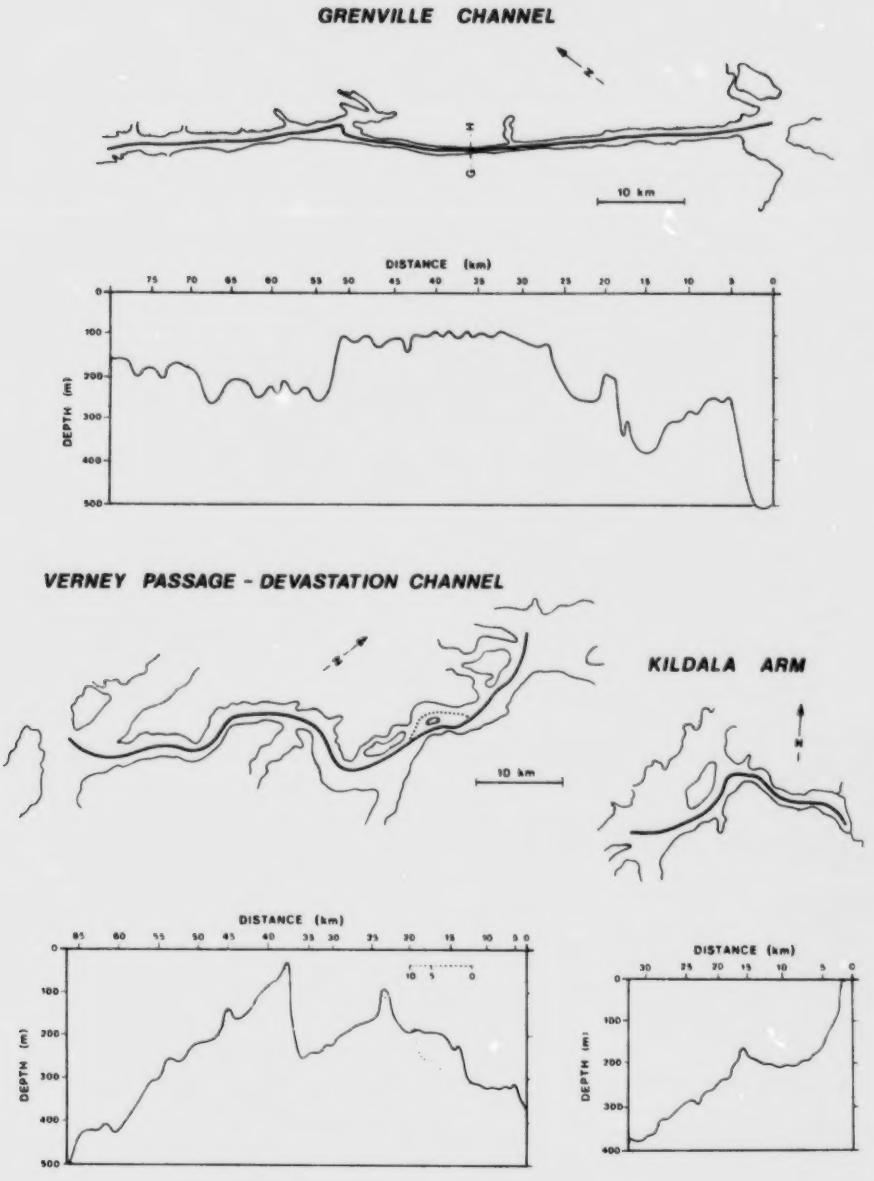

Fig. 2c. Longitudinal section of Grenville Channel, Verney Passage, and Kildala Arm.

Princess Royal Channel and two very shallow sills only 31 m and 35 m deep which cross Verney Passage and Ursula Channel respectively. The deepest portion of Gil Basin is found in Whale Channel and Squally Channel where depths exceed 550 m. The northern boundary of this basin is formed by the aforementioned 211 m deep sill crossing Douglas Channel.

WATER CIRCULATION

The circulation of water in inlets along the British Columbia coast is driven by a combination of three elements; hydraulic gradient, wind stress and tides. The relative importance of each type of forcing varies with time and location. Hydraulic gradient or pressure forces which induce water movement can arise from variations in water density along an inlet's length. This in turn is caused by direct precipitation onto the water or more importantly freshwater runoff discharging at the sides or head of the inlet ("head" refers to the inland end of an inlet and "mouth" to the seawater end). The resulting flow pattern of seaward surface currents with entrainment from below and deeper landward currents to maintain salt balance is termed estuarine circulation. Pickard (1961) has classified Kildala Arm, Douglas Channel and Gardner Canal as "A-1" inlets, the A group fjords being characterized by low salinity in the surface waters at the head, with the A-1 subgroup having the lowest salinity. Estuarine circulation is therefore expected to be well developed at times in the Kitimat fjord system, but to vary in strength according to rate of freshwater input. Wind stress on the surface is also capable of causing water movement with the intensity of circulation depending on both strength and duration of the wind in a particular direction. Wind climate at a location is usually seasonally dependent and this may carry over into the wind driven circulation. Generally, due to the height of surrounding hills, winds are directed topographically up or down the channel. Furthermore, wind generated surface movement can induce motion of deeper water through up or down-welling particularly at the head of an inlet. Tidal forces result in currents which move predominantly back and forth along the channels (rectilinear). Interaction of these currents with the geometry often results in longitudinal, lateral and vertical mixing. While tidal currents lead to mixing they tend not to be a major net advective agent. Estuarine and wind driven circulation usually dominate exchange of the surface waters of the inlet with those external to the inlet.

There are four oceanographically important connections to the Pacific coast where water can enter or leave the system and all abut Gil Basin. The entrances at Campania Sound and Otter Channel are the most important since they are wide and communicate directly with Hecate Strait (Fig. 3). The other two connections are narrow and long: Grenville Channel averages only 600 m in width and extends 80 km to the northeast before joining Hecate Strait through a complex of shoals and passages, while Princess Royal Channel extends a similar distance to the south where it joins Finlayson Channel which connects to Queen Charlotte Sound. The cross sectional areas are estimated at: Campania Sound - $1.3 \times 10^6 m^2$, Otter Channel - $5.2 \times 10^5 m^2$, Princess Royal Channel - $9.5 \times 10^4 m^2$ and Grenville Channel - $2.8 \times 10^4 m^2$.

Bottom waters of the three basins appear to undergo regular renewals and there is no record of anoxic conditions. Minette Bay, however, undergoes seasonal oxygen depletion in its bottom water since it is connected with

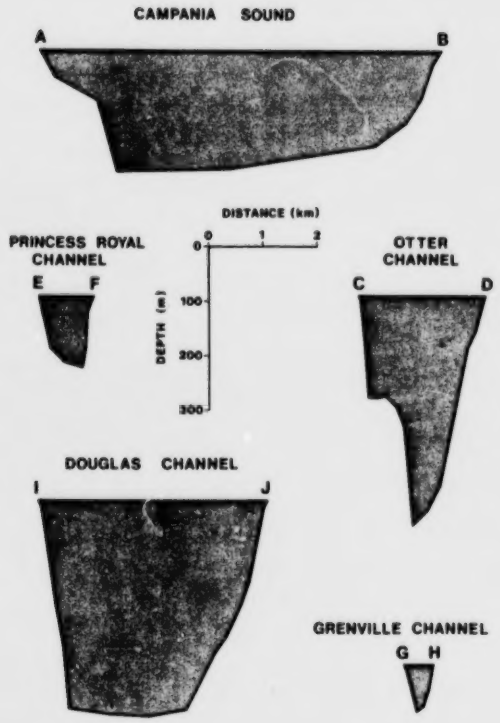

Fig. 3. Some oceanographically important transverse sections of the Kitimat fjord system.

with Kitimat Arm only through shallow 1-2 m deep channels which pass over the tidal flats of the Kitimat River.

CLIMATE AND FRESHWATER DISCHARGE

The fjord system extends about 140 km inland from the Pacific Coast, and the associated watershed even further. It is expected therefore that climate in the broad aspect will vary from maritime near the coast to more continental farther inland. Prevailing westerlies and warm Pacific water combine to produce mild coastal winters and cool summers. Frontal systems from the Pacific and orographic influences dominate the local climate with latitude playing only a minor role (Canada, Department of Transport, 1962). The tendency is for wet winters with little snow at low elevations but enormous quantities of snow can fall on the coast mountains at higher elevations. (Kildala Pass at 1600 m receives a seasonal average snowfall of 2050 cm.) For the most part the west-facing slopes are excessively wet while eastern slopes and the heads of some fjords receive less rain (Hare and Thomas, 1974). In general terms, there are only two characteristic periods during the year. In spring, temperatures tend to increase, rain decreases and the prevailing westerlies intermittently weaken. The summers are marked by few disturbances but the abrupt renewal of the westerlies in September accompanied by Pacific

frontal systems tends to make autumn a season of high precipitation (Fig. 4). While Pacific influences tend to dominate the coastal area, cold Arctic air impounded to the east by the coastal mountains can, in response to pressure changes, flow through mountain passes and result in strong surges of cold air called Squamishes. Cold air descending from local mountains and channeled by the topography lead to disturbances of more local nature known as Williwaws. The strongest winds in winter are assocated with Squamishes although strong up-inlet reversals are possible in response to Pacific storms.

The main rivers which discharge into the fjord system are the Kitimat River at the head of Kitimat Arm, the Dala and Kildala Rivers at the head of Kildala Arm, the Kemano River which enters the north side of Gardner Canal about 30 km from its head, and the Kitlope River near the head of Gardner Canal. Numerous other small creeks and rivers enter along the sides of all the channels. Only two of the rivers are gauged and for the period from 1954-1978 the mean flow rate of the Kitimat River is 134 $m^3 s^{-1}$ and the Kemano River, which is regulated for power, is 79 $m^3 s^{-1}$. (Canada. Department of the Environment, 1979). Pickard (1961) describes Douglas Channel and Gardner Canal as being inlets of the "stored runoff" variety. These inlets

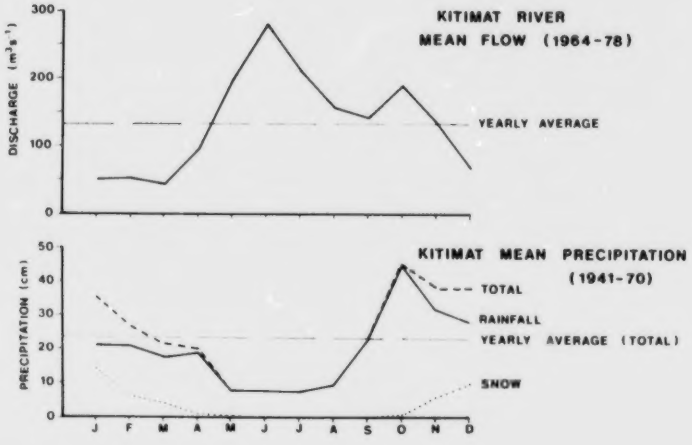

Fig. 4. The monthly mean flow of the Kitimat River from 1964-78 (Canada. Department of the Environment, 1979) and monthly mean precipitation at Kitimat from 1941-70 (Canada. Atmospheric Environment Service, 1973.

receive a peak runoff from May to July as a result of snow and glacier melt. A second peak period is also observed in November in response to autumn rains while in winter precipitation is locked up in snow and ice with the result that rivers whose source is the interior are at their lowest (Fig. 4). As noted earlier, much of the runoff drains into the sides of the channels in many small un-metered rivers. Crude estimates of the watershed areas suggest that this side channel discharge contributes more fresh water to the system than the 2 gauged rivers and may indeed contribute most of the budget for Gardner Canal. To complicate further this picture, the timing and amplitude of peak runoffs is not the same for all rivers discharging into the fjords. Smaller side rivers are more dependent on local conditions and therefore relative importance of river discharge at the head of the channels and at the sides is expected to vary with season and with geographical location.

REFERENCES

Bell, L.M. and R.J. Kallman. 1976. The Kitimat River estuary status of environmental knowledge to 1976. Special Estuary Series No. 6: 296 pp.

Canada. Atmospheric Environment Service. 1973. Climate of British Columbia Climatic Normals 1941-70, Published by British Columbia Department of Agriculture: 90 pp.

Canada. Department of the Environment. 1979. Water Survey of Canada, Monthly and Annual Mean File (Computer Listing).

Canada. Department of Transport. 1962. The Climate of Canada. Meteorological Branch, Air Services, Toronto: 74 pp.

Hare, F.K. and M.K. Thomas. 1974. Climate Canada, Wiley Publishers of Canada Ltd., Toronto: 256 pp.

Holland, S.S. 1976. Land forms of British Columbia, A Physiographic Outline. B.C. Department of Mines. Petrol. Res. Bull. 48: 138 pp.

Holland, J.D.C., E.R. Christiansen, H. Gjaltema, N.J. Lemmen and G.S. Zealand. 1972. Historical review of logging activities and associated problems in the Kitimat District of the Central Coastal Division, Butedale Area 6. In Provisional environmental quality objectives for the Central Coastal Division, Northern Operations Branch, Rep. 1972-4: 1-12. Fisheries and Marine Service, Environment Canada, Vancouver, B.C.

Kitimat Pipe Line Ltd. 1976. Termpol submission re Marine Terminal at Kitimat, B.C. Vol. I-VI.

Pickard, G.L. 1961. Oceanographic features of inlets in the British Columbia mainland coast. J. Fish. Res. Board Can. 18 (6): 907-999.

LA BAROCLINIQUE DES COURANTS SEMI-JOURNALIERS DE LA MARÉE DU CANAL DOUGLAS, C.B.

Ian Webster

Department of Civil Engineering, The University of Western Australia, Nedlands, Western Australia 6009.

RÉSUMÉ

L'examination des records des cinq profondeurs du mesureur-courant à une location tout près du sud du Canal Douglas demontre que les courants semi-journaliers de la marée étaient fort barocliniques dans cet endroit là. Les dégrés des barocliniques ont variées considérablement durant les cinq mois de mesurage. Il est donc suggéré que les resultats barocliniques de l'action réciproque du courant barotropique avec la topographie du canal. Le filoncouche qui croisse le Canal Douglas est examiné pour un gîte possible pour la génération mais il semble que ce soit trap près du mesureur courant pour expliquer les baroclinques près de la surface. En ce qui est de la dispute, que les barocliniques sont dues pour prepager les vagues barocliniques Kelvin, une inspection est donc de rigueur. Le mode un et deux des ondes Kelvin et barotropiques sont aussi sous observation, mais il y a des différences consistantes entre les velocités observées, à chaque profondeur. Ces différences empliquent que les formes théoriques pour les vagues, employées dans l'ajustement du procédé, peut-être incorrectes. Finalement, l'implication des barocliniques observées dans le Canal Douglas pour les courants de mer, le problème en prédiction, est le sujet de discussion.

Webster, I. 1983. The baroclinicity of the semi-diurnal tidal currents in Douglas Channel, B.C. Can. Tech. Rep. Hydrogr. Ocean Sci. 18, 14-32.

Mot-clés: barocliniques, barothropie, Canal Douglas, courant, modèle, ondes Kelvin, théorie.

THE BAROCLINICITY OF THE SEMI-DIURNAL TIDAL CURRENTS IN DOUGLAS CHANNEL, B.C.

Ian Webster
Department of Civil Engineering, The University of Western Australia
Nedlands, Western Australia 6009

ABSTRACT

Examination of current meter records from five depths at a location near the southern end of Douglas Channel, B.C. showed that the semi-diurnal tidal currents were strongly baroclinic in that part of the channel. The degree of the baroclinicity varied considerably during the five month period of the measurements. It is suggested that the baroclinicity results from the interaction of the barotropic tide with the topography of the channel. The sill which crosses Douglas Channel is examined as a possible generation site, but it appears to be too close to the current meters to explain the observed baroclinicity near the surface. The contention that the baroclinicity is due to propagating baroclinic Kelvin waves is also examined. Mode one and mode two Kelvin waves and a barotropic wave are fitted to the observations, but there are consistent differences between the fitted and observed velocities at each depth. These differences imply that the theoretical forms for the Kelvin waves used in the fitting procedure may not be correct. Finally, the implications of the observed baroclinicity in Douglas Channel for the practical tidal current prediction problem are discussed.

Webster, I. 1982. The baroclinicity of the semi-diurnal tidal currents in Douglas Channel, B.C. Can. Tech. Rep. Hydrog. Ocean Sci. 18, 14-32.

Keywords: baroclinic, barotropic, currents, Douglas Channel, Kelvin waves, model, theory

INTRODUCTION

In the period July 1977 to June 1978, Dobrocky Seatech Limited undertook a study of the circulation in the channels which form the seaward approaches to the port of Kitimat in northern British Columbia. The study was designed to delineate the three expected modes of circulation of the system, that is the tidal, the wind driven and the estuarine circulations. The implementation and results of this study are presented by Webster (1980a,b,c), Webster and Ford (1980) and by Buckingham (1980).

As part of this study a one-dimensional, barotropic tidal model was developed for the channel complex. This model is described by Narayanan (1980). The barotropic tidal currents are caused by pressure forces arising from along channel variations in the tidal height. Outside the bottom boundary layer the velocity field associated with a travelling barotropic wave is dependent upon the ratio of the wavelength to the water depth. Since the wavelength of the barotropic tide (typically > 2,000 km in the Kitimat channels) is much greater than the water depths (up to 600 m) the barotropic tidal velocity field is expected to be virtually independent of depth outside the bottom boundary layer.

During the Kitimat study, tide gauge and current meter data were

collected throughout the region for use as input into the barotropic tidal model. It became apparent in analyzing the data from the current meters that the tidal currents in the Kitmat channel system showed a marked degree of baroclinicity, that is they varied in amplitude and in phase with depth. This baroclinicity makes the determination of the barotropic component of current from current meter data more difficult. Also, since the baroclinic components of current appeared to be comparable in size to the barotropic current components they are an important consideration in the practical tidal current prediction problem for the region.

In this paper the nature of the baroclinic currents is examined for a location near the southern end of Douglas Channel which forms part of the Kitimat fjord system. Analyses of current meter data from this location showed major temporal changes in the degree of baroclinicity in the currents. This variability and the possible origin of the baroclinicity are discussed.

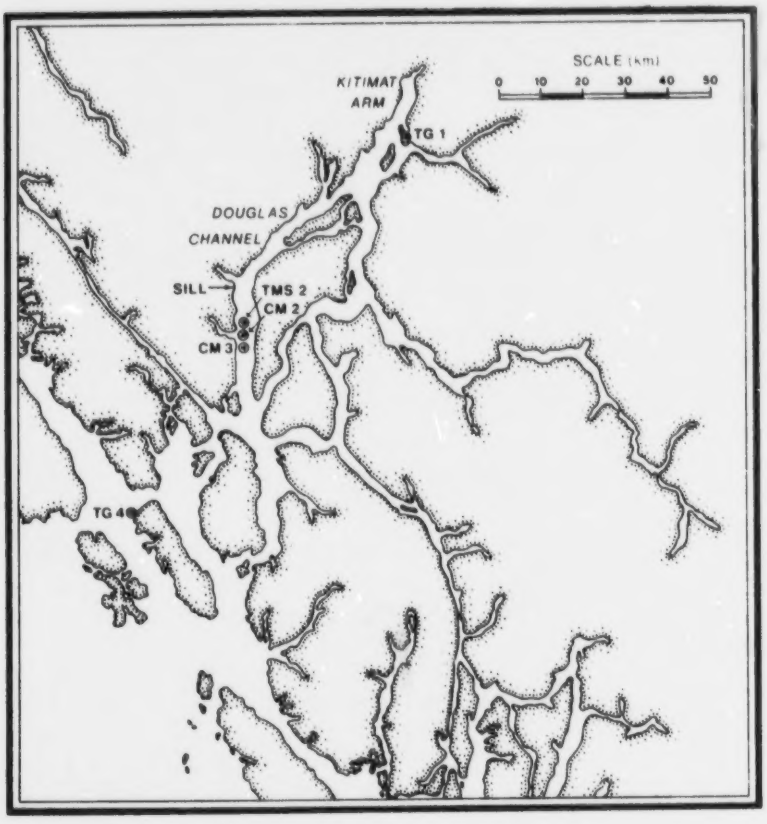

Fig. 1. Locations of Instrumentation.

THE MEASUREMENTS

Current measurements were made at two sites, CM 2 and CM 3, located about 10 km south of the sill which crosses Douglas Channel (see Fig. 1). Aanderaa current meters were located at depths of 5 m and 17 m on a mooring at CM 2 and at depths of 30 m, 165 m and 305 m at the CM 3 mooring (see Fig. 2). Both moorings were located in mid-channel, CM 2 being positioned 1.3 km to the north of CM 3. In addition, an Aanderaa thermistor chain designated TMS 2 was located 0.9 km due north of CM 2. This thermistor chain made temperature measurements at depth increments of 5 m from the surface to a depth of 50 m. The five current meters at CM 2 and CM 3 and the thermistor chain provided measurements concurrently over the five month period July, 1977 to December, 1977. These records were broken in the middle when the instruments were serviced in September, 1977.

In addition to the measurements made in Douglas Channel reference is made to tidal heights measured by tide gauge TG 4 located in Otter Channel (see Fig. 1). This tide gauge was operational for the time period July 1977 to December 1977. A comparison of the amplitudes of the M_2 constituent of tidal height between TG 4 and a tide gauge located in Kitimat Arm (TG 1) over the 2 1/2 month period September 1977 to December 1977 showed the amplitude at TG 1 to be 6% higher than that at TG 4 (1.686 m at TG 1, 1.595 m at TG 4). The phase of the M_2 constituent at TG 4 led that at TG 1 by 3°. Thus, the tidal heights and phases observed at TG 4 should be fairly representative of those within Douglas Channel.

HARMONIC ANALYSES OF CURRENT METER DATA

The amplitudes and phases of the tidal current constituents were computed using harmonic analysis software developed by Foreman (1978). This analysis was applied to each of the two 2 1/2 month sections of velocity record from the five current meters. The results from the harmonic analysis showed that at all depths the tidal currents were principally semi-diurnal in nature. The dominant semi-diurnal constituents were the M_2 (period of 12.42 hours), the S_2 (period of 12.00 hours) and the N_2 (period of 12.66 hours) in decreasing order or importance. These semi-diurnal currents in Douglas Channel ran primarily back and forth in a north/south direction; cross channel flows were generally less than 20% of the long channel flows.

The amplitudes and phases of the velocities in this report will refer to the amplitudes and phases of the north/south velocity components. If $u(t)$ is the contribution to the total north/south component of velocity at time, t, from the tidal constituent having a frequency, ω, then the amplitude, A, and the phase, θ, of this contribution are defined such that:

$$u(t) = A \cos (\omega t - \theta) \qquad (1)$$

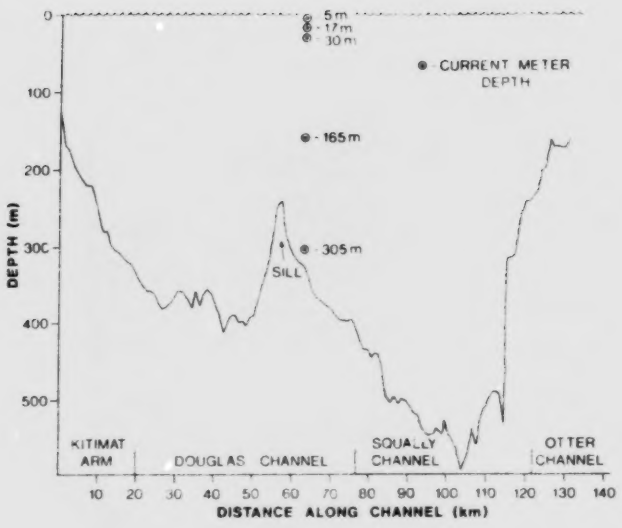

Fig. 2. Bathymetry along Douglas channel and adjoining channels.

Figure 3 compares the velocity amplitudes of the M_2, S_2 and N_2 constituents from the five current meters for the first 2 1/2 month period from July to September. The M_2 amplitude decreases from almost 20 cm s^{-1} at 5 m depth to less than 10 cm s^{-1} at the bottom two meters. Although the S_2 and N_2 amplitudes are less than half the size of the M_2 amplitude these show similar decreases with depth. The corresponding changes of phase of the three semi-diurnal velocity constituents are compared in Figure 4. For each constituent the phases are relative to the phase of tidal height obtained from the harmonic analysis of data from tide gauge TG 4. The phases at 17 m and 30 m depths for the three constituents lead those at 5 m, 165 m and 305 m depths. The similarity of the depth dependencies of amplitudes and phases for the three largest semi-diurnal constituents suggests that the nature of their baroclinicity is likewise similar.

When harmonic analyses were performed on the current meter records from the second 2 1/2 month section of data September to December, 1977 the degree of baroclinicity appeared to be somewhat less than it was in the first period. To examine the temporal variations of the baroclinicity over shorter time scales harmonic analyses were carried out on the velocity time series from the current meters on a weekly basis. A weekly analysis is not able to differentiate the contributions of the individual semi-diurnal constituents (M_2, S_2, and N_2); the resultant semi-diurnal constituent which was calculated for the M_2 frequency was strongly modulated by the presence of the other constituents both in amplitude and in phase. In effect, the weekly harmonic analysis procedure has a transfer function which considerably modified the calculated amplitudes and phases of the M_2 constituent.

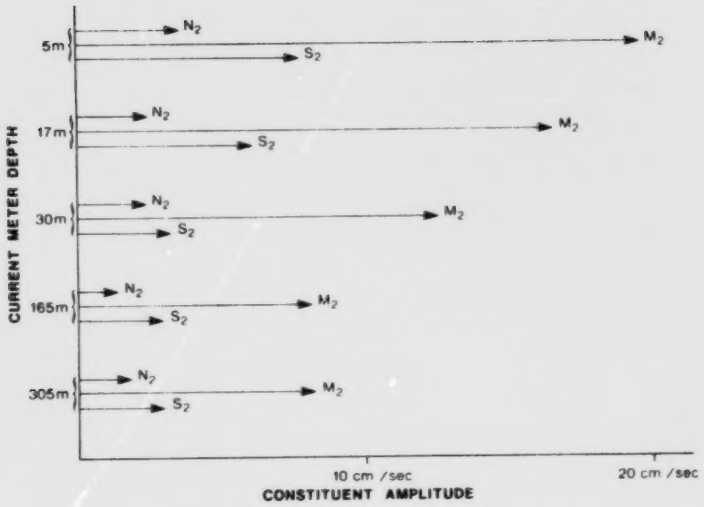

Fig. 3. Amplitudes of semi-diurnal constituents of current velocity (July to September).

One of the results of the barotropic tidal model was that the semi-diurnal barotropic tidal velocities in Douglas Channel were almost directly proportional to the semi-diurnal constituents of tidal height. Weekly harmonic analyses were performed on the tidal height records from the tide gauge TG 4. The resulting semi-diurnal tidal height amplitudes, h, (in cm s^{-1}) were used to calculate 'barotropic' semi-diurnal velocity amplitudes, A_b, (in cm s^{-1}) for each week according to:

$$A_b = 4.9 \times 10^{-2} \text{ h cm } s^{-1} \qquad (2)$$

The proportionality factor was obtained from the results of the tidal model. The velocity amplitudes, A, and the velocity phases, θ, obtained from the weekly analyses of the data from the five current meters were normalized as:

$$A_N = A/A_b \qquad (3)$$

$$\theta_N = \theta - \theta_h \qquad (4)$$

where A_N and θ_N are the normalized semi-diurnal velocity amplitudes and phases and θ_h is the phase of the semi-diurnal tidal height constituent. The legitimacy of this normalization procedure depends upon the velocity amplitudes of the M_2, S_2 and N_2 constituents at each depth being in similar ratios to the tidal height amplitudes for the three constituents.

Also, the relative phases of these constituents of tidal velocity should be similar to the relative tidal height phases. Based upon the results of the harmonic analyses of the 2 1/2 month records, both these criteria appear to be fairly well satisfied.

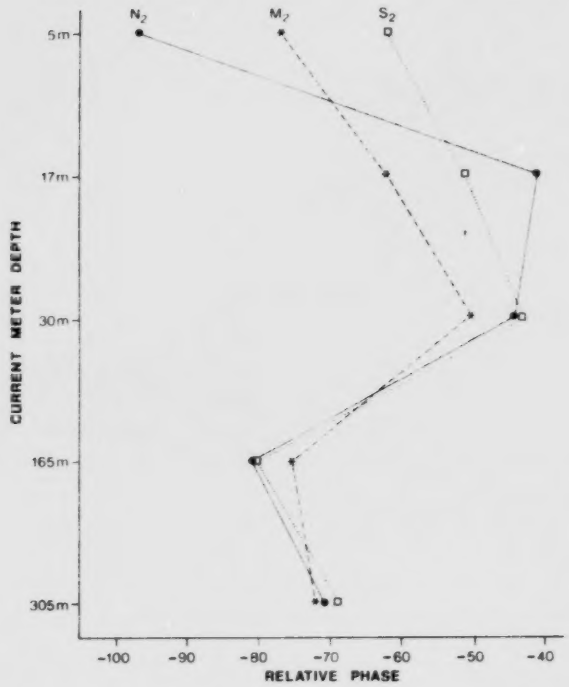

Fig. 4. Phases of semi-diurnal constituents of current velocity relative to phases of tidal height constitutents (July to September).

Figure 5 shows the normalized weekly semi-diurnal velocity amplitudes for the five current meter depths. These data are presented for twenty-one consecutive weeks (except for week #11) starting on July 17, 1977 and ending on December 12, 1977. These normalized amplitudes undergo significant temporal variations. At 5 m depth the amplitudes on weeks #5 and #6 exceed three times the 'barotropic' amplitude; on week #15 the amplitude at 5 m depth is less than the 'barotropic' amplitude. At greater depths the magnitudes of the fluctuations are less, but these still represent a large proportion of the average amplitude at each depth. Figure 6 shows the normalized velocity phases of the semi-diurnal constituents at depths of 5 m, 30 m and 305 m. The phases at 17 m depth tend to be similar to those at 30 m depth and the phases at 165 m depth are mostly similar to those at 305 m depth. Over the period of the record the phases undergo large variations sometimes between one week and the next. Between week #1 and week #21 the normalized phases range from -108^{o} to -59^{o} at 5 m depth; from -76^{o} to -44^{o} at 17 m depth; from -81^{o} to -29^{o} at 30 m depth; from -85^{o} to -63^{o} at 165 m depth and from -103^{o} to -65^{o} at 305 m depth.

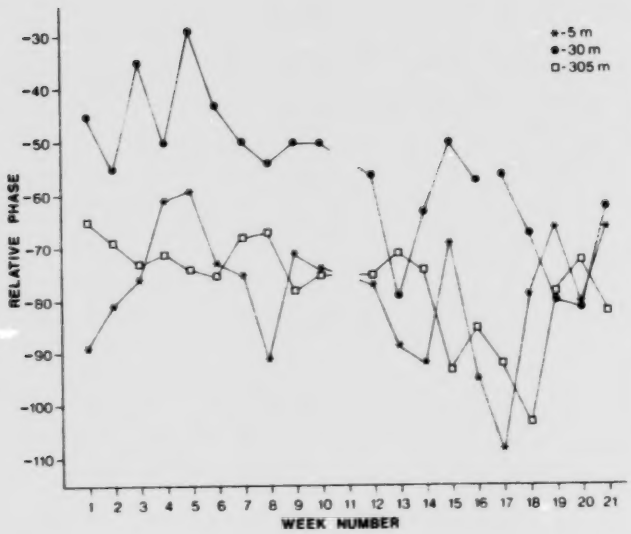

Fig. 5. Observed weekly amplitudes of semi-diurnal velocity normalized with respect to the 'barotropic' velocity amplitudes.

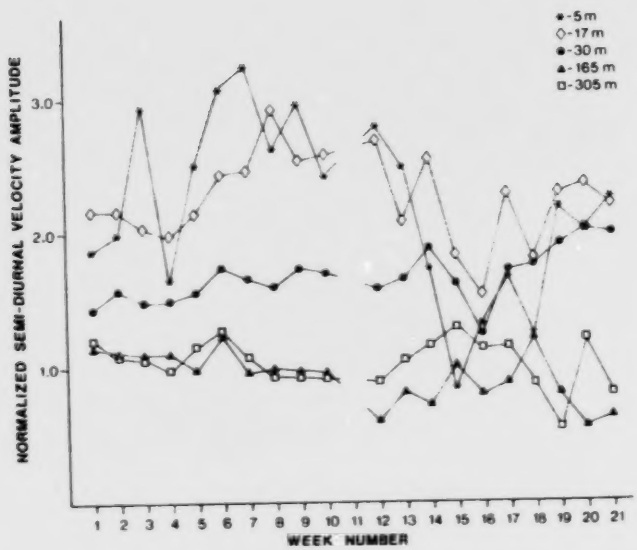

Fig. 6. Observed weekly phases of semi-diurnal velocity relative to the phase of tidal height.

Theoretical Considerations

Batchelor (1967) estimates the thickness of the bottom frictional boundary layer in an oscillating, rectilinear flow as $\delta = K_v(\omega)$ where K_v is the vertical coefficient of eddy viscosity and ω is the frequency of oscillation of the flow. When K_v is taken to be a large value of 1×10^3 $cm^2\ s^{-1}$ and ω is taken to be the semi-diurnal frequency δ is calculated to be 38 m. Since this thickness is considerably less than the depths over which the observed variations in the magnitude of the horizontal velocities occur it would seem unlikely that the variations are due to frictional effects.

Theoretically, baroclinic motions can propagate in a rectangular channel of uniform depth as either internal Kelvin waves or as internal Poincaré waves (Leblond and Mysak, 1978). In their study of baroclinic motions in Johnstone Strait, Thomson and Huggett, 1980 postulate that these motions are due to propagating internal Kelvin waves. They show that possible Poincaré wave solutions to a theoretical consideration of wave propagation in the strait would have large vertical mode numbers and hence would be strongly reduced by dissipative effects. Following the reasoning presented by Thomson and Huggett, it can be shown that Poincaré waves are likely to be of limited importance in Douglas Channel, also. Thus, it is conjectured that the observed baroclinicity in Douglas Channel is due to propagating internal Kelvin waves.

The governing equation for the propagation of an internal Kelvin wave along a straight vertical boundary can be shown to be (LeBlond and Mysak, 1978):

$$\frac{\partial^2 \phi}{\partial z^2} + \frac{1}{\bar{\rho}} \frac{\partial \bar{\rho}}{\partial z} \frac{\partial \phi}{\partial z} + \frac{1}{c^2} \left[\frac{g}{\rho} \frac{\partial \bar{\rho}}{\partial z} - \omega^2 \right] \phi = 0 \qquad (5)$$

This equation is solved subject to the boundary conditions:

$$\phi(0) - \phi(H) = 0$$

where:

- $\phi(z)$ is the vertical displacement amplitude of the internal wave as a function of depth, z.
- c is the horizontal component of the phase speed of the internal wave parallel to the direction of one channel wall (the 'x' direction).
- ω is the angular frequency of the internal wave.
- H is the water depth.
- $\bar{\rho}(z)$ is the mean water density as a function of depth.

Equation (5) can be derived from the fluid momentum and continuity equations subject to the conditions that:

1. The fluid is inviscid and incompressible.
2. The waves are of small amplitude so the equations can be linearized.
3. The water depth, H, is constant.
4. The mean velocities in the fluid are all zero.
5. The horizonal derivatives of density are zero.
6. The Boussinesq approximation.
7. The vertical displacement of water particles as a function of distance x, and time, t, takes the wave-like form:

$$\Phi(x,y,z,t) = \phi(z)\, F(y) e^{i(x-ct-\theta)} \qquad (6)$$

where θ is a phase constant and y is the coordinate in the cross channel direction.

The solutions of equation (5) for specified vertical profiles of density were obtained numerically using computer software developed by P. Fryer (unpublished manuscript). The wave frequency, ω, was taken to be the M_2 frequency, that is $\omega = 1.41 \times 10^{-4}\ s^{-1}$. For the solution to exist as a propagating wave a necessary condition is that the Brunt-Väisälä frequency, N(z), is

$$N = \sqrt{\frac{-g}{\rho}\frac{\partial \bar{\rho}}{\partial z}} > \omega \qquad (7)$$

over part of the water column.

Even in the deep water of Douglas Channel where the stratification was not as strong, values of N always exceeded $1 \times 10^{-3}\ s^{-1}$ over the period July to December, 1977. The solution of equation (5) consists of a series of eigenfunctions which will be termed the first, second, etc., baroclinic modes. Let $\phi_n(z)$ be the n'th mode eigenfunction for a wave propagating in the positive x direction and let c_n and θ_n be the horizontal phase speed and phase corresponding to this solution. Through application of the continuity equation it can be shown that the horizontal velocity field associated with this wave, $\Psi_n(x,y,z,t)$ is given by:

$$\Psi_n(x,y,z,t) = c_n \frac{\partial \phi_n}{\partial z}(x,y,z,t) \qquad (8)$$

The depth dependent amplitude of the horizontal velocity due to the n'th mode wave is thus:

$$\Psi_n(z) = c_n \frac{\partial \phi_n}{\partial z} \qquad (9)$$

The Kelvin wave solution of equation (5) propagates in a direction parallel to and to the left of the channel wall. Although the influence of the Earth's rotation does not appear in equation (5) and so does not affect the calculation of the eigenfunctions, it does result in the amplitude of the Kelvin wave being dependent on the distance, y, away from the channel wall.

This 'y' dependence results from the requirement that in the momentum equation for the cross channel direction, the Coriolis force arising from the along channel flow must be balanced by a lateral pressure gradient. The 'y' component of velocity for the Kelvin wave is still identically zero. If the channel wall is defined as the line y=0 then this dependence can be shown to be:

$$F(y) = e^{-y/r_n} \qquad (10)$$

and $r_n = c_n/f$ is the Rossby internal radius of deformation for the n'th mode where f is the Coriolis parameter.

Thus the wave amplitude is highest against the channel wall and decreases with increasing distance away from the channel wall. The horizontal velocity field associated with the wave will be modified by the same exponential decay factor.

Since Douglas Channel has two fairly straight parallel sides it is possible for internal Kelvin waves to propagate in both directions along it. Values of c_n for the first baroclinic mode were computed to be of the order of 0.8 m s^{-1} giving an internal Rossby radius of deformation of 7 km. Near the current meters the channel is about 4 km wide. For these parameters the amplitudes of fluctuations due to a passing internal Kelvin wave will differ by a factor of 1.8 on the two sides of the channel. For an internal Kelvin wave propagating northwards along Douglas Channel the amplitudes will be largest on its eastern side; for a southward propagating wave the amplitudes on the channels' western side will be largest.

THE FITTING OF THEORETICAL EIGENFUNCTIONS TO OBSERVED CURRENT VELOCITIES

The solution of equation (5) requires that the vertical density profile, $\bar{\rho}(z)$ be specified. Temperature and salinity data from each of the five current meters and the temperature measurements from the thermistor chain TMS 2 were used to estimate an average weekly profile for weeks #1 to #10. Figure 7b shows the computed eigenfunctions of horizontal velocity for the first three baroclinic modes derived using the density profile shown in Figure 7a which was appropriate for week #3. Although the intensity of the stratification varied somewhat over weeks #1 to #10, all the density profiles displayed similar features to that shown in Figure 7a. The density always increased rapidly from the surface to a depth of 20 m and more slowly below this depth. Likewise, the shapes of the eigenfunctions of horizontal velocity also appear similar to those shown in Figure 7b, but the depths of the zero crossings change as the shape of the density profiles change.

The baroclinicity which appears in Figure 3 and the shape of the first mode baroclinic eigenfunction (see Fig. 7b for example) show at least a qualitative similarity with each other. In order to determine quantitatively whether the observed baroclinicity could be accounted for by baroclinic Kelvin waves the theoretical eigenfunctions of horizontal velocity field associated with a barotropic tide (velocity constant with depth) were fitted to the observed semi-diurnal velocities in Douglas Channel for weeks #1 to #10. A least squares fitting procedure was used to obtain the amplitudes and phases of the barotropic contribution and of the two fitted baroclinic modes for each week. Further details of this analysis are given by Webster (1980c).

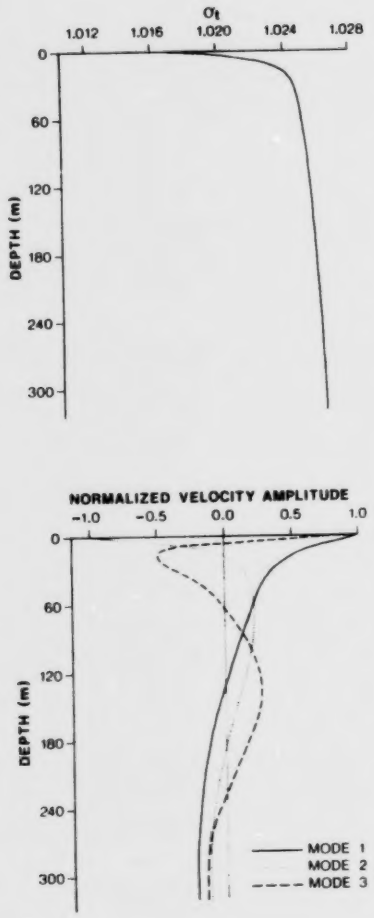

Fig. 7. a) Observed vertical density profile (week #3).
b) Computed baroclinic horizontal velocity eigenfunctions.

The computer amplitudes of the fitted eigenfunctions are shown in Figure 8. Note that these amplitudes have been normalized with respect to the amplitude of the barotropic tide computed from the tidal model for each week. Over the ten week period the normalized amplitude of the fitted barotropic mode varies between 1.16 and 1.45, averaging 1.26. More significantly the phase of the fitted barotropic mode (with respect to the phase of tidal height) varies over a 6° range around -61°. The tidal model predicts phases for the barotropic current to be around -85°. This implies that the semi-diurnal barotropic tide is predominantly a standing wave. For a purely standing wave the horizontal tidal velocity would lag the tidal height by 90°; for a purely travelling wave propagating northwards through Douglas Channel the tidal height and velocity would be in phase. The relative phase between the tidal height and the fitted barotropic velocity of around -60° indicates that the tide is somewhere between a standing and a travelling wave.

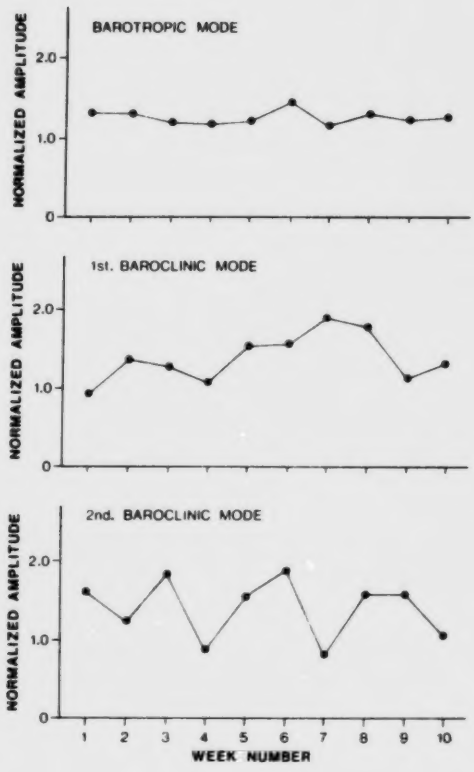

Fig. 8. Fitted normalized velocity amplitudes for barotropic and first two baroclinic modes of velocity.

The modal fitting procedure yields values of the normalized first and second baroclinic amplitudes mostly between 1.0 and 2.0. The phases of the first mode vary from -74 to -13 ; the phases of the second mode fall in the range -15 to 80 . These values show that there was considerable variation in both the amplitudes and phases of the fitted baroclinic eigenfunctions.

SOURCE OF THE BAROCLINICITY

The source of the baroclinicity is almost certainly the interaction of the barotropic tide with the topography of the region. The similarity of the baroclinicity evident in the M_2, S_2 and N_2 components of the tidal currents suggests a tidal origin. If a major part of the baroclinicity were caused by a semi-diurnal component of wind stress, for example, one would expect the nature of the baroclinicity in the S_2 component (period 12.00 hours) to differ markedly from the baroclinicity in the other two components. Before their normalization using a barotropic current computed from the tidal model the amplitudes of the fitted baroclinic modes showed much wider fluctuations from one week to the next than are shown in Figure 8. The stability of amplitudes when normalized compared to the lack of stability without normalizing also suggests a tidal origin for the baroclinicity.

From knowledge of the baroclinic velocity field alone it is not possible to determine the direction of propagation of a baroclinic wave. The sill which crosses Douglas Channel 10 km to the north of the observation sites is the most obvious area of baroclinic wave generation. If the sill were the generation location then the northward flux of energy in the barotropic tide should be greater than the (southward) flux of energy in the baroclinic tide.

The energy transmission through a channel cross section in a tidal period due to a barotropic wave is given by $\langle pu \rangle_{S,T}$ (Thomson and Huggett, 1980). In this expression p is the pressure fluctuation due to the wave (proportional to tidal height) u is the long channel component of velocity and $\langle\ \rangle_{S,T}$ represents integrations over both the cross sectional area of the channel, S, and over the tidal period, T.

For week #6, the northward energy transmission over a tidal period due to the semi-diurnal barotropic tide was 2×10^{13} joules. This computation assumed the relative phase between u and p was -62^{o}, that is the value appropriate for the fitted barotropic tide. When the same calculation was carried out using -85^{o}, the relative phase appropriate for the modelled semi-diurnal current, the energy reduced to 4×10^{12} joules. The energy transmission calculated using the fitted barotropic tide is 5 times as large as that calculated using the modeled barotropic tide. This represents a serious discrepancy.

Since the baroclinic pressure field cannot be evaluated directly, the energy flux calculation for the baroclinic waves could not be completed. An upper bound on the baroclinic energy flux can be obtained by assuming that it is due to a purely travelling Kelvin wave. Thomson and Huggett (1980) show how this energy flux can be calculated once the amplitude and form of a baroclinic mode is known. When this calculation is carried out for week #6 the energy transmission through the channel over one tidal cycle turns out to be 4×10^{10} joules for the first baroclinic mode and 2×10^{10} joules for the second. Even if a phase angle of -85^{o} between the barotropic current and the tidal height is assumed, the northward transmission of barotropic tidal energy is sufficient to account for the observed baroclinicity.

The phases of the first baroclinic mode determined from the fitting procedure are plotted against the computed phase speeds of this mode in Figure 9. A definite relationship between phase speed and phase is not indicated. If the first baroclinic mode were to be generated by the barotropic tidal flow across the sill then the relationship between phase speed, c, and phase, θ, at an observation site at a distance, x, from the sill should look like:

$$\theta = \frac{\omega x}{c} + \theta_o \qquad (11)$$

where ω is the seni-diurnal frequency and θ_o is a constant representing the relative phase of the barotropic and baroclinic modes at the sill. The dotted line in Figure 9 shows the relationship if θ_o were -140^{o}.

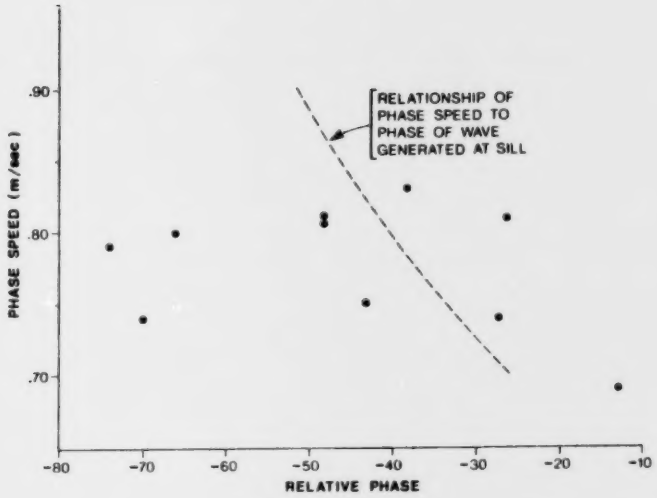

Fig. 9. Phase speed versus fitted relative phase for the baroclinic mode.

The propagation of energy in baroclinic waves takes place along their characteristics. For a baroclinic Kelvin wave the equations for these characteristics in a zero mean flow can be shown to be (Leblond and Mysak, 1978):

$$\frac{dz}{dx} = \pm \left(\frac{\omega^2}{N^2 - \omega^2} \right)^{\frac{1}{2}} \qquad (12)$$

Assuming the baroclinic waves are generated at the top of the sill then this equation can be used to estimate the distance away from the sill at which the wave energy reaches the surface. If N is assured constant between the current meter depths then the energy characteristic will decrease depth by Δz over a distance Δx where:

$$\Delta x = \pm \left(\frac{N^2 - \omega^2}{\omega^2} \right)^{\frac{1}{2}} \Delta z \qquad (13)$$

Using values of N calculated from the current meter density data and taking the Δz's as the changes in depth between current meters then equation (13) can be evaluated in a stepwise fashion to determine the total horizontal distance travelled before a characteristic originating at 240 m depth (sill depth) reaches the surface. This technique is schematicised in Figure 10. Table 1 details the calculation for week #1 for which the characteristic reached a depth of 5 m a distance of 21 km away from the sill. For the other nine weeks this distance was not less than 17 km.

Since this distance is about twice the distance of the current meters to the sill (10 km) baroclinic energy propagated directly from the sill does not appear to be responsible for the observed baroclinicity at the current meters.

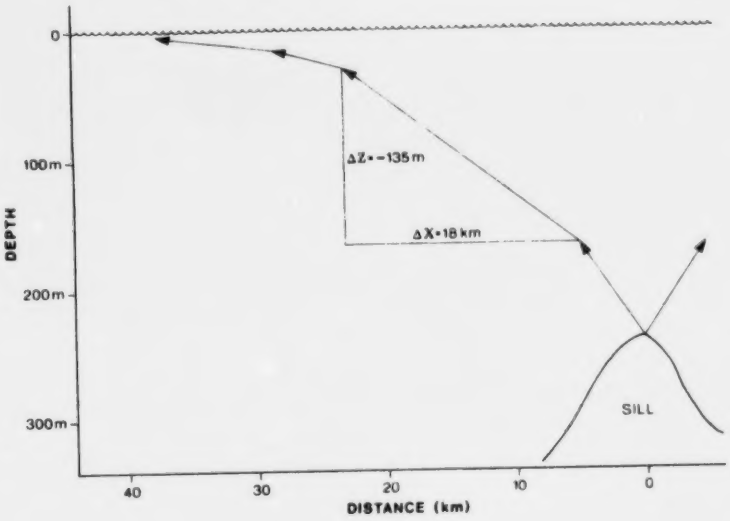

Fig. 10. Schematic of baroclinic energy propagation from Douglas Channel sill (week #1).

Table 1. Calculation of Characteristic Depth for Week #1

Depth Range	N(sec^{-1})	Δz(m)	Δx(km)
240 m to 165 m	0.006	75	3
165 m to 30 m	0.01	135	10
30 m to 17 m	0.03	13	3
17 m to 5 m	0.06	12	5
		total	21

It is evident that the observed baroclinicity in Douglas Channel is not simply explained as Kelvin waves propagating from the sill of the forms theoretically developed. Perhaps the sill is not the generation point for the baroclinicity. Alternatively, the forms of the baroclinic Kelvin waves used in the fitting procedure may be incorrect. The differences between the energy fluxes computed using the fitted barotropic tide and the modelled barotropic tide suggest a fundamental problem in either the barotropic tidal model or in the baroclinic fitting procedure. The differences between the observed velocities and the fitted velocities for each current meter depth have a consistent nature from week to week. This consistency suggests that the differences are not primarily due to a noise-like phenomenon in the current meter data. Perhaps the fitting procedure should include baroclinic waves of higher mode than two. Also, the baroclinic wave structures were calculated from vertical profiles of density which had to be interpolated from the available data. As a result these calculated wave structures used in the fitting procedure are subject to considerable uncertainty.

Perhaps a more serious shortcoming of the analysis used is the assumption of zero mean horizontal velocity in the derivation of the baroclinic eigenfunctions. Douglas Channel has significant horizontal water movements evidently associated with its estuarine and wind driven circulations. Near the surface (5 m depth) where these mean horizontal currents tended to be largest their magnitudes usually exceeded 10 cm s^{-1} and were often over 20 cm s^{-1} in the ten week period over which the fitting was accomplished. Since these currents are not insignificant compared to the horizontal phase speeds of the first and second baroclinic modes one might expect that their presence would have a major influence on the nature of the baroclinic waves in the channel. For higher order modes having smaller wave speeds the mean currents in the channel might be expected to have an even greater influence on the form of the baroclinic waves.

SUMMARY AND CONCLUSIONS

A high degree of baroclinicity was indicated in the semi-diurnal currents measured in the southern part of Douglas Channel over the period July, 1977 to December, 1977. Both the amplitudes and phases of these currents showed marked changes with depth. The amplitudes of the semi-diurnal current at 5 m depth often exceeded twice the amplitude of the estimated barotropic currents in this section of the channel; at mid-depth and near the bottom of the channel the tidal current amplitudes were similar to the expected barotropic current. Moreover, the observed baroclinicity showed significant temporal variability. Over the five month observation period the semi-diurnal current at 5 m depth was observed to range in amplitude from less than the barotropic current amplitude to more than three times as large.

Probably the baroclinicity results from the interaction of the barotropic tide with the topography of the area. Variations in the amount of energy which appears in the baroclinicity would result from changes in the density and mean flow structures in the channel. The sill which crosses Douglas Channel to the north of the current meters was examined as a possible generation site. Although a generation site to the north of the current meters is plausible on the grounds of flow energetics, the method of characteristics suggests that the sill is too close to the current meters for baroclinicity generated there to be observed by the current meters near the surface.

The observed baroclinicity displays a form which is at least qualitatively similar to that of a baroclinic Kelvin wave. Accordingly, the observed semi-diurnal currents were fitted by a sum of baroclinic Kelvin waves having mode numbers of one and two and a barotropic wave. The theoretical velocity structure of each mode of the Kelvin waves was determined numerically using measured density profiles from Douglas Channel. The results of the fitting procedure did not show conclusively that the observed baroclinicity was due to waves of the forms fitted. The theoretical Kelvin waves were derived using the simplifying assumptions that the bottom was flat, the mean current shear in Douglas Channel was zero, the friction was zero, and that the waves could be derived from linearized equations. Since all these assumptions are in error to some degree the derived Kelvin wave forms are at best approximations.

The determination of the source and the generation mechanism of the baroclinicity is essential for the successful prediction of near surface tidal currents in Douglas Channel. If kinetic energy is distributed among a series of baroclinic waves having different mode numbers then the baroclinic contribution to the total current will change in amplitude and phase with increasing distance away from the source of the baroclinicity due to the differing horizontal phase speeds of the modes. A semi-diurnal first mode baroclinic wave having a horizontal phase speed of 0.8 m s^{-1} changes phase by 555° along the 55 km length of Douglas Channel; a semi-diurnal second mode baroclinic wave having a horizontal phase speed of 0.5 m s^{-1} changes phase by 885° in the same distance. By comparison, the phase change along the channel of a propagating barotropic wave of phase speed 60 m s^{-1} is only 7°. The first and second mode baroclinic waves will therefore each make additive and subtractive contributions to the barotropic current simultaneously in different locations in the channel. If a superposition of one or more baroclinic waves is the appropriate representation of the baroclinicity in Douglas Channel then predictive schemes for near surface tidal currents should consider potentially significant spatial variability in the currents which arises as a consequence.

REFERENCES

Batchelor, G.K. 1967. An Introduction to Fluid Dynamics. Cambridge Univ. Press. 615 pp.

Buckingham, W.R. 1980. Kitimat Physical Oceanographic Study 1977-1989. The Response of Douglas Channel to Meteorological Forces. Contract Report Series 80-3 (part 5), Institute of Ocean Sciences, Patricia Bay, B.C., unpublished Manuscript, 52 pp.

Foreman, M.G.G. 1978. Manual for Tidal Currents Analysis and Prediction. Pacific Marine Sciences Report 78-6, Institute of Ocean Sciences, Patricia Bay, B.C., unpublished manuscript.

LeBlond, P.L. and L.A. Mysak. 1978. Waves in the Ocean. Elsevier, 602 pp.

Narayanan, S. 1980. Kitimat Physical Oceanographic Study 1977-1978. Tidal circulation model. Contract Report Series 80-3 (part 4), Institute of Ocean Sciences, Patricia Bay, B.C., unpublished manuscript.

Thomson, R.E. and W.S. Huggett. 1980. M_2 Baroclinic Tides in Johnstone Strait, B.C. Journal of Physical Oceanography, 10, pp. 1509-1539.

Webster, I.T. 1980a. Kitimat Physical Oceanographic Study 1977-1978, Data Collection and Analyses. Contract Report Series 80-3 (part 1), Institute of Ocean Sciences, Patricia Bay, B.C., unpublished manuscript, 51 pp.

Webster, I.T. 1980b. Kitimat Physical Oceanographic Study 1977-1978, Estuarine Circulation. Contract Report Series 80-3 (part 3), Institute of Ocean Sciences, Patricia Bay, B.C., unpublished manuscript, 81 pp.

Webster, I.T. 1980c. Kitimat Physical Oceanographic Study. Temporal Variations of the Baroclinic Tide in Douglas Channel. Contract Report Series 80-3 (part 6), Institute of Ocean Sciences, Patricia Bay, B.C., unpublished manuscript, 36 pp.

Webster, I.T. and L. Ford. 1980. Kitimat Physcial Oceanographic Study A manual for General Data Access. Contract Report Series 80-3 (part 2), Institute of Ocean Sciences, Patricia Bay, B.C., unpublished manuscript, 110 pp.

ACKNOWLEDGEMENTS

I gratefully acknowledge the assistance of R. Macdonald, J. Poulin and D. Wonnacott in preparing this paper.

LES COURANTS DE SURFACE APPROCHANT LE KITIMAT

W.S. Huggett and S.O. Wigen
Institute of Ocean Sciences, Sidney, B.C.

RÉSUMÉ

Cet atlas fait voir sur la carte marine de douze heures de courant s'écoulant du Laredo Sound jusque à Kitimat. Ces études ont été faites en 1953 et 1954. Ces cartes-marine sont basées sur 1680 heures de perche-flotante à la trace; et 388 heures de courant-compteur. Durant la condition des immenses courants, une étendue disparate fût apliquer-si necessaire-afin d'apporter de la vélocité à ces courants. La où plusieurs vélocitées ont été corriger, elles sont disponibles à une simple location; pourvie qu'elles soient en accord communces vélocitées ont été au-des-sous du commun. Si ces observations sont disparates, la priorité fût donner à celles, que furent observer durant les marées-hautes. La vélocité est donner en neouds.

Huggett, W.S. and S.O. Wigen, 1983. Surface currents on the approaches to Kitimat. Can. Tech. Rep. Hydrogr. Ocean Sci. 18, 34-65.

Mot-clés: courants, Kitimat, Laredo Sound, perche flottante

SURFACE CURRENTS IN THE APPROACHES TO KITIMAT

W.S. Huggett and S.O. Wigen
Institute of Ocean Sciences, Sidney, B.C.

ABSTRACT

This Atlas shows twelve hourly current charts of the surface flow from Laredo sound to Kitimat compiled from studies carried out in 1953 and 1954. These charts are based on 1680 hours of driftpole tracking and 388 hours of current metering. A range factor has been applied as necessary to bring velocities to those to be expected during large tide conditions. Where several corrected velocities are available at a single location and time, they have been averaged, provided they are in close agreement. If the observations are disparate precedence has been given to those observed during the larger tides. Velocities are given in knots.

Huggett, W.S. and S.O. Wigen, 1983. Surface currents on the approaches to Kitimat. Can. Tech. Rep. Hydrogr. Ocean Sci. 18, 34-65.

Keywords: currents, driftpoles, Kitimat, Laredo sound

INTRODUCTION

Development of the aluminum industry at Kitimat in the early 1950's created a new major shipping route on the B.C. coast. From Queen Charlotte Sound the route entered the coastal passages at Laredo Sound, and continued via Laredo Channel, Caamano and Campania Sounds, Whale Channel and Douglas Channel to Kitimat Arm. To aid in providing safe navigation the Department of Transport provided lights and navigational aids, and the Canadian Hydrographic Service surveyed major portions of the route and published new charts northward from Whale Channel. Field programs carried out by the Canadian Hydrographic Service also included a study of surface and near-surface currents along the route and in adjacent passages. These studies were carried out by the Tides and Current Section from July 4 to September 12, 1953 and June 23 to August 6, 1954. No data were collected during the winter months.

Winds during the periods of observations were calm to moderately-fresh (0-20 knots), and from all quadrants of the compass. On days of strong winds, heavy rain or fog no observations were taken, mainly because all positioning of the drift-poles was done by sextant fixes. Douglas Channel can be affected by the wind, especially winds from the north which, when coupled with the river run-off, generate a persistent southerly surface current and through entrainment velocities up to 2 knots are present at the south end of the channel. This current continues seaward through Whale Channel.

In view of the possibility that the current survey data might have other applications, and because of the present interest in the waterways leading to Kitimat, this paper is intended to outline the method of survey and data interpretation, and to present the hourly flow patterns based on the survey.

C.G.S. *Parry*, a 26 metre vessel with seiner-type hull provided the base for the survey. Captain Hugh Halkett served as master, Mr. Wigen as officer-in-charge of the survey, and Mr. Huggett as senior assistant. The ship had a normal complement of 15 persons including surveyors, officers and crew. Observations were carried out both from the *Parry* and from two 9 metre launches. Most of the measurements were made by tracking free-floating drift poles, but some current meter observations were made from the ship at anchor.

Drift Pole Construction, Deployment and Tracking

Drift poles were constructed with a 3.6 metre length of 50 x 50 mm dressed lumber, weighted at the lower end with angle iron or sheet lead, and buoyed at the top with one or two cork fish floats about 150 mm in diameter. Each carried a plastic flag less than 0.3 m square, on a strip of wood, and had a wire loop at the top end for easy recovery and for towing behind a launch. They were designed to float vertically with less than one foot showing to present a minimum of surface area above the water to diminish wind influence, and have as near a uniform cross-section as possible throughout their length.

For tracking their movement, triangulation stations along the shore, marked during the hydrographic survey, were relocated and whitewashed for easy visibility. Plotting boards showing the location of these stations and the coastline were prepared for use in the launches. A launch with one or two surveyors and coxswain would release up to 4 poles in the channel cross-section being surveyed, and the movement of each pole was then tracked by a series of timed sextant fixes. A "fix" consisted of measuring the two angles subtended by 3 appropriate stations. Positions were then plotted on the board with a station pointer, the distance travelled between successive fixes scaled and the speed calculated. A separate page of field notes was kept for each pole, with fixes and times being recorded on every second line, and scaled distances, time intervals, and velocities being entered on the intermediate lines. Poles drifting out of the area being surveyed or coming close to shore were redeployed to start a new line. To avoid having the motion of the pole disturbed by the wash or wake from the launch, the boat would routinely be brought to a position about 10 feet away from the pole for the fix, always in the same direction relative to the pole.

Since these observations were limited to daylight hours, to obtain a full tidal cycle the observations are by necessity spread over a number of days at any one location.

Current Metering

Nineteen current meter stations were occupied by the *Parry*. Most of these were 25-hour stations located on shoals of 70 metres or less and all but four were south of Whale Channel. The Channels to the north of Whale Channel provided few suitable sites within the *Parry's* anchoring capability.

The Gurley-Price current meter used at these stations recorded speeds only, and the direction of the flow was estimated by either visual observation of the orientation of the current meter or by a drogue suspended

to the appropriate depth. The speed of the flow was measured at depths of 1.8, 5.5 and 9.1 metres and occasionally at 3.6 metres if a flow gradient or shear was evident. Stations were occupied for 25 hours, unless the ship was driven off station by sea conditions.

For the most part current meter records have been used as a backup to the drift-pole records because the vessel was normally anchored over shoals where currents were not typical of those experienced in the main channels.

Interpretation and Compilation of Data

Current observations have been compiled into a series of hourly flow charts. Where several velocities are available at a single location and time, they have been averaged provided they are in close agreement. If the observations were disparate precedence has been given to those observed during the larger tides.

In the current metering, speeds at 1.8, 3.6 and 5.5 metres tended to be larger than those at the 9.1 metre depth. Generally again the higher values have been accepted.

Two sets of 12 hourly flow charts are appendixed to this report, the southern set extending from Laredo Sound to Whale Channel, and the northern, from Whale Channel to Kitimat. Velocities are given in knots.

The observational program on which these flow charts are based included a total of 388 hours of current metering and 1680 driftpole hours of tracking.

Source records of these surveys are available in the Tidal and Current Section at the Institute of Ocean Sciences, Sidney, B.C.

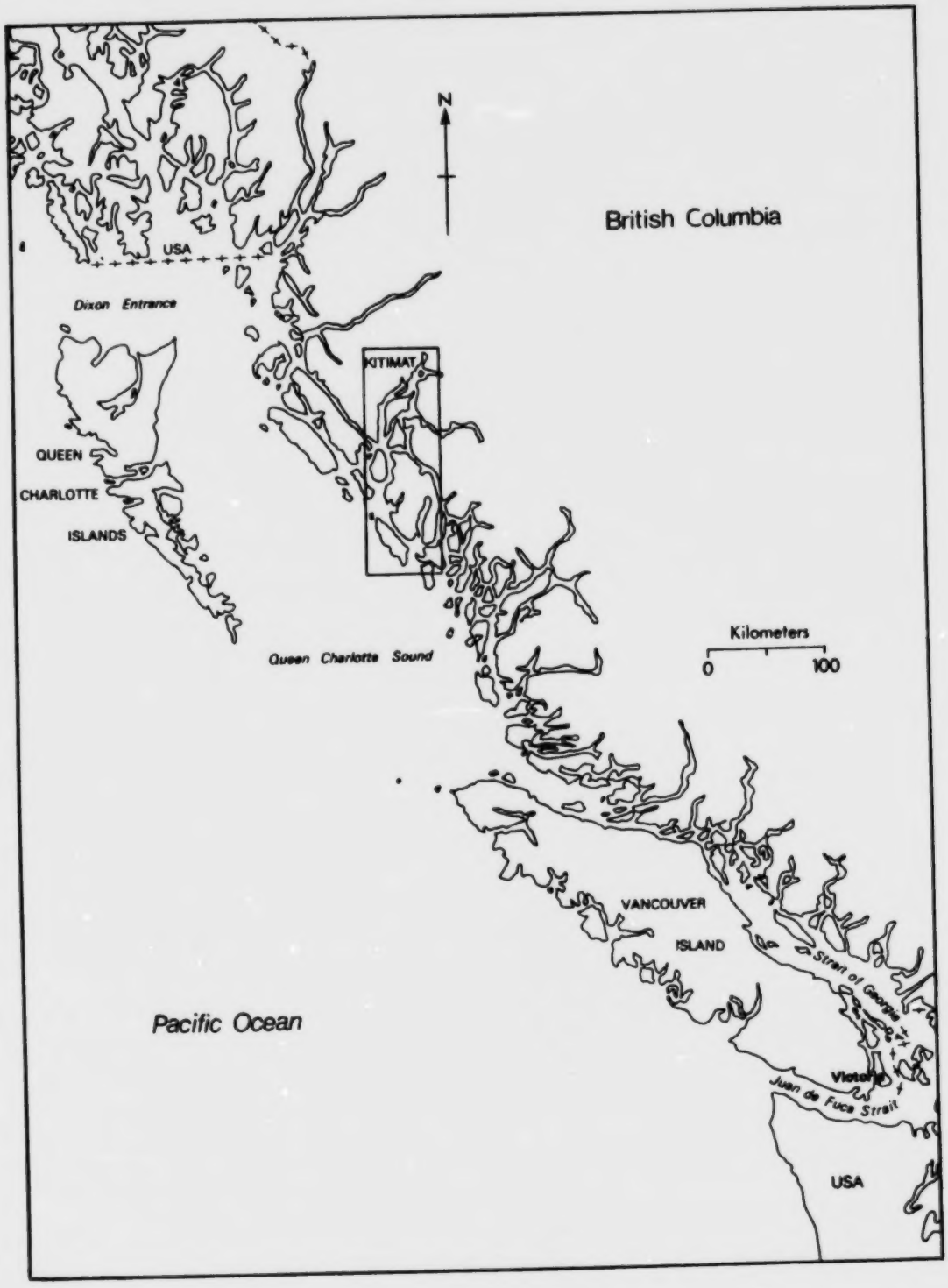

Figure 1. Study Area

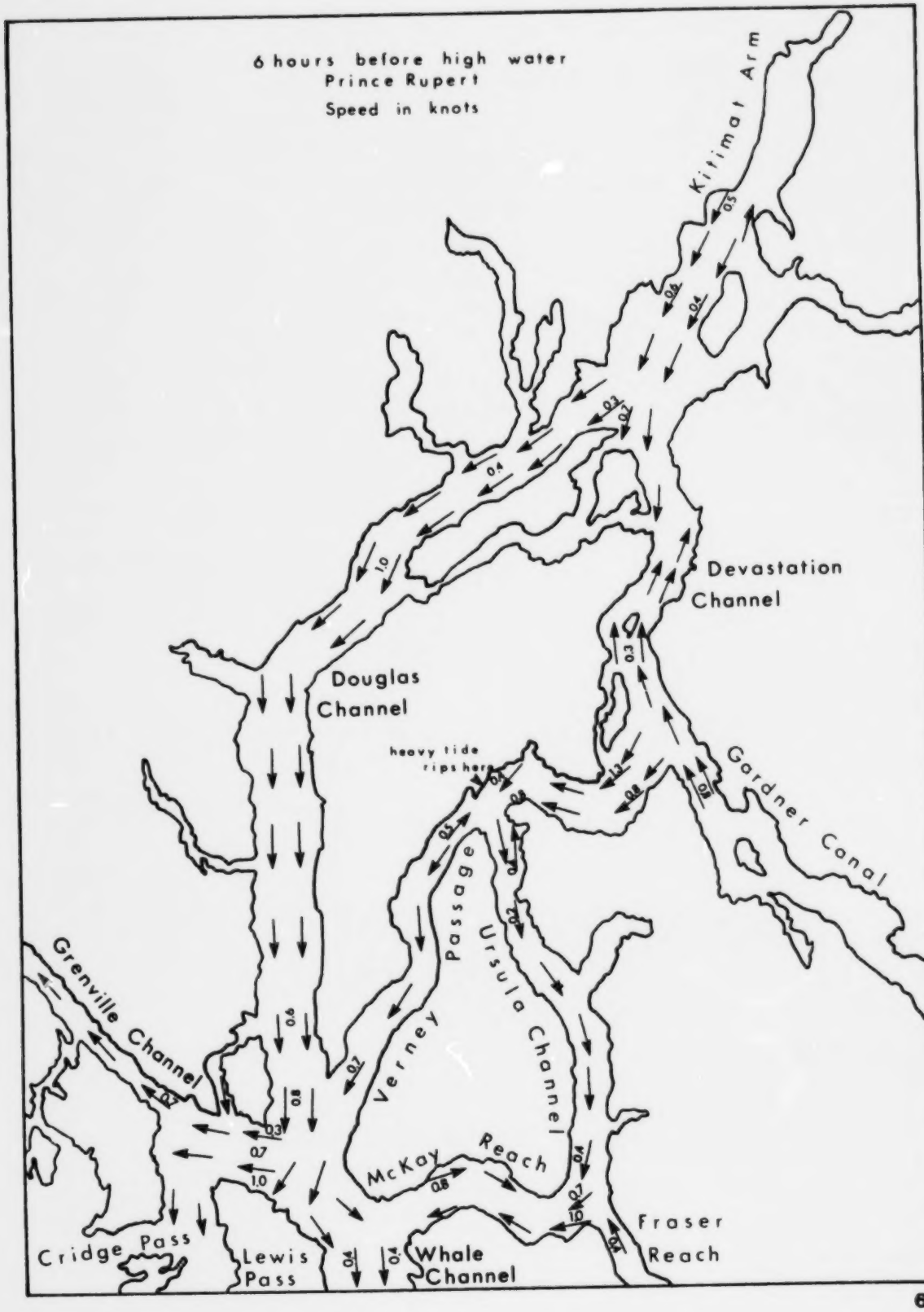
6 hours before high water
Prince Rupert
Speed in knots
Kitimat Arm
Devastation Channel
Douglas Channel
heavy tide rips here
Gardner Canal
Grenville Channel
Verney Passage
Ursula Channel
McKay Reach
Fraser Reach
Cridge Pass
Lewis Pass
Whale Channel

6B

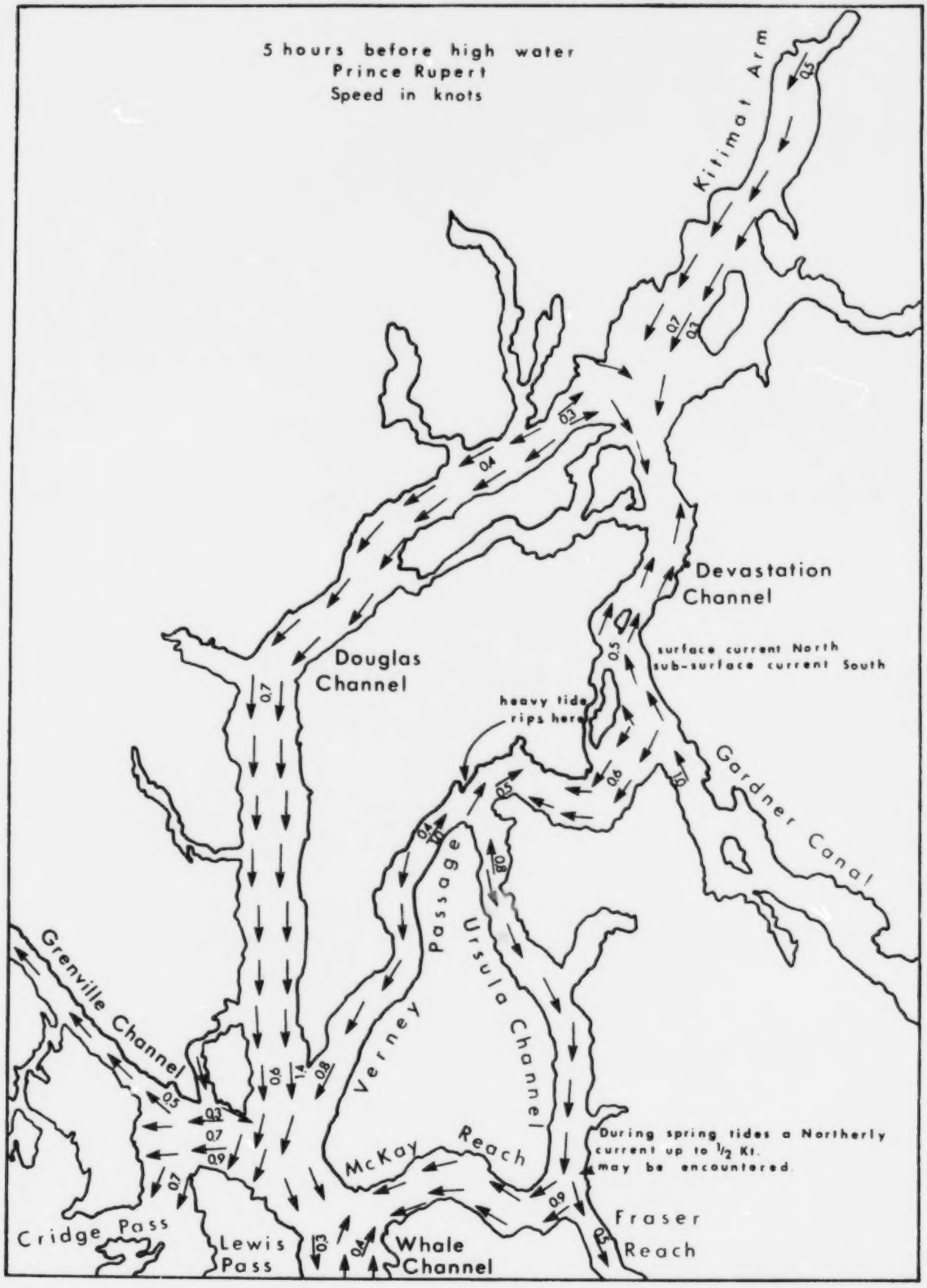
5 hours before high water
Prince Rupert
Speed in knots
Kitimat Arm
Devastation Channel
surface current North
sub-surface current South
Douglas Channel
heavy tide rips here
Gardner Canal
Grenville Channel
Verney Passage
Ursula Channel
McKay Reach
During spring tides a Northerly current up to ½ Kt. may be encountered.
Cridge Pass
Lewis Pass
Whale Channel
Fraser Reach

5B

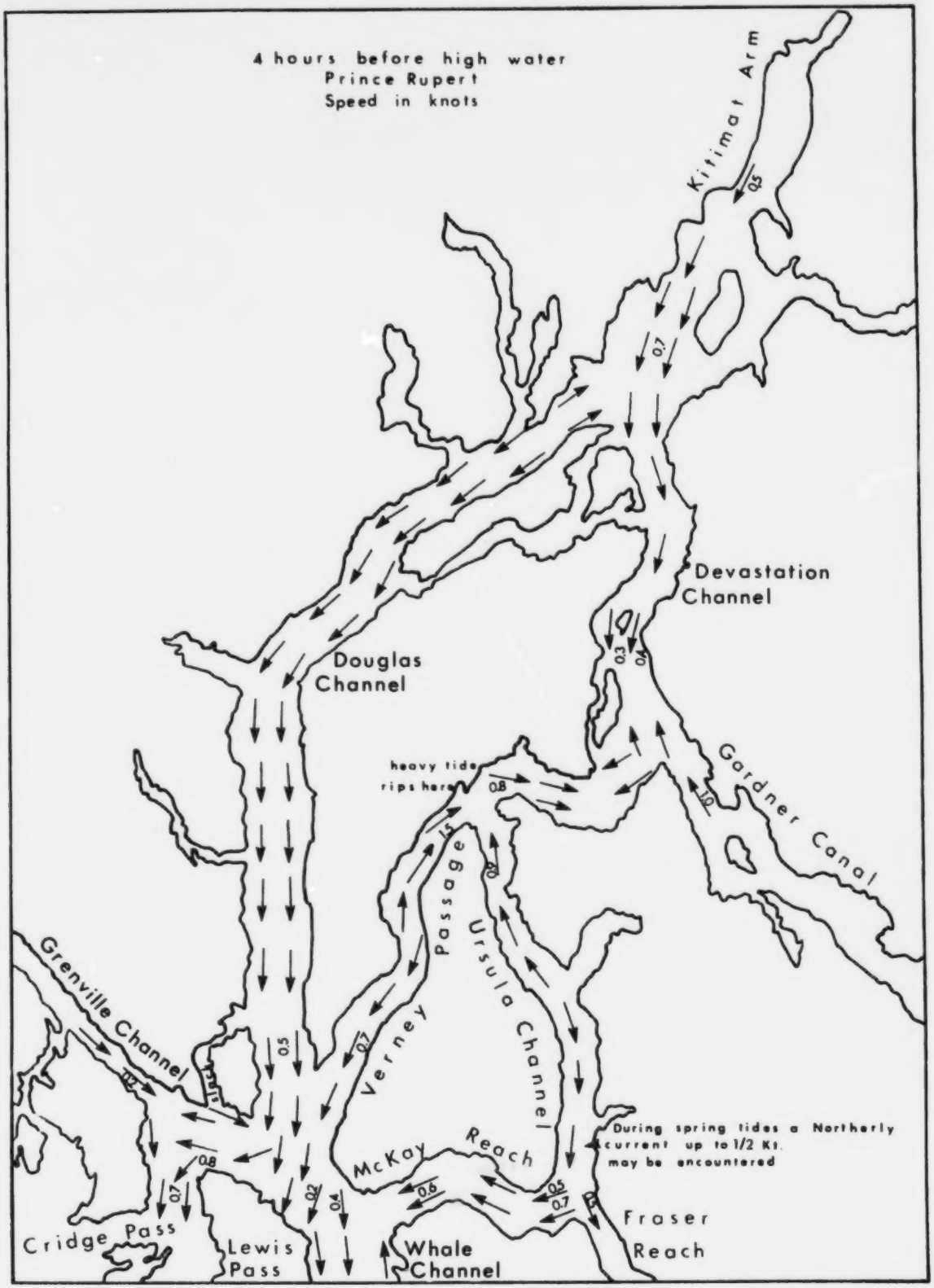
4 hours before high water
Prince Rupert
Speed in knots
Kitimat Arm
0.5
0.7
Devastation Channel
0.3
0.4
Douglas Channel
heavy tide rips here
0.8
1.0
Gardner Canal
1.5
2.0
Grenville Channel
0.5
0.7
Verney Passage
Ursula Channel
0.8
0.7
0.2
0.4
McKay Reach
0.6
0.5
0.7
During spring tides a Northerly current up to 1/2 Kt. may be encountered
Cridge Pass
Lewis Pass
Whale Channel
Fraser Reach

4 B

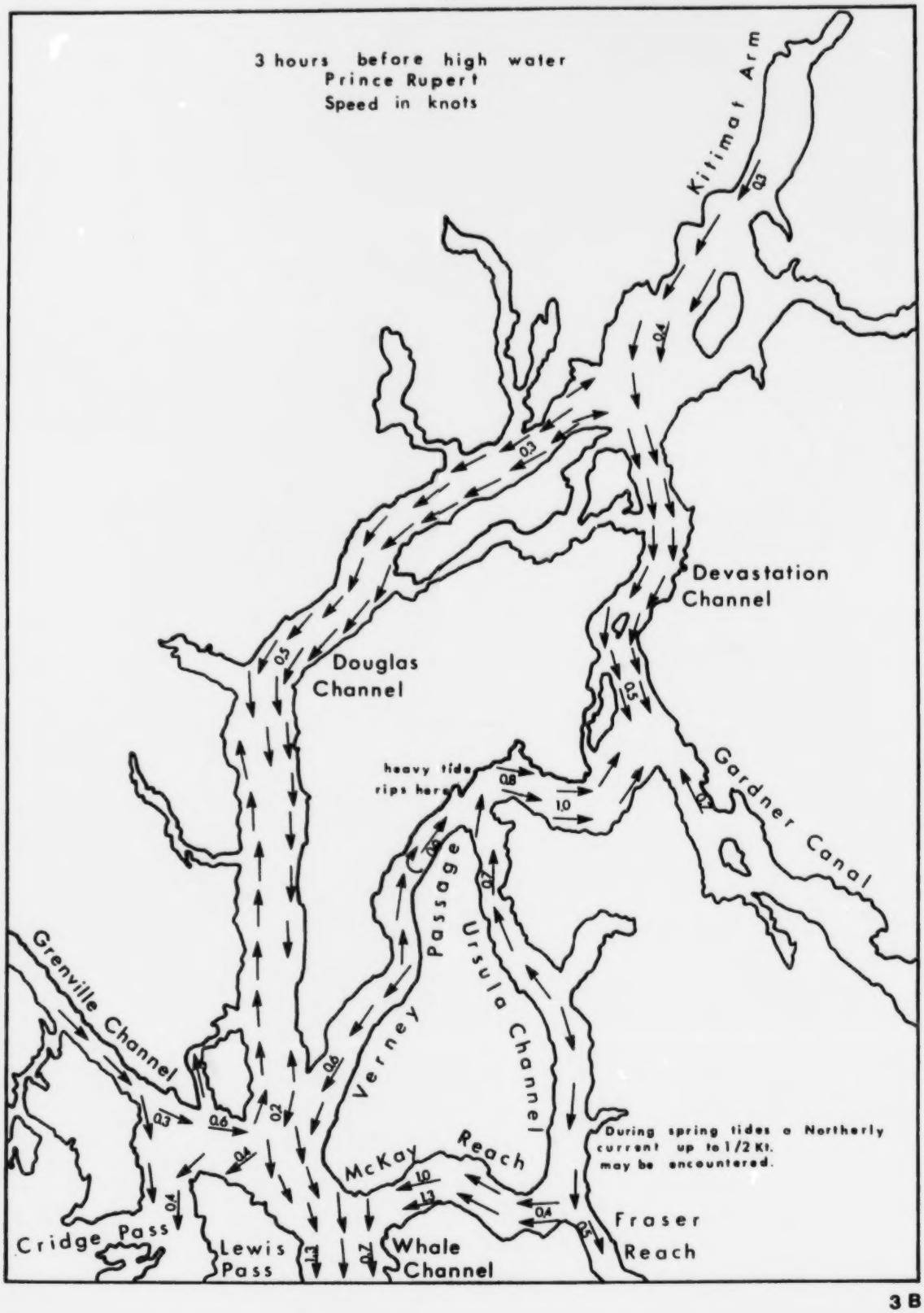
3 hours before high water
Prince Rupert
Speed in knots
Kitimat Arm
Devastation Channel
Douglas Channel
heavy tide rips here
Gardner Canal
Grenville Channel
Verney Passage
Ursula Channel
McKay Reach
During spring tides a Northerly current up to 1/2 Kt. may be encountered.
Cridge Pass
Lewis Pass
Whale Channel
Fraser Reach

3B

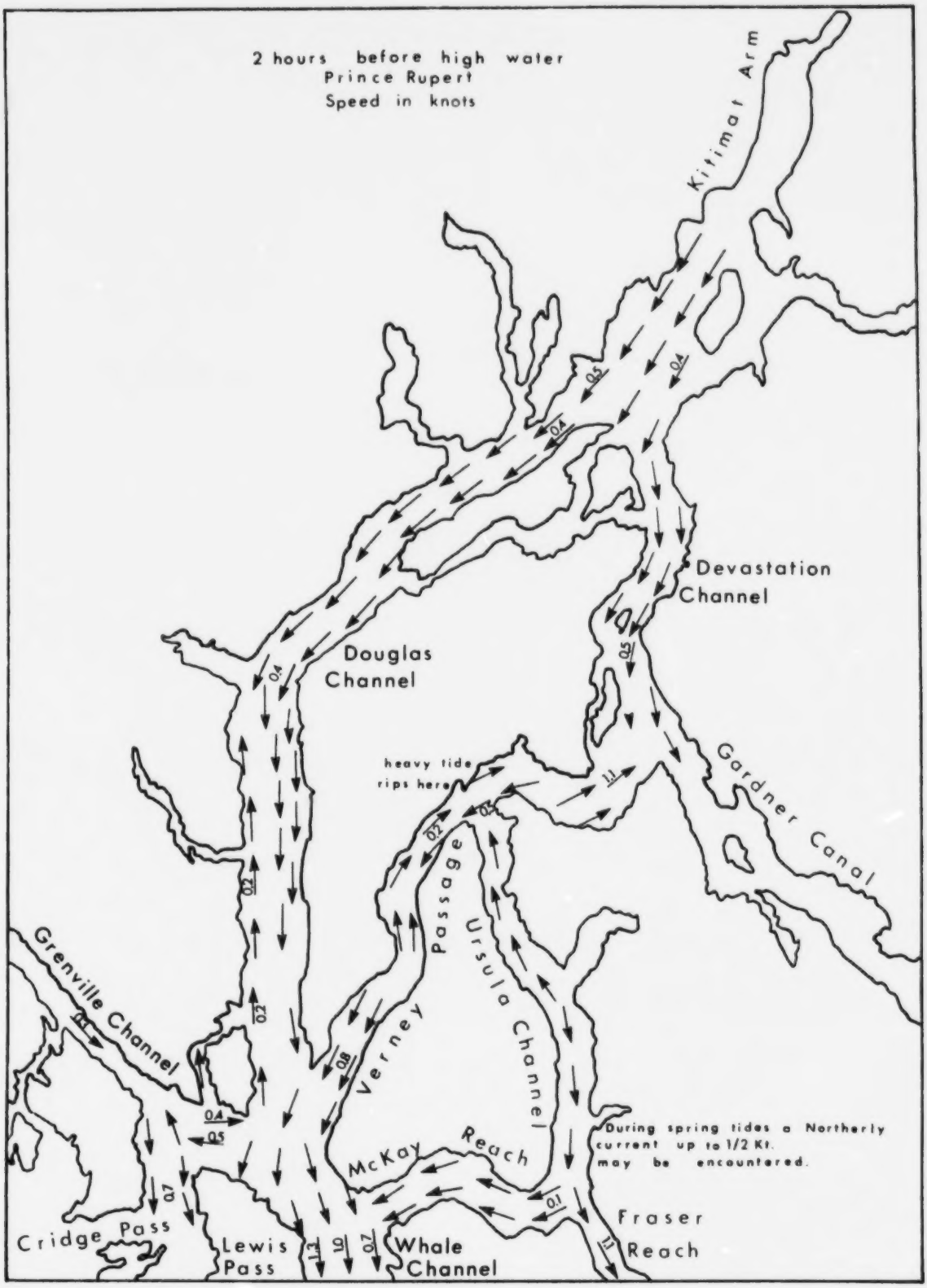
2 hours before high water
Prince Rupert
Speed in knots
Kitimat Arm
Devastation Channel
Douglas Channel
heavy tide rips here
Gardner Canal
Grenville Channel
Verney Passage
Ursula Channel
McKay Reach
During spring tides a Northerly current up to 1/2 Kt. may be encountered.
Cridge Pass
Lewis Pass
Whale Channel
Fraser Reach

2 B

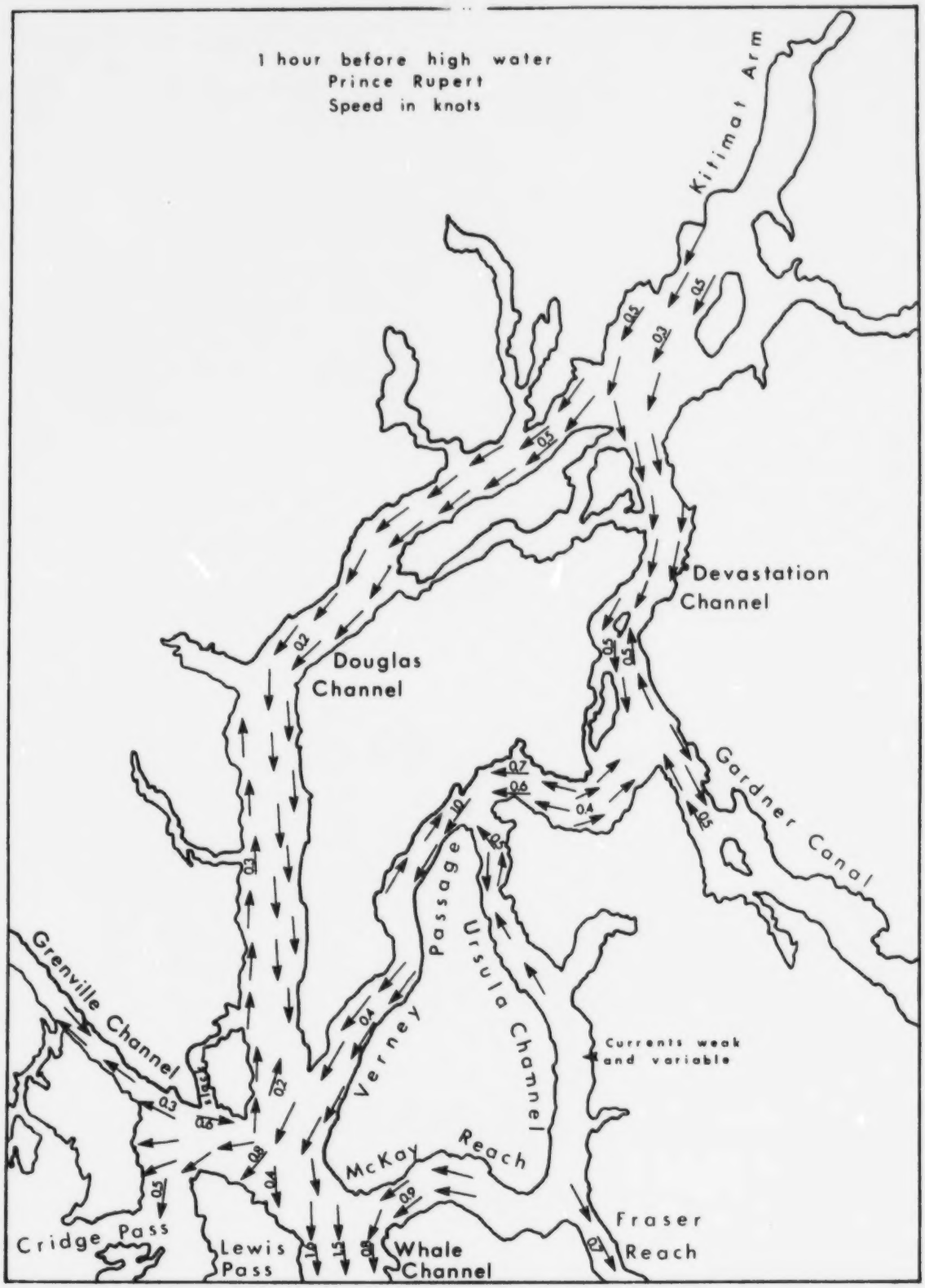
1 hour before high water
Prince Rupert
Speed in knots
Kitimat Arm
Devastation Channel
Douglas Channel
Gardner Canal
Grenville Channel
Verney Passage
Ursula Channel
Currents weak and variable
McKay Reach
Fraser Reach
Cridge Pass
Lewis Pass
Whale Channel

1 B

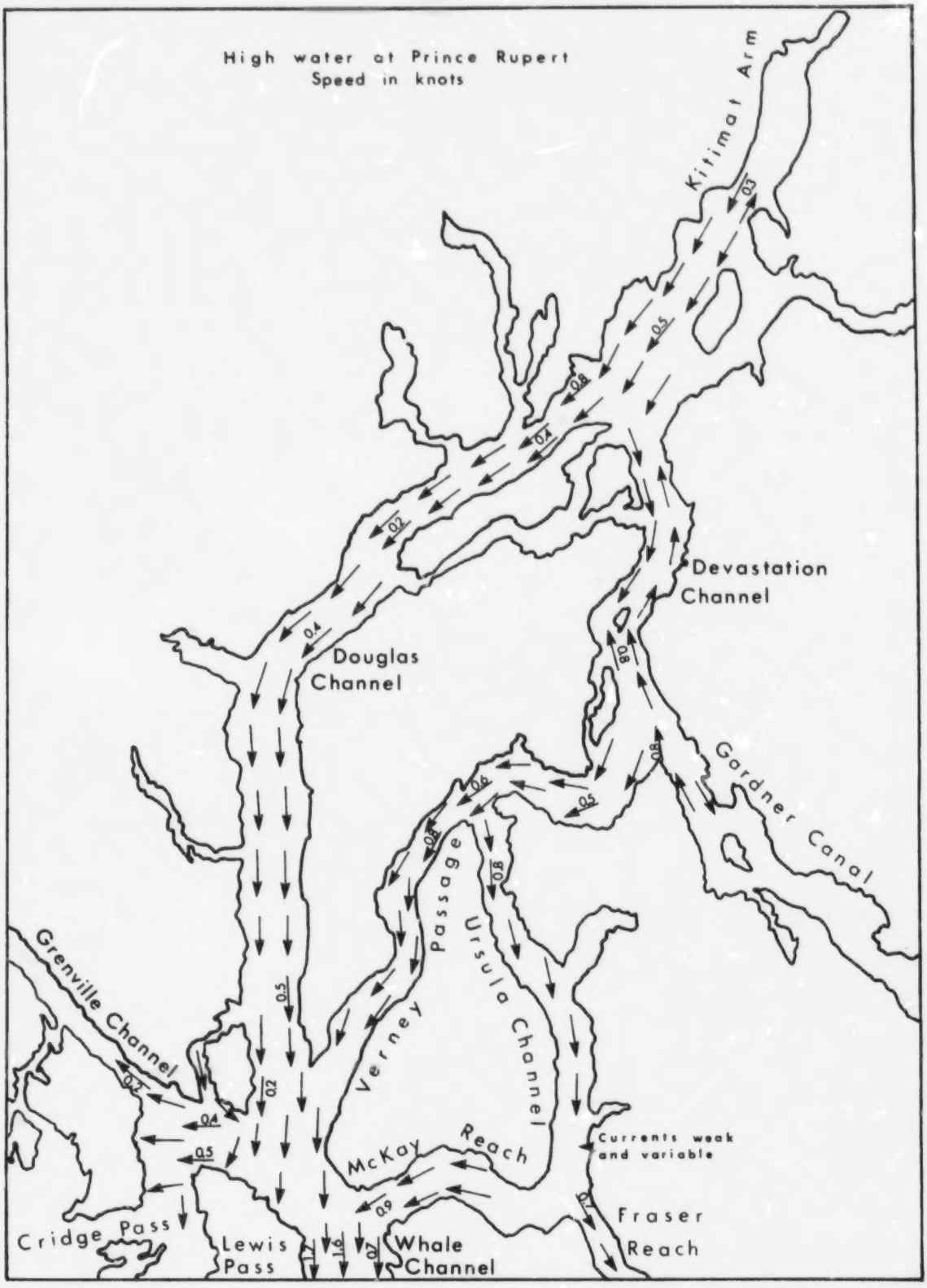
High water at Prince Rupert
Speed in knots
Kitimat Arm
Devastation Channel
Douglas Channel
Gardner Canal
Grenville Channel
Verney Passage
Ursula Channel
McKay Reach
Currents weak and variable
Fraser Reach
Cridge Pass
Lewis Pass
Whale Channel
HW

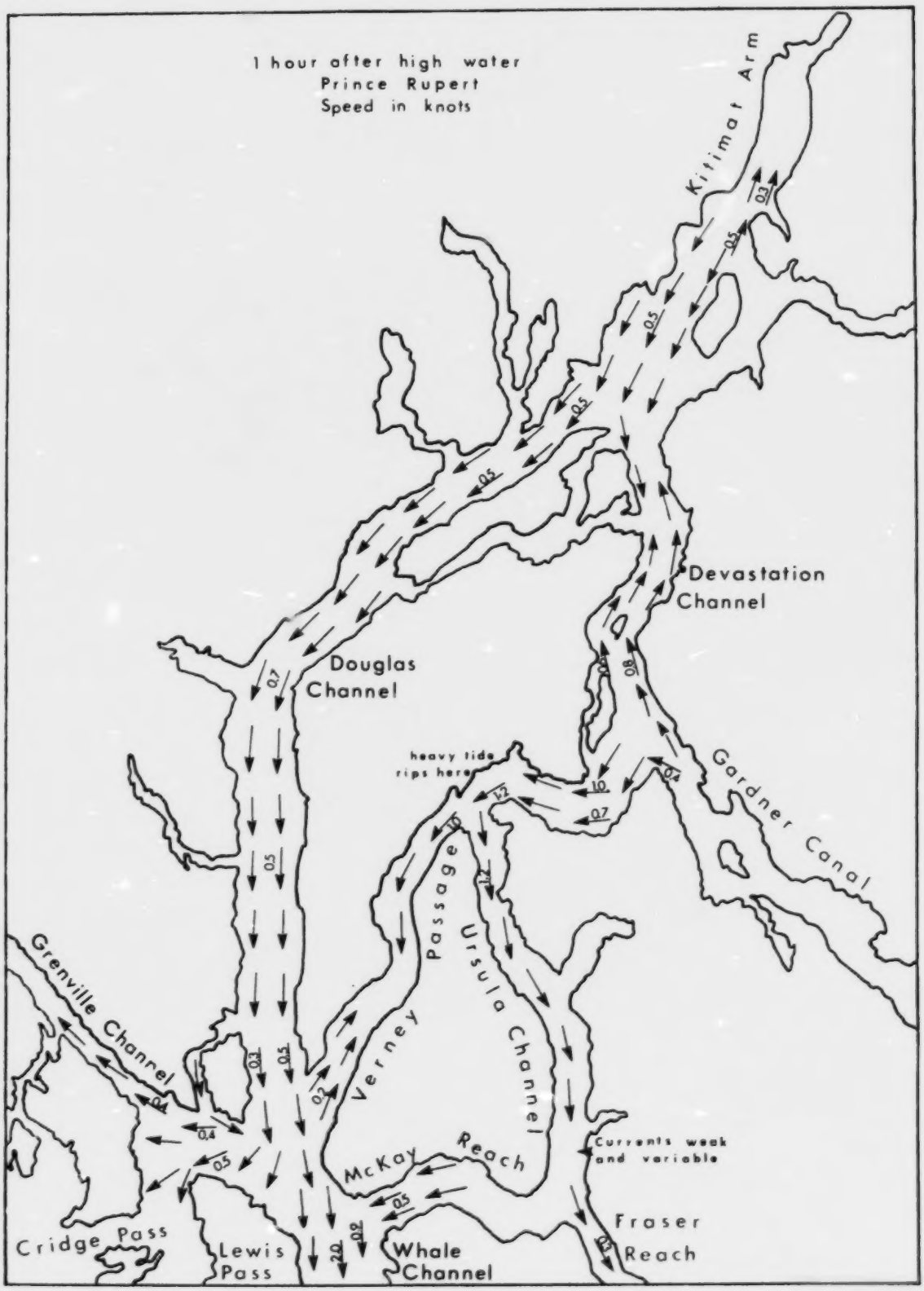
1 hour after high water
Prince Rupert
Speed in knots
Kitimat Arm
Devastation Channel
Douglas Channel
heavy tide rips here
Gardner Canal
Grenville Channel
Verney Passage
Ursula Channel
McKay Reach
Currents weak and variable
Cridge Pass
Lewis Pass
Whale Channel
Fraser Reach

1 A

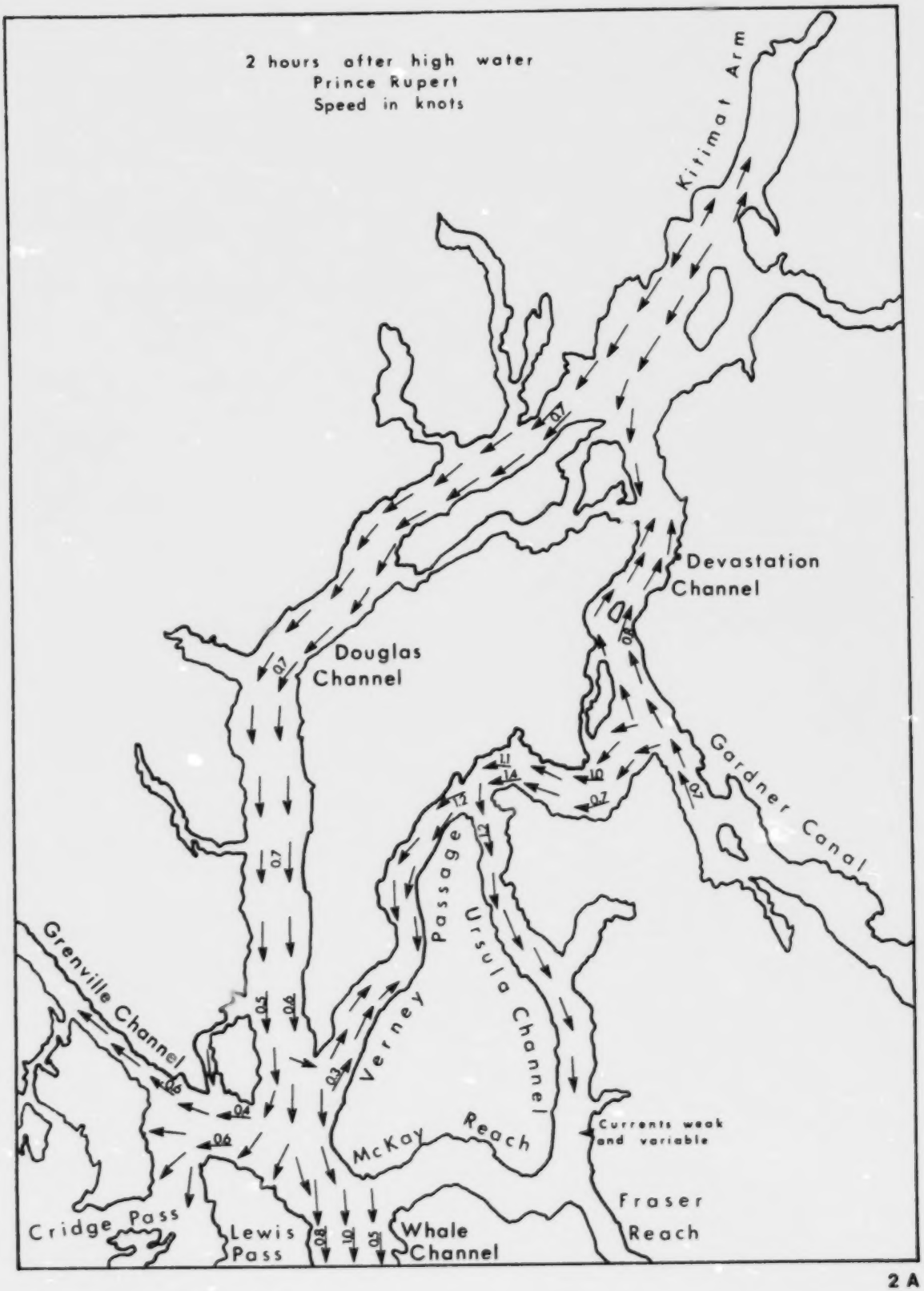
2 hours after high water
Prince Rupert
Speed in knots
Kitimat Arm
Devastation Channel
Douglas Channel
Gardner Canal
Grenville Channel
Verney Passage
Ursula Channel
McKay Reach
Currents weak and variable
Fraser Reach
Cridge Pass
Lewis Pass
Whale Channel

2 A

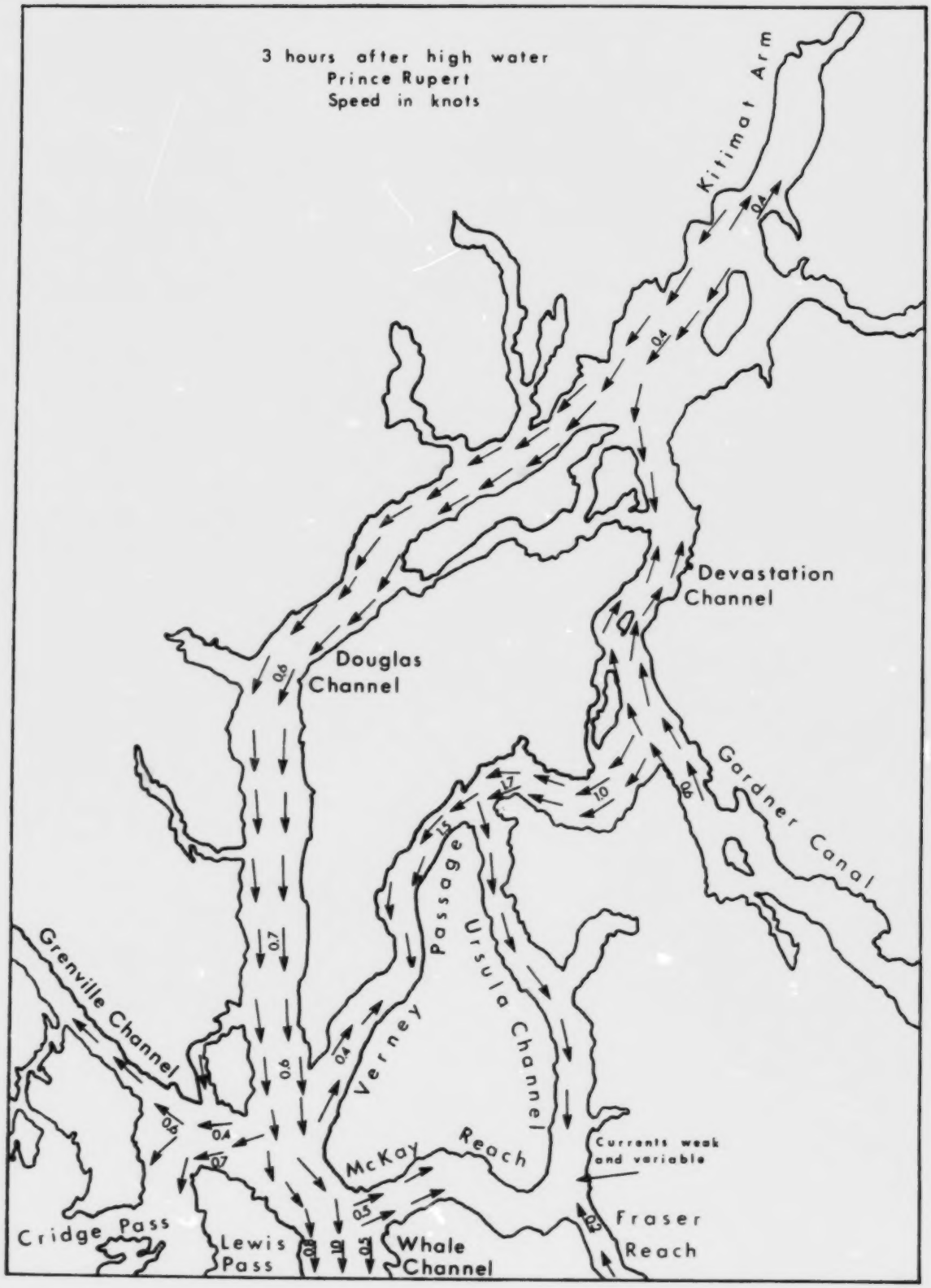
3 hours after high water
Prince Rupert
Speed in knots
Kitimat Arm
Devastation Channel
Douglas Channel
Gardner Canal
Grenville Channel
Verney Passage
Ursula Channel
McKay Reach
Currents weak and variable
Fraser Reach
Cridge Pass
Lewis Pass
Whale Channel
0.4
0.6
0.7
0.9
1.7
1.0
1.5
0.5
0.3

3 A

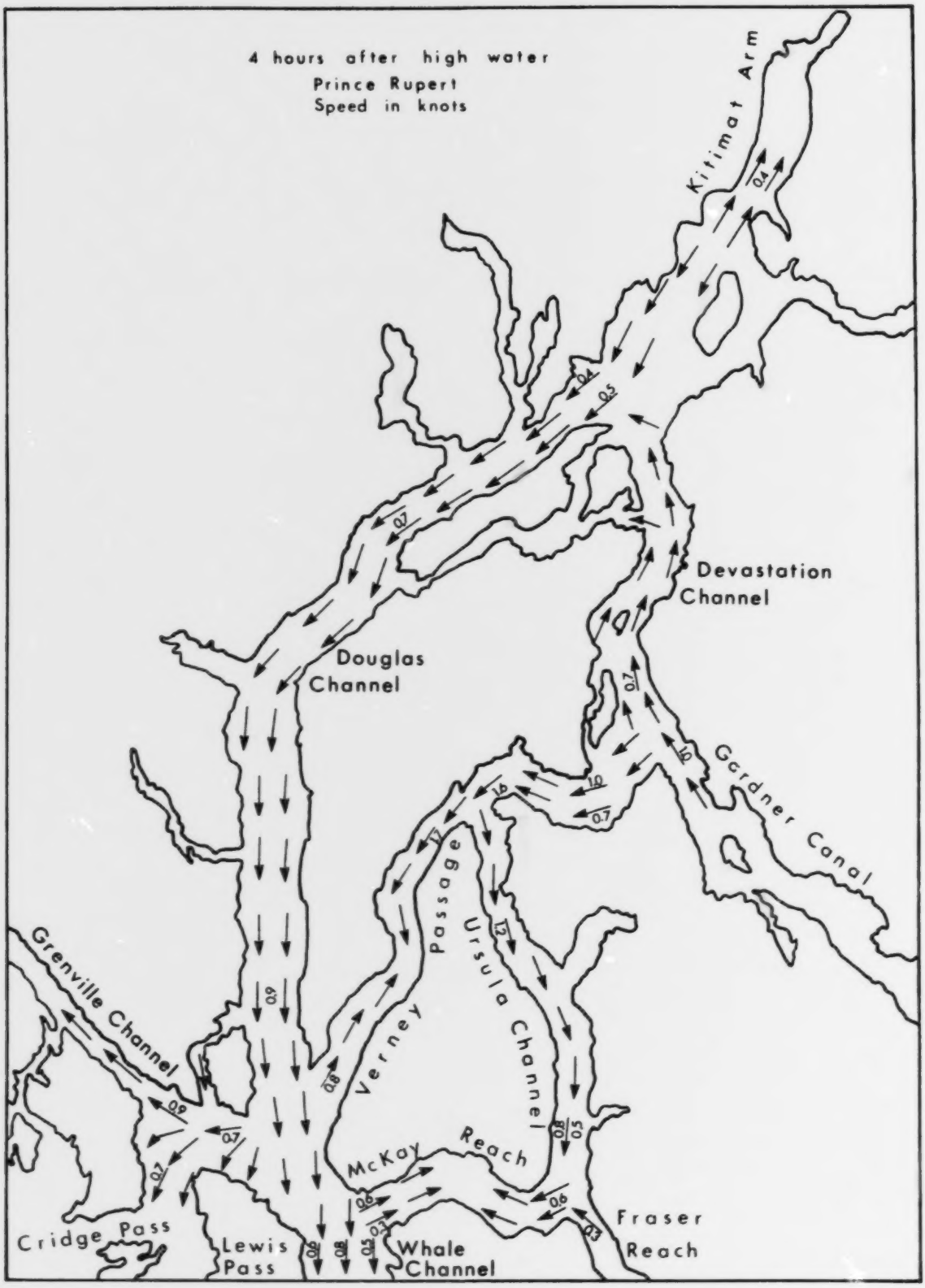
4 hours after high water
Prince Rupert
Speed in knots
Kitimat Arm
Devastation Channel
Douglas Channel
Gardner Canal
Grenville Channel
Verney Passage
Ursula Channel
McKay Reach
Fraser Reach
Cridge Pass
Lewis Pass
Whale Channel

4 A

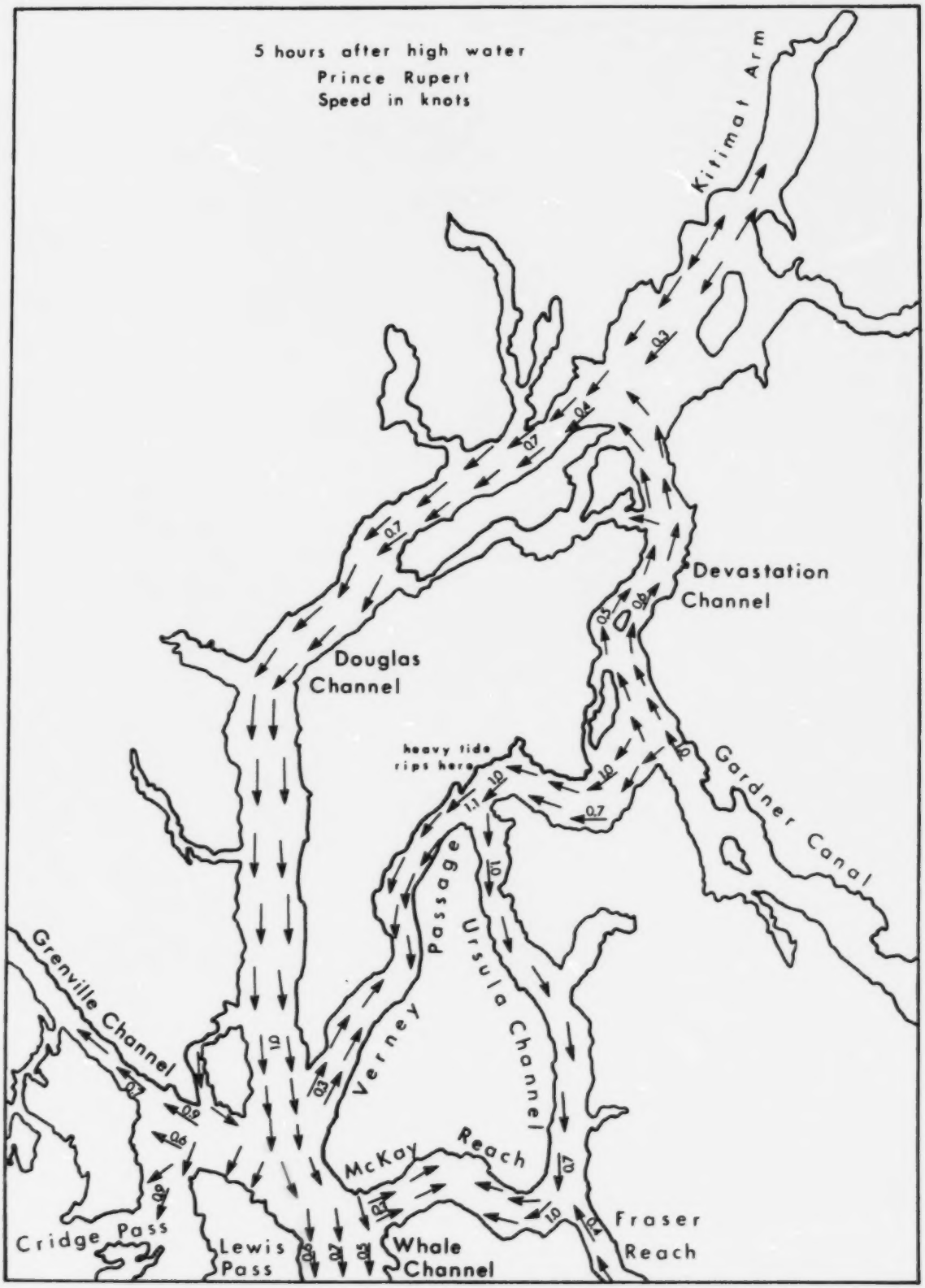
5 hours after high water
Prince Rupert
Speed in knots
Kitimat Arm
Devastation Channel
Douglas Channel
heavy tide rips here
Gardner Canal
Grenville Channel
Verney Passage
Ursula Channel
McKay Reach
Cridge Pass
Lewis Pass
Whale Channel
Fraser Reach

5 A

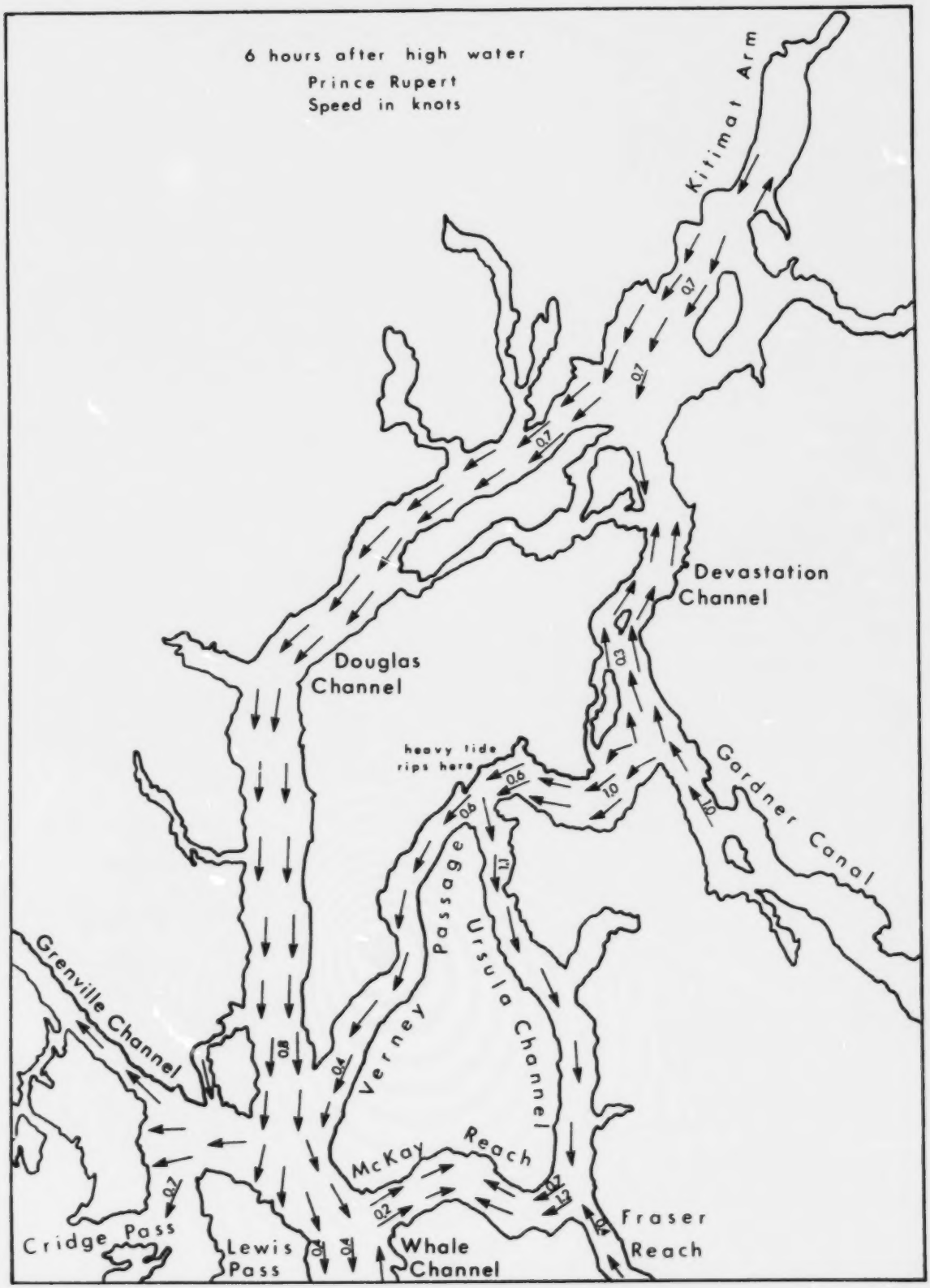
6 hours after high water
Prince Rupert
Speed in knots
Kitimat Arm
Devastation Channel
Douglas Channel
heavy tide rips here
Gardner Canal
Grenville Channel
Verney Passage
Ursula Channel
McKay Reach
Fraser Reach
Cridge Pass
Lewis Pass
Whale Channel

6A

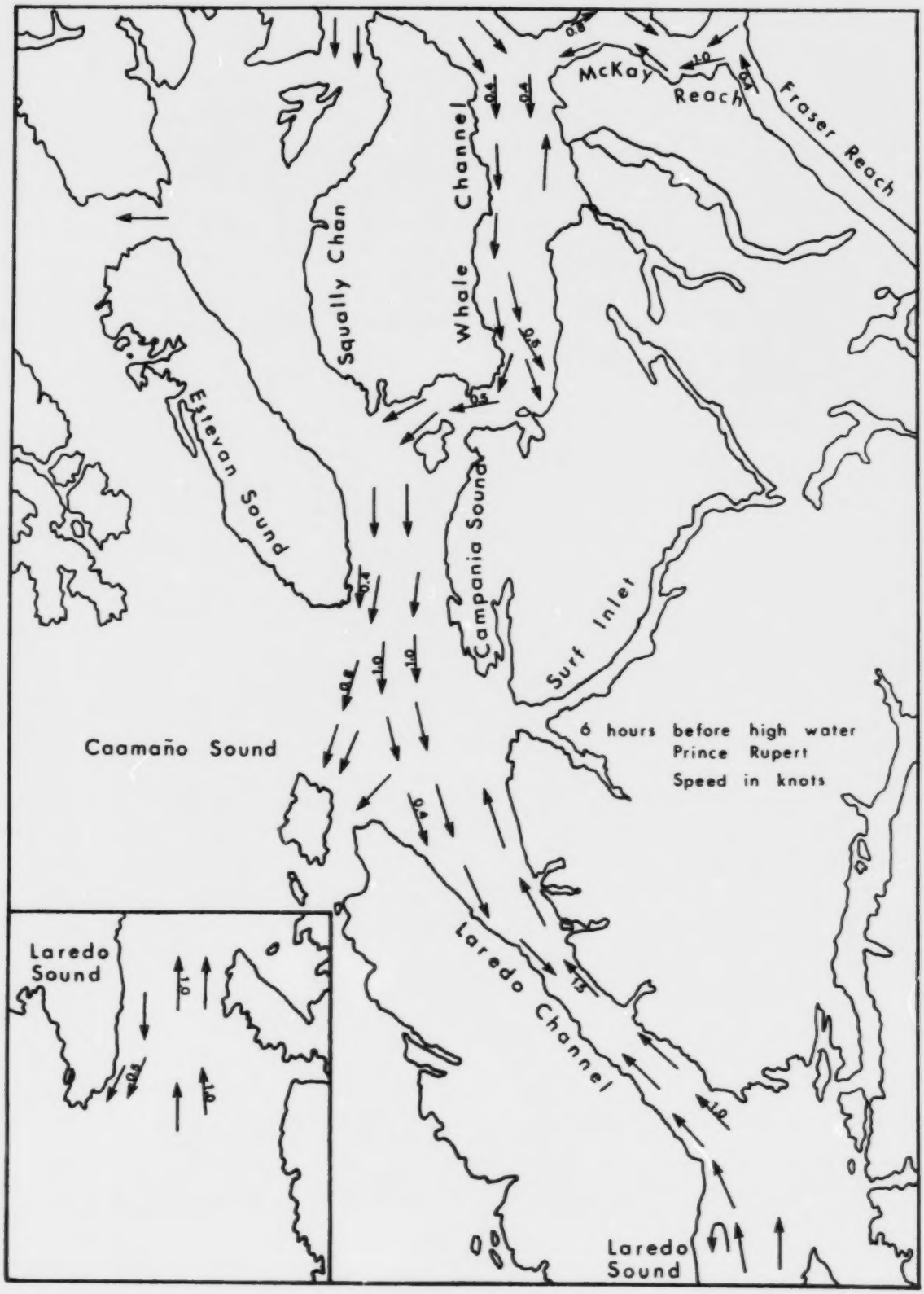
McKay Reach
Fraser Reach
Whale Channel
Squally Chan
Estevan Sound
Campania Sound
Surf Inlet
Caamaño Sound
6 hours before high water
Prince Rupert
Speed in knots
Laredo Channel
Laredo Sound
Laredo Sound

6 B

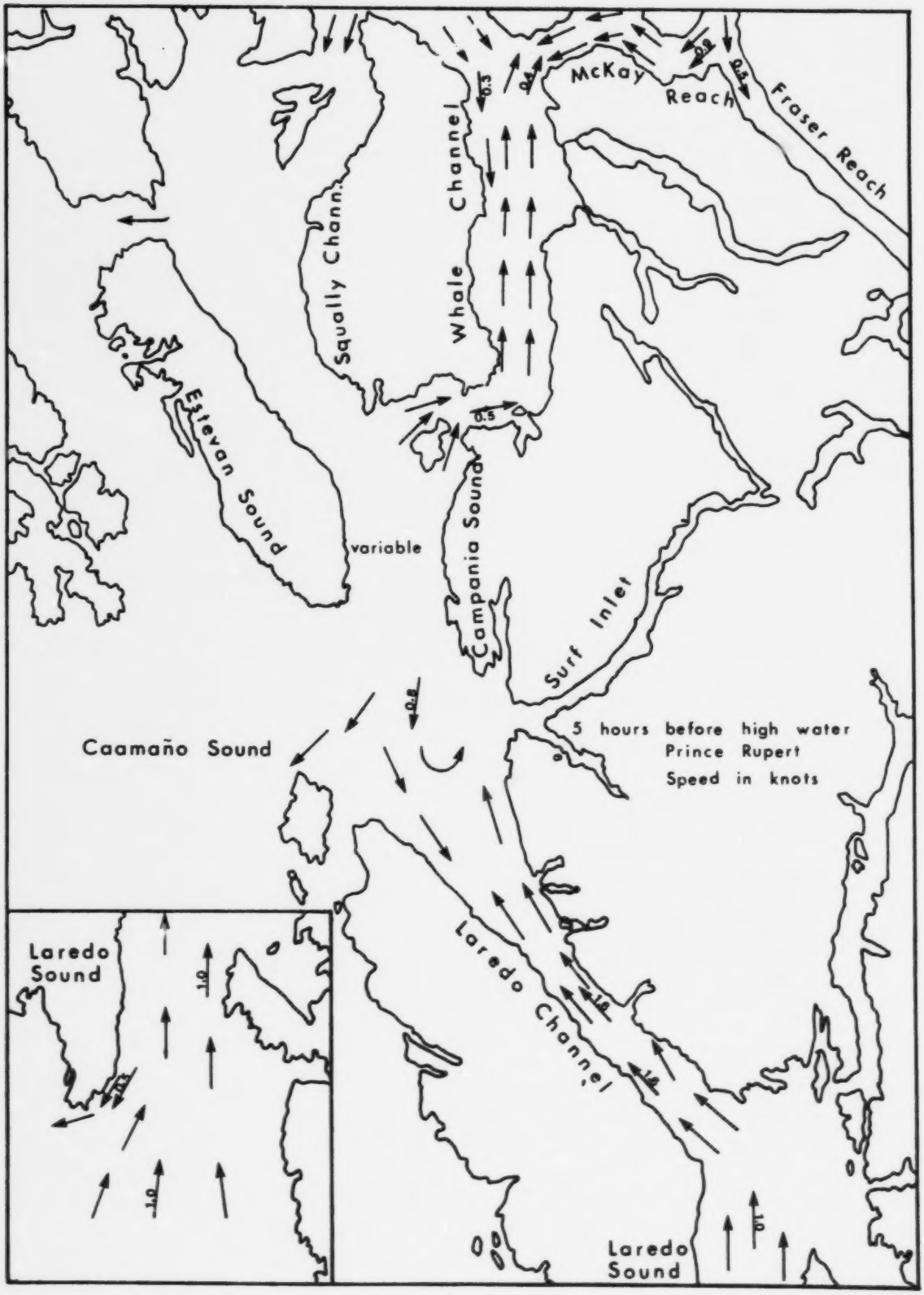
McKay Reach
Fraser Reach
Whale Channel
Squally Chann.
Estevan Sound
Campania Sound
Surf Inlet
variable
Caamaño Sound
5 hours before high water
Prince Rupert
Speed in knots
Laredo Channel
Laredo Sound
Laredo Sound

5B

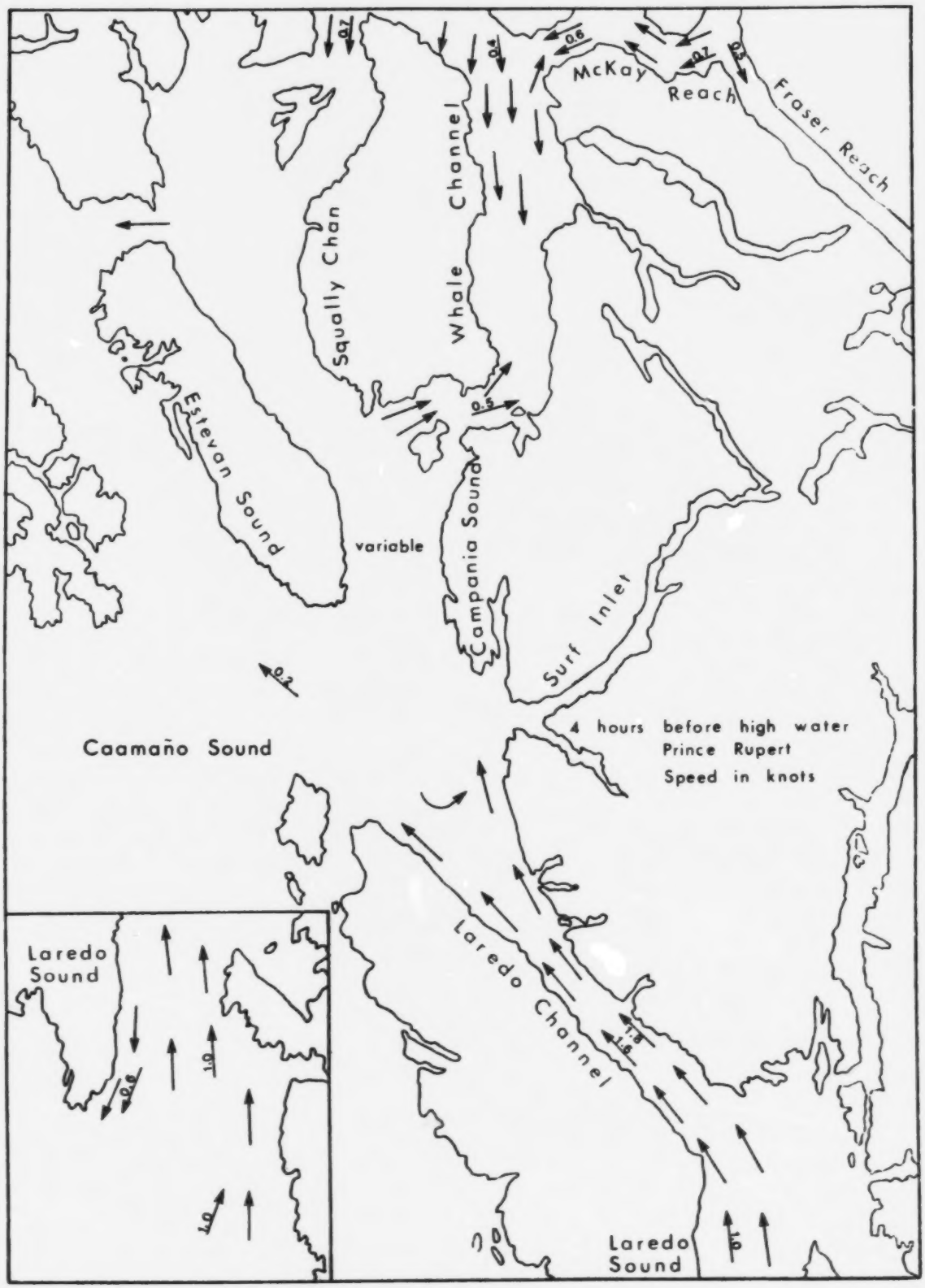
McKay Reach
Fraser Reach
Whale Channel
Squally Chan
Estevan Sound
variable
Campania Sound
Surf Inlet
Caamaño Sound
4 hours before high water
Prince Rupert
Speed in knots
Laredo Channel
Laredo Sound
Laredo Sound

4B

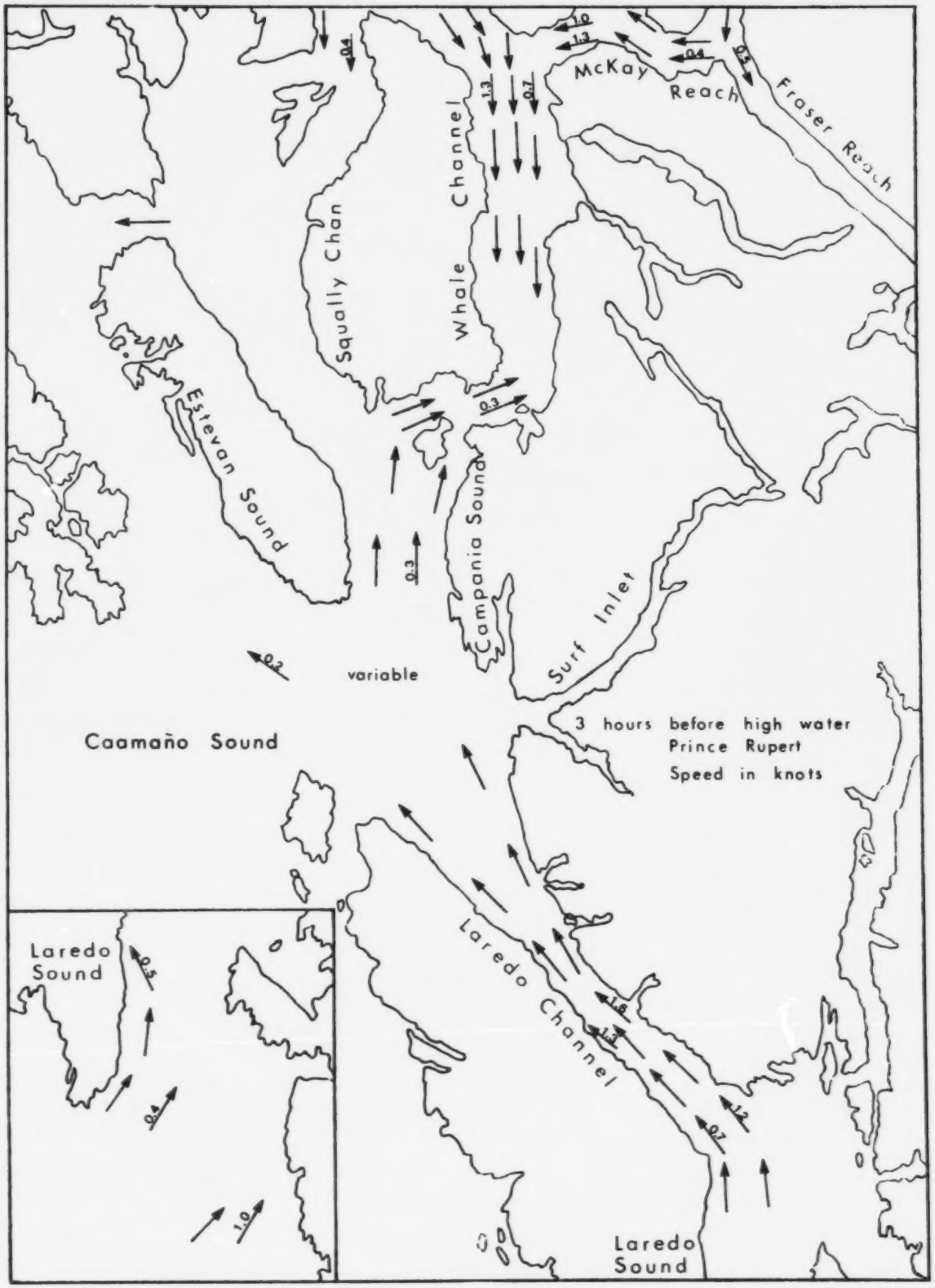
McKay Reach
Fraser Reach
Whale Channel
Squally Chan
Estevan Sound
Campania Sound
Surf Inlet
variable
Caamaño Sound
3 hours before high water
Prince Rupert
Speed in knots
Laredo Channel
Laredo Sound
Laredo Sound

3B

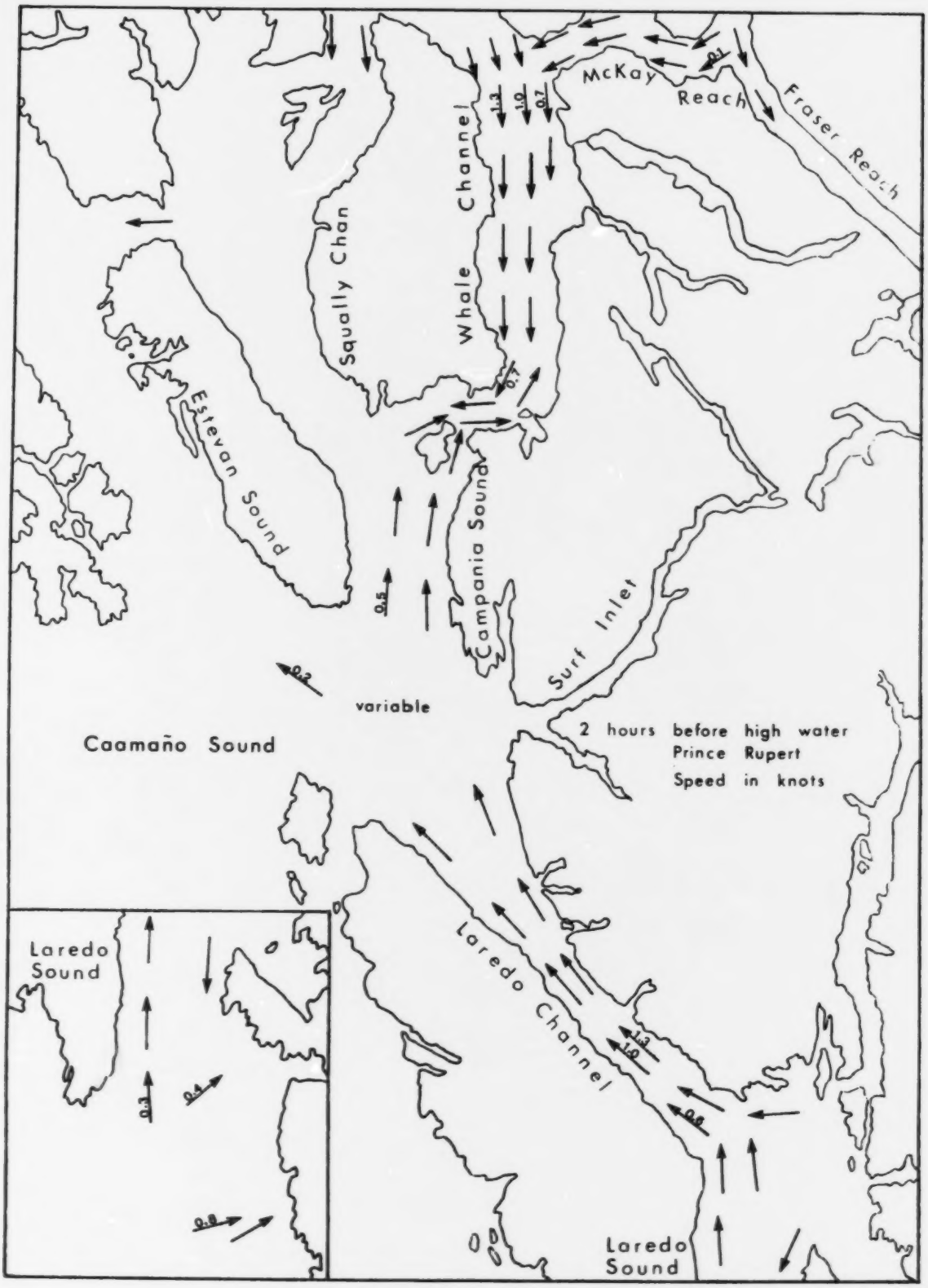
McKay Reach
Fraser Reach
Squally Chan
Whale Channel
Estevan Sound
Campania Sound
Surf Inlet
variable
Caamaño Sound
2 hours before high water
Prince Rupert
Speed in knots
Laredo Sound
Laredo Channel
Laredo Sound

2 B

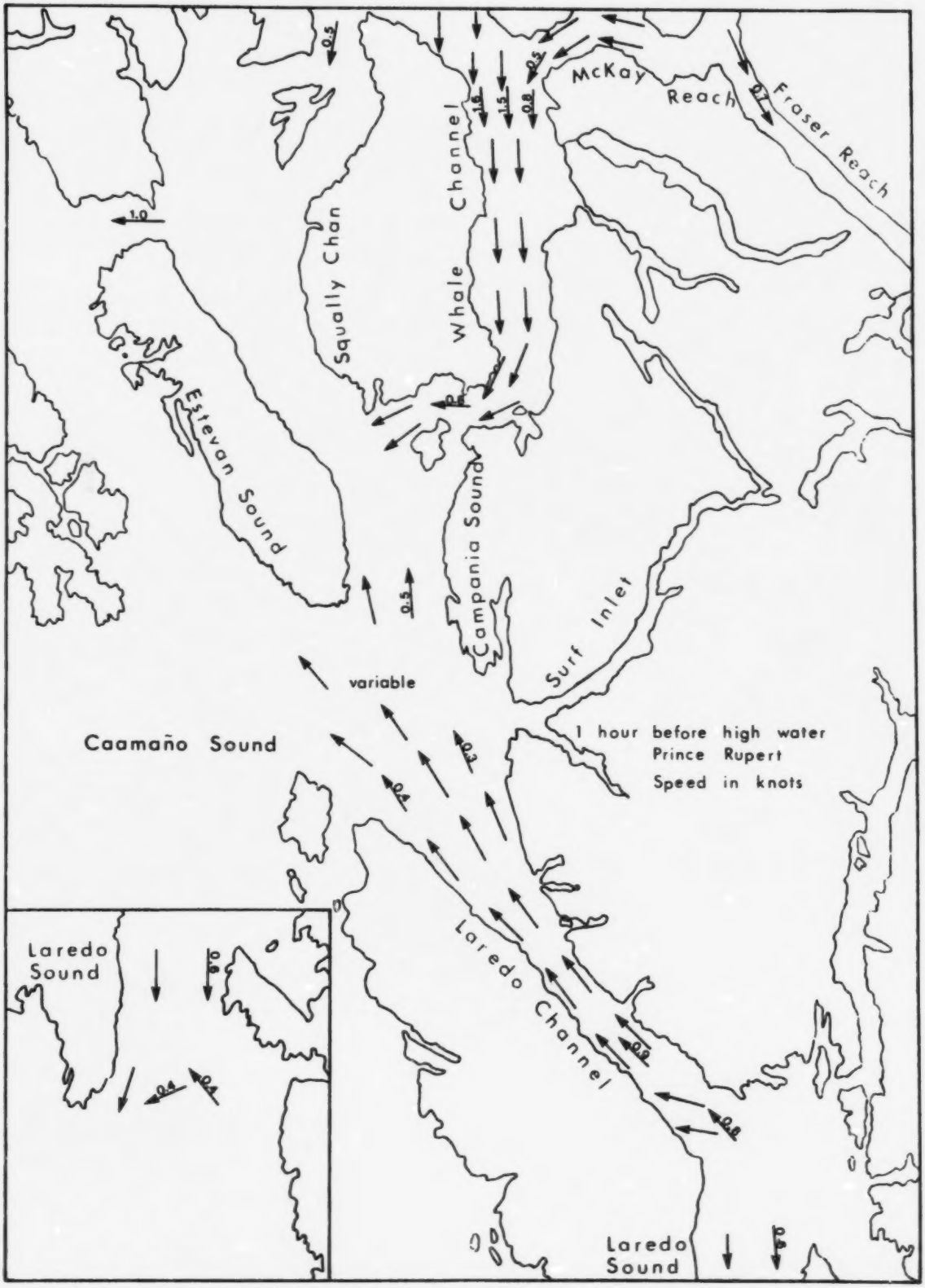
McKay Reach
Fraser Reach
Whale Channel
Squally Chan
Estevan Sound
Campania Sound
Surf Inlet
variable
Caamaño Sound
1 hour before high water
Prince Rupert
Speed in knots
Laredo Sound
Laredo Channel
Laredo Sound

1 B

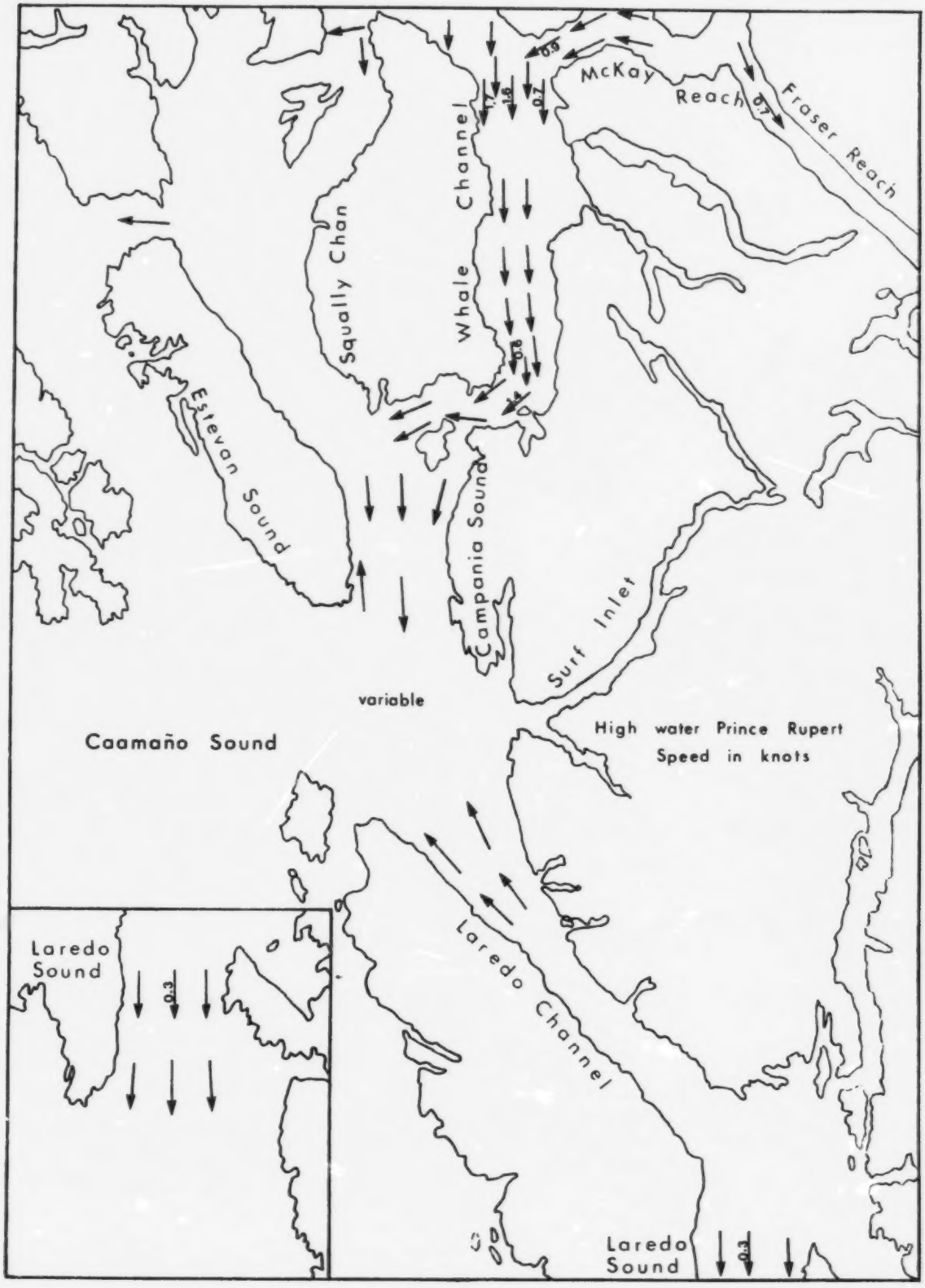
McKay Reach
Fraser Reach
Squally Chan
Whale Channel
Estevan Sound
Campania Sound
Surf Inlet
variable
Caamaño Sound
High water Prince Rupert
Speed in knots
Laredo Sound
Laredo Channel
Laredo Sound
HW

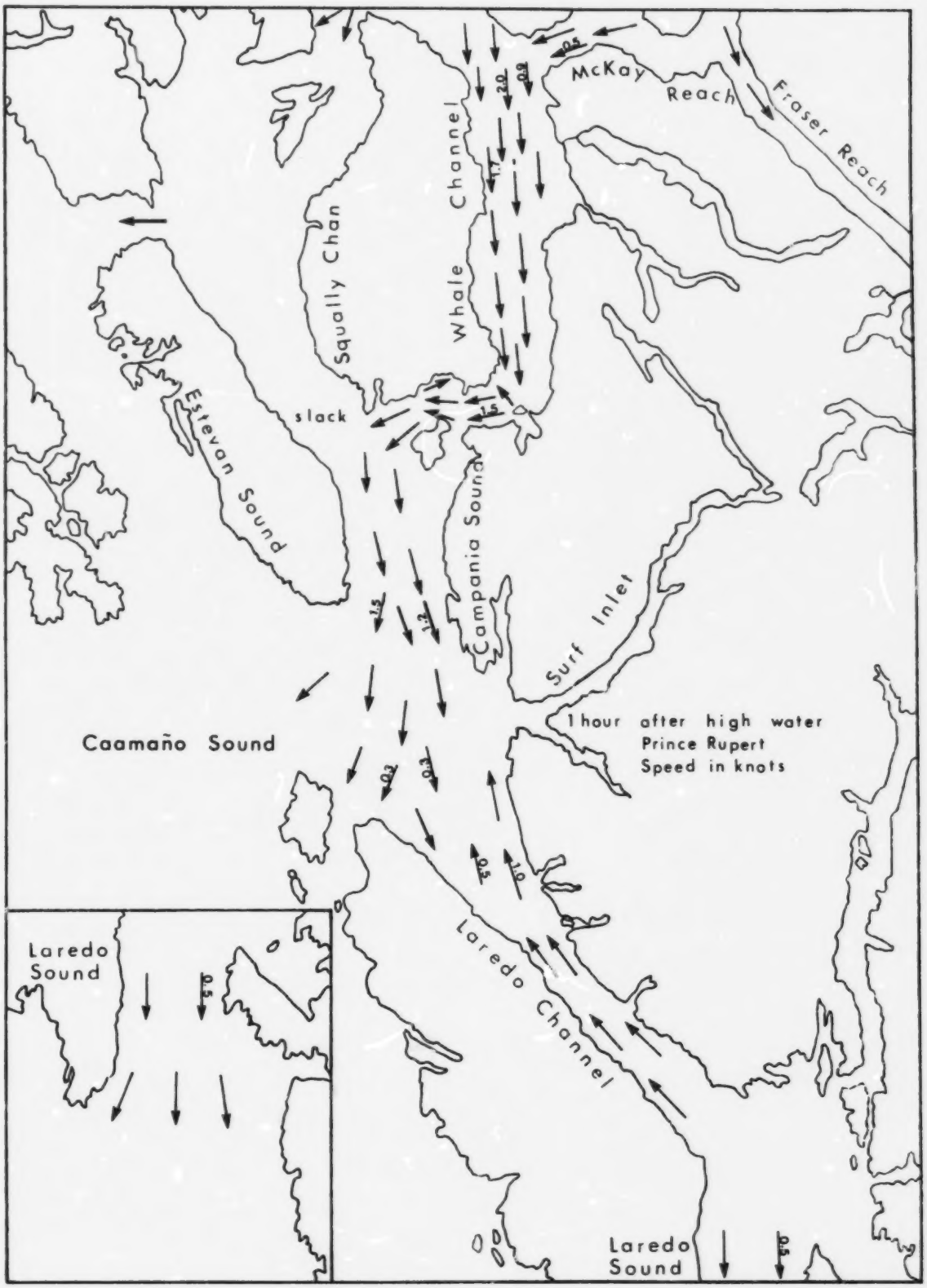
McKay Reach
Fraser Reach
Whale Channel
Squally Chan
Estevan Sound
slack
Campania Sound
Surf Inlet
Caamaño Sound
1 hour after high water
Prince Rupert
Speed in knots
Laredo Channel
Laredo Sound
Laredo Sound

1A

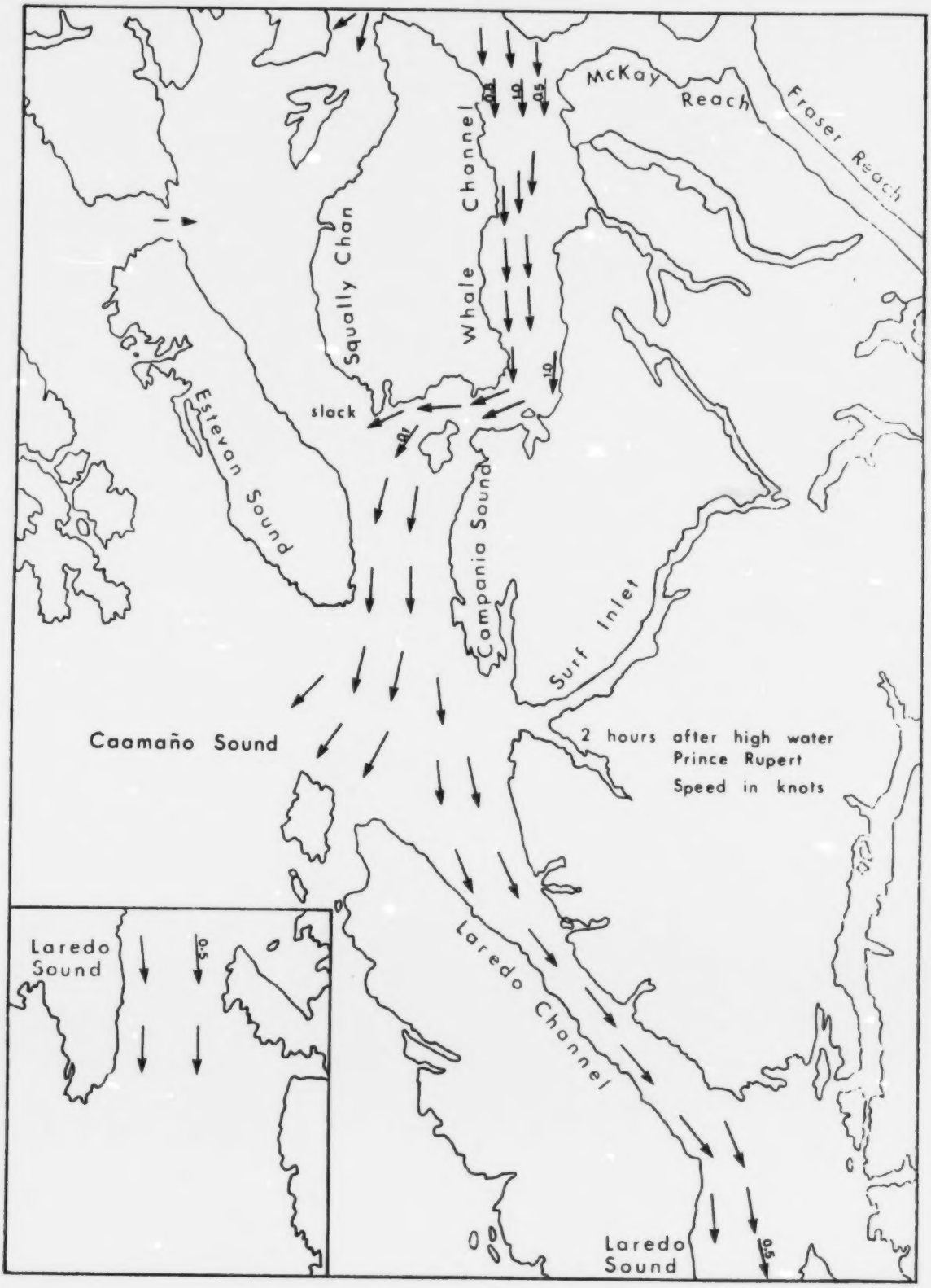
McKay Reach
Fraser Reach
Whale Channel
Squally Chan
Estevan Sound
slack
Campania Sound
Surf Inlet
Caamaño Sound
2 hours after high water
Prince Rupert
Speed in knots
Laredo Channel
Laredo Sound
Laredo Sound
0.3
1.0
0.5
1.0
0.1
0.5
0.5

2A

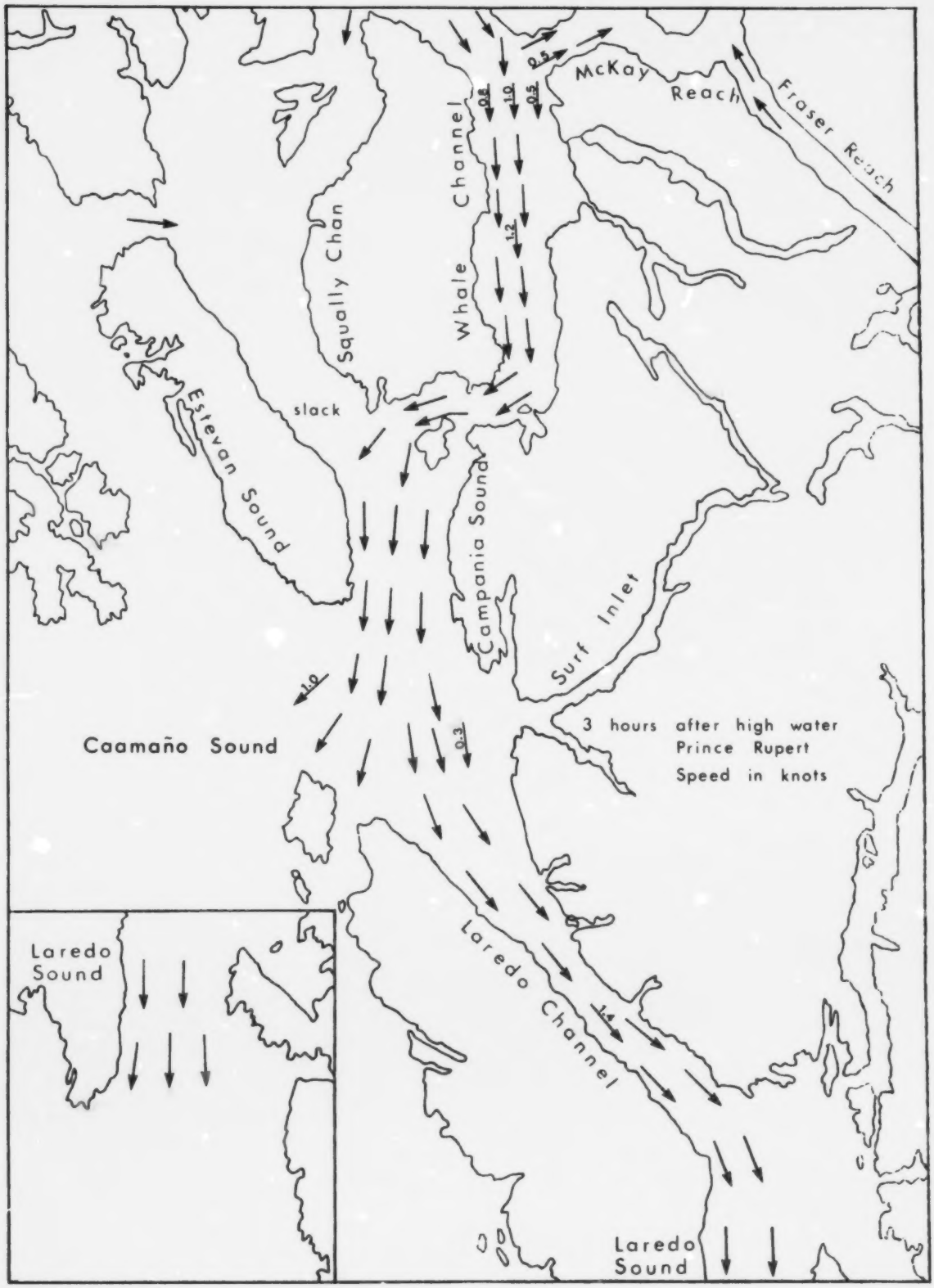
McKay Reach
Fraser Reach
Whale Channel
Squally Chan
Estevan Sound
slack
Campania Sound
Surf Inlet
Caamaño Sound
3 hours after high water
Prince Rupert
Speed in knots
Laredo Channel
Laredo Sound
Laredo Sound
0.5
0.8
1.0
0.5
1.2
1.0
0.3
1.4

3A

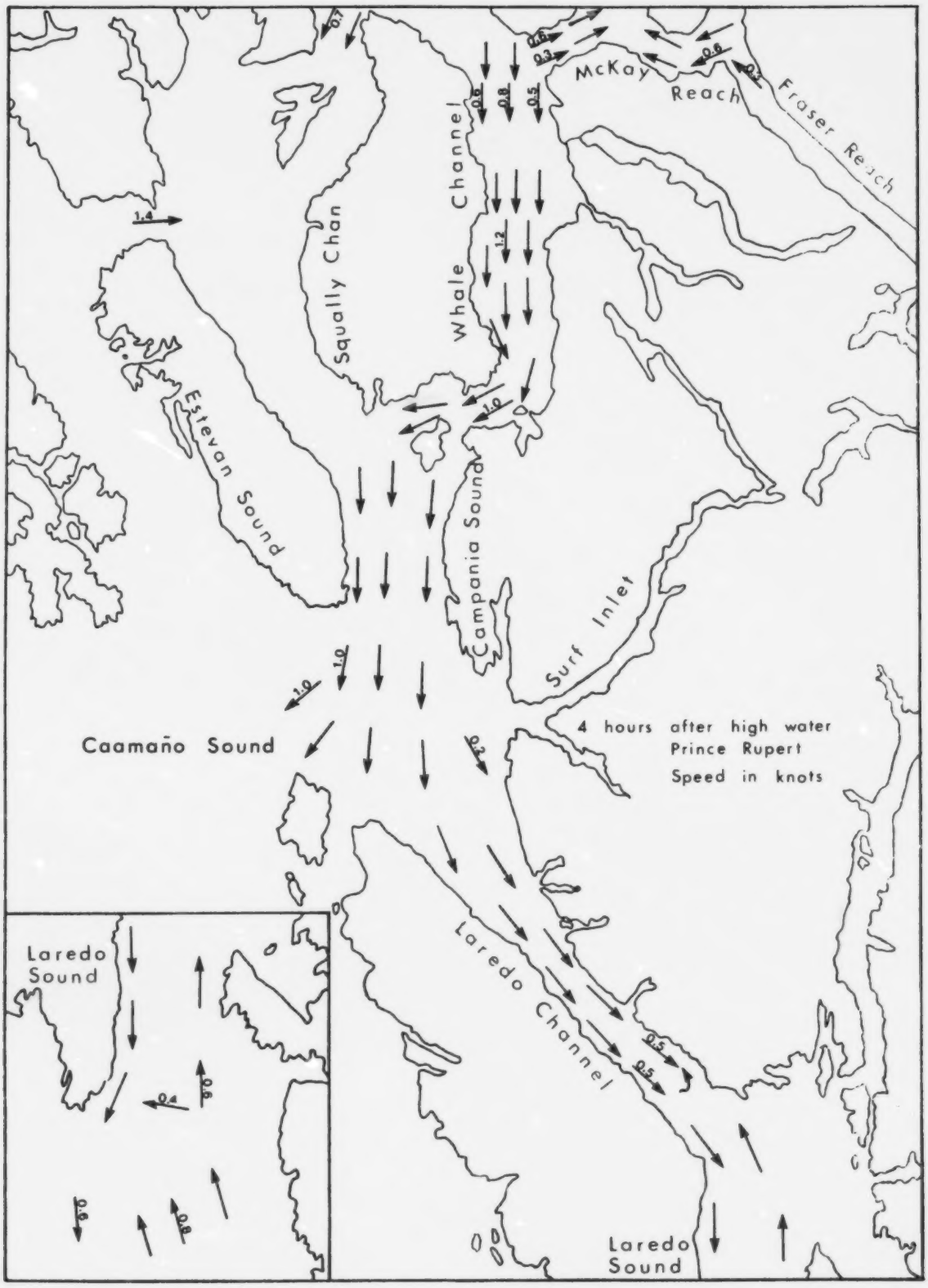
McKay Reach
Fraser Reach
Whale Channel
Squally Chan
Estevan Sound
Campania Sound
Surf Inlet
Caamaño Sound
Laredo Channel
Laredo Sound
Laredo Sound
4 hours after high water
Prince Rupert
Speed in knots

4A

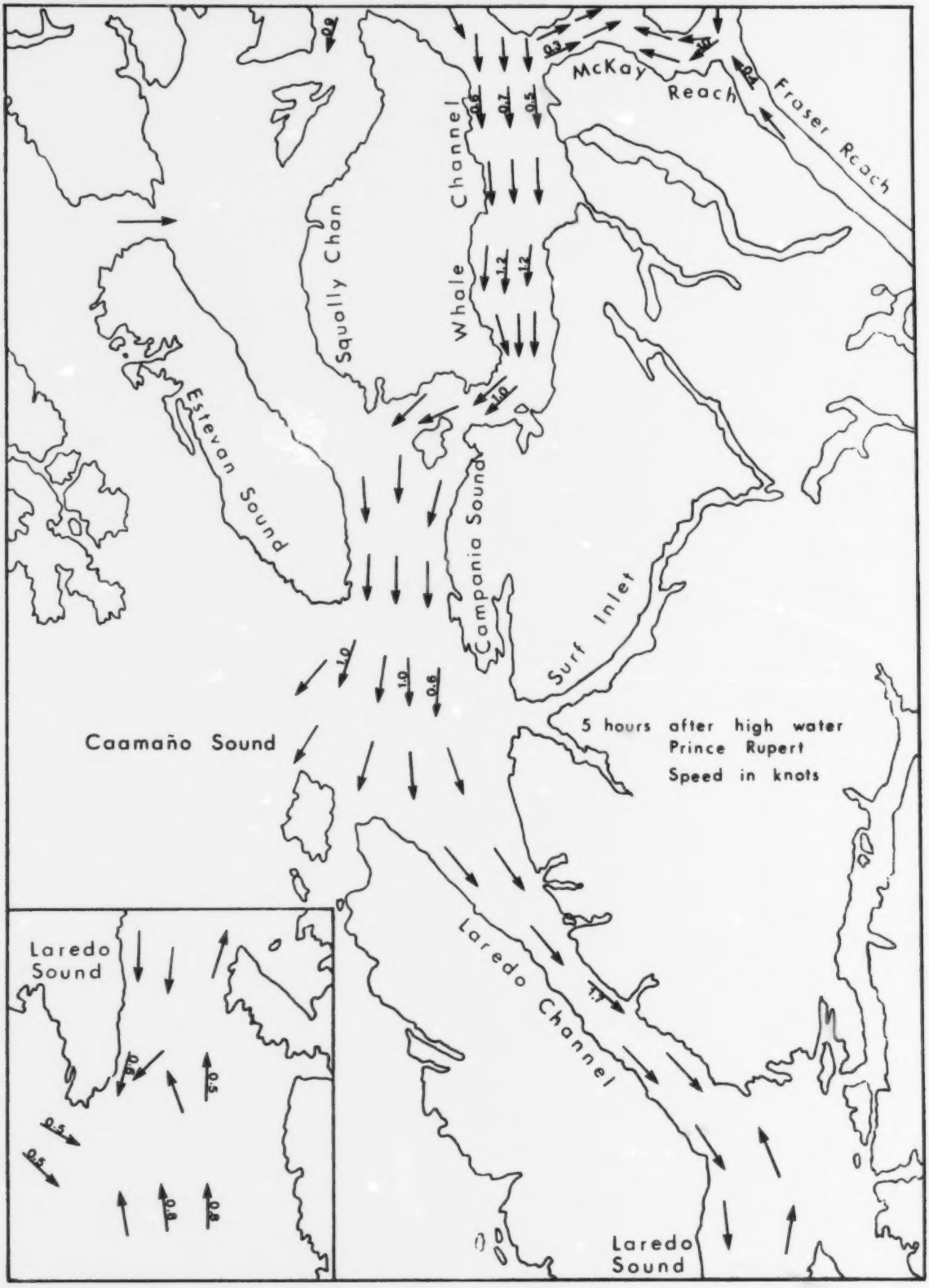
McKay Reach
Fraser Reach
Whale Channel
Squally Chan
Estevan Sound
Campania Sound
Surf Inlet
Caamaño Sound
5 hours after high water
Prince Rupert
Speed in knots
Laredo Channel
Laredo Sound
Laredo Sound

5A

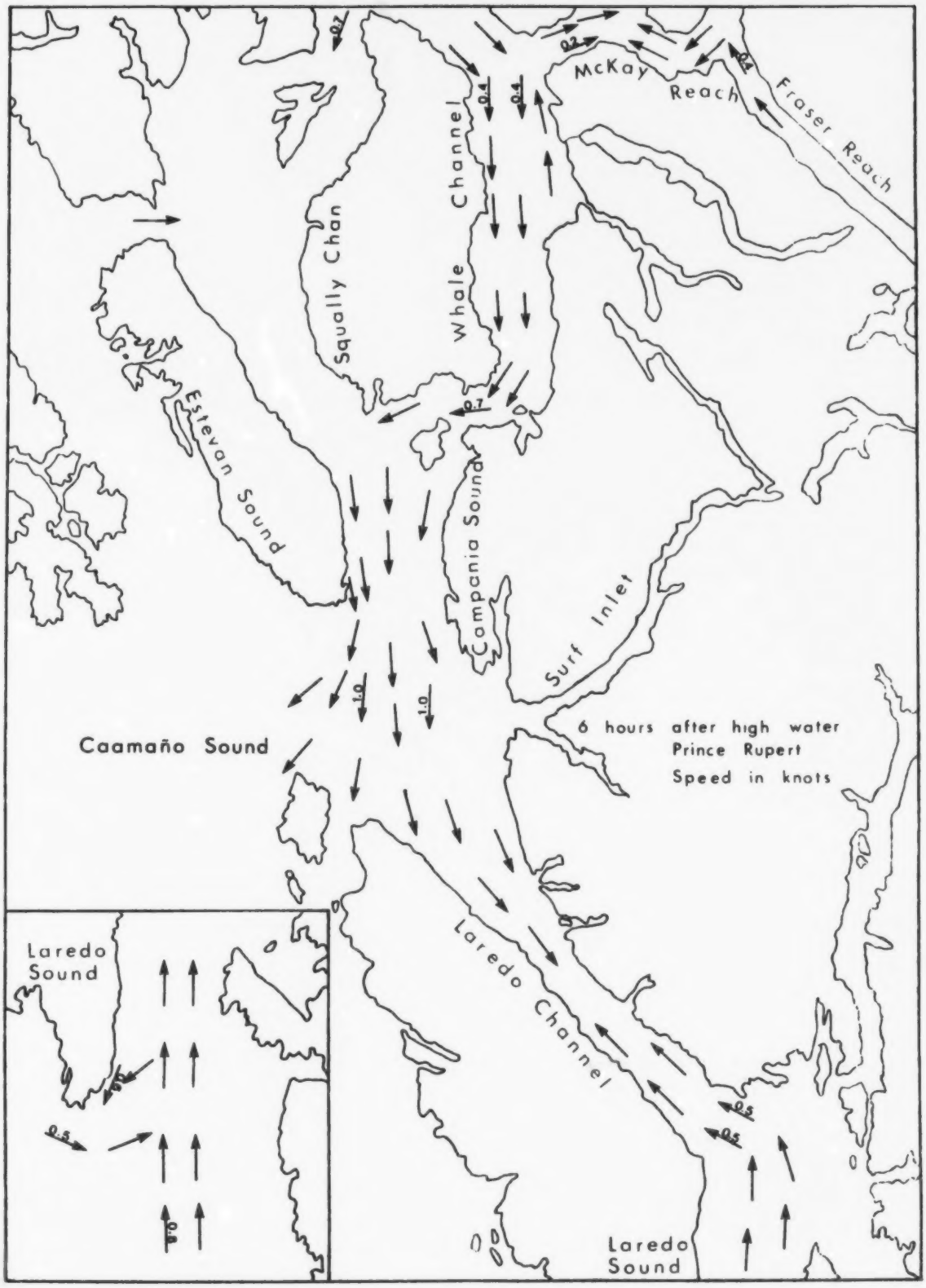
McKay Reach
Fraser Reach
Whale Channel
Squally Chan
Estevan Sound
Campania Sound
Surf Inlet
Caamaño Sound
Laredo Channel
Laredo Sound
Laredo Sound
6 hours after high water
Prince Rupert
Speed in knots
0.7
0.2
0.4
0.4
0.4
0.7
1.0
1.0
0.5
0.5
0.5
0.5

6A

CHARACTÈRE-CHIMIQUE DE L'EAU DANS LE SYSTÈME KITIMAT FJORD

R.W. Macdonald, W.J. Cretney, C.S. Wong
Institute of Ocean Sciences, Sidney, B.C.

P. Erickson
Seakem Oceanography Limited, Sidney, B.C.

RÉSUMÉ

L'eau de mer, phosphate, nitrate, silicate, et oxygène dissout ensemble avec la salinité et la température, furent mesurer pendant quatre croissières, durant quelque deux ans. Un changement dans ces domaines fût employé pour inférer le mouvement de l'eau. Le système du passage Kitimat, fût dynamique, avec deux remplacements annuel d'eau de fond et d'une grande intrusion d'eau des côtes marines, aux profondeurs intermédiares - et particulièrement en hiver.

Macdonald, R.W., W.J. Cretney, and C.S. Wong, 1983. Chemical characteristic of water in the Kitimat fjord system. Can. Tech. Rep. Hydrogr. Ocean Sci. 18, 66-87.

Mot-clés: circulation, eau de fond, fjord, inclination, Kitimat, mélanger, nitrate, oxygène, phosphate, renouvellement, salinité, silicate, température

CHEMICAL CHARACTERISTICS OF WATER IN THE KITIMAT FJORD SYSTEM

R.W. Macdonald, W.J. Cretney, C.S. Wong
Institute of Ocean Sciences, Sidney, B.C.

P. Erickson
Seakem Oceanography Limited, Sidney, B.C.

ABSTRACT

Sea water properties of dissolved phosphate, nitrate, silicate, and oxygen together with salinity and temperature were measured during four cruises spanning two years. Changes in these properties were used to infer water movements. The Kitimat fjord system was found to be dynamic with two annual replacements of bottom water and large intrusions of coastal water at intermediate depth, particularly in winter.

Macdonald, R.W., W.J. Cretney, C.S. Wong and P. Erickson. 1983. Chemical characteristics of water in the Kitimat fjord sytem. Can. Tech. Rep. Hydrogr. Ocean Sci. 18, 66-87.

Keywords: bottomwater, circulation, fjord, Kitimat, mixing, nitrate, oxygen, phosphate, renewal, salinity, temperature, upwelling

INTRODUCTION

Four oceanographic cruises were conducted in the Kitimat fjord system from February, 1977 to February 1979. The reactive nutrients (silicate, orthophosphate, and nitrate plus nitrite) were measured along with salinity, temperature and oxygen. This paper interprets these data with respect to the sea water properties and circulation within the system. The general characteristics of the Kitimat fjord system have already been reviewed and compilations of the raw data are available (Macdonald et al, 1983a, b, 1978).

METHODS

In this paper the four cruises have been referred to according to month and year; Feb-77, Jun-78, Oct-78 and Feb-79. Because the first cruise (Feb-77) was a preliminary investigation, some differences between it and the three later cruises occurred. Sampling was carried out from the C.S.S. Parizeau for the first cruise and from the M.V. Sea Lion for the others. Station locations for the 1977 cruise differed (Fig. 1), and nutrient samples were frozen and returned to the shore based laboratory for determination. On board analysis was performed with an Auto-Analyzer II within a few hours of sampling during the later cruises.

Nutrient concentrations were determined by standard Technicon Industrial Methods, details of which are available elsewhere (Macdonald et al, 1983). The precision of analysis was generally about 2% (2σ) and accuracy, better than 5% (2σ). A slight deterioration ($\sim$1%) in precision and accuracy may have resulted in the frozen samples (Macdonald & McLaughlin, 1983).

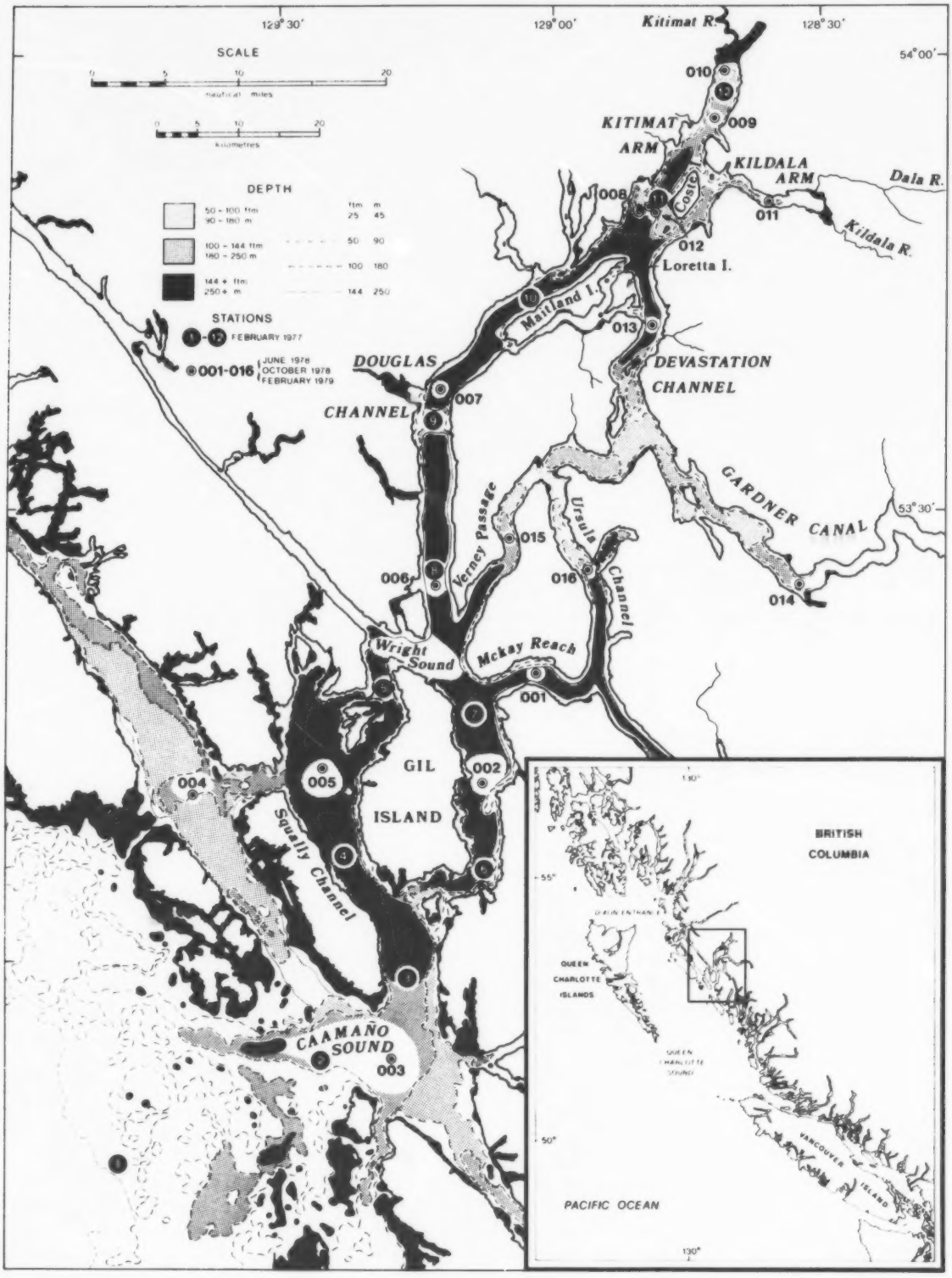

Fig. 1. Study area and station locations.

Oxygen was measured by the micro-Winkler technique (accuracy 0.9 mmol m^{-3}), salinity with a Hytech model 621 induction salinometer (accuracy ±0.02 °/oo), and temperatures with protected and unprotected reversing thermometers (accuracy ±0.02 C°).

Nutrient ternary diagrams were constructed to assist interpretation. For this purpose, phosphate concentration was multiplied by 11.4, (the approximate ratio of silicate to phosphate) to improve display, and each nutrient was calculated as a percent of the total, all concentration units being mmol m^{-3}). These diagrams allowed a quick evaluation of composition changes. Conventional techniques such as nutrient-salinity or nutrient-temperature plots, longitudinal sections and vertical profiles were used to examine trends in absolute concentrations.

The composition of nutrients as shown on the ternary plot is represented on longitudinal sections (Figs. 4, 10, 14 and 18) in the following manner. A convenient arbitrary reference composition (silicate: nitrate: 11.4 x phosphate = 47.2: 26.4: 26.4) is selected. The changes in the silicate and nitrate, both relative to phosphate, between the reference composition and other nutrient compositions are calculated. Arrows are then drawn on each datum in the longitudinal sections such that the x and y projections are proportional to these changes. An increase in silicate concentration relative to the phosphate concentration is denoted by an arrow pointing to the right, an increase in nitrate concentration relative to phosphate concentration is denoted by an arrow pointing to the right, an increase in nitrate concentration relative to phosphate concentration, by an arrow pointing upwards.

RESULTS AND DISCUSSION

Although the February 1977 cruise is chronologically first, it is too far removed in time to provide continuity with the other cruises. It does, however, provide a valuable comparison with the other winter cruise and will be discussed in that light later.

CRUISE JUN-78

Figure 2 is a plot of salinity versus temperature. Several numbered regions are evident and their location is shown also on the ternary plot (Fig. 3) and the longitudinal section (Fig. 4).

Region 1, the surface layer, was characterized by reduced salinities and elevated temperatures. Nutrient and oxygen data suggested the sub-divisions marked on Figure 4. Region 1A, the top 5-10 m, was separated from deeper water by a sharp pycnocline. Dilution by river water was evident (Fig. 3) as a silicate addition that was particularly strong at stations in Kitimat and Kildala Arms (008, 009, 010, 011). At these stations salinities above the pycnocline were from 3 to 8 °/oo. The nutrient composition (mmol m^{-3}) of river water (Kitimat) during the cruise was estimated to be: phosphate 0.1-0.2, silicate 30-40, and nitrate 0-2. For the surface water, silicate enrichment was accompanied by nitrate depletion, probably a result of dilution by low-nitrate river water mixed with sea water below about 20 m (20-25 mmol m^{-3}), and biological removal of nitrate in the euphotic zone. Compared to the

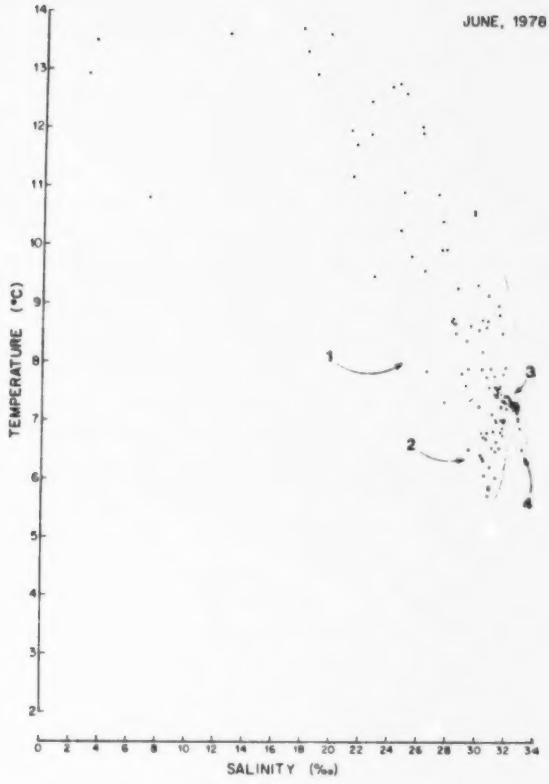

Fig. 2. Scatter plot of temperature versus salinity for samples collected during Jun-78.

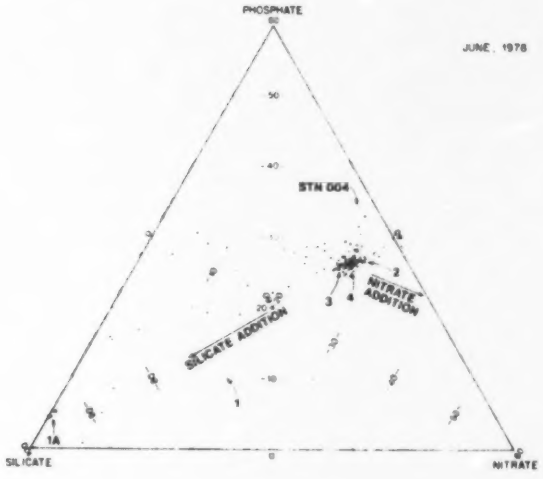

Fig. 3. Ternary plot for phosphate, silicate and nitrate, Jun-78. Phosphate was multiplied by 11.4 and all nutrients calculated as a percent of total. Numbers refer to regions on the longitudinal section (Fig. 4).

reference composition, region 1A water showed strong silicate enrichment and nitrate depletion relative to phosphate (arrows in Fig. 4). The character of the surface water changed from estuarine to oceanic between station 006 (Douglas Channel) and station 005 (Squally Channel). Here the salinity increased from 19 to 28 °/oo with an accompanying decrease in silicate enrichment. Region 1B (Fig. 4) was characterized by total depletion of silicate and by oxygen supersaturations of 110-150%. Nitrate concentration was also found to be at or near zero. One Region 1B location was found beneath the pycnocline at Kitimat Arm and another in the surface layer at stations 1 and 2. Pickard (1961) has referred to the sub-pycnocline O_2 supersaturation and the obvious cause: biological production. In Kitimat Arm relative silicate depletion and nitrate enhancements were evident well below the layer in which O_2 supersaturation was detected. This may have been caused by the relative rate at which nutrients were recycled, silicate being lost to the upper layer by settling of diatoms or diatom rich fecal pellets. Region 1C, which deepens seaward of station 006, was richer in silicate toward the head of the inlet, but did not have the large silicate additions evident at the surface.

The ternary plot (Fig. 3) shows biological growth in region 1 as points displaced toward or falling on the zero nitrate line. Nitrate is apparently depleted faster than the other two nutrients. However, station 003 and particularly station 004 appear to be more depleted in silicate than nitrate (Figs. 3, 4), apparently a characteristic of non-estuarine coastal water. Further evidence for this is found in the results of other cruises.

Region 2, the remnant of winter cooling, was characterized by a temperature minimum at 20-30 m. (A similar tongue of cold water at the head of a fjord has been studied by Ebbesmeyer et al (1975) and with more data their model could be applied to Kitimat Arm to yield mixing parameters.) This type of water was not found seaward of station 006, an indication of downward mixing or advection. The temperature minimum was lower toward the head of the inlet; 5.71°C at station 010 and 6.81°C at station 006. The S-T plot (Fig. 2) clearly showed water which had been cooled, and this type of water extended to the bottom of Gardner Basin (Fig. 4). During this cruise (June) the water density at the bottom of Gardner Basin (σ_t = 25.0) was lower than that of the water at the entrance sill (σ_t = 25.5). Although renewal of bottom water in Gardner Canal was not detected during the cruise, it could potentially have started.

Region 3 contains water with a very narrow range of temperature (7.2 - 7.4°C) and salinity (31.5 - 32.7 °/oo) and probably results from uplift of bottom water during renewal of the outer two basins. Evidence of this uplift is found in elevated nutrient and reduced oxygen concentrations, particularly in water from near the head of the fjord. Region 2 and region 3 can also be differentiated by thier relative silicate enrichments (Fig. 4) or by silicate-nitrate ratios (Fig. 5). A universal feature of the uplift is vertical compression of layers as they expand horizontally (Gade & Edwards, 1980). Isopleths for oxygen (Fig. 6) show lower concentrations toward the head of the inlet and the compression of region 3 (see Fig. 4), particularly inside the sill near station 007. While region 3 can be identified by the uniform S-T characteristics, the nutrient and oxygen distributions point decisively to an uplift origin for that water mass.

Region 4, the bottom water, was identified on the T-S plot as water with salinity exceeding 32.7 °/oo. Temperature decreased with depth in the bottom

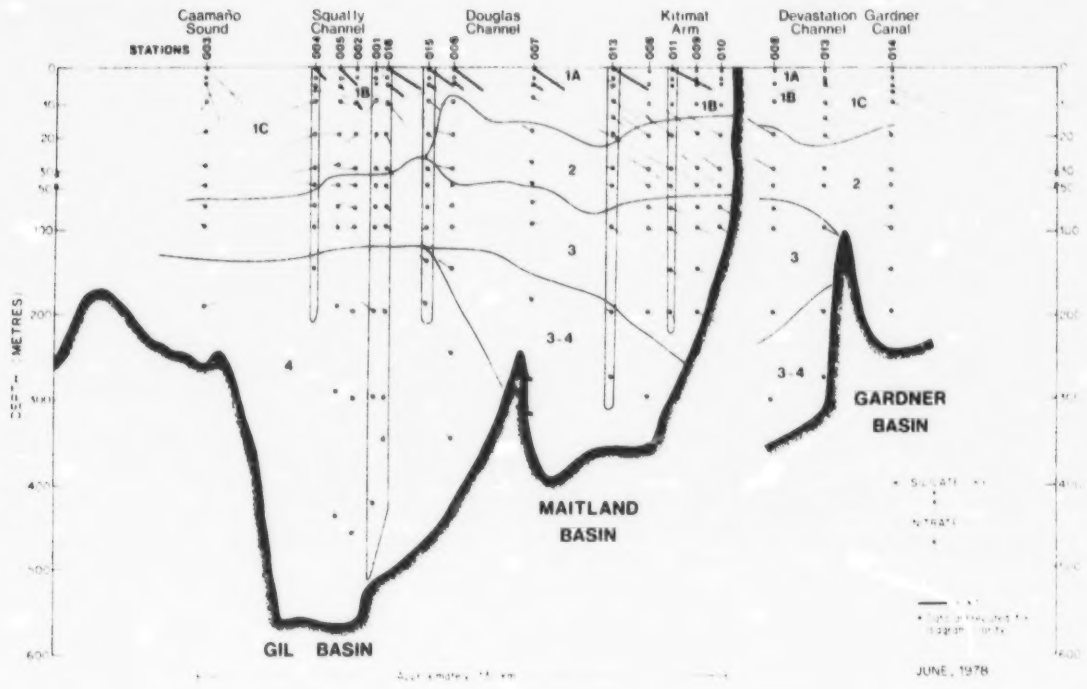

Fig. 4. Longitudinal section on which numbered regions are identified according to water properties (Jun-78). For explanation of arrows see methods.

water. Upwelling of coastal water in spring or summer has been shown to result from wind driven divergence (Dodimead et al, 1976; Dodimead, 1980). This process has been considered to drive the renewal of bottom water by an influx of dense water which is cold, nutrient rich, and oxygen depleted. The renewal was apparently well advanced by the time of the cruise since Gil Basin had already been completely flushed, and Maitland Basin at least partially flushed. Renewal was still active since the highest nutrient concentration (phosphate 2.4, silicate 54, nitrate 29.7 mmol m^{-3}) and lowest temperature (6.5°C) were found at 195 m at station 003, just inside the sill.

Vertical profiles for stations 006 and 011 best represent the various water bodies (Fig. 7). At station 006 the warm, fresh, high silicate containing water (Region 1) overlies the colder water of region 2. Uplifted water (Region 3) has a slight silicate maximum with concurrent phosphate and nitrate maxima. At station 011 the silicate maximum at the surface is sharply offset by the minimum just under the pycnocline at 10 m. This minimum is accompanied by elevated oxygen concentration.

CRUISE OCT-78

Figures 8, 9 and 10 are the T-S scatter plot, the ternary diagram and the longitudinal section respectively for this cruise.

As in June, region 1 was characterized by reduced salinity and warm temperatures of about 8-10° C. Silicate was an excellent indicator, and the

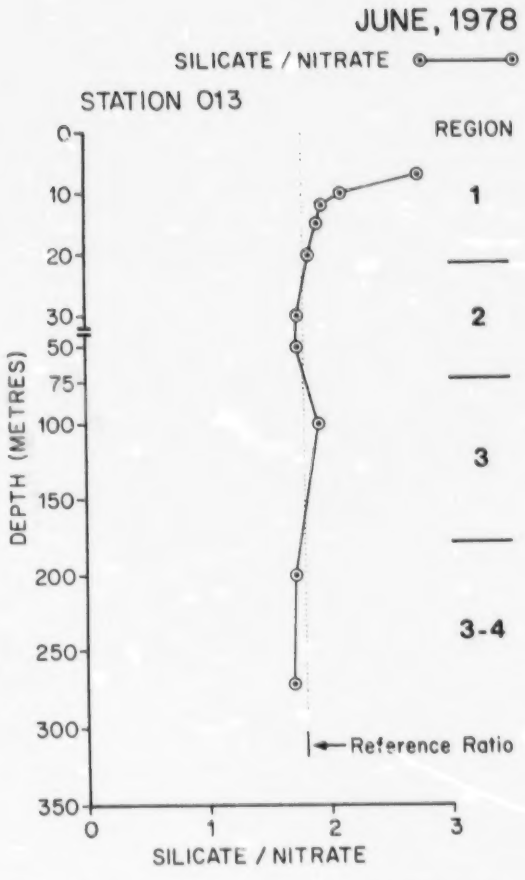

Fig. 5. A plot of silicate/nitrate ratio versus depths. Region 2 water shows a slight decrease in the ratio (Jun-78).

ternary diagram showed runoff as a straight line amounting to silicate addition. Nitrate removal by biological activity, which was so obvious in June, was no longer in evidence.

Region 2, the winter cooled water, remained as a small tongue at 50-100 m and was found only in Kitimat and Kildala Arms. The nutrient concentration, salinity, and temperature for this water was similar to that observed at station 006 in June. Erosion of Region 2 over the summer had apparently taken place since it occupies a smaller volume withdrawn towards the head of the inlet and depressed in the water column. Estuarine circulation, where fresh water flows seaward at the surface and gradually becomes saline by entrainment, requires a deeper inflow of salt water to balance the salt budget. This explains the general movement of the cool water toward the head of the inlet, but its depression by almost 50 m in the water column is unexpected since upwelling normally accompanies entrainment. Neither cross-channel variation nor internal tides can satisfactorily explain the results. Evidently the deep water movements in Kitimat Arm - Douglas Channel during summer cannot be completely explained by a simple entrainment model.

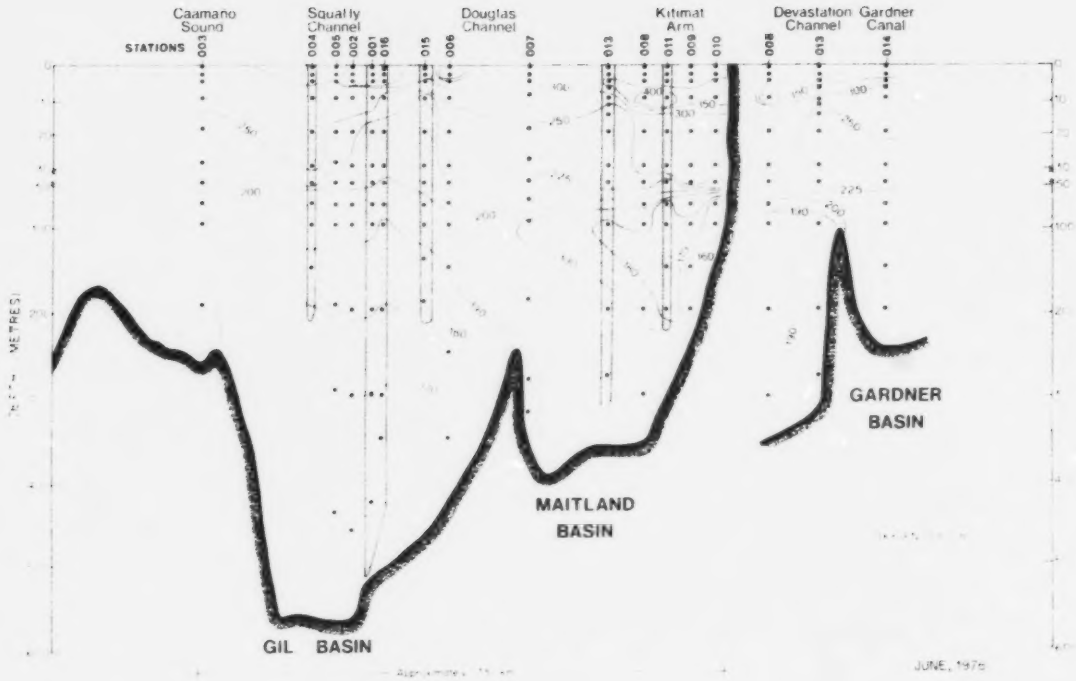

Fig. 6. Isolines of oxygen observed in Jun-78 during deep water renewal. Of particular note is the decrease of oxygen toward the head of the inlet in region 3 (Fig. 4), the old uplifted bottom water.

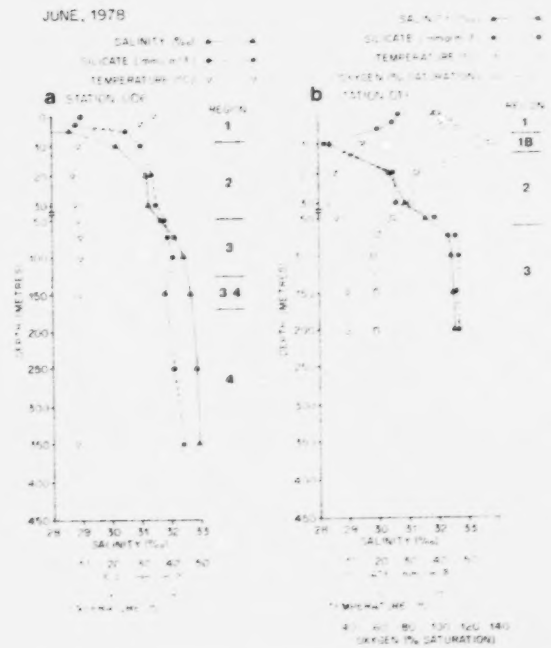

Fig. 7. Vertical profiles reflecting the various properties of the regions shown in Figure 4. (Jun-78).

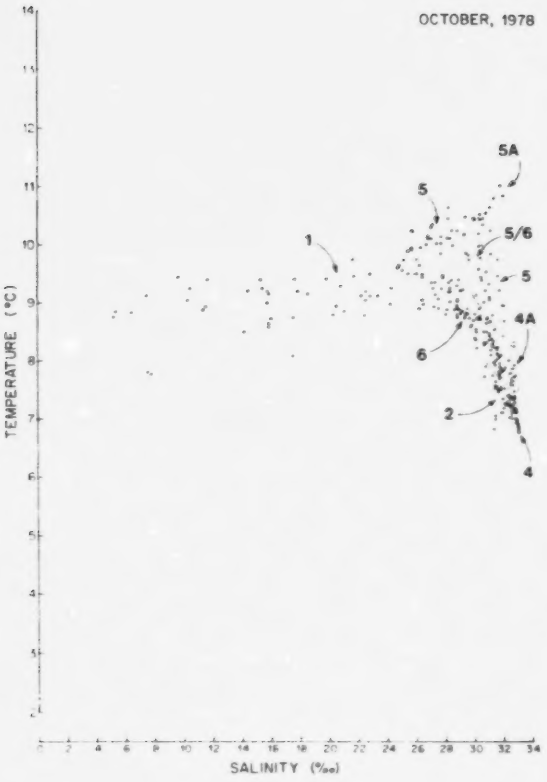

Fig. 8. Scatter plot of temperature versus salinity for samples collected during Oct-78.

By October, region 3 was no longer an important water mass, except perhaps in Gardner Basin. The bottom water there which by virtue of density was poised for renewal in June, had been completely flushed. The salinity increased from 31.9 to about 32.3 °/oo, the temperature from 7 to 7.5°C, and oxygen decreased from 211 to 175 mmol m^{-3}. The new water properties in Gardner Basin were consistent with flushing by region 3 water from about 100 m.

Region 4, the bottom water in the outer two basins, was more saline and colder than it was in June. Renewal apparently continued after the June cruise and completely flushed Gil and Maitland Basins. The nutrient concentrations were higher than in June and oxygen concentrations, lower; however, the concentrations closely match those measured at the bottom of station 003 (195 m) during June. While some of the oxygen decrease and nutrient increase in bottom water may have been caused by decomposition of detritus, much of it may have resulted from renewal with upwelled water from Hecate Strait. As indicated by the ternary plot and the arrows on Figure 10, silicate was slightly enriched in the bottom water compared to the previous cruise.

Region 4A was identified on the T-S plot (Fig. 8) by an isohaline line at 32.8 °/oo. The water appeared to have intruded over the sill with with the core temperature highest toward the shelf; 8.25°C at station 003, 7.35°C

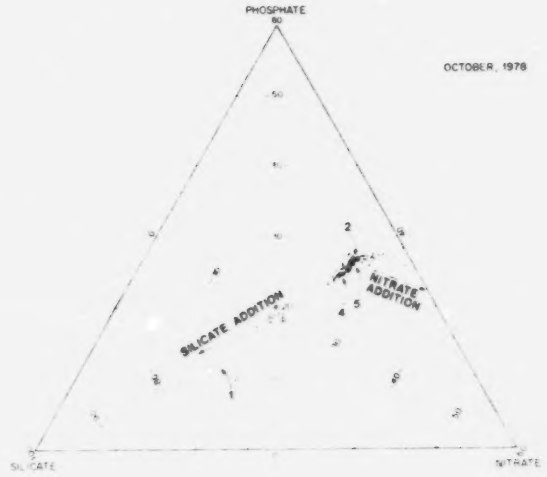

Fig. 9. Ternary plot for phosphate, silicate and nitrate, Oct-78.

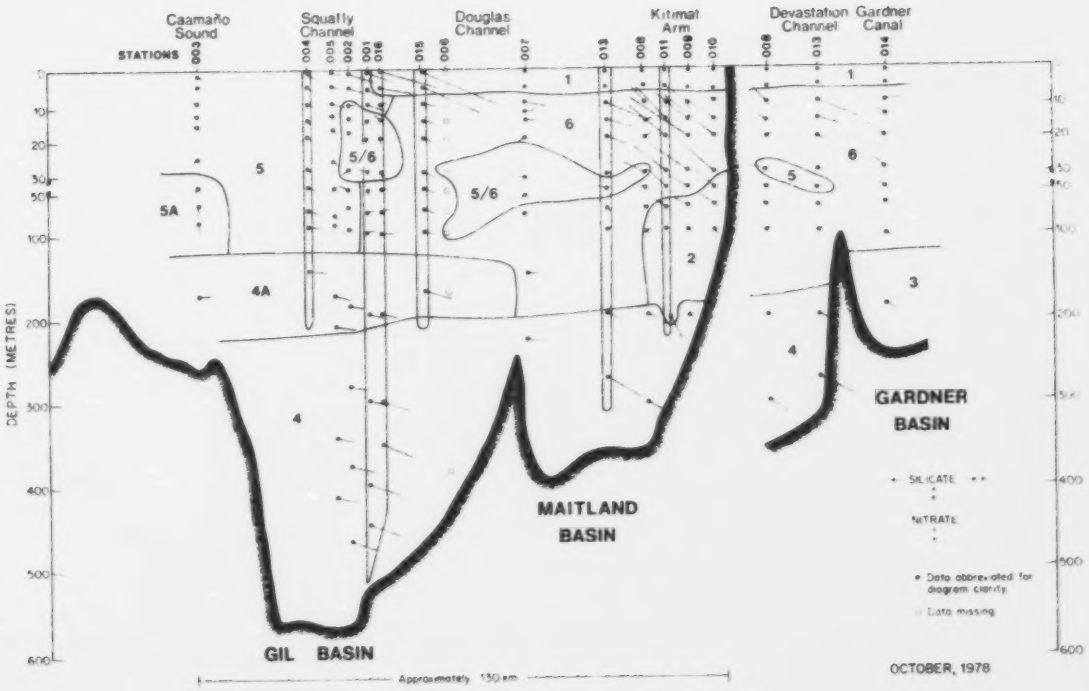

Fig. 10. Longitudinal section on which numbered regions are identified according to water properties (Oct-78).

at station 015. In October, it had not penetrated as far as station 007 in Douglas Channel. Nutrient concentration and ratios were very uniform for this water as shown by the constant direction and magnitude of the arrows in Figure 10.

Region 5 is warm and has a subsurface temperature maximum of about 10.5°C. In contrast region 6 is cooler and temperature decreases monotonically with depth (Fig. 8). Region 5 is found at the seaward end of the fjord and is closer in its T-S characteristics to water in Hecate Strait (c.f. Dodimead, 1980). Region 5 also tends to have lower nutrient and higher oxygen concentration than region 6. An intrusion of region 5 water into Douglas Channel (Fig. 10) is identified by the T-S characteristics at several stations and by nutrient concentrations. The intrusion is observed at two depths for station 006 (Fig. 11a) where temperature maxima are coincident with oxygen maxima and nitrate minima at 30 and 100 m. The T-S plot for station 006 (Fig. 11b) clearly shows the intrusion. There appears to be a discontinuity in the intrusion between station 002 and 006 (Fig. 10). This is an artefact of the drawing since stations 001, 015, and 016 are located in side channels. Type 5 water, it seems, has been forced into Douglas Channel and McKay Reach, a process which may in part explain the depression of region 2 during the summer.

Between the pycnocline and region 2 at station 008, 009, 010 and 011, an anomalous region is found. T-S characteristics place this water in region 6, but the water is depleted in silicate and enriched in nitrate as shown by the arrows on Figure 10. Points from this region are located in the open cluster toward the right on the ternary plot. Compare the silicate profile at station 007 (Fig. 11c) and station 011 (Fig. 11d). Silicate depletion at station 011 is not accompanied by an oxygen maximum, and appears to be a remnant of biological production.

In both June and October, upwelling took place at stations 1, 15 and 16, as was evidenced by the upward displacement of water properties, particularly nutrients. The small basin in Kildala Arm (Stn. 011) was not flushed during the summer. The highest nutrient and lowest oxygen concentrations were found there (phosphate 2.95, silicate 58, nitrate 28.3, oxygen 107 mmol m^{-3}), and salinity had decreased only slightly between the two cruises.

CRUISE FEB-79

Figures 12, 13 and 14 are the T-S scatter plot, ternary diagram and longitudinal section, respectively.

The T-S plot shows that water near the surface is much colder than in October. The tighter grouping of data points on the ternary diagram is a result of mixing and a reduction of nutrient-altering processes such as runoff of biological production. Indeed, fresh water input accompanied by silicate was obvious only in the surface at station 011.

Region 2, the zone of winter cooling, which has developed to about 30-50 m is characterized by a slight silicate enrichment. Silicate from runoff mixed downwards is the probable explanation. The silicate depletion zone found below the pycnocline at the head of the inlet in October no longer appears. There is, however, a small zone of nitrate enrichment at about 30-100 m, particularly

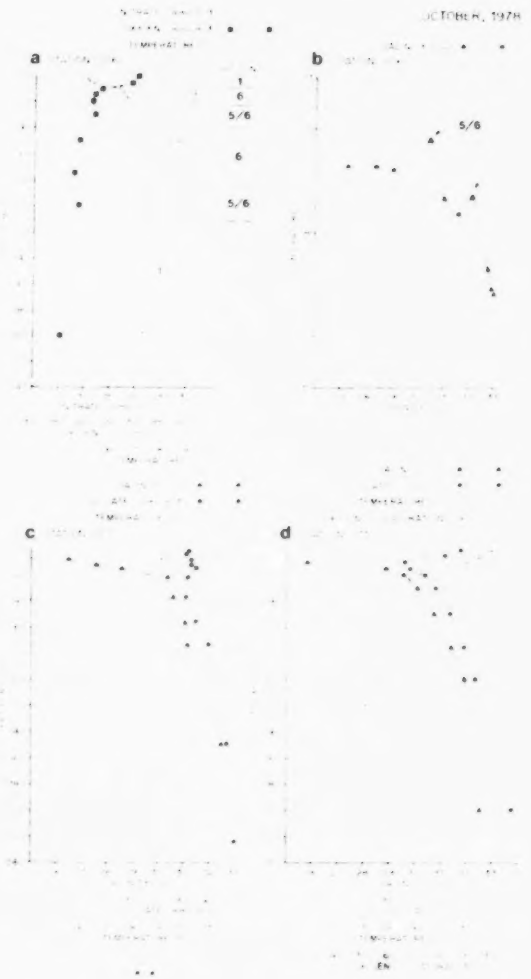

Fig. 11. a) Vertical profiles of temperature, oxygen and nitrate showing the difference in properties between region 6 and region 5/6 (Oct-78).
b) The temperature-salinity plot for the same station shown in Fig. 11(a).
c) Vertical profiles for station 007 (Oct-78).
d) Vertical profiles for station 011 (Oct-78).

at stations 008 and 011 (see arrows on Fig. 14). Although the effect is small, it is real and appears as the small appendix indicated on the ternary plot. We have no ready explanation for its origin.

The bottom water in Gil and Maitland Basins was much warmer (from 6.76 to 7.38°C) and less saline than in October. Apparently type 4A water had been mixed downward during the interval between October and February. The water at the bottom of station 005 in Feb-79 was almost identical in properties to that found at 260 m in Oct-78. Basing estimates on salinity, the water in both basins had undergone at least 2/3 replacement. To supply the necessary volume of water, the intrusion of 4A water must have continued for some time

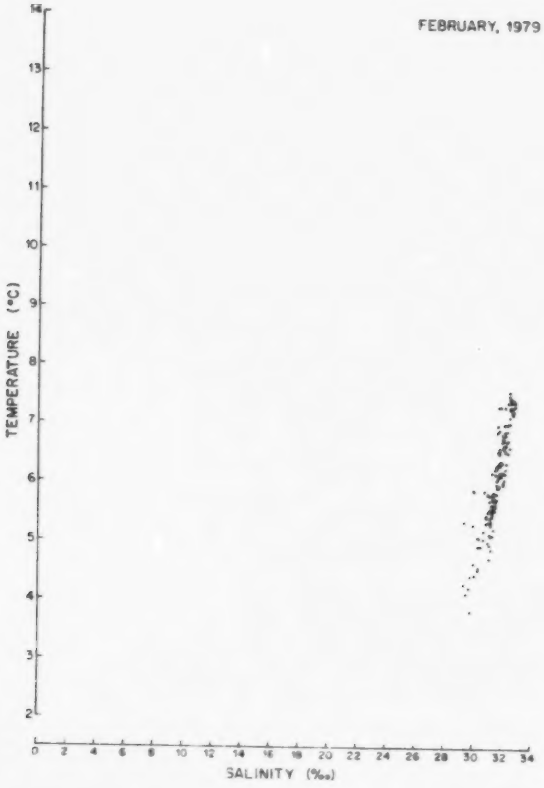

Fig. 12. Scatter plot of temperature versus salinity for samples collected during Feb-79.

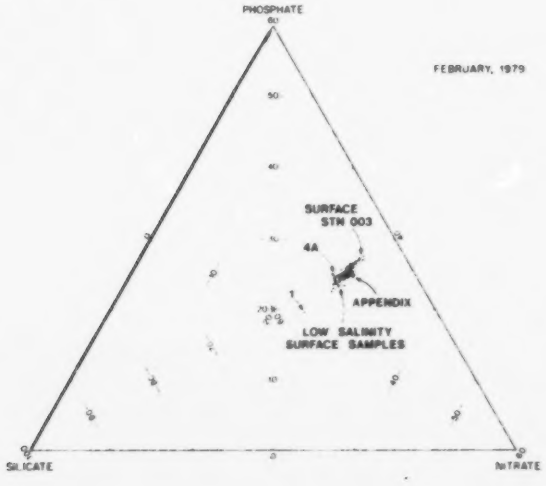

Fig. 13. Ternary plot for phosphate, silicate and nitrate, Feb-79.

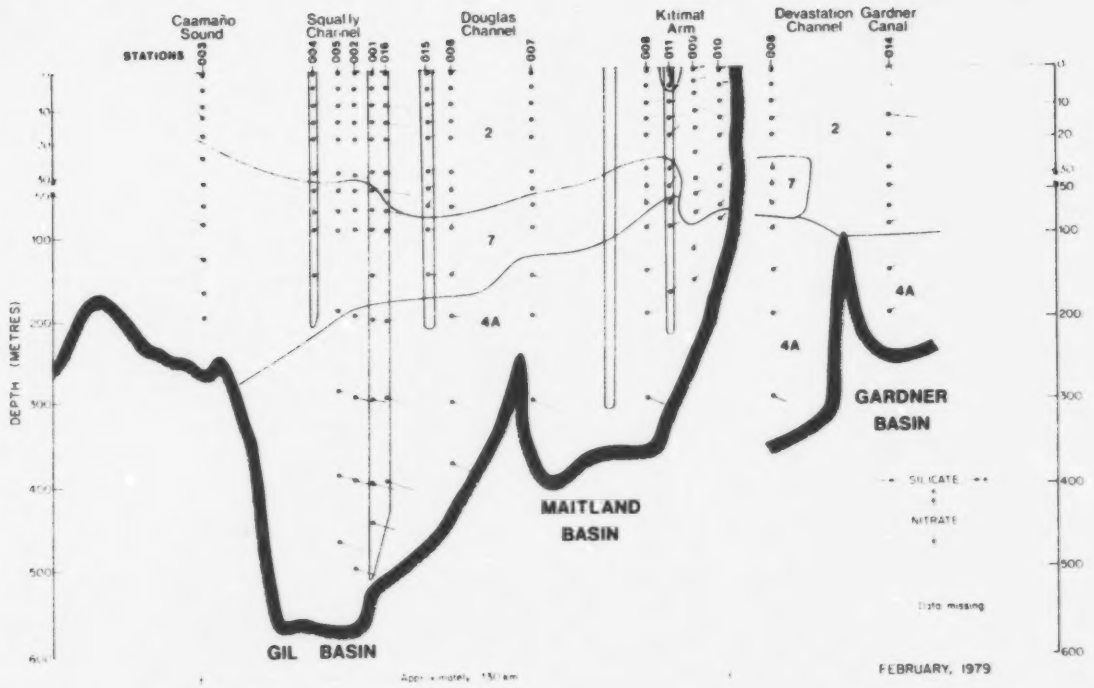

Fig. 14. Longitudinal section on which numbered regions are identified according to water properties (Feb-79).

after the Oct-78 cruise. The bottom water in Gardner Basin was also fresher (32.6 °/oo in October to 31.94 °/oo in February at 200 m), warmer, and the oxygen concentration had increased from 174 to 205 mmol m^{-3}. To accomplish these changes, renewal must have occurred by downward mixing of water similar to type 4A from about 150 m, the sill depth of Gardner Canal.

Mixing depends to some extent on topography (McClimans, 1980) and is enhanced where baroclinic modes predominate (Svendsen, 1980). M_2 (semi-diurnal) internal tides exist at mid-latitudes provided the Brunt-Väisalä frequency, N(z), is greater than the wave frequency and the latitude is greater than 30°, i.e.:

$$N(z) = \left[-\frac{g}{\rho} \frac{\partial \rho}{\partial z} \right]^{\frac{1}{2}} > W_{M_2} \simeq 1.4 \times 10^{-4} s^{-1}$$

where g is the gravitation acceleration constant, ρ is density and z depth. This criterion is met everywhere and at all times of the year in the Kitimat system (Webster, 1981). Conditions for mixing are therefore favourable both topographically and tidally, which helps to explain our observations.

There is evidence that uniform downward mixing does not adequately describe the process leading to warmer and fresher bottom waters in winter since replacement appears to take place with some longitudinal variability, progressing from the outer basin inwards. A time series (approximately one week intervals) throughout fall and winter months is required before bottom water property changes during this period can be completely understood, and perhaps modeled.

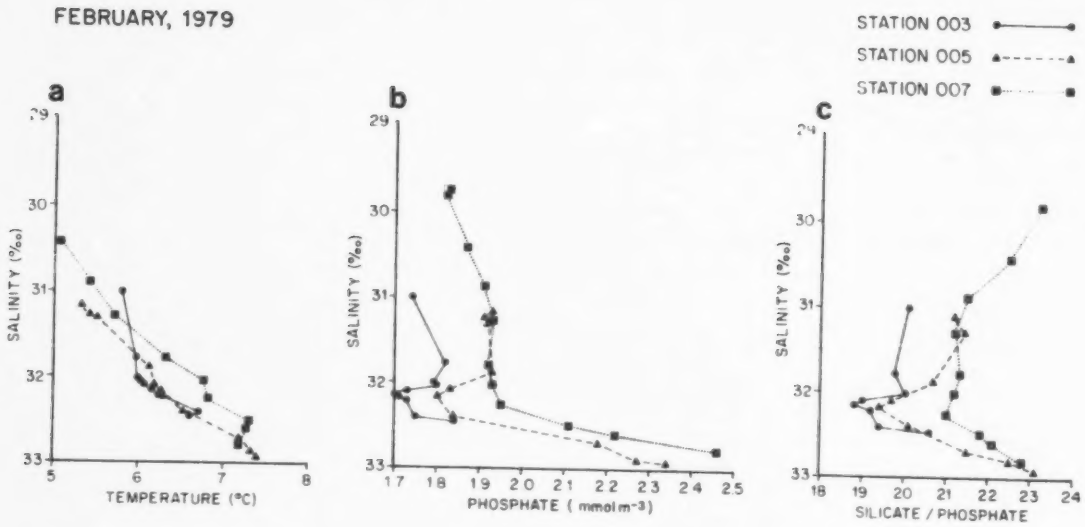

Fig. 15. a) Temperature-salinity plot showing the slight temperature decrease at about 32-32.5 °/oo (Feb. 79).
b) Phosphate-salinity plot showing the nutrient minimum at 32-32.5 °/oo (Feb-79).
c) Silicate-phosphate ratio versus salinity showing the relative depletion of silicate at 32-32.5 °/oo (Feb-79).

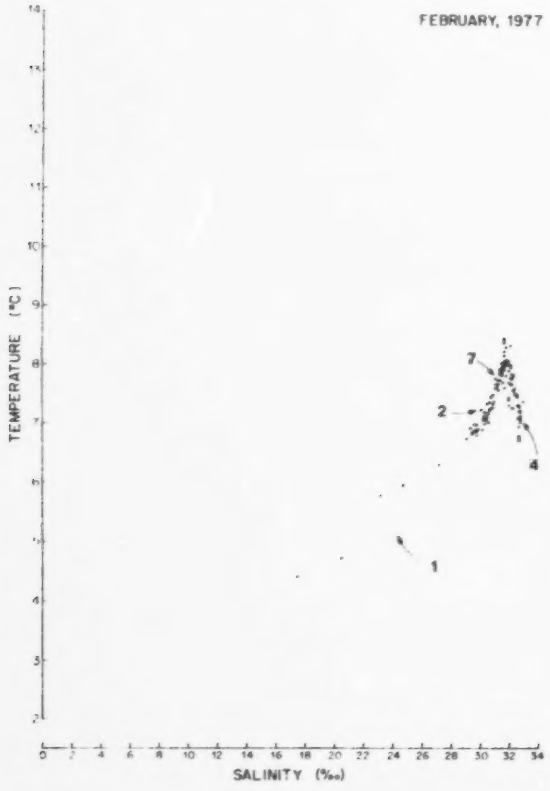

Fig. 16. Scatter plot of temp. versus salinity for samples collected Feb-77.

Region 7 (Fig. 14) is identified by a temperature minimum or an inflection on the T-S curve (Fig. 15a) accompanied by a nutrient minimum and oxygen maximum. Region 7 is also slightly depleted in silicate as shown in Fig. 14, and detected on nutrient-salinity plots (Fig. 15b) or by silicate/phosphate ratios (Fig. 15c). The T-S characteristics of this water are similar to those of Hecate Strait (Dodimead, 1980) and imply that this water has been recently advected into the system.

The wind record for Kitimat shows prolonged periods of strong northerlies commencing sometime in November. These "katabatic" winds drive the surface layer seaward. Webster's (1980) observations indicate currents exceeding 25 cm s^{-1} at 30 m in response to this wind stress, and residual return flow of about 5 cm s^{-1} at 165 m. If continuous, this return flow transports water about 130 km per month, and can therefore easily explain the rapid penetration of shelf water into the system at that time of the year (the penetration of type 4A water seen in Oct-79 could be the beginning of this process). Furthermore, the water properties change at about 30-75 m from region 2 to region 7 in agreement with the 30-60 m shear zone observed by Svendsen (1980) for wind driven circulation in six fjords.

CRUISE FEB-77

The T-S scatter plot (Fig. 16) contrasts sharply with that of Feb-79). The temperature maximum, which was observed at all stations, dominates. A surface layer freshened by runoff is also evident and is probably the result of warm winter in 1977.

The ternary plot (Fig. 17) is quite similar to that for the Feb-79 cruise, but the distribution center is shifted toward silicate depletion, perhaps the result of interannual variation. Station 1, outside the sill, and station 2 at the sill are the most depleted in silicate and show that water in Hecate Strait has a nutrient composition different from that observed in the fjord.

Figures 14 and 18 show that the same regions are evident for both winter cruises. Region 7 is the most interesting, being characterized in 1977 by a temperature maximum, nutrient minimum and relative silicate depletion. This water probably has a recent origin in Hecate Strait. The pronounced silicate depletion at station 1 and 2 supports this point of view. The great difference between the two winter cruises is that water from the shelf was warm in 1977, but cold in 1979. The longitudinal temperature section for Feb. 19-77 (Fig. 19) shows the influence that shelf water can have on total heat in the inlet. Compare also the T-S diagrams (Figs. 12, 16).

The onset of northerlies in the fall, and their dominance of the percentage wind frequency from November to February, occurs annually (Bell & Kallman, 1976). If, as we suggest, large volumes of shelf water from 70-150 m are forced into the Kitimat system in response to surface outflow conditions then the annual temperature of this intermediate water should be controlled in winter by shelf water properties. During Jan-Feb, the water column in Queen Charlotte Strait is well mixed down to about 100-150 m (c.f. Dodimead, 1980). Thus, the long time series of surface temperature measurements at Cape St. James Lighthouse at the south end of the Queen Charlottes (Fig. 20) may be used to predict the temperature of this intermediate water. Note the similarity in temperature of the intermediate water (8.0°C in Feb-77, 6.4°C

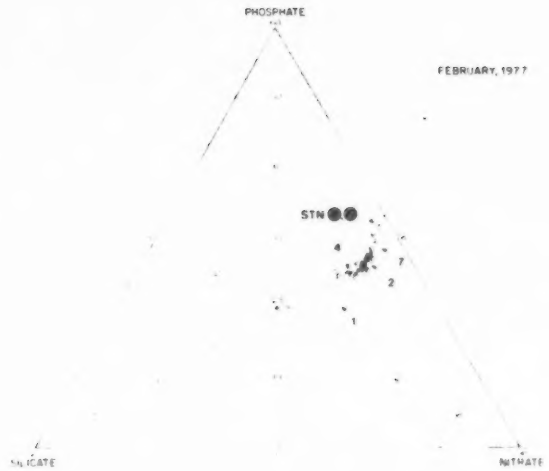

Fig. 17. Ternary plot for phosphate, silicate and nitrate, Feb-77.

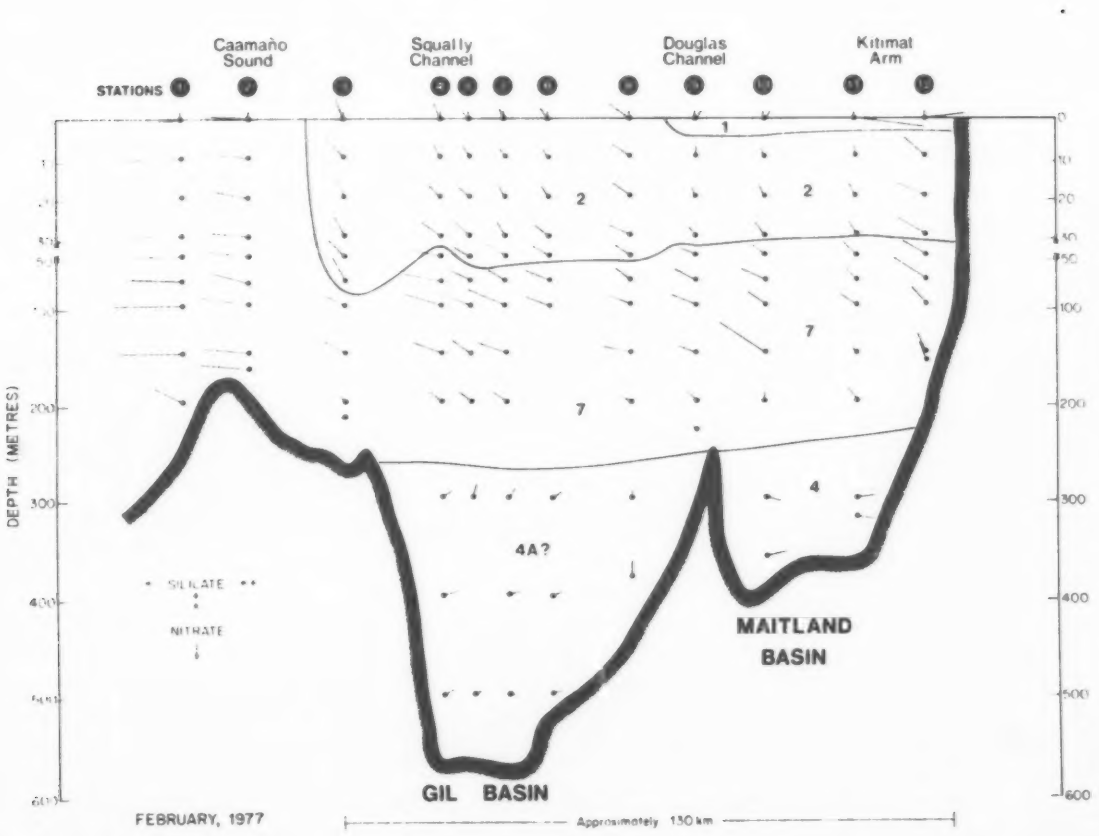

Fig. 18. Longitudinal section on which numbered regions are identified according to water properties (Feb-77).

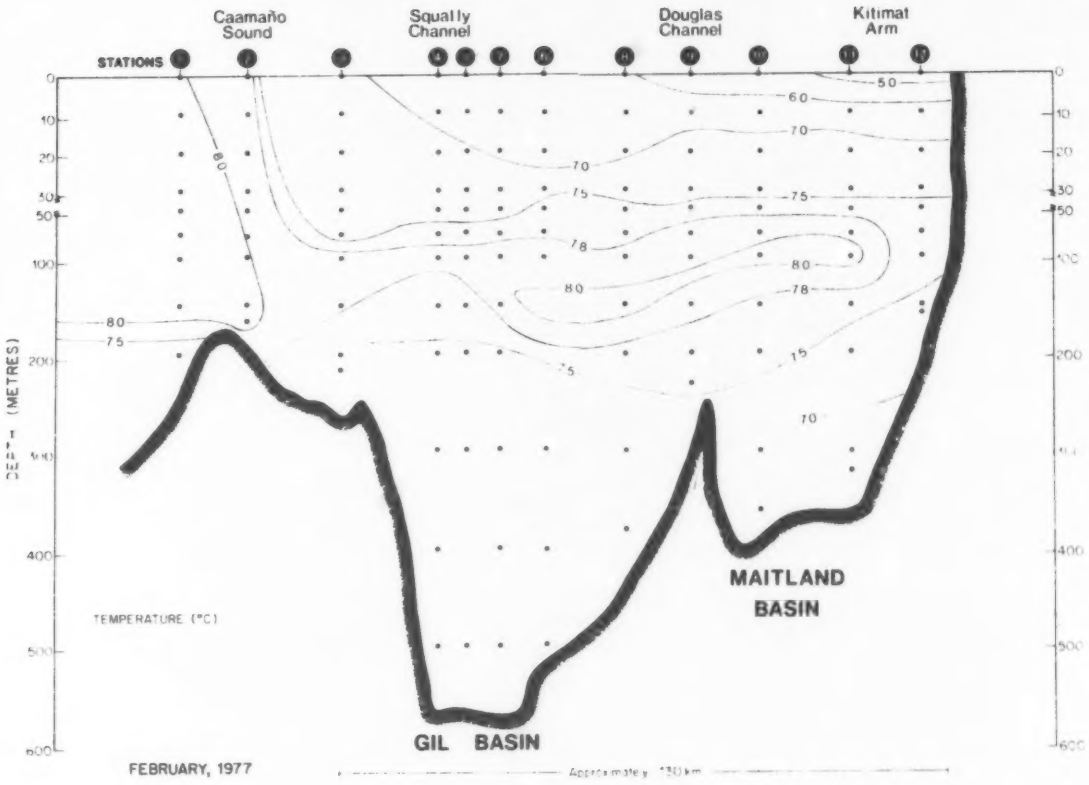

Fig. 19. Longitudinal section showing temperature distribution (Feb-77).

in Feb-79) with the temperature of the Queen Charlotte Strait surface water (Fig. 20). Although there are few winter data collected in the Kitimat fjord system (c.f. Tabata, 1980), two other data sets exist where temperature comparisons with Fig. 20 could be made. Webster (1980) reports intermediate water temperatures in Douglas Channel for mid-December, 1977 (8.3°C) and mid-March, 1978 (6.4°C), and Waldichuk et al (1978) found this water to be about 7°C for mid-April, 1962. The agreement between the intermediate water temperatures in Douglas Channel and those at Cape St. James is compelling, but further time series are required to determine the regularity and importance of this phenomenon.

While temperature can be a capricious indicator of intermediate water intrusion, nutrient-salinity relationships (Fig. 21a, b) are more reliable. Comparison of Figures 21 and 15 shows that the intrusion was broader and more diffuse in 1977.

In February, 1977, the water at the bottom of Gil Basin was fairly warm (7-7.3°C) and less saline than it was in Feb-79. The oxygen concentration, 150 mmol m^{-3}, was about the same for both years. Water similar to 4A might have mixed downward prior to the Feb-77 cruise in what may be an annual event. If so, this downward mixing was probably weaker in 1977 since Maitland Basin had been only partially flushed.

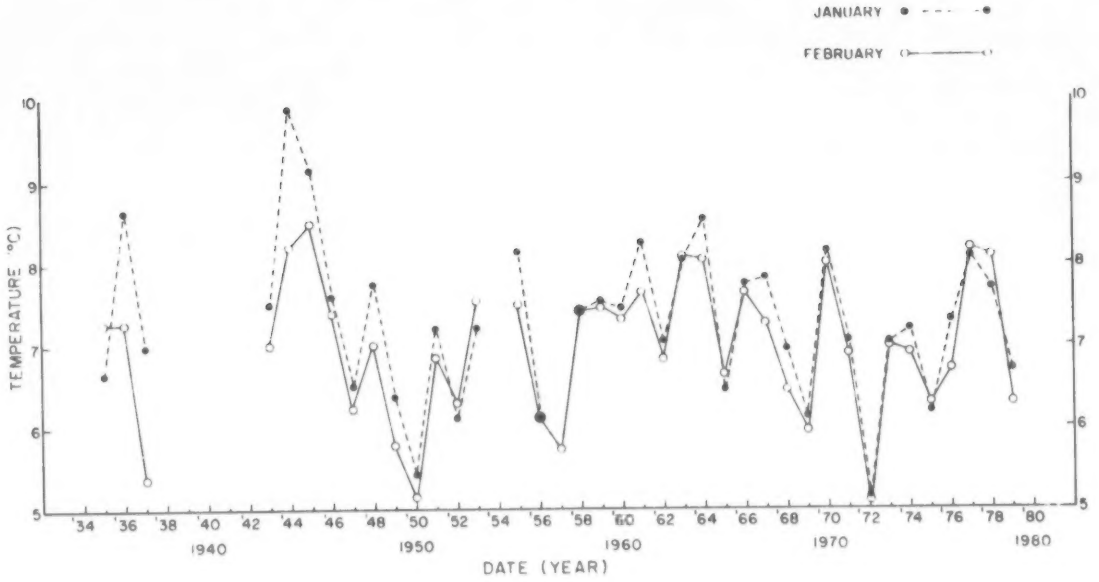

Fig. 20. Surface temperature records at Cape St. James over the period 1935-1979. Data were compiled from Dodimead (1980) and Giovando (1978a, b, c, d, 1980).

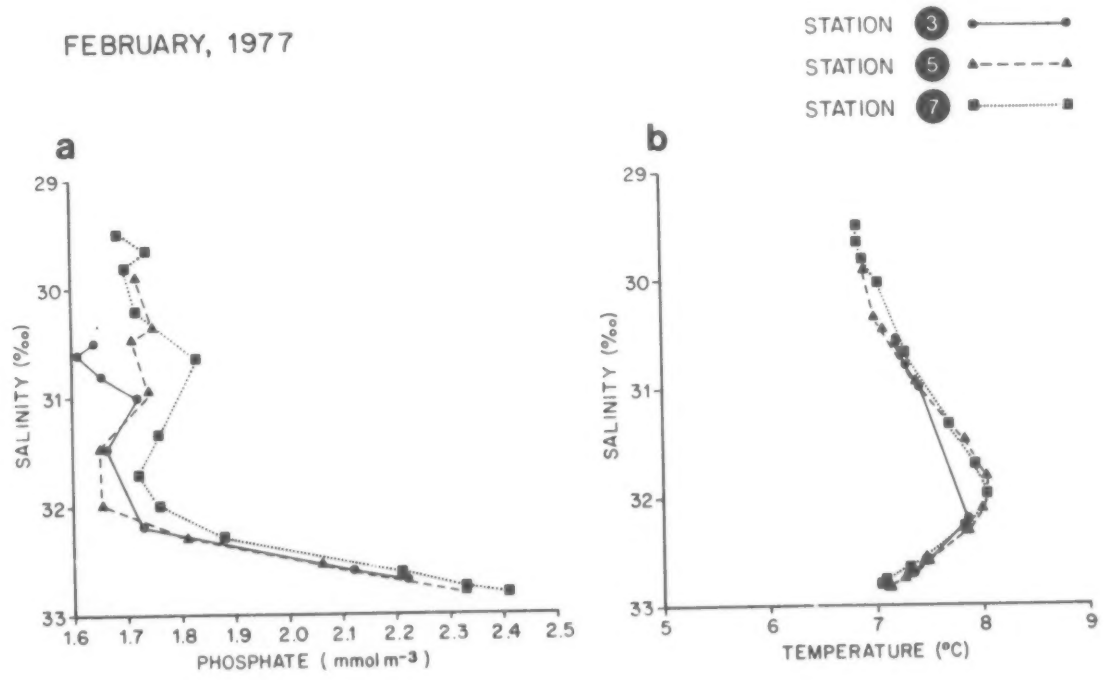

Fig. 21. a) Phosphate salinity plot showing the nutrient minimum at 31-32.5 °/oo (Feb-77).
b) Temperature-salinity plot showing the mid-winter temperature maximum at 31-32.5 °/oo.

CONCLUSIONS

Our limited data suggest that the water motions in the Kitimat fjord system are dynamic and strongly influenced by events on the shelf. Bottom water undergoes replacement in two different ways. In spring through summer, cold, dense, oxygen-depleted water upwells on the shelf and replaces the water in the two outer basins by uplifting the old water. Flushing proceeds inwards, and Gardner Basin is the last to undergo renewal. Gardner Basin may be flushed with old, uplifted water from the other two basins. Although in 1978 renewal increased the oxygen content of Gardner Basin, this may not always be the case since oxygen isopleths are closely spaced at the depth from which renewal takes place (Fig. 6). The small basin in Kildala Arm may not undergo renewal until later in the year, possibly November. During the second type of renewal, water mixes downward. This occurs in autumn, and results in increased temperatures and decreased salinity.

During winter, probably due to katabatic winds, surface water is driven seaward. In response, water from 30-150 m is rapidly forced into the system from Hecate Strait. This intrusion is detectable through nutrient properties, and could have temperatures from 5-9°C. Other water properties such as planktonic assemblages (Stone, 1980) or $^{16}O/^{18}O$ ratio may be useful tracers in future studies.

Upwelling is apparent at the shallow sills of Verney Passage and Ursula Channel during periods of fresh water input. This is probably caused by estuarine circulation and coupled with vigorous tidal mixing results in nutrients distributed through the euphotic zone. McKay Reach and Wright Sound may reap the benefit of this upwelling with sustained primary production.

ACKNOWLEDGEMENTS

We gratefully acknowledge the many people who assisted in collecting these data with special thanks to W. Richardson for the careful nutrient determinations. We also thank the officers and crews of the C.S.S. *Parizeau* and M.V. *Sea Lion* for their cooperation during cruises, and J. Poulin and T. Lehman for their assistance in preparing the manuscript. We are indebted to R. Thomson and W. Bell for providing critical and perceptive comment on the preliminary drafts.

REFERENCES

Dodimead, A.J. 1980. A general review of the oceanography of the Queen Charlotte Sound - Hecate Strait - Dixon Entrance region, Canadian manuscript Report of Fisheries and Aquatic Sciences, No. 1574, 248 pp.

Dodimead, A.J., . Favorite and K. Nasu. 1976. Review of oceanography of the sub-arctic Pacific region. 1960-1971. Bull. 33 Int. N. Pac. Fish. Comm. 187 pp.

Gade, H.G. and A. Edwards. 1980. Deep water renewal in fjords. In Fjord Oceanography, Plenum Press, Freeland, Farmer & Levings, eds. pp 453-89.

Giovando, L.F. 1980. Observations of seawater temperature and salinity at British Columbia shore stations 1974-1978. Pacific Marine Science Report Series a) 80-10, 125 pp., b) 80-1, 111 pp., c) 78-12, 111 pp., d) 78-8, 111 pp., e) 78-2, 111 pp.

Macdonald, R.W., B.D. Bornhold and I. Webster. 1983 (a). The Kitimat fjord system: An introduction. In Proceedings of a Workshop on the Kitimat marine environment, R.W. Macdonald, ed., Canadian Technical Report of Hydrography and Ocean Sciences, 18, 2-13.

Macdonald, R.W., W.J. Cretney, C.S. Wong and P. Erickson. 1983 (b). Kitimat hydrocarbon baseline study 1978-9 III; Oceanographic support data, Canadian Data Report of Hydrography and Ocean Sciences, 18, 66-87.

Macdonald, R.W., D.M. Macdonald and P.S. Munro. 1978. Oceanographic data report Kitimat Arm, Porpoise Harbour Feburary 1977. Pacific Marine Science Report 78-24, 61 pp.

Macdonald, R.W., F.A. McLaughlin. 1982. The effect of storage by freezing on dissolved inorganic phosphate, nitrate and reactive silicate for samples from coastal and estuarine waters. Water Research, 16, 95-104.

McClimans, T.A. 1980. Energetics of mixing processes in fjords. In Fjord Oceanography, Plenum Press. pp. 215-218.

Pickard, G.L. 1961. Oceanographic features of inlets in the British Columbia mainland coast. J. Fish. Bd. Canada, 18, pp. 907-999.

Stone, D.P. 1980. The distribution of zooplankton communities in a glacial run-off fjord and exchanges with the open sea. In Fjord Oceanography, Plenum Press. pp. 291-298.

Svendsen, H. 1980. Exchange processes above sill level between fjords and coastal water. In Fjord Oceanography, Plenum Press. pp. 355-362.

Tabata, S. 1980. An inventory of physical oceanographic information for the waters of Queen Charlotte Sound, Hecate Strait, Dixon Entrance and their vicinity. Pacific Marine Science Report 80-7, 24 pp. and tables.

Waldichuk, M., J.R. Markert and J. Meikle. 1968. Physical and chemical oceanographic data from the west coast of Vancouver Island and the northern British Columbia coast, 1957-1967. Volume II, Fisher Channel - Cousins Inlet, Douglas Channel - Kitimat Arm and Prince Rupert Harbour and its contiguous waters. Fisheries Research Board of Canada, Manuscript Report Series No. 990, 303 pp.

Webster, I. 1983. The baroclinicity of the semi-diurnal tidal currents in Douglas Channel, B.C. In Proceedings of a workshop on the Kitimat Marine Environment, R.W. Macdonald, ed., Canadian Technical Report of Hydrography and Ocean Sciences, 18, 14-33.

DÉPOSITIONS DANS LE CANAL DOUGLAS ET KITIMAT ARM

Brian D. Bornhold
Geological Survey of Canada
Pacific Geoscience Center, Sidney, B.C.

RÉSUMÉ

Le Canal Douglas et Kitimat Arm consiste de trois bassins de dépositions majeures. Deux de ceux-ci sont de 400 m de profondeur, et contient des dépôts inconsolidés, avec plus de 600 m d'épaisseur. Ils sont séparés d'un filoncouche proéminent à la profondeur de 211 m, qui est composé de plus de 900 m de matière moraine. Le troisième bassin, étant tout à fait plein, est à la base du nord du Kitimat Arm et du sud du Kitimat Valley, il est aussi séparé des autres bassins par un filoncouche rocheux qui est maintenant ensevelé par les depôts du delta Kitimat. De la dique du delta Kitimat, les contours et centres seismiques, et les répercutions à basse-fréquences décrivent les unites stratigraphiques: teroirs dépôts glaciomarines, sable stratifié, boue sableuse, boue transparente, dépôts de moraines graveleuses, mince couche de boue stratifié et boue sableuse ensemble avec quelque fois, des échelons sableux; aussi des dépôts mamelonnés, et des dépôts bouges. Le plus gros des dépôts du fjord (passage) fût deposé durant le déglacement, entre, environ, 13,100 et 11,000 ans B.P. avec les mêmes filoncouches moraines étant reproduites par l'éparpillement de la glace à environ 12,000 ans B.P. Le dépôt deltaique près du Kitimat à commencé à environ 9-9500 ans B.P., et, ainsi donc à conduit aux plus récentes unites stratigraphiques dans les bassins; - les boues (combinant boue et boue sableuse) avec des dépositions hémiplaquiques, les éboulements de terre, les débris, et les courants turbulents.

Bornhold, B.D. 1983. Sedimentation in Douglas Channel and Kitimat Arm. Can. Tech. Rep. Hydrogr. and Ocean Sci. 18, 88-114.

Mot-clés: bouge, Canal Douglas, datant, déposition, répercusion, seismique

SEDIMENTATION IN DOUGLAS CHANNEL AND KITIMAT ARM

Brian D. Bornhold
Geological Survey of Canada
Pacific Geoscience Center, Sidney, B.C.

ABSTRACT

Douglas Channel and Kitimat Arm consist of three major depositional basins. Two of these are 400 m deep and contain unconsolidated sediments more than 600 m thick. They are separated by a prominent sill at a depth of 211 m which is composed of more than 900 m of predominantly morainal material. The third basin, which is completely filled, underlies northern Kitimat Arm and southern Kitimat Valley and is separated from the other basins by a bedrock sill, now buried by Kitimat delta sediments. Seismic profiling, low-frequency echosounding and coring have delineated the following stratigraphic units: tills (?) and glaciomarine sediments; stratified sands and sandy muds; acoustically transparent muds; coarse, gravelly morainal sediments; thin, surficial stratified muds and sandy muds with occasional sand layers; and hummocky, slumped sediments on the Kitimat delta front. Much of the sediment in the fjord was deposited during deglaciation between approximately 13,100 and 11,000 yr B.P. with the main morainal sill being produced by stagnation of the ice at about 12,000 yr B.P. Deltaic sedimentation near Kitimat began about 9-9500 B.P. and led to the deposition of the most recent stratigraphic unit in the basins, interstratified muds and sandy muds, through hemipelagic deposition, landslides, debris flows and turbidity currents.

Bornhold, B.D. 1983. Sedimentation in Douglas Channel and Kitimat Arm. Can. Tech. Rep. Hydrogr. and Ocean Sci. 18, 88-114.

Keywords: coring, dating, Douglas Channel, sedimentation, seismic profiling, slumping

INTRODUCTION

Douglas Channel and Kitimat Arm (Fig. 1) lie within the Kitimat Ranges, a physiographic sub-province of the British Columbia coast mountains characterized by mountain peaks up to 3000 m high composed predominantly of massive granitic rocks, a relative scarcity of glaciers compared to mountain ranges to the north and south, and a prominent system of large-scale lineaments (Holland, 1976). These lineaments take the form of long straight valleys and channels, one set trending northwesterly, and the other trending north to northeasterly. Both sets appear to be fundamentally structurally controlled (Holland, 1976) but have been extensively modified by Pleistocene glaciation as well as by fluvial erosion and deposition. The fjord channels and adjacent subaerial valleys contain thick sequences of glacial, glaciomarine, marine, deltaic and fluvial sediments and many of the inlet basins continue to fill rapidly through the progradation of fjord-head deltas.

The purposes of this study were to identify and describe the major sedimentary units within Douglas Channel and Kitimat Arm and to attempt to explain the sedimentary history of the fjord system in the light of what is known about Quaternary events in the area. Data from four cruises of the

Geological Survey of Canada were used in this investigation: CSS Parizeau in February 1977 (Bornhold 1977), joint cruises with Earth Physics Branch (Energy, Mines and Resources) in October 1977 and May 1978 using CSS Vector (Lewis et al. 1978), and CSS Parizeau in October 1979 (Fig. 2).

METHODS

Bathymetry

A bathymetric map of Douglas Channel was prepared by contouring Field Sheets 3319-L, 3320-L, and 3310-S, obtained from the Canadian Hydrographic Service, at a 50 m contour interval.

Sub-bottom profiling

An O.R.E. high-resolution sub-bottom profiling system with 12 hull-mounted transducers was used at a frequency of 3.5 kHz, a bandwidth of 1 kHz, and approximately 5 kW power during the Vector and Parizeau 1979 cruises. A Simrad 11 kHz echosounder was used during the Parizeau 1977 cruise.

Air-gun seismic relection profiles were obtained with a 16 cm^3 air gun source fired every second at 7600 kPa, and a hydrophone array with a built-in preamplifier. The 80-3000 Hz interval was recorded on an EPC 4100 graphic recorder. All seismic profiling was carried out at ships' speeds of 5 to 10 km/h.

Seismic Refraction

A reversed seismic refraction line 7.5 km long was carried out in Kitimat Arm using an 80 cm^3 air gun source and an Aquatronics Model SM44 sonobuoy and Aquatronics FM receiver.

Coring

Gravity coring was conducted using a 550 kg Alpine corer, with an internal diameter of 6.35 cm and an 80 kg Benthos corer with an internal diameter of 6.67 cm.

Cores were split and described as soon as possible following each cruise. Water contents were determined for selected samples within the cores.

GEOLOGIC SETTING

Douglas Channel and Kitimat Arm cut across the Coast Crystalline Belt of plutonic and metamorphic rocks which forms the western mainland of British Columbia. The rocks bordering the channel consist of Paleozoic schists, gneisses and metasediments as well as diorites, granodiorites and monzonites of uncertain age (Roddick 1970), but probably younger than late Mesozoic. These plutonic rocks continue up the Kitimat Valley with minor Jurrassic andesitic rocks along the southwestern side of the valley (Duffell

Fig. 1. Bathymetric map of Douglas Channel and Kitimat Arm. Based on Canadian Hydrographic Service field sheets contoured at a 50 m interval.

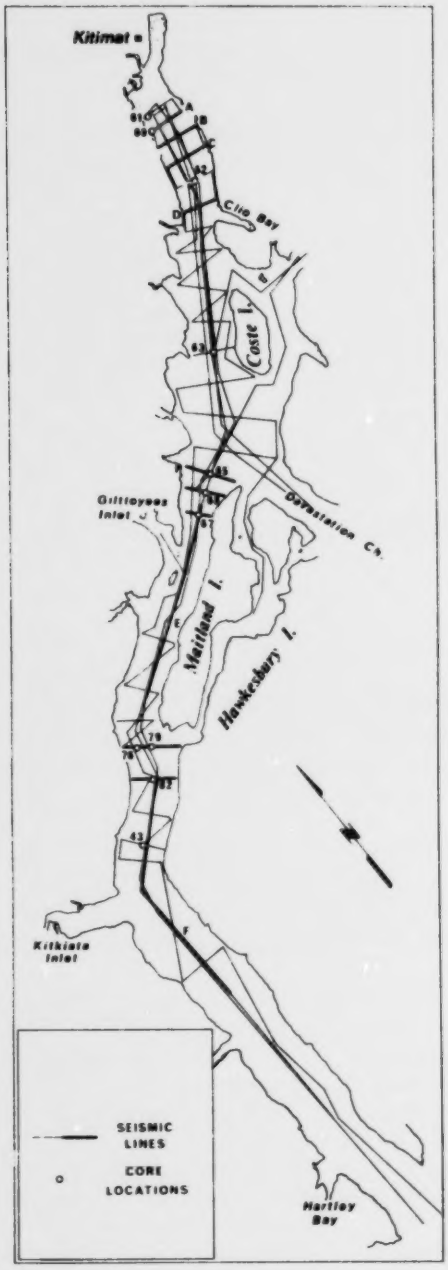

Fig. 2. Location of seismic lines and gravity cores. The heavier sections denote seismic lines illustrated in other figures.

and Souther 1964).

Duffell and Souther (1964) suggest that the Kalum-Kitimat Valley is the surface expression of a major fault in which the east side of the valley has moved upward and northward relative to the west side. This inference is based on the differences in rock types on either side of the valley, the occurrence of hot springs near Lakelse Lake between Kitimat and Terrace, and the linear nature of the feature. Roddick (1970) implies a similar movement, presumably along faults through the Douglas Channel area.

The surficial geology has been studied in the Kitimat Valley by Dolmage (1956), Duffell and Souther (1964), Armstrong (1966), Clague and Hicock (1976), and Clague (1977), and has been summarized by Bell and Kallman (1976). Pleistocene marine muds containing shells occur at elevations up to 122 m above sea level at least 80 km inland from the present Kitimat delta. These sediments are associated with sands and gravels of marine deltaic origin (Clague and Hicock 1976) up to elevations of about 230 m. Locally marine muds contain a thin till, the result of a minor late glacial readvance.

BASIN MORPHOLOGY

Douglas Channel possesses a typical fjord morphology with steep bedrock walls and smooth sediment-floored basins separated by sills of rugged relief. The channel system is approximately 70 km long and is divided into two principal basins, here called "Gil Basin" and "Maitland Basin" (Fig. 3) separated by a major sill located just south of Kitkiata Inlet (Fig. 1, 4). South of the sill Gil Basin deepens to more than 460 m in Douglas Channel and continues into Whale Channel where depths of 570 m are attained.

The main sill in Douglas Channel at 211 m depth stands approximately 200 m above the adjacent Maitland Basin floor and 60 m above the adjacent Gil Basin floor (Fig. 4). The steepest slopes occur on the south side of the sill with a broad area, several kilometres wide, of hummocky, irregular relief on the north side.

Maitland Basin is separated into two sub-basins by a minor sill between northern Maitland Island and the entrance to Gilttoyees Inlet. Maitland Basin attains a maximum depth in the more southerly sub-basin, 420 m in small depressions near southern Maitland Island and 410 m in a larger depression mid-way between the southern tip of Maitland Island and the main sill at Kitkiata Inlet. To the north of the smaller sill in Maitland Basin, the greatest depths are found in a broad depression near the junction of Devastation and Douglas Channels, between Coste and Maitland Islands. This part of the basin lies between 350 and 380 m with the greatest depths between northernmost Maitland Island and the mainland.

The floor of Maitland Basin rises gently and smoothly to a depth of about 210 m at the foot of hummocky, deltaic sediments of the Kitimat Delta (Fig. 5). These delta-front sediments extend approximately 6 km south of the subaerial edge of the Kitimat delta. Their morphology and origin through periodic slumping of unconsolidated sediment masses on the delta and along the fjord walls have been discussed in some detail by Swan (1978), Packman and Bradshaw (1977), Luternauer and Swan (1978) and Prior et al, (1982).

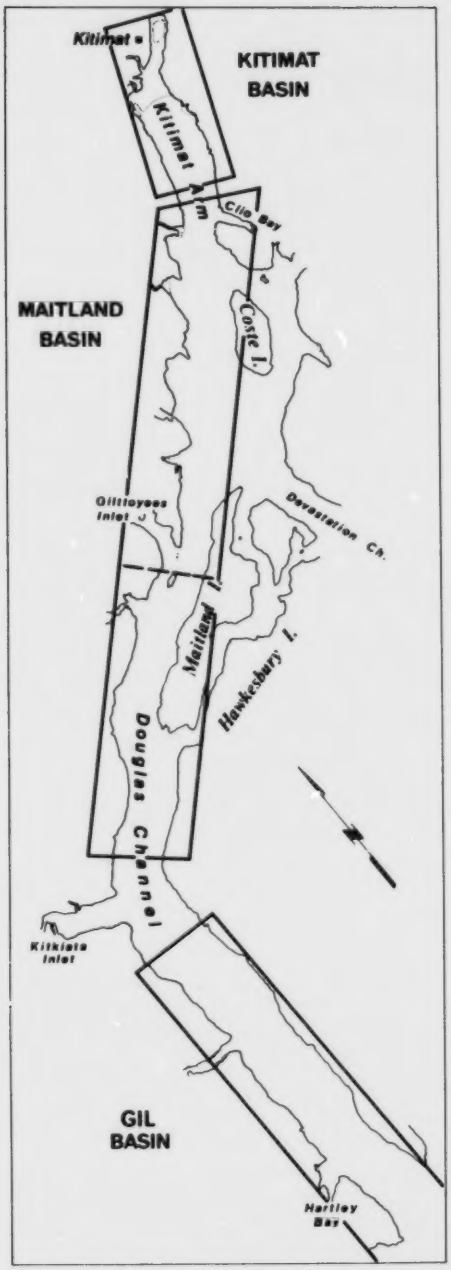

Fig. 3. Location map showing the main depositional basins in Kitimat Arm and Douglas Channel. Dashed line marks position of small bedrock sill which subdivides Maitland Basin.

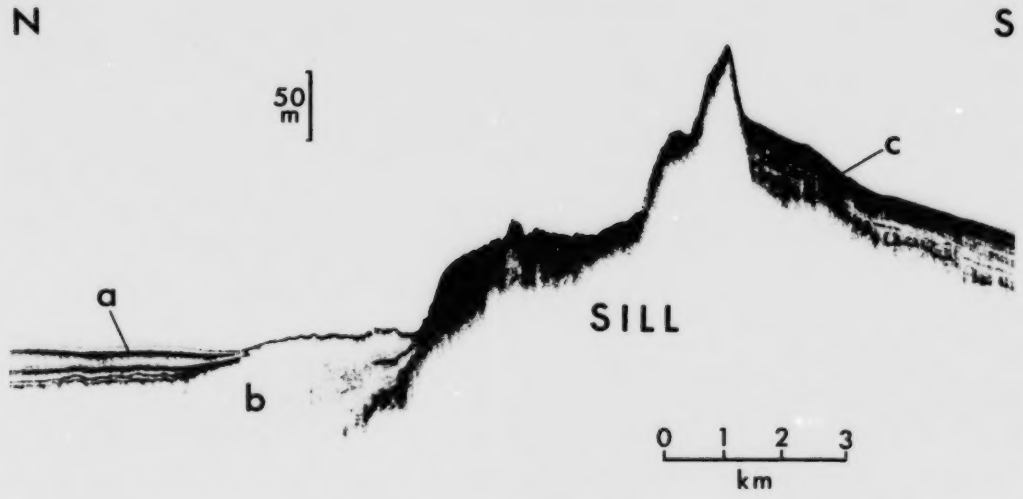

Fig. 4. High-resolution (3.5 kHz) seismic reflection profile across the main sill near Kitkiata Inlet (Line F, Fig. 3) showing the steep-sided sill, the surficial stratified sediments (a) north of the sill overlying a thick sequence of transparent sediments (b) which outcrop near the sill, and the highly reflective, stratified sediments (c) which lap onto the south side of the sill.

A third basin, here called "Kitimat Basin" (Fig. 3, 6), at one time occupied northernmost Kitimat Arm but is now entirely filled with sediment. The history of this basin is discussed in more detail below.

RESULTS

Seismic Velocities

A reversed seismic refraction profile was undertaken down Kitimat Arm using an air gun source and a sonobuoy receiver in an attempt to obtain information on the seismic velocity distribution within the sedimentary section and thereby to determine the true thickness of particular stratigraphic units. Because of the low-frequency acoustic source and filtering at the receiver, the seafloor was not, in fact, "seen" in this refraction experiment; the velocity of the surficial sediments is probably very close to that of the overlying seawater. A reliable interval velocity of 1862 m/s was obtained, however, for the sediment section from a few meters depth to very near the sediment-bedrock interface. Probably because of a highly irregular bedrock surface, no reasonable bedrock velocities were obtained in this experiment.

For the purposes of computing actual sediment thicknesses, a velocity of 1600 m/s has been assumed for surficial sediments (50 m) and the measured average value of 1862 m/s has been used to calculate thicknesses deeper in the sedimentary section as well as total sedimentary thicknesses.

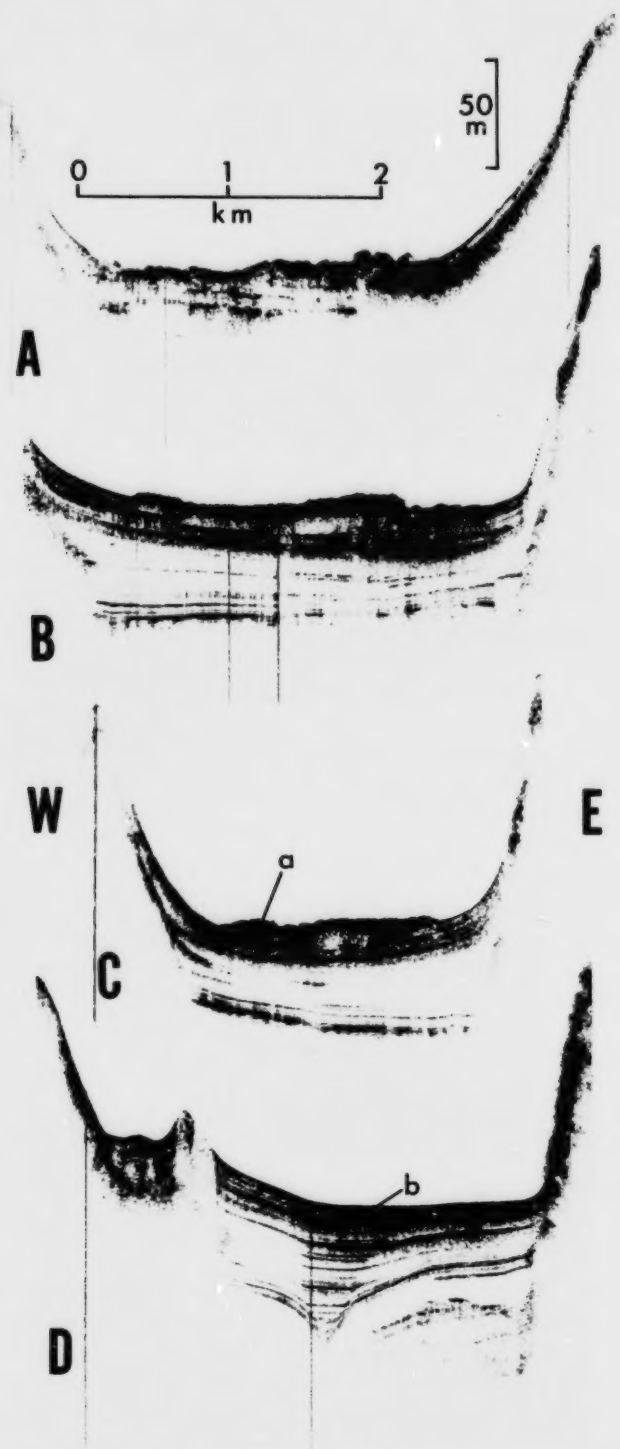

Fig. 5. High-resolution (3.5 kHz) seismic relection profiles across Kitimat Arm (see Fig. 3 for locations) showing the hummocky, surficial sediments (a) overlying smooth stratified sediments in northern Kitimat Arm and the smooth, reflective strata (b) at the surface in southern Kitimat Arm.

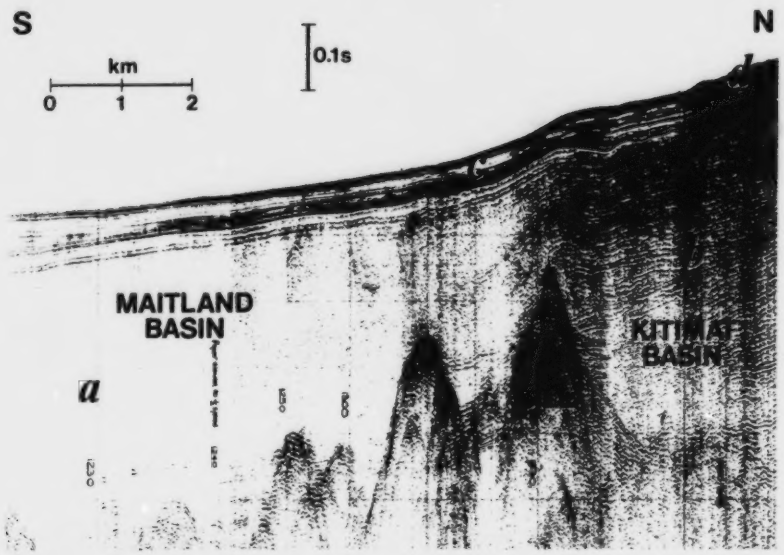

Fig. 6. Deep seismic relection profile across the sill between Kitimat Basin and Maitland Basin. a-transparent sediments, Maitland Basin; b-stratified sediments, Kitimat Basin; c-stratified surficial sediments in both basins; d-chaotic, landslide material originating on Kitimat delta slope.

Stratigraphic Units

Total sediment thickness

The variations in total sediment thickness along the axis of the fjord shown in Fig. 7, are based on air-gun seismic reflection profiles. Sediment thicknesses greater than 0.5 s (two-way travel time; approximately 500 m) are found beneath the main sill near Kitkiata Inlet, between Coste Island and Maitland Island and in Kitimat Arm north of Clio Bay. Unlike the main sill, composed of glacial and glaciomarine sediments, the smaller sill off central Maitland Island is bedrock.

A schematic summary of the stratigraphic successions in each of the three basins is given in Fig. 8.

Gil Basin

Based on air-gun and 3.5 kHz seismic profiling two distinct sedimentary units can be recognized in Gil Basin (Fig. 8). The lower stratigraphic unit (unit c, Fig. 9; unit b, Fig. 10) ranges from 0.2 to 0.5 s (180-500 m) in thickness and consists of a sequence of highly reflective, stratified sediments. The intensity and number of reflectors appear to increase towards the surface and many of the reflectors near the top of the unit are irregular and appear to continue laterally into horizons associated with the sill between the two main basins (Fig. 9). These irregular strata are overlain unconformably by a sequence of smooth, parallel reflectors which dip southward away from the sill.

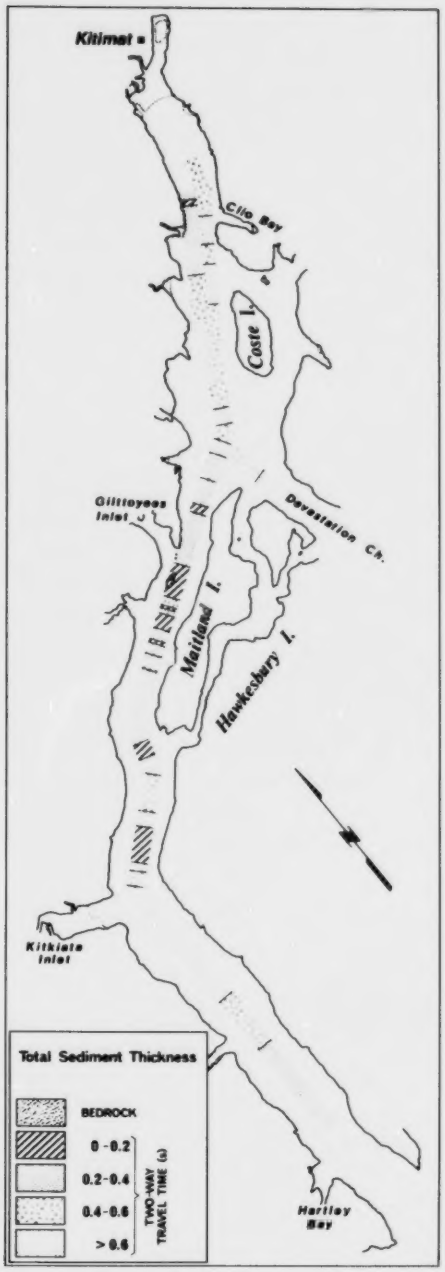

Fig. 7. Total sediment thickness above bedrock based on air-gun seismic reflection profiles.

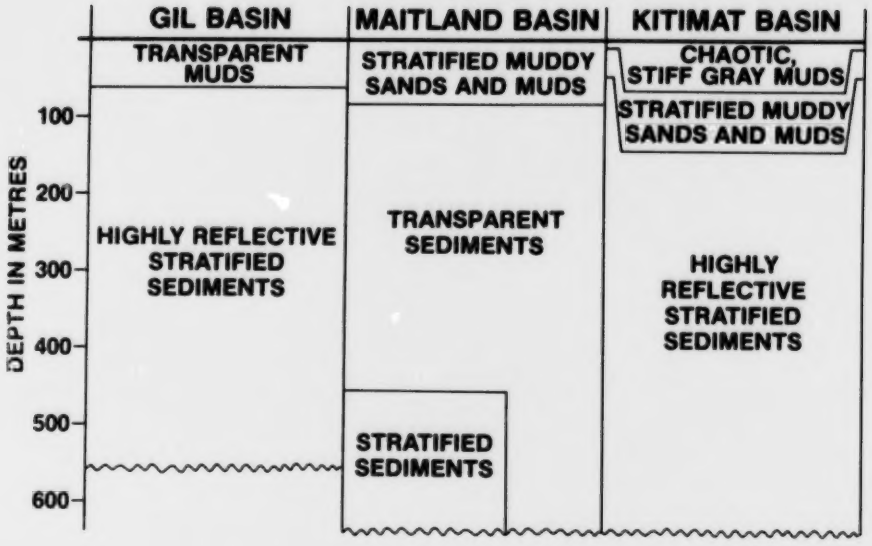

Fig. 8. Schematic summary of stratigraphic successions in Gil, Maitland and Kitimat Basins.

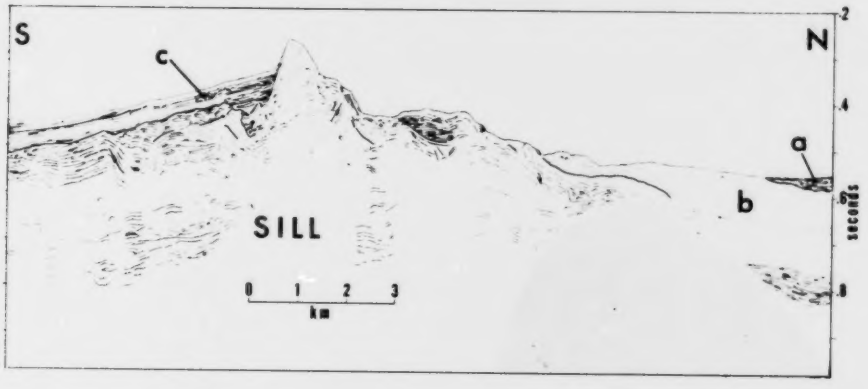

Fig. 9. Deep seismic reflection profile (line F) across the main sill. The sedimentary units are the same as those shown in Fig. 4, the stippled pattern is bedrock. The vertical scale is two-way travel time (seconds).

The upper stratigraphic unit in Gil Basin (Fig. 8; unit a, Fig. 10) is a northward-thinning wedge of more transparent sediments up to 60 m thick. This unit pinches out against the underlying stratified sequence approximately 3.5 km south of the main sill. Erosion in southernmost Douglas Channel, near the junction with the southern end of Devastation channel, has removed an unknown thickness of this surficial unit and approximately 15-20 m of the underlying stratified sediments (Fig. 10).

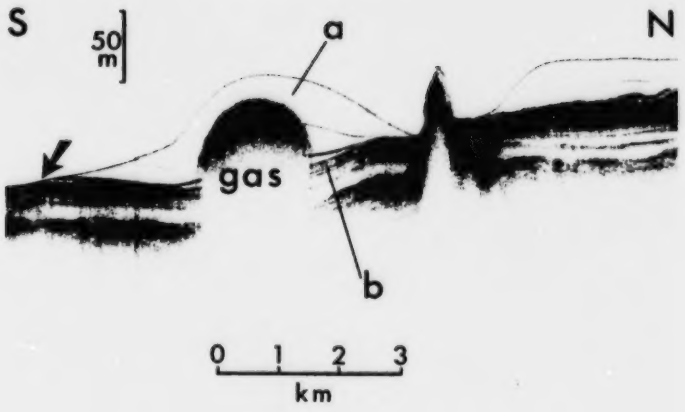

Fig. 10. High-resolution (3.5 kHz) seismic relection profile in Douglas Channel south of Hartley Bay. This profile shows: (i) the nearly transparent surficial sediments (a) overlying reflective, highly stratified sediments (b); (ii) evidence of erosion of both units (a) and (b) (arrow); and, (iii) a small pocket of gas.

An "acoustic mask", or "acoustic termination anomaly" (Kvenvolden et al. 1979), interpreted to be a small pocket of gas, similar to those described elsewhere in British Columbia inlets (Schurer and McFarlane, 1980) occurs within these surficial sediments in southernmost Douglas Channel (Fig. 10). At its shallowest point, this "mask", which obliterates deeper reflectors, lies about 20 m below the sea floor.

Main Sill

The sill between Gil and Maitland Basins is characterized by an absence of coherent reflectors directly beneath the peak, by undulating and high-angle parallel reflectors on the flanks, and by small basins infilled by horizontal strata (Fig. 9). The total sediment thickness beneath the sill exceeds 0.8 s (800 m). Several reflectors can be traced from the sill sediments into the adjacent basinal sedimentary units. Canadian Hydrographic Service field sheets show a great abundance of gravel on the sea floor in this area in contrast to the basin floors to the north and south which are dominated by mud.

Maitland Basin

Three sedimentary units, consisting of a discontinuous stratified unit overlain by an extensive transparent unit, in turn overlain by a discontinuous highly stratified sequence, are recognized in Maitland Basin (Fig. 8). The lowest unit in Maitland Basin consists of up to 0.2 s (190 m) of generally stratified sediments (unit c, Fig. 11) overlying a very irregular bedrock surface with up to 0.35 s (280 m) relief. In some areas, such as near the main sill the basal parts of the unit appear more transparent than the upper parts; elsewhere strong parallel reflectors occur throughout (Fig. 11). In general, the top of the unit slopes gently downward with increasing distance from Kitimat.

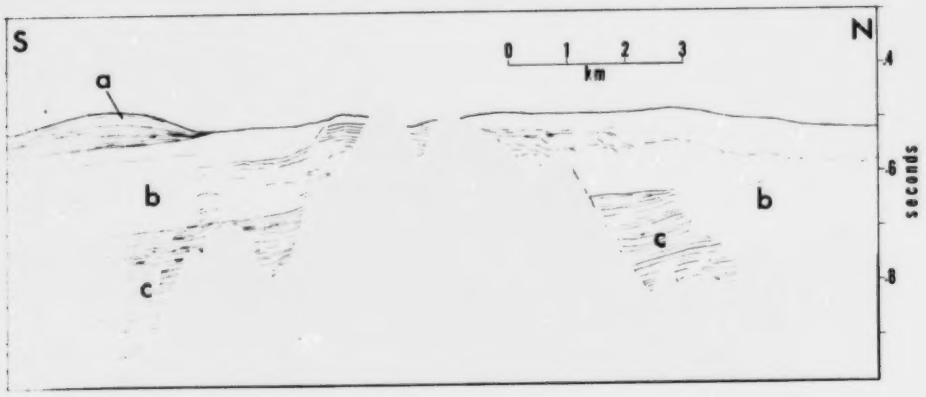

Fig. 11. Deep seismic reflection profile west of Maitland Island (line E, Fig. 2) showing the surficial stratified unit (a), the thick transparent sediments (b), and the deeper stratified sediments (c) over bedrock (stippled).

This lower stratified sequence appears to be absent in the area between northern Maitland Island and southern Coste Island, the broad area at the confluence of Devastation, and Douglas Channels (Fig. 11). It reappears in Kitimat Arm and similar sediments can be seen beneath the present Kitimat delta.

Overlying these stratified sediments is an acoustically transparent unit (Fig. 8), ranging from 0.1 to 0.4 s (100 - 375 m) thick, which occurs throughout Maitland Basin (unit b, Fig. 11). These sediments occur as a drape of relatively uniform thickness over the underlying sediments and the steep fjord walls, frequently to more than 100 m above the present basin floor (unit b, Fig. 12). Acoustically similar sediments are not present in Gil Basin or Kitimat Basin. A few short, prominent reflectors can be seen within this unit particularly near the main sill (Fig. 9) and the sill between the Maitland and Kitimat Basins; in the latter case the reflectors dip steeply to the south and can be traced to the stratified sediments which fill Kitimat Basin. In the high-resolution profiles, two prominent horizons can be detected in these otherwise transparent sediments (unit b, Fig. 13) at a depth of 0.025 and 0.06 s (20 and 48 m) below the top of the unit. Near the small bedrock sill which separates the two sub-basins within Maitland Basin, erosion has removed several metres of the uppermost part of this unit (Fig. 13).

Two cores, 67 and 43 (Fig. 3, 14, 15), were obtained from areas where this transparent unit appears to be exposed on the basin floor. The sediments consist of olive, olive grey and dark grey very sandy muds and soft muds grading downwards to stiff muds. In core 67 coarse sand and clasts of very stiff mud more than 3 cm in diameter occur in a softer mud matrix and overlie a firm, homogeneous mud (Fig. 14). In core 43, a soft very sandy mud, containing medium sand to granules, wood and a well-rounded pebble (2 cm diam.), overlies 154 cm of stiff, gray muds which contain no sand (Fig. 15).

Water contents in core 67 range from 35 to 57 percent; the two near-

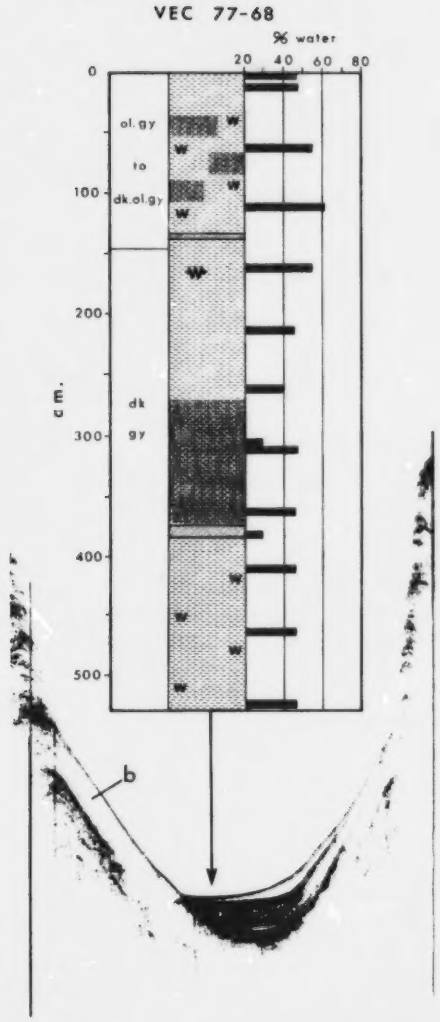

Fig. 12. Log of core 68 off northern Maitland Island. For legend see Fig. 15. Seismic profile shows stratified surficial unit overlying tranparent gray muds (b).

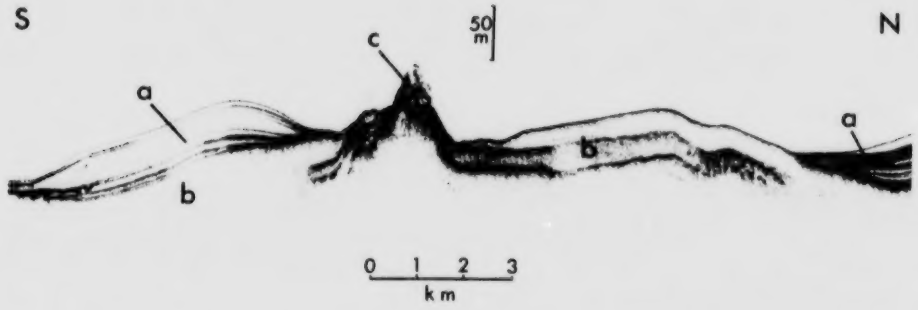

Fig. 13. High-resolution seismic profile across the low bedrock sill off northern Maitland Island showing the erosion of the outcropping transparent unit (b) near sill and the two parallel reflectors near the top of the transparent unit.

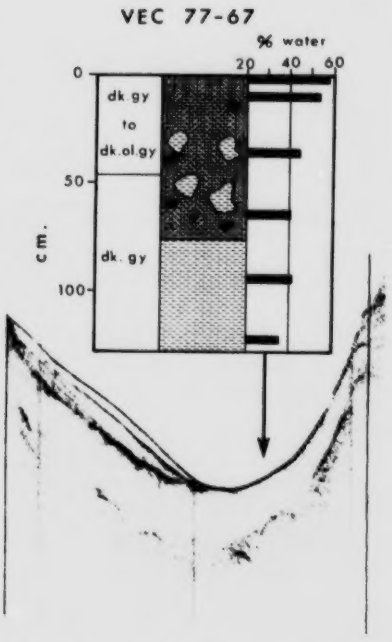

Fig. 14. Log of core 67 taken off northern Maitland Island in an area of thick transparent sediments, with surficial stratified sediments confined to one side of the basin.

surface values taken at 0 and 10 cm were 56.9 and 52.4 percent, respectively, whereas the samples between 37 and 122 cm ranged from 35 to 45 percent with a mean of 40.5 percent. In core 43 no near-surface water contents were determined; values between 40 and 160 cm depth ranged from 37 to 43 percent with a mean of 38.7 percent, comparable to values obtained at similar depths in core 67.

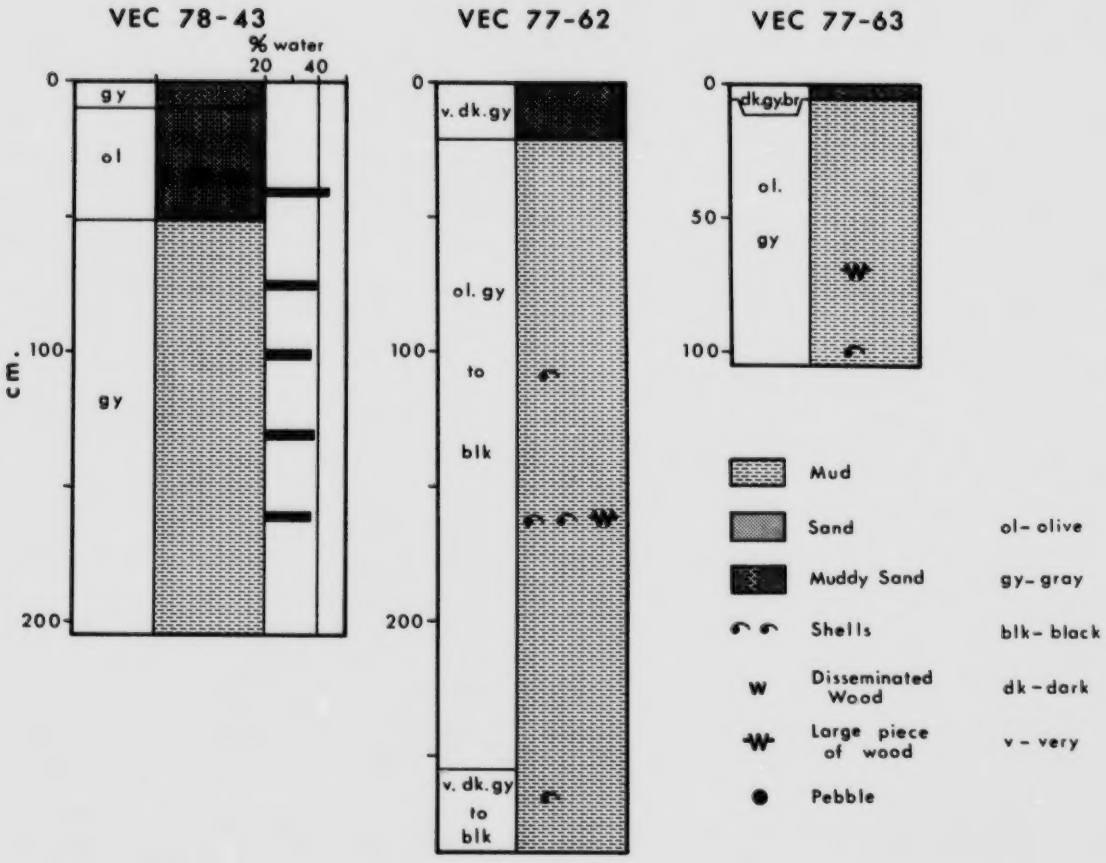

Fig. 15. Logs of three cores in Douglas Channel and Kitimat Arm.

The uppermost unit in the basin consists of two lenses of highly stratified sediments (Fig. 16; unit a, Fig. 17) up to 70 m in thickness. The larger can be traced from beneath the hummocky Kitimat delta-front sediments, through Kitimat Arm into the broad area between Maitland and Coste Islands and finally pinches out against the underlying transparent sediments off northwestern Maitland Island (Fig. 16 and 17). The smaller lens extends from near the mouth of Gilttoyees Inlet to a point 7.5 km southwest of the southern tip of Maitland Island (Fig. 14). The reflectors in the more northerly sub-basin appear to be more intense than those in the smaller lens.

These sediments do not, in general, cover the entire basin floor but, rather, occur "banked up" along one side of the fjord and frequently are absent from the deepest parts of the basin (Figs. 14, 18). From the isopach map of this unit (Fig. 16) and a comparison of the axis of maxium sediment thickness with the fjord thalweg (Fig. 19), the sedimentary unit can be seen to be displaced to the west and north sides of the fjord sub-basins.

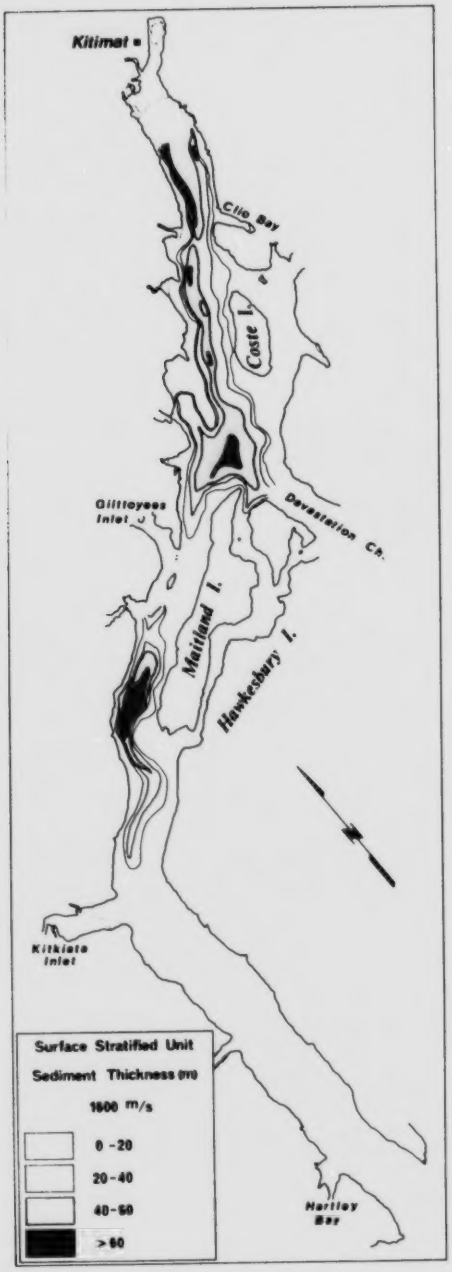

Fig. 16. Isopach map of the surficial stratified unit.

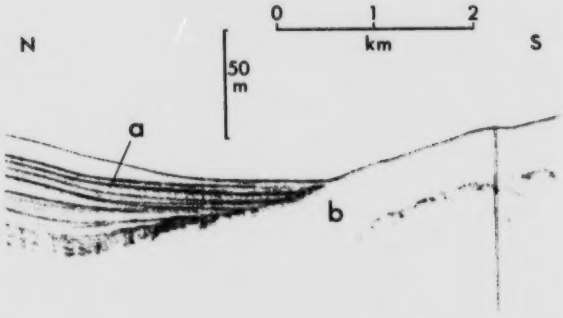

Fig. 17. High-resolution seismic reflection profile in mid-channel approximately between cores 67 and 68 (Fig. 3) showing the surficial stratified (a) pinching out against the underlying transparent sediments (b).

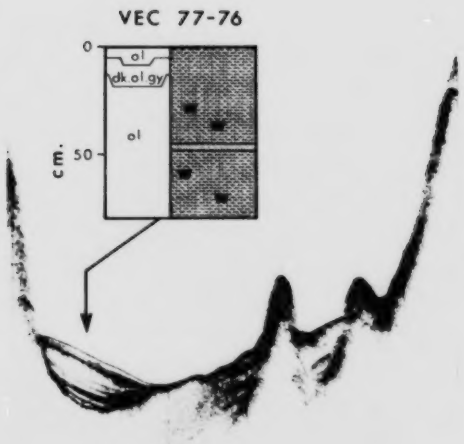

Fig. 18. Log of core 76 off southern Maitland Island and seismic profile showing inclined bedding surfaces of the surficial stratified unit.

Most of the cores obtained in Douglas Channel have been from this unit and have consisted of interstratified olive to olive-gray, soft muds and sandy muds with occasional 1 to 4 cm sand layers (Fig. 12, 15, 18, 20 and 21). Disseminated conifer needles, twigs, and shell fragments are common and occasional larger pieces of wood are encountered. Radiocarbon age determinations were obtained on two such pieces of wood from this unit: 6780 ± 185 yr B.P. (S = 1494) at 162 cm in core 62 and 1300 ± 220 yr B.P. (S = 1496) at 20 cm in core 82.

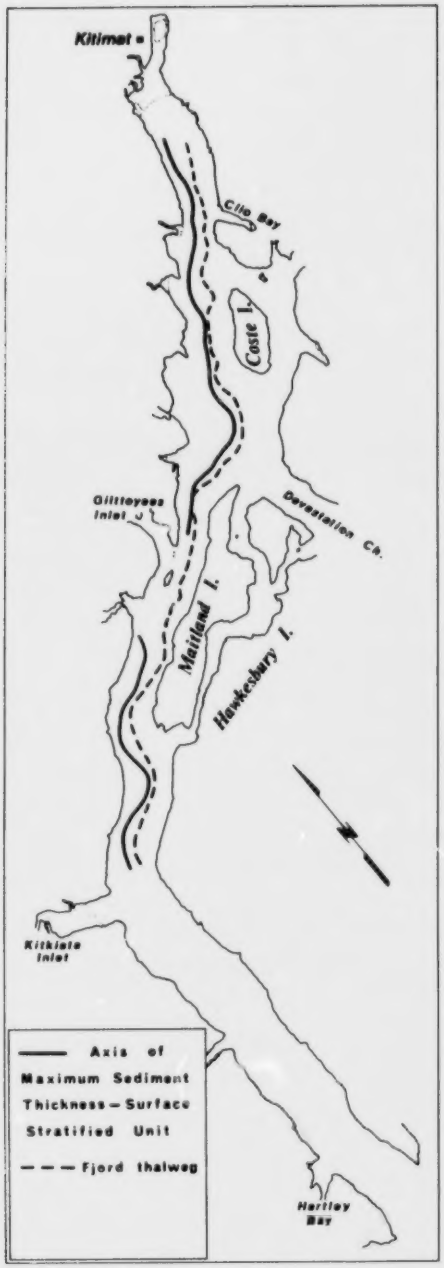

Fig. 19. Map of the fjord thalweg in northern Douglas Channel and the axis of thickest sediment accumulation unit.

Water contents for muds and sandy muds range from 35 to 65 percent with a mean of 47.7 percent and standard deviations of 5.7 percent for core 68 in the more northerly lens and a mean of 63.1 percent and standard deviation of 4.62 percent for core 82 in the more southerly lens (Figs. 12 and 21) suggesting somewhat higher values associated with less sandy sediments found farther down the fjord. There is a tendency towards somewhat lower values in the deeper parts of some cores. Sand layers have water contents of 20 to 30 percent.

Kitimat Basin

A prominent, buried bedrock barrier opposite Clio Bay (Fig. 6) separates a thick (> 0.65s; 600 m) sequence of highly stratified sediments overlying bedrock in Kitimat Basin (unit b, Fig. 6) from the transparent sediments (unit b, Fig. 6) in Maitland Basin to the south. Reflectors dip southward with occasional strata above the sill top continuing into the transparent sediments in Maitland Basin. These stratified sediments in Kitimat Basin continue upwards without interruption into the stratified sediments of the upper unit (unit c, Fig. 6) (0.05 s; 40 m) which can be traced directly into Maitland Basin as the uppermost stratified sequence (Fig. 8).

The surficial unit in northern Kitimat Arm (unit d, Fig. 6) consists of chaotic, stiff gray muds which have been described in some detail by Swan (1978). Submersible observations (R. Hoos, personal communication) revealed a surface of extremely rugged relief with near-vertical mud walls several metres high frequently with protruding broken cables and logs.

The surface morphology can be attributed to slumping events along the delta front and fjord walls, such as occurred in 1974 and 1975. In the better-documented 1975 event, approximately 60 x $10^6 m^3$ (Swan 1978) was displaced downslope and resulted in a deepening of the area by approximately 26 m (Golder and Associates 1975). The resulting deposit is 5 to 10 m thick. The event occurred as a result of minor construction activity nearby and took place during an extreme low tide. Such events are apparently common in areas near rapidly prograding fjord-head deltas in British Columbia (eg. Terzaghi 1956; Golder and Associates 1975) and Norway (Bjerrum 1972).

DISCUSSION

Deglaciation of Douglas Channel and Kitimat Arm

The observed distribution of sedimentary units in the fjord can be integrated with the results of surficial mapping in Kitimat Valley (Clague 1977) and radiocarbon age determinations in the area to describe the late Quaternary history of the Douglas Channel system.

Deglaciation in the southern part of the fjord probably began about 13,000 yr B.P. A radiocarbon date of 12,700 ± 120 yr (GSC - 2290) from near Prince Rupert indicates that the outer mainland coast was free of ice by that time (J.J. Clague, personal communication). Ice receded rapidly to approximately Kitkiata Inlet where it apparently stabilized sufficiently long to produce the morainal sill which separates Gil and Maitland Basins. The irregular, reflective stratified sediments in Gil Basin which pass into the

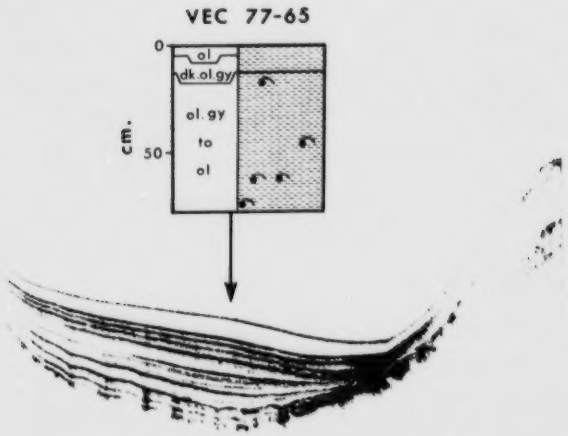

Fig. 20. Log of core 65 just north of Maitland Island and seismic profile showing a thick sequence of stratified sediments.

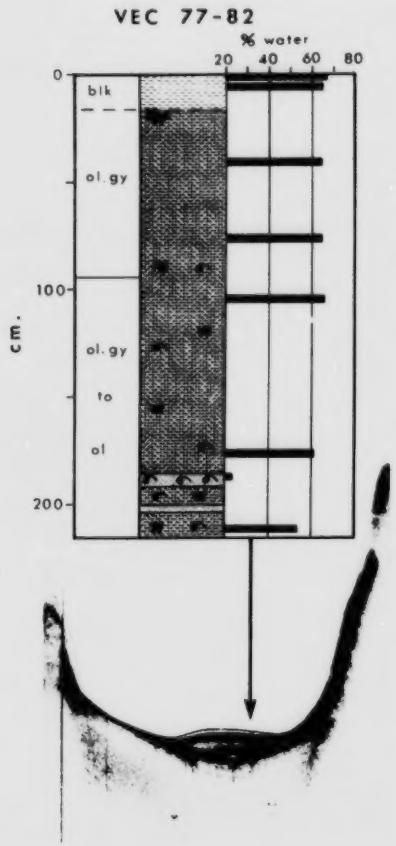

Fig. 21. Log of core 82 south of Maitland Island and seismic profile showing a lens of stratified sediments over a thick sequence of transparent sediments.

chaotic, gravelly sediments of the sill, are interpreted as ice-contact materials deposited during this recession. The smooth, parallel reflectors which overlie them are thought to be glaciomarine outwash which emanated from the stationary ice front. Based on the total time available to deglaciate Douglas Channel - Kitimat Valley and the number of such recessional moraines which occur within it, it is doubtful that ice remained stationary near Kitkiata Inlet for more than a few hundred years. Allowing time for a stillstand to produce the main sill, ice withdrew up Douglas Channel at an average rate of 8-10 km/100 years.

Following the emplacement of this main sill, at about 12,000 yr B.P., ice withdrew to a position near Kitimat where it again stabilized to produce a small moraine (Clague 1977). The oldest radiocarbon date from the Kitimat area is 10,000± 160 yr B.P. (J.J. Clague, personal communication) on marine shells and indicates that the area was certainly ice-free at least by that time and more probably prior to 11,000 yr B.P. since radiocarbon ages from farther north in the Kitimat Valley (Lakelse Lake) show that ice had already withdrawn more than 40 km up the valley by 10,800 yr B.P.

The thick blanket of acoustically transparent, grey marine muds and sandy muds, with occasional ice-rafted pebbles, seen in the deep and shallow seismic reflection records and cored at sites 67 and 43 was deposited following the retreat of the ice from the fjord. Very similar sediments are presently accumulating in several Alaskan fjords near receding glaciers (Carlson et al. 1978; Molnia 1979; Carlson et al. in press) at rates of between 0.5 and 4 m per annum. If similar rates are applied to Douglas Channel, all of the sediment fill in the main basin can easily be accounted for in 500 to 1000 years. This time estimate is not unrealistic given the constraints of the radiocarbon age determinations cited above. These calculations do not, however, preclude the presence of much older glacial or glaciomarine sediments in the lowermost part of the sedimentary section.

As ice stagnated near Kitimat tremendous volumes of stratified outwash were shed from the front of the moraine and filled the small Kitimat Basin in northernmost Kitimat Arm. As these coarse sediments overlapped the bedrock sill they occasionally became interstratified with the transparent glaciomarine muds which were accumulating in Maitland Basin immediately to the south.

Following this brief stagnation near Kitimat ice retreated rapidly up the Kitimat Valley to near Terrace and, after a brief readvance (Duffell and Souther 1964) shortly after 10,800 yr B.P. (Clague 1980), receded completely from the Kitimat Valley. During the recession up the Kitimat Valley, thick deposits of grey marine clay, similar to those encountered in Douglas Channel, were deposited in the valley (Duffell and Souther 1964; Clague 1976). Along the margins of the basin, extensive marine deltas formed and rapidly filled large areas of the valley with thick sequences of sands and gravels (Clague and Hicock 1976). As the sea withdrew from the valley, fluvial sand and gravel deposits of more limited extent developed in the valley. Sea level reached its present position between 7700 and 8500 yr B.P. (Clague 1980).

Recent Fjord Sedimentation

When the marine basins in Kitimat Valley had filled and sea level had fallen substantially, fluvial sediments were brought to the ancestral Kitimat delta which began to prograde into Kitimat Arm. Although no precise dates are available for the initiation of deltaic sedimentation, it probably began about 9000 - 9500 yr B.P. since sea level was at least 38 m above present near Kitimat 9880 ± 160 yrs B.P. (GSC - 522) (Clague 1980).

The uppermost stratified unit in Maitland Basin in all likelihood began to be deposited at this time since it appears to be the result of hemipelagic sedimentation from surface waters interstratified with occasional coarser layers produced by sediment gravity flows, such as debris flows and turbidity currents (Middleton and Hampton 1973) originating near the foot of the delta or on the fjord walls in Kitimat Arm. These latter sediments are deposited episodically, most commonly as a result of subaqueous landslides on or near the delta where sediments with high water contents accumulate very rapidly. These landslides develop downslope into debris flows through agitation, which breaks up the physical structure of the mass, and through a consequent increase in water content which further reduces the strength of the sediment. The debris flows themselves are further transformed into turbidity currents through the erosion of the nose of the debris flow as it moves downslope (Hampton 1972). The turbidity currents, generally with densities only slightly greater than that of surrounding seawater, continue to flow along the basin floor. Similar mechanisms have been suggested to account for the stratified sandy sediments in fjords in Norway (Holtedahl 1965), New Zealand (Glasby 1978), and Alaska (Carlson et al. in press).

Few direct measurements of natural turbidity currents in fjords exist; one possibility is a measurement of 38 cm/s for approximately one hour in Alice Arm, British Columbia which was attributed to a slump-generated turbidity current (Littlepage 1978). Velocities of turbidity currents in fjord lakes in British Columbia have been estimated at 10 - 30 cm/s (Pharo and Carmack 1979; R. Gilbert personal communication).

One interesting aspect of recent deposition in Maitland Basin is the tendency for the upper stratified sediments to occur along the sides of the basin, a pattern which has been extremely stable since the initiation of gravity flow sedimentation 9 - 10,000 yr B.P. Two major influences on the flow paths in fjord basins of currents in the 10 - 40 cm/s range are the Coriolis force, which tends to force the flow to the right in the northern hemisphere, and topography, which can redirect the flow (Pharo and Carmack 1979). There is a very clear tendency for sediments to be thicker on the north and west sides of the fjord (Fig. 19) indicating an important control by Coriolis force. The axis of maximum sediment thickness does meander somewhat with respect to the thalweg, suggesting as well some topographic control by the fjord walls.

There is some evidence to suggest that the surface plume of sediment-laden water emanating from the Kitimat delta is deflected to the right (west) by the Coriolis force. No significant thickness of recent sediments occurs anywhere except associated with the upper stratified unit; older, stiff, gray clays outcrop over large areas of the basin floor. Although at present suspended particulate data are insufficient to assess the significance of

Coriolis force in deflecting the plume and thereby controlling sediment accumulation patterns, there is a tendency for surface salinities to be lower on the west side of Kitimat Arm (Bell and Kallman 1976). Tabata and Pickard (1957) observed the same type of salinity distribution in Bute Inlet and attributed it to Coriolis force. The influence of the Coriolis force on sedimentation plumes has been observed by Pharo and Carmack (1979) in Kamloops Lake, British Columbia where markedly higher turbidity on the north side of the lake is reflected in the underlying bottom sediments by coarser mean grain size, higher sedimentation rates and lower trace element concentrations and by Pickrill and Irwin (in press) in Lake Tekapo, New Zealand where higher sedimentation rates were noted along the east side of the lake.

Sedimentation Rates

From a study of the distribution pattern of the most recent sediments in the fjord basin it can be seen that some caution is required in using sedimentation rate determinations. Clearly over the past 9 - 10,000 years rates on the floor of the fjord have varied from 0 (or less where erosion has occurred) to more than 7 $m/10^3$ yr. Thus, sedimentation rate determinations are, in general, applicable only at the site where the measurements are made or in areas of comparable stratigraphic thickness, and average basin-wide sedimentation rates are probably of little value for most studies of sediment accumulation in fjords such as this.

One unresolved aspect of sediment accumulation rates in Douglas Channel concerns the discrepancy between estimates based on ^{210}Pb measurements and those based on radiocarbon age determinations. From the work of Macdonald et al, (1978) and Macdonald (1983) using ^{210}Pb, sediments in the upper stratified sediments are accumulating at a rate of 4.7 mm/yr (uncompacted) or 2.1 mm/r (compacted) off southern Maitland Island, a rate which is in good accord with stratigraphic inferences based on the late Quaternary history of the region. Radiocarbon dating of wood in sediments in the same area, however, yielded an age of 1300 ± 220 yr at a depth of 20 cm, or 0.15 mm/yr; sediments here are more than 35 m thick. Similarly, a radiocarbon data of 6780 ± 185 yr at 162 cm in Kitimat Arm yields an accumulation rate of 0.24 mm/yr in an area of very thick sediments. These rates are clearly less than one-tenth those determined by ^{210}Pb methods, and, furthermore, do not agree well with the estimates based on the total sediment thickness and the inferred time of initiation of deposition. Studies are planned in Douglas Channel to attempt to resolve these discrepancies.

CONCLUSIONS

Glacial ice began to withdraw up Douglas Channel at approximately 13,000 yr B.P. depositing stratified glacial and glaciomarine sediments in Gil Basin. By about 12,000 yr B.P. ice stagnated near Kitkiata Inlet shedding coarse glaciomarine outwash into Gil Basin and producing the large morainal sill which separates Gil Basin from Maitland Basin. After this brief halt, the retreat up Maitland and Kitimat Basins continued rapidly with ice pausing again at Kitimat, about 11,000 years ago, before continuing up the Kitimat - Terrace Valley.

Since Kitimat Basin was separated from Maitland Basin by a prominent bedrock sill, coarse, stratified glaciomarine sediments were deposited only in Kitimat Basin until it had completely filled, probably about 9,500 years ago. As Kitimat Basin was filling, a thick sequence of acoustically transparent grey muds, with occasional ice rafted pebbles, accumulated in Maitland Basin from suspended sediments settling through the water column to the sea floor.

As sea level approached its present position, about 8 - 9,000 years ago, deltaic sedimentation began in the Kitimat area which, through periodic landslides, debris flows and resultant turbidity currents led to the deposition of interstratified muds and sandy muds in Maitland Basin. Both the surface plume of sediment-laden river water and the bottom-following turbidity currents appear to have been significantly influenced by Coriolis force resulting in a thicker build-up of sediments on the north and west sides of the inlet.

Farther down the fjord, recent sediments are accumulating only in the deeper parts of Gil Basin. Bottom current activity in the vicinity of the main sill near Kitkiata Inlet is apparently too vigorous to permit deposition. It is interesting to note that at certain localities in the deepest parts of Gil Basin, where side channels enter Douglas Channel, significant erosion of both recent and late glacial sediments has taken place reflecting a significant local influence on the deep circulation by these other inlets.

ACKNOWLEDGEMENTS

I should like to express my appreciation to Dr. T. Lewis, Chief Scientist during the two Vector cruises, to R. Hyndman, E. Davis, M. Burgess, V. Allen, D. Swan and J. Collyer and to the officers and crews of the CSS Vector and CSS Parizeau for their cooperation and assistance.

At various stages during the preparation of the manuscript valuable discussions were held with J.J. Clague, R.W. Macdonald, R. Gilbert, D. Prior, W. Wiseman, H. Freeland, D. Stucci and R. Gillie. The manuscript was critically reviewed by J.J. Clague, R.W. Macdonald, T. Lewis, and R.A. Pickrill.

R.G. Currie very kindly provided the air-gun seismic profile in Douglas Channel, G. Riley assisted in describing the cores and W. Price and B. Sawyer drafted the figures.

REFERENCES

Armstrong, J.E. 1966. Glacial studies, Kitimat-Terrace area. Geol. Surv. Can. Pap. 66-1: 50.

Bell, L.M. and R.J. Kallman. 1976. The Kitimat River Estuary - Status of Environmental knowledge to 1976. Dept. of Estuary Working Group, Environment Canada, Special Estuary Series No. 6: 296 pp.

Bjerrum, L. 1972. Subaqueous slope failures in Norwegian fjords. Norwegian Geotechn. Inst. Bull. 37: 29 pp.

Bornhold, B.D. 1977. Echo-sounding and sub-bottom profiling in Douglas Channel and Kitimat Arm, British Columbia. Geol. Surv. Can. Pap. 77-1B: 265-268.

Carlson, P.R., B.F. Molnia, J. Hampton, A. Post, and T.J. Atwood, 1978. Post-deglaciation sedimentation in Yakutat Bay, Alaska. EOS 59: 296.

Carlson, P.R., M.C. Wheeler, B.F. Molnia, and T.J. Atwood. In press. Neoglacial sedimentation in Glacier Bay, Alaska. U.S. Geol. Surv. Circular.

Clague, J.J. 1977. Surficial geology, Kitimat, British Columbia. Geol. Surv. Can. Pap. Open File 470.

Clague, J.J. 1980. Late quaternary geology and geochronology of British Columbia. Part 1: Radiocarbon Dates: Geol. Surv. Can. Pap. 80-13: 28 pp.

Clague, J.J. and S.R. Hicock. 1976. Sand and gravel resources of Kitimat Terrace, and Prince Rupert, British Columbia. Geol. Surv. Can. Pap. 76-1A: 273-276.

Dolmage, V. 1956. Geology of Kitimat Area, British Columbia (103 IE1/2). Geol. Surv. Can. Mem. 329: 177 pp.

Duffell, S. and J.G. Souther. 1964. Geology of Terrace map area, British Columbia (103 I E½). Geol. Surv. Can. Mem. 329, 117 pp.

Glasby, G.P. 1978. Sedimentation and sediment geochemistry of Caswell, Nancy and Milford Sounds p. 19-37. In G.P. Glasby (Ed.) Fjord studies: Caswell and Nancy Sounds, New Zealand. New Zealand oceanogr. Inst. Mem. 79.

Golder, Brawner and Assoc. 1975. Report to B.C. Water Resources Service on investigation of seawave at Kitimat, B.C.: 9 pp.

Hampton, M.A. 1972. The role of subaqueous debris flow in generating turbidity currents. J. Sediment. Petrol. 42: 775-793.

Holland, S.S. 1976. Landforms of British Columbia - A Physiographic Outline. B.C. Dept. Mines Petrol. Res. Bull 48: 138 pp.

Holtedahl, H. 1965. Recent turbidities in Hardangerfjord, Norway. p. 107-141. In W.P. Whitiard and R. Bradshaw. (Ed.) Submarine Geology and Geophysics - Colston Papers. Butterworths, London.

Kvenvolden, K.A., C.H. Nelson, D.R. Thor, M.C. Larsen, G.D. Redden, J.B. Rapp. 1979. Biogenic and thermogenic gas in gas-charged sediment of Norton Sound, Alaska. Proc. 11th offshore Technology Conf.: 479-483.

Lewis, T., B. Bornhold, M. Burgess, E. Davis, R. Hyndman. 1978. Preliminary Results, PGC 77-6 Cruise, Vector, 1977. Geothermal Service of Canada, Internal Report. 78-2: 90 pp.

Littlepage, J.L. 1978. Oceanographic and marine biological surveys Alice Arm and Hastings Arm, British Columbia 1974-1977. Rept. to Climax Molybdenum Corp., Terrace, B.C. 77 pp.

Luternauer, J.L. and D. Swan. 1978. Kitimat submarine slump deposit(s): a preliminary report. Geol. Surv. Can. Pap. 78-1A: 327-332.

Macdonald, R.W., D.M. Macdonald, and P.S. Munro. 1978. Oceanographic data report Kitimat Arm, Porpoise Harbour February 1977. Pac. Mar. Sci. Rept. 78-24: 61 pp.

Macdonald, R.W. 1983. The distribution and dynamics of suspended particles in the Kitimat fjord system, In Proceedings of a workshop on the Kitimat Marine Environment, R.W. Macdonald, ed., Can. Tech. Rept. of Hydrogr. and Ocean Sciences, 18, 116-137.

Middleton, G.V. and M.A. Hampton. 1973. Sediment gravity flows: mechanics of flow and deposition. p. 1-38. In G.V. Middleton and A.H. Bouma (ed.) Turbidities and Deep-Water Sedimentation, Pacific Section, Soc. Econ. Paleont. Mineral., Los Angeles, Calif.

Molnia, B.F. 1979. Sedimentation in coastal embayments, northeastern Gulf of Alaska. Proc. 11th Annual Offshore Technology Conference: 665-670.

Packman, G.A. and V. Bradshaw. 1977. Environmental surveillance of Kitimat Arm, British Columbia. Environ. Protection Service Rept. EPS-5-PR-77-7: 33 pp.

Pharo, C.H. and E.C. Carmack. 1979. Sedimentation processes in a short residence-time intermontane lake, Kamloops Lake, British Columbia. Sedimentology 26: 523-541.

Pickrill, R.A. and J. Irwin. In press. Sedimentation in a deep glacier-fed lake, Lake Tekapo, New Zealand. Sedimentology.

Prior, D.B., B.D. Bornhold, J.M. Coleman and W.R. Bryant. 1982. The morphology of a submarine slide, Kitimat Arm, British Columbia. Geology, 10, 588-92.

Roddick, J.A. 1970. Douglas Channel - Hecate Strait map-area, British Columbia, (103 H). Geol. Surv. Can. Pap. 70-41: 56 pp.

Schurer, P.J. and W.T. McFarlane. 1980. Investigation of shallow water sediments offshore from Vancouver Island. Proc. Can. Coastal Conf. '80', Burlington, Ontario.

Swan, D. 1978. Acoustic imaging of the seabed in northern Kitimat Arm, B.C. unpublished B.Sc. Thesis, Dept. Geophysics and Astonomy, Univ. of B.C.: 72 pp.

Tabata, S. and G.L. Pickard. 1957. The physical oceanography of Bute Inlet, B.C. Jour. Fish. Res. Bd. Can. 14: 487-520.

Terzaghi, K. 1956. Varieties of submarine slope failure. Proc. Eighth Texas Conf. on Soil Mechanics and Foundation Engineering, Univ, Texas, Bur. Engineering Re., Austin, Texas.

LA DISTRIBUTION ET DYNAMIQUE DES PARTICULES EN DISPONIBILITÉ DANS LE KITIMAT FJORD

R.W. Macdonald
Institute of Ocean Sciences, Sidney, B.C.

RÉSUMÉ

La distribution des dépôts en disponibilité dans le système Kitimat fjord a été déterminé durant deux périodes; un écoulement maximum et minimum. On trouve dans les eaux profondes de basses concentrations des matières particulières ($0.1\ \mu L^{-1}$) et une grandeur representative dans les eaux marines paisibles. Prés du fond de re-suspension, on trouve souvent une prédominance characteristique des excellentes particules. Des procédés flaconneux et épais ont été identifier par une perte d'excellentes particules, et la formation en grosseur de plusieurs particules qui disparaissent en hauteur alors que la salinité augmente de 0-20 °/oo. En vue de tout ceci, le mélange d'eau douce et d'eau de mer est de ce fait, non conservateur, en ce qui concerne les matières particulieres. Un sac de dépôts (où sédiment) estimé par une variété de techniques, comprenant l'ajustement des particules, Pb-210 geo-chronologie, la puissance absorbée par les cours d'eau et les dépositions post-glaciales produit une image trés consistante. La plupart des dépôts en disponibilité, sont jeter tout pres de l'entrée des fleuves.

Macdonald, R.W. 1983. The distribution and dynamics of suspended particles in the Kitimat fjord system. Can. Tech. Rep. Hydrogr. Ocean Sci. 18, 116-137.

Mot-clés: compteur de coulter, estuaire, fjord, flaconneux, floculation, Kitimat, particulières, re-suspension, sedimentation, deposition, en disponibilité

THE DISTRIBUTION AND DYNAMICS OF SUSPENDED PARTICLES IN THE KITIMAT FJORD SYSTEM

R.W. Macdonald
Institute of Ocean Sciences, Sidney, B.C.

ABSTRACT

The distribution of suspended sediments in the Kitimat fjord system has been determined during two periods; maximum and minimum runoff. The deep waters are found to have low concentrations of particulate matter ($0.1\ L^{-1}$) and a size distribution representative of quiescent marine water. Near bottom resuspension is often found and is characterized by a predominance of fine particles. Above and within the pycnocline, flocculation processes have been identified by a loss of fine particles and formation of larger ones which disappear from the upper layer as salinity increases from 0-20 $^{o}/oo$. In view of this, mixing of fresh and sea water is expected and found to be non-conservative with respect to particulate matter. Sediment budgets estimated by a variety of techniques including particle settling, Pb-210 geochronology, river input and post-glacial deposition yield a consistent picture. Most of the suspended sediments are dropped within short distances of the river mouth.

Macdonald, R.W. 1983. The distribution and dynamics of suspended particles in Kitimat fjord system. Can. Tech. Rep. Hydrogr. Ocean Sci. 18, 116-137.

Keywords: coulter counter, estuary, fjord, flocculation, Kitimat, particle size distribution, resuspension, sedimentation, settling, suspended particulates

INTRODUCTION

During 1978-9 an oceanographic baseline study was conducted to determine the hydrocarbon levels in water, sediments and biota of the Kitimat fjord system. As a major part of this study, samples were collected during three cruises in June and October, 1978 and February, 1979. Measurements were made on hydrocarbons and support data were obtained on the water properties: salinity, temperature, reactive nutrients and oxygen content. Determination of suspended particulates was also carried out at 12 of the stations taken in October, 1978 and at 15 stations in February, 1979 for a total of 323 data points. The data have been reported elsewhere (Macdonald et al, 1983) and the interpretation of these data is provided here.

The Kitimat system is, morphologically speaking, a complex of connected fjords (Fig. 1) but in terms of the water properties it may be considered as an estuary. Macdonald, Bornhold and Webster (1983) have briefly reviewed some of the background features. Runoff occurs principally from two metered rivers, the Kitimat and the Kemano, but numerous smaller streams also contribute fresh water along the sides of the channels. The runoff is generally turbid and is expected to be important and perhaps dominant in terms of suspended particulate inputs to the system. Peak periods for runoff, and the associated land derived detritus are during May-July and October, while a winter minimum during January-March is observed (Fig. 2).

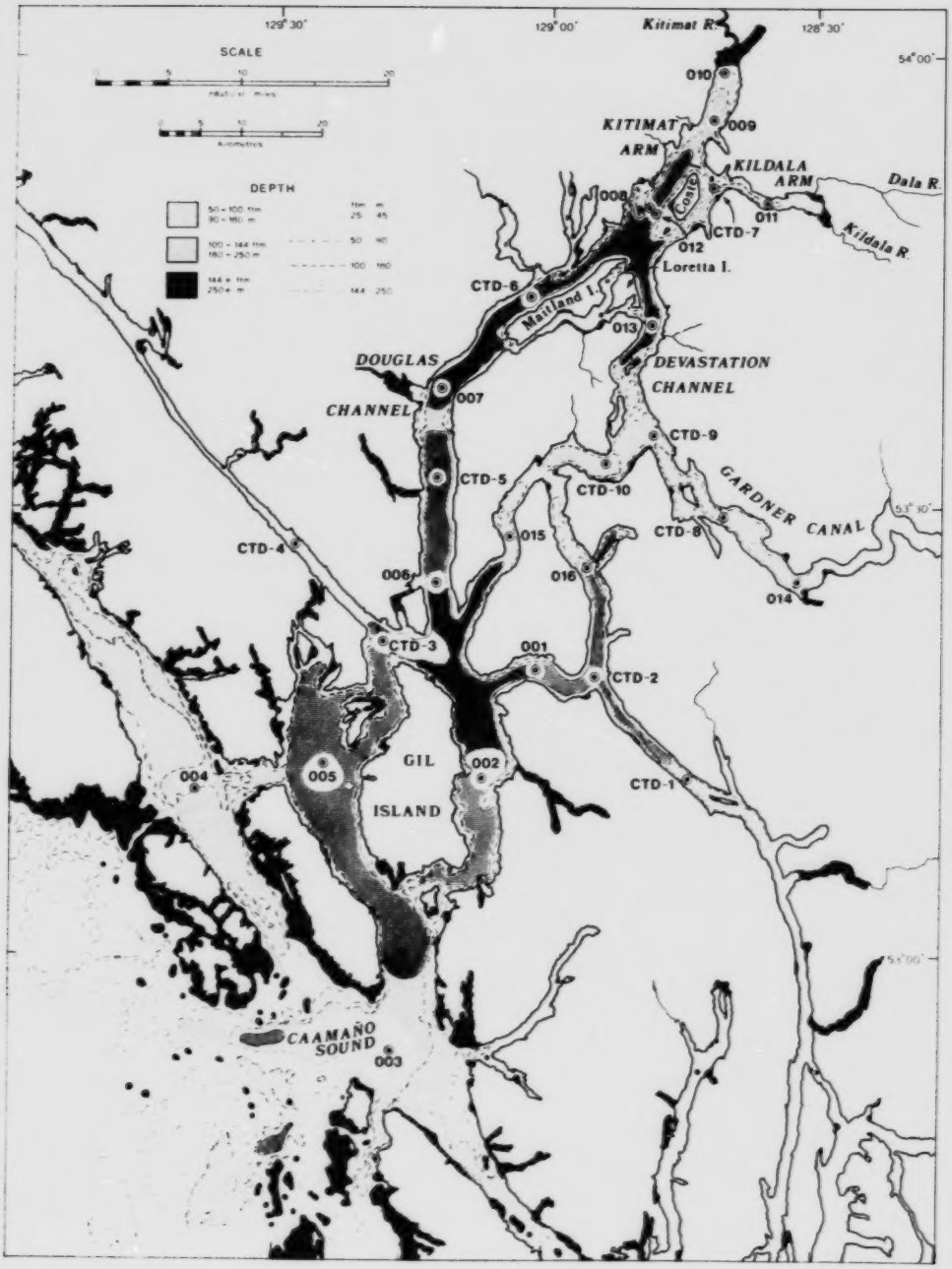

Fig. 1. Study area and station locations

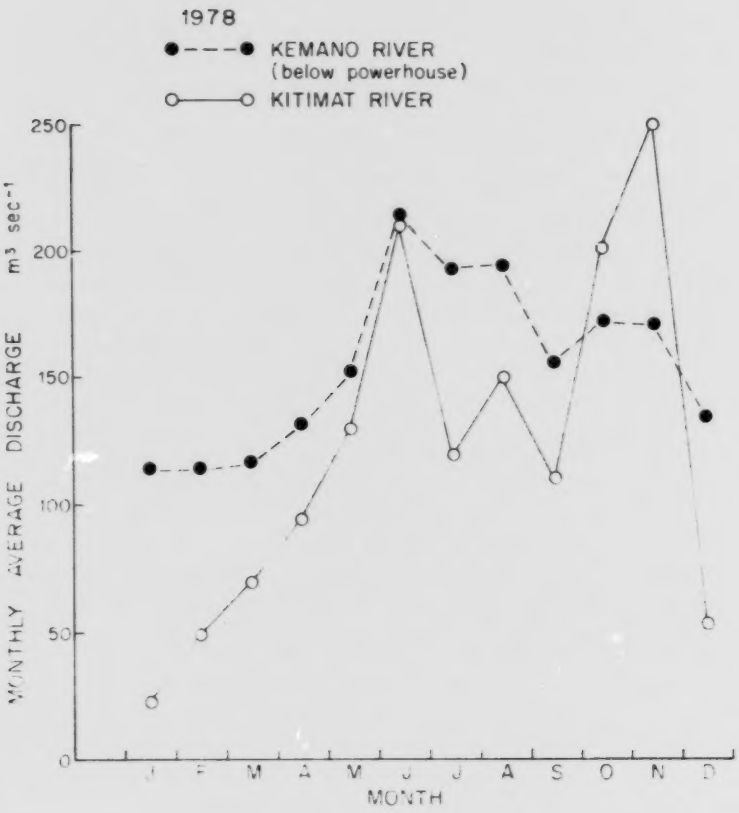

Fig. 2. Annual flow pattern in 1978 on the two metered rivers. The Kemano River is partly controlled by a power plant.

EXPERIMENTAL METHODS

Sampling and Analysis

Sampling was carried out from the MV Sea Lion and station locations were determined from charts using radar fixes. Stations at which samples were obtained for suspended particulates are shown in Figure 1.

Hydrocasts were made with 3 L capacity PVC water bottles (Seakem Oceanography Ltd.) at standard depths (H.O. Publication 607, 1968) with some modifications in the surface layer to obtain greater detail. After subsamples had been taken for dissolved O_2 measurement, the suspended particulate (S.P.) samples were obtained by twice rinsing a glass 300 mL screw cap bottle and then carefully filling it to prevent bubble formation. The same glass bottles were re-used from station to station.

Measurement of S.P. has been carried out by a variety of techniques some of which are summarized in Matsumoto and Wong (1977). During the present study, particle size distribution (P.S.D.) was measured immediately after

collection of the water using a Coulter Counter (Sheldon and Parsons, 1967). The concentration of particles between 4-64 μm in diameter was measured using the model TAII Coulter Counter in conjunction with a 200 μm aperture tube. Calibration was performed with standard 9.69 μm polystyrene beads and with 27.3 μm lycopodium. Due to the relatively small number of particles in sea water, samples were counted for a set time of 100 seconds. The counted volume, approximately 16 mL, was calibrated by determining the time required to count a 2 mL volume.

Suspended sediment was also determined for a few samples during the cruise in October, 1978, by suction filtration of 1-2 L of water through pre-weighed 0.45 μm Nuclepore filters. Each filter was washed with a small volume of distilled water and dried to constant weight defined as three consecutive weighings which agreed to ±0.05 mg.

Data Analysis

Data on P.S.D. are difficult to summarize in a simple fashion. In the present study, particle numbers were counted in 13 size ranges for each of 323 samples, a total of 4199 data points. A general approach has been to determine the volume of particles in each channel and sum the results for all channels to arrive at a total volume expressed as $\mu L\ L^{-1}$ (ppmV). In this process, information on the shape of the P.S.D. is lost.

In order to assist interpretation, Kitchen et al. (1975) have used characteristic vector analysis. The method is adequately reviewed by them and others (Chanut et al. 1977) but briefly consists of the following. The particle count data are converted to normalized volume. All of the data (323 samples, 13 channels) may then be considered as a 323 x 13 matrix and the characteristic vectors may be found. The procedure produces a set of row vectors which when multiplied by the appropriate scalar multipliers and added, reproduce the original data exactly. Each sample is thus represented by 13 scalar multipliers. The advantage of this procedure is that the vectors are arranged in order of importance and by considering only the first two for the present data set over 90% of the variance is removed. Plotting the first multiplier versus the second results in a visual display by which data may be quickly grouped.

RESULTS AND DISCUSSION

Particulate Distribution, October 1978 and February 1979

The two cruises during which particulates were measured occurred during a period of high runoff, October 1978, and during a period of low runoff, February 1979 (Fig. 2). Due to malfunctioning of the counter, a complete data set was not obtained during the October cruise, although the northern part of Douglas Channel, Kitimat Arm and Gardner Canal and its approaches were successfully sampled.

Figures 3(a) and 3(b) are the result of plotting scalar multiplier 1 versus scalar multiplier 2 for samples taken during the two cruises. Both plots have been scaled according to the range of scalar multipliers, but in October, 1978, much higher suspended sediment concentrations were encountered

resulting in a relative compression of background points in Figure 3(a). Error or variability has also been expanded in Figure 3(b), a fact which should be borne in mind during interpretation. The characteristic vectors are not the same for the two data sets and therefore points located at relatively the same place in Figures 3(a) and 3(b) may have slightly different particle size distributions.

Although the multipliers do not necessarily have any physical significance (Simonds, 1963) it is found here that scalar multiplier 1 loosely corresponds with total S.P. concentration, with volume of particulates increasing from left to right. Scalar multiplier 2 operates as a shape factor with points at the bottom of Figures 3(a) and 3(b) having much of their volume contributed by fine particles, while points at the top are generated by samples exhibiting bi-modality or significant contributions from larger particles. During computer analysis each sample was designated with a number and these are included in the figures only where they are mentioned in the text.

In Figures 3(a) and 3(b) the majority of points are clustered toward the left. The regions of dense clustering may be considered as "background" and represent water samples which were low in particulate content (less than 0.1 $\mu L\ L^{-1}$). This water was found below the pycnocline but far enough from the bottom not to be subjected to particulate input through resuspension.

Natural collections of small particles often have a size distribution which can be formulated by an equation of the form (Bader, 1970):

$$N = K\ x^{-c}$$

where K and c are positive constants, N is the number of particles larger than a given size (cummulative number) and x is a size parameter (eg. volume or radius). Nine of the lowest background samples from Figure 3(a) were averaged and plotted according to equation 1 resulting in the open circles in Figure 4. A similar procedure for the February 1979 background data points resulted in the closed triangle (Fig. 4). A representative plot showing volume versus size of particle for these background samples is shown in Figure 5(g). The form shown in Figure 4 has been observed previously and is thought to be characteristic of quiescent marine water (Bader, 1970). The deep waters of the Kitimat fjord system are therefore not extraordinary in terms of their P.S.D. and reflect their marine origin. The hyperbolic curve for the February data shows that in winter there are fewer particles larger than 6.8 μm. Settling coupled with a decrease in terrigenous or biogenous supply of particles is the likely explanation.

Noteworthy in Figure 4 is the "knee" at a particle size of about 8.8 μm. A "knee" has frequently been observed but has not been explained. Previous theoretical studies (Lehrman et al. 1974, Brun-Cottan, 1976) indicate that Stokes' Law is no longer obeyed when eddy diffusivity competes with settling. Brun-Cottan has suggested that 4-5 μm may be the critical size below which particles no longer conform to Stokes' behaviour. The actual size must be a balance between particle density, shape and size, and eddy diffusivity. The "knee" may be the point, in natural waters, at which turbulent diffusion and settling rate become competitive. Periodicity in the rate of supply of particles could cause alteration in the posiition of the "knee".

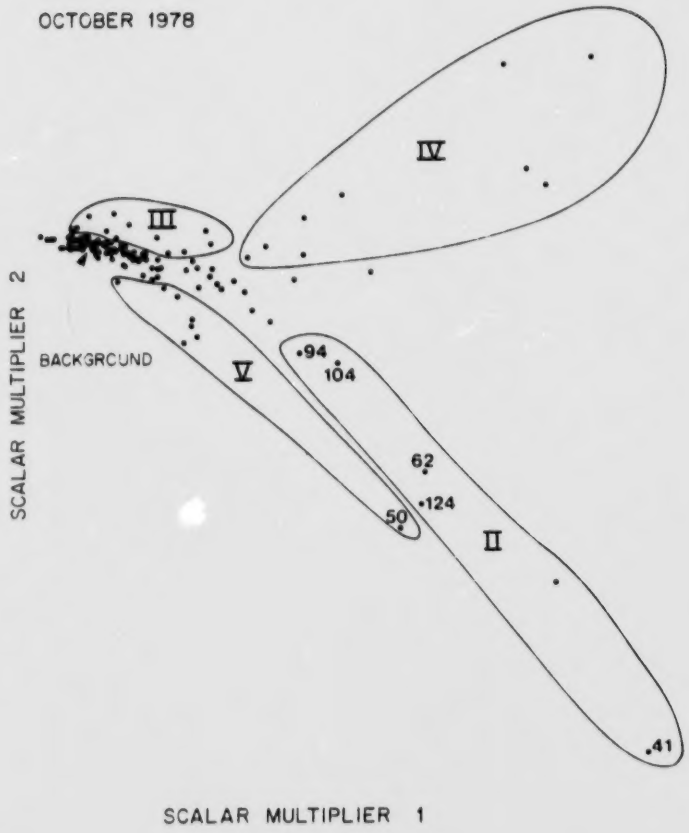

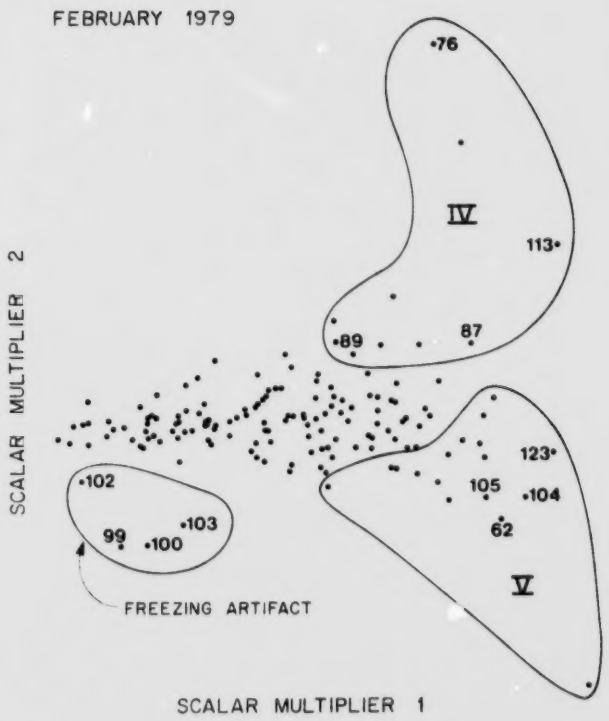

Fig. 3(a)(b). Plots of scalar multiplier 1 vs scalar multiplier 2 for the October 1978 and February 1979 particulate data. Scalar multipliers were generated by a characteristic vector analysis. The following regions are identified: I-Background, II-Surface samples, Kildala Arm and Gardner Canal, III-Below pycnocline 22-29 $^{o}/_{oo}$, 5-20 m, IV-Markedly bi-model samples, V-bottom resuspension.

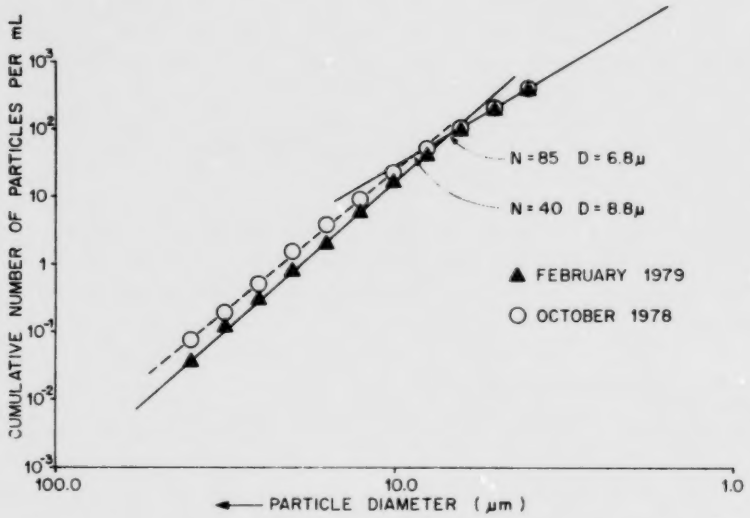

Fig. 4. Hyperbolic plot (Bader, 1970) of the distribution of particle size for background samples in October 1978 and February 1979. Figure 5 (g) shows the shape of the volume vs size curve for the 1978 data.

Several other groupings can also be distinguished in Figure 3(a),(b). The region marked II includes points from surface bottles taken in Gardner Canal and Kildala Arm during maximum runoff. Surface samples from CTD 9 (104) and CTD 10 (94) at the entrance to Gardner Canal might also be marginally included in this group. Volume contribution was predominantly from fine particles (Fig. 5(a)). All samples in this region had low salinities which were, with the exception of 104 and 94, less than 7.7 $^{o}/oo$. Samples of this sort were not found in February when surface salinities were much higher.

The third region identified on Figure 3(a) contains samples taken just below the pycnocline (22-29 $^{o}/oo$, 5-20 m). These samples appear to have been altered from background by the addition or formation of large particles and it is logical to suppose that settling from above or flocculation has taken place.

The region marked IV on Figures 3(a) and (b) contains samples which exhibit bimodality. In October 1978 the samples were taken at 1 m and 5 m from stations in Kitimat Arm or Douglas Channel (Station 8, 9, 10, CTD-7). Here the particulate concentration was high and there tended to be many larger particles resulting in a bimodal volume distribution (eg. Fig. 5(b)). In February (Fig. 3(b)) the samples in region IV also came from the top 10 meters but had high salinities (29 $^{o}/oo$). Figures 6 (c, d, e, f) show four of the volume-size distributions for this region; for two of the samples there is a second peak in particle concentration at about 20 m. This peak is at a slightly smaller size than the peak at 30-40 m observed in October (Fig. 5 (b, c, d) and perhaps reflects a different salinity - time history for runoff water during the two seasons or differing current speeds (c.f. Kranck 1973).

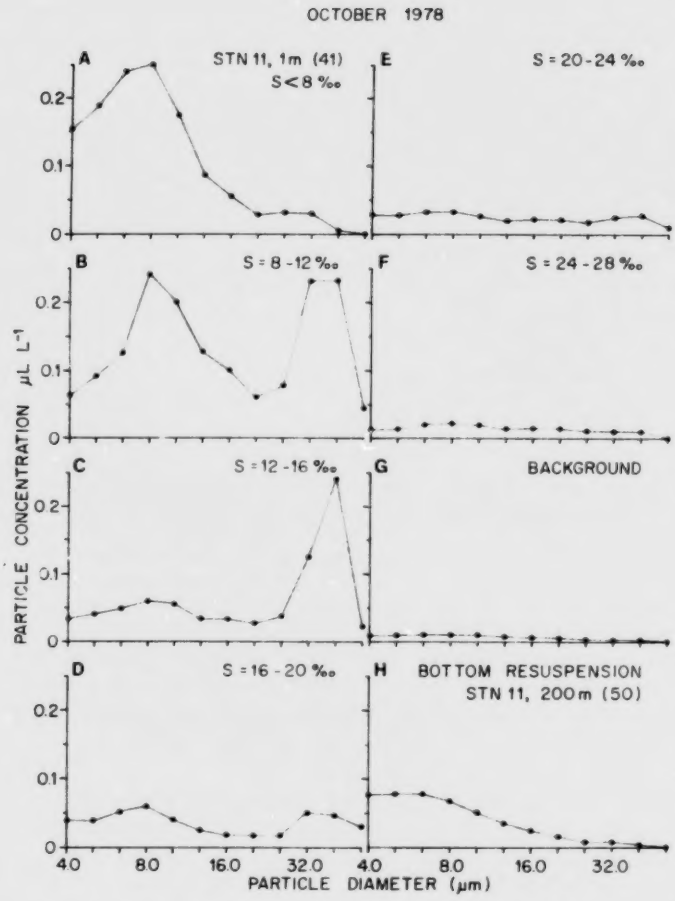

Fig. 5. Particle volume concentration vs size for selected samples, October 1978.

The alteration of particle size distribution with change in salinity can be seen in Figure 5 in which average volume concentration as a function of size is plotted for several salinity intervals. At low salinities (less than 8 °/oo) the total volume of particles is comprised predominantly of small particles grouped around 8 µm. As salinity (and mixing time) increases, the distribution begins to show marked bimodality with a second peak at about 32 µm. For salinity in the range 12-16 °/oo the contribution of fine particles around 8 µm is much reduced and in the 16-20 °/oo range, many of the particles around 32 µm have apparently been removed. The mechanism consistent with the observed behaviour is flocculation of runoff-derived fine particles as salinity is increased to 8-16 °/oo by mixing with sea water. Larger particles so formed settle out. The exact nature of the flocculation process is a complex function of the salinity time path along which the water passes but it has been observed before both in the laboratory (Sholkovitz, 1978) and in the field (Syvitski, 1979). It is interesting that in the above-mentioned laboratory study it was found that removal of trace elements (by flocculation) increased as salinity increased from 0 °/oo to between 15 °/oo - 18 °/oo but little additional removal occurred thereafter.

Flocculation and settling of particles should require that particulates be non-conservative when fresh and saline water are mixed. Figure 7 shows particulate concentration as a function of salinity, and curvature below 18 °/oo salinity is consistent with the loss of some particulates. This type of behaviour has been noted by others (Bornhold et al., 1972; Matsumoto and Wong, 1977), but Meade (1968) and Syvitski and Murray, 1981 have argued for conservative mixing. Recently, Farrow et al., 1982 have convincingly shown that suspended particulate loading is not conservative in Knight Inlet, B.C.; a highly turbid fjord. Since most authors agree that flocculation and agglomeration take place, and that sediments often form well-defined zones related to source (Manheim et al., 1972; Sharma, 1979; Syvitski and Macdonald, 1982), the mixing of turbid fresh water with sea water must ultimately be non-conservative. Disagreement in the literature has probably resulted from differences in time scale or turbulence. In the present study, volume concentration of particulates in Kitimat River water was not measured but estimates based on filtration measurements indicate that it was greater than 4 $\mu L\ L^{-1}$, and therefore the curvature in Figure 7 is not exaggerated. The dense cluster of points above a salinity of 28 °/oo represents background.

The open squares in Figure 7 and 8 denote bottom bottles and show the effect of resuspension. These points could also be differentiated on Figures 3(a,b) as the region marked V. Points found in this group appear to be background samples perturbed by the addition of fine particles. Figure 5(h) shows a representative plot of volume versus size for this type of sample.

In winter, during minimum runoff, the surface turbid layer was not found (compare Figs. 7 and 8). However, surface samples (Fig. 3(b), February 1979) from Station 10 (104, 105) Station 4 (123) and Station 6 (62) were placed in group V. Furthermore the shape of the volume versus size curve shown in Figure 6(a) resembles Figure 5(h). The salinity of surface water at all of these stations was above 29 °/oo so that flocculation of runoff derived particles should have already occurred. It is concluded that the particulate concentration in these winter surface samples has been augumented by resuspension of shallow water deposits rather than through runoff.

On Figure 3(b) there is a small region including numbers 99, 100, 102 and 103 which appears anomalous in that particulate concentrations are low and skewed toward fine particle size (Fig. 6(b)). These samples were taken at station 9 where very cold conditions caused some of the samples to freeze on deck before analysis. Frozen samples were rejected outright but the remaining samples were thought to have been unaffected and so were analyzed. The utility of characteristic vector analysis is shown by identifying these artifact-contaminated samples.

Density of Particulates

During the October 1978 cruise, particulate concentration ($mg\ L^{-1}$) was determined for some of the samples by filtration. The comparison between these data and those measured by Coulter Counter is shown in Figure 9.

Although the density of many silicate minerals is approximately 2.7 g cm^{-3}, aggregated particles suspended in a fluid may often have densities less than this as a result of occluded water and organic matter and may be as low as

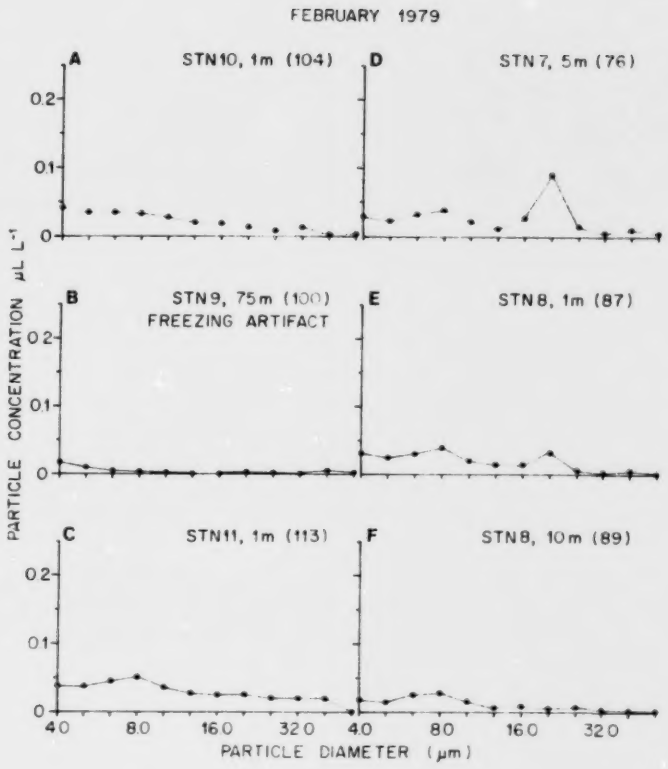

Fig. 6. Particles volume concentration vs size for selected samples, February 1978.

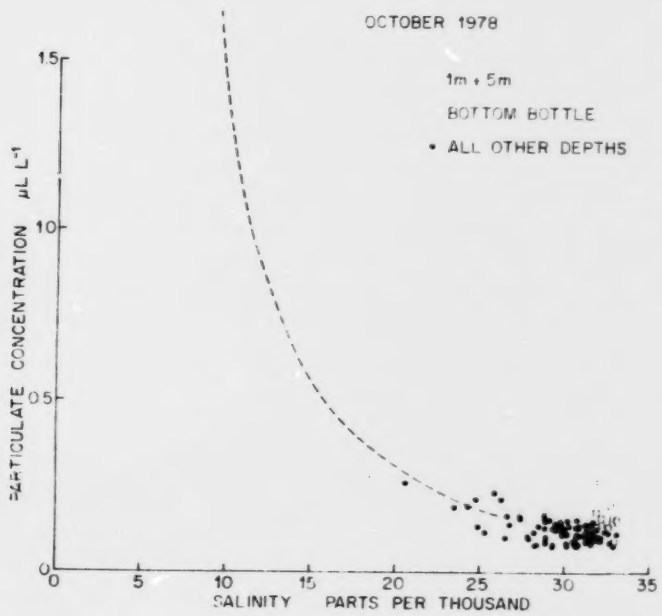

Fig. 7. Particulate concentration as a function of salinity, October 1978.

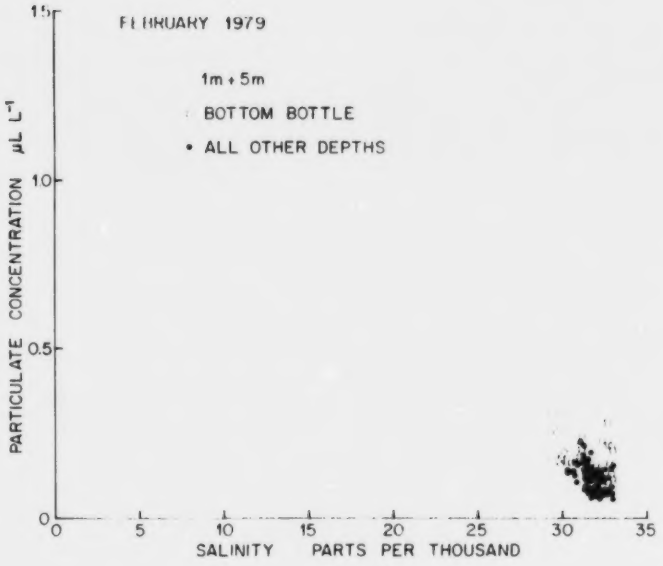

Fig. 8. Particulate concentration as a function of salinity, February 1979.

1.056 g cm^{-3} (Krone, 1976). The in situ density is the important parameter for the estimation of settling velocity, but there is a paucity of data, presumably due to the difficulty in making the measurements (Brun-Cottan, 1976). In a recent article, Gartner and Carder (1979) have used simultaneous volume (wet) and mass (dry) determinations for a selection of clay minerals to calculate in situ density. Following their method and terminology the following calculations ensue. The Coulter Counter measures wet volume ($V_p + V_w$) where V_p is the volume of the particulate matter and V_w is the volume of occluded water. Filtration measures the dry mass of the particle M_p. From these two experimental measurements the apparent density is calculated as:

$$\rho_\alpha = \frac{M_p}{V_p + V_w} \qquad (2)$$

The in situ density, however, is expressed as:

$$\rho = \frac{M_p + M_w}{V_p + V_w} \qquad (3)$$

Where M_w is the mass of occluded water. If the density of dried solids, ρ_d, is known, then the in situ density is:

$$\rho = \rho\alpha\ (1 - \rho_w/\rho_d) + \rho_w \qquad (4)$$

where ρ_w is the denisty of the water associated with the particle and may be

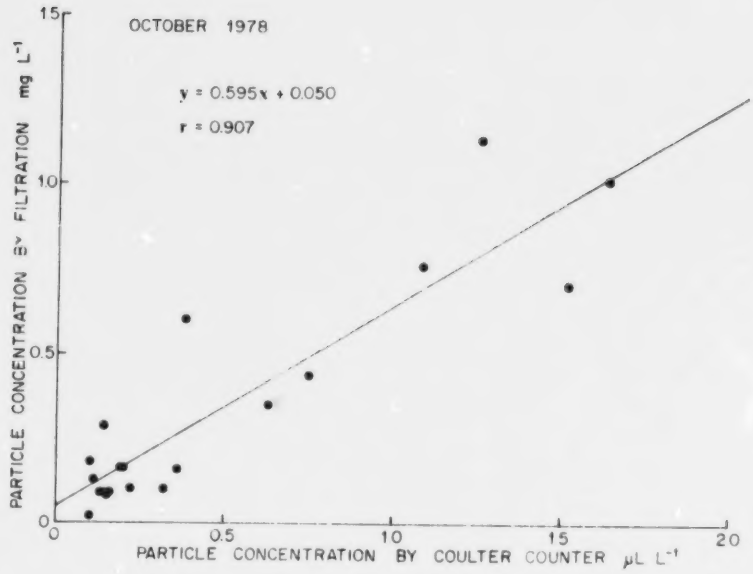

Fig. 9. Plot of particulate concentration determined by Coulter counting vs particulate concentration determined by filtration.

accurately assessed from a knowlege of salinity and temperature. Pycnometry performed on the dried solids of several cores in the Kitimat region has yielded a dry density of 2.55 ± 0.10 g cm^{-3} and is taken to be a reasonable estimate of ρ_d. The density of sea water used is 1.02 ± 0.01 g cm^{-3}. Using these density estimates and the simultaneous Coulter Counter and filtration data for 1 m and 5 m samples (turbid water above the pycnocline), the in situ density of particulates was found to be 1.38 ± 0.18 (2s) g cm^{-3}. Since Coulter Counter determines the total volume for a range of particles from 4-64 µm while filtration with a 0.45 µ filter traps smaller particles, it is expected that the density calculation will be an overestimate. Particles greater than 40 µm tended to be negligible for most samples (Fig. 5). Particles finer than 4 µm on the other hand, may have contributed non-trivial amounts. Their significance was estimated by extrapolating the hyperbolic plot for a worst case (Fig. 5(a)) to determine the number of particles in each size class from 4 to 0.45 µm. This process resulted in a decrease in the in situ density by 13%.

Particle Transport in the Surface Plume

The main sources of particulate matter in the Kitimat fjord system are runoff, biological production and atmospheric fallout. Of these the first is dominant, especially near river mouths, and displays an annual cycle (Fig. 2). The suspended solids brought in by rivers along the B.C. mainland coast consist predominantly of glacial flour with other important components including organic matter and dissolved elements, which may contribute to particle formation and transformation.

Solids introduced to the marine environment by rivers may be classified according to their transport properties. Much of the solid phase is coarse, and is transported by saltation (c.f. Biggs, 1978). This material drops out too quickly to be transported far by the surface plume. Fine sand (125 m), for example, settles about 10 m in 15 minutes. Further transport of coarse sediment requires other processes such as turbidity flows (Holtedahl, 1965; Terzaghi, 1956) or deep water sand flows (Syvitski, 1980). Finer material which remains suspended in the surface kplume forms the visually turbid water often associated with estuaries. Measurements or estimates of particle loading in the river can be quite different to those found in the plume. For example the Fraser river has a mean annual flow of 1960 $m^3 s^{-1}$ and a total sediment discharge of about 18×10^6 tonne a^{-1} (Water Survey of Canada 1967-77). A similar result is met when calculations are performed on the Mackenzie River (Bornhold, 1979; Davies, 1975) or the Mississippi (Manheim, et al., 1972).

For the finer material, settling according to Stokes' Law is a relatively slow method of downward transport. Efficient removal of the fines requires other mechanisms with three processes possible; flocculation of the solids, downward diffusion of the water and particulates, and fecal pelleting by zooplankton. The processes are inter-dependent: diffusion and entrainment of salt contributes to flocculation and flocculation assists fecal pelleting.

Flocculation commences as salt becomes entrained in the upper layer. According to the kinetics of particle agglomeration, the time-dependent decrease in numbers of particles may follow either a first order or second order rate law under mixed or quiescent conditions respectively (Stumm and Morgan, 1970). Where settling also occurs, the situation is more complex especially when a wide range of particle sizes are present. Kranck, (1980) has recently performed laboratory experiments on concentration as a function of settling time and her data show that settling by flocculation occurs in two distinct periods and her data show that settling by flocculation occurs in two distinct periods. Initially floc formation is strongly dependent on concentration such that after about three hours, particle concentrations between 30-2335 ppm had all decreased to 10 ppm by settling. Thereafter the concentration decrease was proportional to time raised to the minus four-thirds power. In the salt solutions grains of all sizes settle at a similar rate. As Kranck (1980) points out these experiments probably cannot be extrapolated to nature since turbulence increases particle collision but limits growth size. naturally occurring organic and inorganic material excluded from her experiments could also be important factors in particle dynamics.

Downward diffusion transports fresh water from the upper layer resulting in a decrease in salinity in deeper water. Particulates associated with the fresh water will also be kmoved out of the upper layer by the process.

Fecal pelleting effectively removes fine material by packaging it into coarser units which can sink rapidly. The rate at which zooplankton can remove particulate matter from their host water depends on several factors including concentration of S.P., number and type of zooplankton, rate of feeding and selectivity. There is evidence that zooplankton are selective with respect to particle size (Richman et al., 1977) suggesting that a certain degree of flocculation may be required before particles can be effectively trapped and removed.

If the initial rapid settling of coarse material is followed by slower, and less size-discriminating processes such as flocculation, diffusion and fecal pelleting, and if particles settle almost vertically to the bottom, then sediments should record the process. A good example of this behaviour has been documented by Hoskin et al., (1978). In Blue fjord, an Alaskan Inlet, glacier meltwater containing up to 300 mg L^{-1} suspended solids formed a surface plume with particulates up to 200 mg L^{-1} at the head of the inlet; within 5 km, only a few mg L^{-1} of solids remained. In the sediments they observed a decrease in grain size mode distance from the head for the first 2 km and thereafter no trend in the sediments for the remainder of the 7 km fjord.

The vertical flux, F, of material too fine to be quickly sedimented by individual grain settling is given by:

$$F = Cv_z - E_z \frac{\partial c}{\partial z} + P \qquad (5)$$

where C is concentration, v_z is settling velocity, E_z is the vertical eddy diffusivity, P accounts for fecal pelleting and z is depth, positive downwards. The relative importance of each of these terms is estimated below for the Kitimat estuary.

The downward flux of particles by gravitational settling can be calculated in principle by applying Stokes' law to each particle size provided in situ density and water viscosity are known (McCave, 1975; McCave and Swift, 1976). The in situ density of particles has already been estimated at 1.38 g cm^{-3} and viscosity can be calculated from the measured salinity and temperature (Horne, 1968). There are a number of uncertainties in this process some of which McCave (1975) has discussed: (i) Settling velocity is a function of shape and Stokes' law applies strictly to smooth rigid spheres. The particles measured here certainly violate this requirement; this may not cause serious error however. McNown et al. (1951) experimented with shapes having longest to shortest axial ratios of up to 8:1. A correction factor between 0.96 and 1.7 applied to the equivalent spherical diameter was all that was required. In addition aggregates are expected to be roughly spherical (McCave, 1975). Small particles (less than 4-5 μm) do not settle according to Stokes' law (Brun-Cottan, 1976) and are ignored in the calculations. (ii) The in situ density (1.38 calculated here for particles from 4 to 80 μm) agrees very well with the 1.44 g cm^{-3} calculated by McCave (1975) for Brun-Cottans' data and 1.43 g cm^{-3} given by Pierce, 1975. It is, however, an average for all of the particles and it is assumed here that it applies to all sizes. (iii) Perhaps the most serious error is that small numbers of large particles lead to poor counting statistics, and large particles can be important in terms of transport. As McCave (1975) notes we have little alternative but to use Stokes' law keeping in mind the approximations. The ensuing estimates of downward transport of particles in the upper layer are given in Table 1.

The second term in equation 5 relates to diffusion. Estimation of the rate of downward transport by this mechanism is very difficult to do. Aside from temporal and spatial variability, entrainment may result in a net upward water motion which if fast enough could prevent particles from sinking. In a recent paper, Smethie (1980) has noted that "vertical eddy diffusivity is inversely dependent on stratification and directly dependent on energy input, although the functional relationship is unknown". If it is assumed that Kitimat behaves like Narrows Inlet with a high energy regime for the surface and low

Table 1. Downward flux calculated for the particle size distributions.

Station	Depth m	S.P. mg L^{-1}	Downward Flux g cm^{-2} d^{-1}
9	1	1.02	6.4×10^{-4}
9	5	0.96	7.9×10^{-4}
10	1	5.85	-
10	5	0.70	4.9×10^{-4}
8(a)	1	0.41	4.9×10^{-4}
8(a)	5	0.54	6.8×10^{-4}
8(b)	1	0.27	1.9×10^{-4}
8(b)	5	0.32	2.7×10^{-4}
CTD-7	1	1.02	9.3×10^{-4}
CTD-7	5	0.48	4.4×10^{-4}
CTD-7	1	0.80	1.6×10^{-4}
CTD-7	5	0.40	3.8×10^{-4}

energy regime for the deep water (away from sills) then K_z is about 0.5 cm^2 s^{-1} in the upper layer, dropping to perhaps 0.1 cm^2 s^{-1} at the pycnocline (Smethie, 1980). Based on a diffusivity of 0.1 cm^2 s^{-1} at the bottom of the upper layer and on the observed gradients in particulate matter (5 m resolution), diffusion could transport $0\text{-}3 \times 10^{-5}$ g cm^{-2} d^{-1} for the stations reported in Table 1. Relative to transport by settling, diffusion appears to be slow in removing particulates from the upper layer. As a cautionary note, strong winds or tides could result in rapid mixing, and diffusion may be more important during times when estuarine circulation is not well developed.

The effect of zooplankton in removing inorganic material from the upper layer has previously been estimated from the rate of formation of fecal pellets (Manheim et al., 1972). Zooplankton concentrations of 25-815 m^{-3} have been measured near the surface in the Kitimat fjord system including Kitimat Arm (Dilke et al., 1979; Higgins and Schmidt, 1975). Syvitski and Lewis (1980) found that for a variety of clay minerals, *Tigriopus californicus*, a copepod, produced 2-19 fecal pellets per day with a mean pellet size less than 140 μm. Furthermore pellet production was dependent on clay mineral concentration with an egestion rate of less than one pellet per day for tremolite concentrations less than 10 mg L^{-1}. Zooplankton (copepods and euphausids) native to Howe Sound average only half the number of pellets per time as the laboratory cultured *T. californicus*. Syvitski and Lewis (1980) report rather high densities of 2.6-3.1 g cm^{-3} for fecal pellets containing a large fraction of clay mineral. If the upper bounds for the above factors are chosen and an upper layer thickness of 10 m is assumed, the fecal pellet production rate amounts to 6.7×10^{-5} g cm^{-2} d^{-1}. Fecal pellet production above the pycnocline does not appear to be an important process for removing particulates in the plume relative to flocculation,

however it may still be important for sending inorganic fines to the bottom since zooplankton grazing continues at depth. Zooplankton pellets may also be able to accumulate on the bottom where hydrodynamic vigour does not allow flocs to settle.

How long fines can be carried in the upper layer depends on the concentration of particulates, and varies with experimental conditions. In the present study downward flux is approximately linearly correlated with concentration (Table 1). Furthermore particles of all grain sizes disappear from the upper layer at similar rates, supporting the Kranck (1973, 1975) model. In nature a steady state is reached at which the particle size distribution is controlled by settling of larger flocs and their replacement by growth from smaller flocs. Turbulence controls the growth rate and size of flocs, with the result that individual grains of all sizes settle at similar rates and are therefore not subject to "Stokes' law" sorting.

If a linear relation between downward flux and concentration is assumed and if the depth of the pycnocline is z_p cm then for an area ℓ cm square,

$$\frac{1}{\ell^2}\frac{dm}{dt} = -kC \qquad (6)$$

where C is concentration (g cm^{-3}), m (g) is the total mass of particulates in a water column of volume $z_p\ell^2$ and k is the first order rate constant (cm d^{-1}).

$$m = C\ell^2 z_p \qquad (7)$$

$$\frac{dm}{dt} = \frac{k}{z_p} m \qquad (8)$$

From Table 1, k is approximated to be 800 cm d^{-1}. If the depth of the upper layer is held constant at 10 m (Webster, 1980),

$$\frac{m}{m_o} = e^{-\frac{k}{z_p}t} = e^{-0.8t} \qquad (9)$$

where t is measured in days, and m_o is the initial concentration of fine particulates in the plume. In view of laboratory experiments (Kranck, 1980) this equation will probably be in serious error at concentrations in excess of 10 ppm where faster settling appears possible. According to equation 9 about half of the fine S.P. will be lost from the upper layer after a day and only ∿1% will remain after 5 days. This estimate is relatively crude since no attempt has been made to consider spatial or temporal variability brought on by tidal, wind and runoff changes, or to consider diffusive or biological removal of particles from the upper layer.

From the above discussion the following sequence of events seems to occur for the Kitimat estuary during periods of maximum runoff: (i) Coarse particles (>125 μm) fall out of the plume within minutes after they reach the sea. (ii) The finer material may then undergo a transition period of rapid removal depending on the salinity-time path of the water parcel; rapid flocculation and settling occur for perhaps several hours until the S.P. concentration drops to about 10 ppm. (iii) The finer material continues to be removed from

the upper layer during a period of about 5 days.

The residence time of fresh water in the fjord channel can be calculated from the integrated volume of fresh water above the pycnocline and the runoff rate. Based on runoff data (Webster, 1980 a,b) the residence time for fresh water in Gardner Canal is about 7 days. The residence time for Douglas Channel-Kitimat Arm varies from a minimum of five days when all of the fresh water from Gardner Canal passes through Douglas Channel to 30 days when none of it does. Given the time scale for loss of particles, the majority settle out of the upper layer relatively close to the source. Subsequent transport below the pycnocline may even move them back toward the river (Hoskin et al., 1978).

Estimates of sedimentation calculated by the variety of techniques are summarized in Table 2, but certain factors should be borne in mind when comparing these. While estimates of particulate input to andtransport in the water column are essential because they help to set time, distance and size scales for particulate mediated processes, they do not necessarily correlate with what is accumulating at a specific point on the bottom. Recent seismic surveys (Bornhold, 1981) show both longitudinal and lateral variability in thickness of post glacial sediments indicating that sediment accumulation is not uniform. Both aspects, settling and accumulation must be addressed before a complete understanding of the effect of land-derived particulates on fjords can be reached.

Table 2. Particulate budgets for the upper basin of Douglas Channel.

	Method of Determination	Sedimentation Rate g $cm^{-2}d^{-1}$	g $cm^{-2}a^{-1}$
1.	Water column measurements during a maximum runoff period (this study).	$1\text{-}10\times10^{-4}$	(0.04-0.37)
2.	Kitimat River input (mean annual discharge of 135 m^3s^{-1} and a suspended sediment load of 5-15 mg L^{-1} deposition area $\sim$ 100 km^2.		(0.02-0.06)
3.	Sedimentation traps, June-Sept (Werner and Hyslop, 1968). Correction applied for shape (Hargrave and Burns, 1979). Collected material was 78-94% inorganic with shell and wood contribution the remainder.	$4\text{-}7\times10^{-4}$	(0.15-0.3)
4.	Lead-210 dating (Macdonald et al., 1978; Cretney et al., 1983).		(0.06-0.27)
5.	Post glacial deposition (Bornhold, pers. comm.) maximum post-glacial sediment thickness - 60 m average water content 30% (wt). Time of accumulation - 10,000 years.		<0.92

ACKNOWLEDGEMENTS

I thank P. Erickson for his assistance during the cruises, and B. Bornhold and K. Kremling for critically reivewing the manuscript. J. Poulin assisted in the preparation of the manuscript.

REFERENCES

Bader, H. 1970. The hyperbolic distribution of particle sizes. J. of Geophys. Res. 75: 2722-2830.

Biggs, R.B. 1978. Coastal bays in coastal sedimentary environments. R.A. Davis ed., Springer Verlag, N.Y. 420 pp.

Bornhold, B.D. 1975. Suspended water in the southern Beaufort Sea. Beaufort Sea Technical Report #256 23 pp.

Bornhold, B.D. 1983. Sedimentation in Douglas Channel and Kitimat Arm. Can. Tech. Rep. Hydrogr. Ocean Sci. 18, 88-115.

Brun-Cottan, J.,1976. Stokes settling and dissolution rate model for marine particles as a function of size distribution. J. Geophys. Res. 81: 1601-1606.

Chanut, J.P., S.A. Poulet, D. Cossa and J.C. Marty. 1977. In proceedings "First World Conference on Mathematics at the Service of Man", Barcelona, Spain.

Cretney, W.J., C.S. Wong, R.W. Macdonald, P. Erickson and B. Fowler. 1983. Hydrocarbon levels in the marine environment of Kitimat Arm and its seawter approaches. Can. Data Rep. Hydrogr. Ocean Sci., 18, 162-195.

Davies, K.F. 1975. Mackenzie River input to the Beaufort Sea, 1975. Beaufort Sea Technical Report #15, 72 pp.

Dilke, B.R., S. McKinell and R.I. Perry. 1979. Ship of Opportunity Program, March 1978 - March 1979. Data Report #46. Institute of Oceanography, University of British Columbia. 111 pp.

Farrow, G.E., J.P.M. Syvitski and V. Tunnicliffe. 1982. Suspended particulate loading on the macrobenthos in a highly turbid fjord Knight Inlet, British Columbia, Can. J. Fish. Aquat. Sci. (in press).

Feely, R.A. and M.F. Lamb. 1979. A study of the dispersal of suspended sediment from the Fraser and Skagit River into northern Puget Sound using LANDSAT imagery, Interagency Energy/Environment R&D Program Report, EPA-600/7-79-165. 46 pp.

Gartner, J.W. and K.L. Carder. 1979. A method to determine specific gravity of suspended particles using an electronic particle counter. J. Sed. Petrol. 42: 631-633.

Hargrave, B.T. and N.M. Burns. 1979. Assessment of sediment trap collection efficiency. Limnol. and Oceanogr. 24: 1124-1136.

Higgins, R.J. and A.H. Schmidt. 1975. Kitimat River Estuary study (1974-1975). Unpublished manuscript, Pacific Environment Institute, Vancouver, B.C.

Holtedahl, H. 1965. Recent turbidities in Hardangerfjord, Norway. In W.P. Whitiard and R. Bradshaw (eds.) Submarine Geology and Geophysics - Colston Papers. Butterworths, London. 107-141.

Horne, R.A. 1969. Marine Chemistry, Wiley , N.4. 568 pp.

Hoskin, C.M., D.L. Burrell and G.R. Freitag. 1978. Suspended sediment dynamics in Blue Fjord, Western Prince William Sound, Alaska. Est. & Coast. Mar. Sci. 7: 1-16.

H.O. Publication #607. 1968. Instruction manual for obtaining oceanographic data, 3rd edition, U.S. Naval Oceanographic Office.

Kitchen, J.C., D. Menzies, H. Pak and J.R.V. Zanefeld. 1975. Particle size distribution in a region of coastal upwelling analyzed by characteristic vectors. Limnol. & Oceanogr. 20: 775-783.

Kranck, K. 1973. Flocculation of suspended sediment in the sea. Nature, 246: 348-350.

Kranck, K. 1975. Sediment deposition from flocculated suspension. Sedimentology 22: 111-123.

Kranck, K. 1980. Experiments on the significance of flocculation in the settling of fine grained sediment in still water. Can. J. Earth Sci. 17: 1517-1526.

Krone, R.B. 1976. Engineering interest in the benthic boundary layer. In McCave, I.N., ed., The Benthic Boundary Layer, N.Y. Plenum Press: 143-156.

Lehrman, A., D. Lal and M.F. Decey. 1974. Stokes settling and chemical reactivity of suspended particulates in natural waters in "Suspended Solids in Water", R.J. Gibbs ed. pp. 17-47, Plenum Press, N.Y.

Macdonald, R.W., W.J. Cretney, C.S. Wong and P. Erickson. 1983. Kitimat Hydrocarbon Baseline Study, Can. Data Rep. Hydrogr. Ocean Sci., in prep.

Macdonald, R.W., D.M. Macdonald and P.S. Munro. 1978. Oceanographic Data Report, Kitimat Arm, Porpoise Harbour, February 1977. PMSR 78-24, 61 pp.

Macdonald, R.W., B.D. Bornhold and I. Webster. 1983. The Kitimat Fjord System: An Introduction. Can. Tech. Rep. Hydrogr. Ocean Sci. 18, 2-13.

Manheim, F.T., J.C. Hathaway and E. Uchupi. 1972. Suspended matter in surface waters of the northern Gulf of Mexico. Limnol. & Oceanogr. 17: 17-27.

Matsumoto, E. and C.S. Wong. 1977. The distribution of suspended particles in the southern Beaufort Sea. J. Oceanogr. Soc. Japan, 33: 227-232.

McCave, I.N. 1975. Vertical flux of particles in the ocean. Deep-Sea Res. 22: 491-502.

McCave, I.N. and S.A. Swift. 1976. A physical model for the rate of deposition of fine-grained sediments in the deep sea. Geol. Soc. of America Bull. 87: 541-546.

McNown, J.S., J. Malaika and H.R. Pramanik. 1951. Particle shape and settling velocity. Proceedings of the International Association for Hydraulic Research, 4th Meeting, Bombay. pp. 511-522.

Meade, R.H. 1968. Relations between suspended matter and salinity in estuaries of the Atlantic seaboard, U.S.A. Int. Assoc. Sci. Hydrology. Bern 1967, vol. 4 (I.A.S.H. Pub. 78, 1968).

Pierce, J.W., 1975. Suspended sediment transport at the shelf break and over the outer margin in marine sediment transport and environmental management. D.J. Stanley and D.J.P. Swift, eds Wiley-Interscience, N.Y., pp. 437-460.

Richman, S., D.R. Heinle and R. Huff. 1977. Grazing by adult estuarine calanoid copepods of the Chesapeake Bay. Mar. Biol. 42: 69-84.

Sharma, G.D. 1979. The Alaskan Shelf; hydrographic, sedimentary and geochemical environment. Springer Verlag, N.Y. 498 pp.

Sheldon, R.W. and T.R. Parsons. 1967. A practical manual on the use of the Coulter Counter in marine science. Coulter Electronics, Toronto. 66 pp.

Sholkovitz, E.R. 1978. The flocculation of dissolved Fe, Mn, Al, Cu, Ni, Co and Cd during estuarine mixing. Earth & Planet. Sci. Lett. 41: 77-86.

Simonds, J.L. 1963. Application of characteristic vector analysis to photographic and optical response data. J. Opt. Soc. Am. 53: 968-974.

Smethie, W.M. 1980. Estimation of vertical mixing rates in fjords using naturally occurring radon-222 and salinity as tracers. In Fjord Oceanography, Plenum Press, Freeland, Farmer & Levings, eds., pp. 241-249.

Stumm, W. and J.J. Morgan. 1970. Aquatic Chemistry. Wiley Interscience, N.Y., 583 pp.

Syvitski, J.P.M. 1980. Flocculation, agglomeration and zooplankton pelletization of suspended sediment in a fjord receiving glacial meltwater. In Fjord Oceanography, Plenum Press, Freeland, Farmer & Levings, eds., pp 615-624.

Syvitski, J.P.M. and A.G. Lewis. 1980. Sediment ingestion by *Tigriopus californicus* and other zooplankton: mineral transformation and sedimentological considerations. J. Sed. Petrol 50: 869-880.

Syvitski, J.P.M. and J.W. Murray. 1981. Particle interaction in fjord suspended sediment, Mar. Geol. 39: 215-242.

Syvitski, J.P.M. and R.D. Macdonald. 1982. Sediment character and provenance in a complex fjord; Howe Sound, British Columbia, Can. J. Earth. Sci, 19: 1025-1044.

Terzaghi, K. 1956. Varieties of submarine slope failures, 8th Texas Conf. on soil mechanics and foundation engineering. Special Publ. #29, Bureau of Engineering Research, U. of Texas.

Webster, I. 1980(a). Kitimat physical oceanographic studies, 1977-1978: III Estuarine Circulation. Contractor Report Series, 80-3, 81 pp. Institute of Ocean Sciences, Sidney, B.C.

Webster, I. 1980(b). Kitimat physical oceanographic study 1977-1978. 1. Data collection and analyses. Contractor Report Series 80-3, 51 pp. Institute of Ocean Sciences, Sidney, B.C.

Werner, A.E. and W.F. Hyslop. 1968. Accumulation and composition of sediments from polluted waters off the British Columbia Coast, 1963-1966. Fisheries Research Board of Canada, Manuscript Report Series No. 963, 81 pp.

VARIATIONS DE LA TEMPERATURE DU FOND DES EAUX DÛMENT OBSERVÉE ET ENREGISTRÉE DANS LE FOND DES DÉPÔTS ALICE ARM ET LE CANAL DOUGLAS

Trevor Lewis
Geological Survey of Canada
Pacific Geoscience Centre, Sidney, B.C.

RÉSUMÉ

Les changements du système dans l'Alice Arm et Douglas Channel, Colombie Britanique la température du fond des eaux fût mesurée aussi bien que le fond des dépôts mous. Une valeur de limite pour les dépots ascendants, conduit par la chaleur, détermine la température du fond des eaux. Consequemment un record passé la température du fond des eaux, est entreposé dans les dépôts, comme une agitation descendante et éparpillée. A fin de mesurer l'équilibrium terrestre des courants chauds, employant les techniques océaniques, ces agitations doivent être enlevées de ces données. Mais c'est aussi possible de determiner les changements passés de la température du fond des eaux, pour une période d'environ un an; par l'ajustement des données des agitations d'un modèle simple de température entrelacée. On a découvert dans l'Alice Arm, une variation annuelle avec un maximum de 5.5°C en septembre, et un minimum de 5.0°C en mars. Dans le système du Kitimat, la tempèrature du fond des eaux de tous les grands bassins était à moins de 0.15° de chacun; la plupart du temps. On à observer une variation annuelle de 7.25° en avril jusqu'à 6.80° en septembre. La regularité de ces variations annuelles ne peux pas être déterminé car le temps de ces observations est de trop courte durée.

Lewis, Trevor. 1983. Bottom water temperature variations as observed, and as recorded in the bottom sediment, Alice Arm and Douglas Channel, British Columbia. Can. Tech. Rep. Hydrogr. Ocean Sci. 18, 138-161.

Mot-clés: Alice Arm, Douglas Channel, écoulement, modèle, température

BOTTOM WATER TEMPERATURE VARIATIONS AS OBSERVED, AND AS RECORDED IN THE BOTTOM SEDIMENTS, ALICE ARM AND DOUGLAS CHANNEL, BRITISH COLUMBIA

Trevor Lewis
Geological Survey of Canada, Pacific Geosciences Center, Sidney, B.C.

ABSTRACT

In Alice Arm and Douglas Channel, British Columbia, changes in the temperature of the bottom water and the upper 6 m of soft, bottom sediments were measured. The bottom water determines the sediment interface temperature, a boundary value for upward conduction of heat in the sediments. Consequently a record of past bottom water temperatures is stored in the sediments as a downward propagating, dispersive temperature perturbation. To measure equilibrium terrestrial heat flow using oceanic techniques, such perturbations must be removed from the data. But it is also possible to determine past changes in bottom water temperatures up to about a year by fitting calculated perturbations from simple models of the interface temperature. In Alice Arm an annual variation was detected, 5.5°C in September, and 5.0°C in March. In the Kitimat system bottom water temperatures in all of the large basins were within 0.15° of each other most of the time. An annual variation from 7.25°C in April to 6.80°C in September was observed. The regularity of such annual variation cannot be determined from observations over such a short interval.

Lewis, Trevor. 1983. Bottom water temperature variations as observed, and as recorded in the bottom sediment, Alice Arm and Douglas Channel, British Columbia. Can. Tech. Rep. Hydrogr. Ocean Sci. 18, 138-161.

Keywords: Alice Arm, Douglas Channel, heat flow, model, temperature

INTRODUCTION

The amount of heat flowing upwards to the earth's surface, the terrestrial heat flow, is a very important parameter for studying the earth's crust. It delineates zones of subduction, partial melting of the crust, crustal extension and other crustal anomalies, and is needed for calculating temperatures at depth since the physical properties of the earth's crust are very temperature dependent. If the crust near the surface is an impermeable solid, then heat is conducted up to the surface, and is equal to the product of the temperature gradient and the thermal conductivity of the crust. But the terrestrial heat flow is very small, about three orders of magnitude smaller than the heat flux from the sun at the earth's surface. Since the surface temperature is a boundary condition for conduction in the solid crust, and since it is controlled by many, larger influences, including the temperature of the air or water above the crust, the heat flow near surface is disturbed by changes in air or water temperature.

On land, measurements are made at great depths in mines or down boreholes to avoid the largest disturbances. Even then corrections must be made for the effects of topography and past climatic changes. Along the Coast Plutonic Complex in British Columbia where boreholes and mines are scarce and the topography exceptionally rugged, oceanic techniques for measuring heat flow have been used in the deep basins of the fjords (Hyndman, 1976; Lewis et al., in preparation). These measurements depend upon a knowledge of the past temperature of the bottom waters since the water temperature controls the mud to water interface temperature.

Studies of the B.C. mainland inlets, including measurements of temperature, were initiated by Pickard (1961), and the Institute of Oceanography at the University of B.C. continued sporadic cruises to obtain additional data (Data Reports, 1963-1972). Recently more detailed studies concentrated on two areas (Fig. 1): Alice Arm (Littlepage, 1978; Krauel, 1981), and the Douglas Channel - Kitimat Area (Webster, 1980). Heightened interest in these two areas is caused by proposed developments related to mining, transportation and industrial expansion.

During two cruises, PGC 77-6 in October, 1977, and PGC 78-4 in May, 1978, we measured temperature profiles in the water, temperature gradients in the bottom sediments to a maximum depth of 7 m, and the thermal conductivity of sediments in situ and in cores at several sites within these areas. The purpose of this paper is to present the data we acquired from the two areas and models of the changes in bottom water temperatures based on the temperature perturbations recorded in the sediments. The water movements causing the temperature changes are not discussed here.

Since the temperature at the water-sediment interface is a boundary condition which is fairly constant, any changes in the temperature can be considered to be a perturbation which propagates down into the sediments. As such a change propagates, it disperses and decreases in amplitude. Although there is no unique answer if we try to determine the past temperature at the boundary from measurements of temperature within the sediments, for simple models we can obtain the amplitudes and times of changes of the past temperature of the bottom waters.

THEORY

The effect of a varying boundary temperature on temperatures within a semi-infinite, homogeneous solid is well known. Jaeger (1965) has derived an expression for the anomaly caused by a sinusoidal change with time in the boundary temperature for a model having variations in the temperature $V(z,t)$ as a function of time, t, and the depth, z:

$$V(z,t) = V_o\, e^{-\phi z} \cos(\omega t - \phi z) \qquad (1)$$

for $V(o,t) = V_o \cos(\omega t)$

where z is measured positive into the solid,
ω is the angular frequency of the wave,

$\phi = (\frac{\omega}{2\kappa})^{\frac{1}{2}}$,

κ is the thermal diffusivity, defined as $\kappa = \frac{k}{pc}$, where
k is the thermal conductivity, ρ the density, and c, the heat capacity per unit mass.

For a step change of V_1 in the boundary temperature between times t_1 and t_2 in the past, where time is measured backwards from the present, the temperature is now perturbed by the amount (Jaeger, 1965):

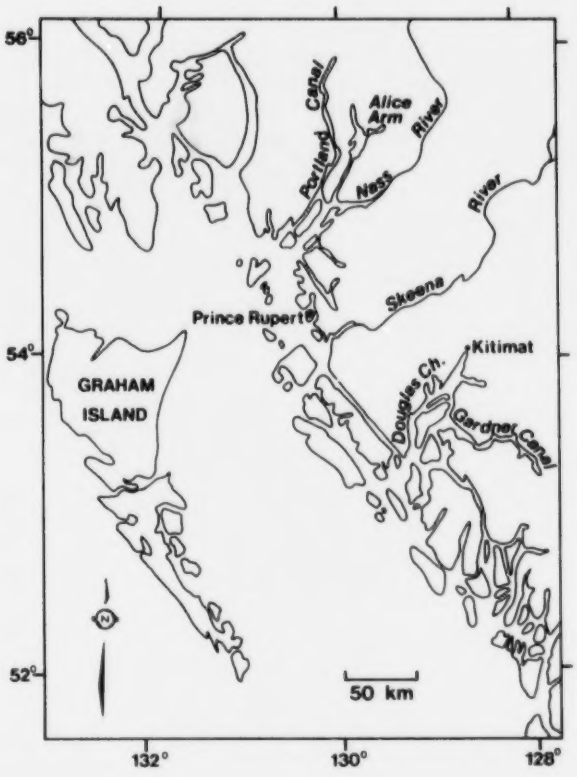

Figure 1. Locations of Alice Arm and Douglas Channel.

$$V(z,t) = V_1 \left\{ \text{erf} \left[\frac{z}{\sqrt{4\kappa t_1}} \right] - \text{erf} \left[\frac{z}{\sqrt{4\kappa t_2}} \right] \right\} \qquad (2)$$

where $\text{erf}(x) = \frac{2}{\sqrt{\pi}} \int_0^x e^{-y^2} dy$

and other symbols are as previously defined.

Similarly for a surface temperature which was linearly increasing with time (Carslaw and Jaeger, 1959) at the rate a degrees per unit time, the anomaly produced within the solid is

$$v(z,t) = at \left\{ (1 + \frac{z^2}{2\kappa t}) \text{ erfc } (\frac{z}{\sqrt{4\kappa t}}) - \frac{z}{\sqrt{\pi\kappa t}} e^{-\frac{z^2}{4\kappa t}} \right\} \qquad (3)$$

for surface temperatures

$V(o,t) = 0, \quad t \leq 0$

$V(o,t) = at \quad t \leq 0$

where $\text{erfc}(x) = 1-\text{erf}(x)$

These anomalies may be combined, and/or added to the temperatures resulting from the constant equilibrium terrestrial heat flow.

In the sediments of the inlets, p, the fraction by weight that is water, can vary from 0.35 to 0.80 causing the thermal conductivity, κ, to vary by 70% (Figure 2). If we assume values for the conductivity and density of rock and water and we use this measured conductivity of the sediments as a function of p, we can calculate the diffusivity of the sediments as a function of p. This result varies by a factor of 2.

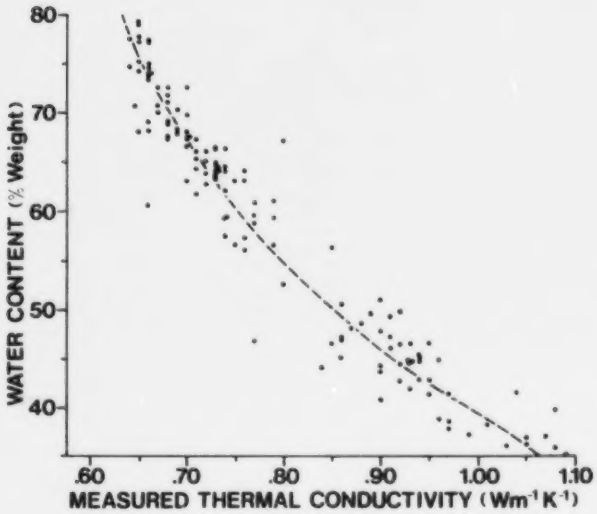

Figure 2. The measured values of thermal conductivity of sediment cores as a function of water content by per cent weight. The dotted line is the relation determined by Ratcliffe (1960).

Figures 3 and 4 show the temperature perturbations within sediments for a boundary temperature with an annual sinusoidal variation and a step increase in the past. Such changes affect the temperatures measured in the top 7 meters of the sediments and the average gradient. Such anomalies may be considered a record of past changes in water temperatures.

Simple models can be fitted to many of the observations. For simplicity we assume that the diffusivity does not vary as the function of depth at a particular station. The largest variations in diffusivity are caused by changes in the thermal conductivity, and Fig. 2 indicates how large the variation in the thermal conductivity of cores can be. At most sites, however, the conductivity is nearly constant, and simple modelling can be used. More complex models are not warranted by the limited number, and the quality of some of the water temperature data.

METHODS OF MEASUREMENT

All temperatures were measured using calibrated thermistors as sensors inside water-proof probes at atmospheric pressures. Water temperatures were

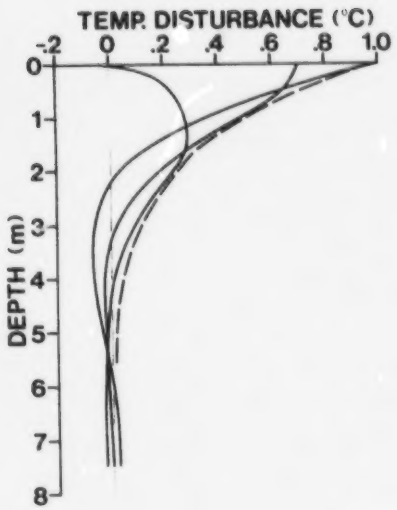

Figure 3. Temperature anomaly within the sediments ($\kappa = 1.9 \times 10^{-7}$ m^2/s) caused by an annual sinusoidal variation in water temperature. The solid curves indicate the value of the anomaly at the beginning and middle of the first quarter of an annual cycle; the dashed line indicates the envelope of the curves, which are symmetric about the zero temperature.

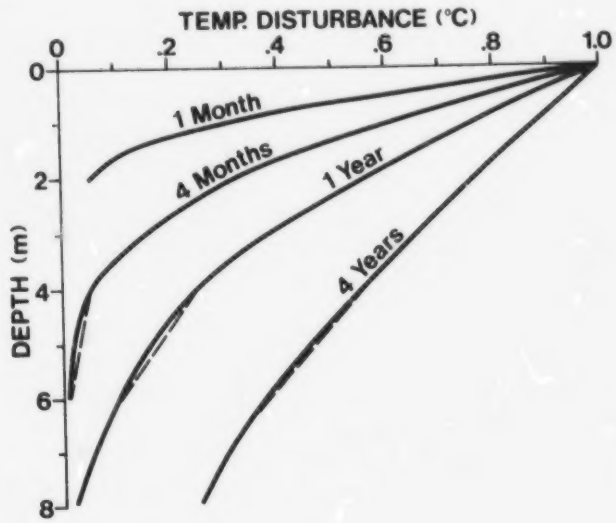

Figure 4. Temperature anomaly within the sediments ($\kappa = 1.9 \times 10^{-7}$ m^2/s) caused by a single step change previously in the water temperature at the specified time.

measured by a single thermistor, inside a pressure-tight probe on a light-weight, 4-conductor cable, lowered by a portable winch used for borehole logging (Lewis, 1975). Temperature resolution was 0.002 K and absolute accuracy is 0.01° C.

Temperatures within the top few meters of the sediments were measured by thermistors inside slim probes up to 7 meters long. The electronics and batteries contained in pressure cases at the top of each probe measure and record the results, and on one probe acoustically telemeter the data back to the surface as well. Hyndman et al. (1979) described the telemetering instrument used on PGC 78-4 cruise which measures the sediment's thermal conductivity in situ, as well as the gradient. On PGC 77-6 cruise a 5 m Bullard probe was used most frequently, although a 7 m gravity corer with three outrigger thermistor sensors was also used. An example of the quality of the data, and of how linear the undisturbed gradients can be is presented in Figure 5.

The description of methods of obtaining data used by others (Data Reports, 1963; 1966; 1969; 1970, 1972, Dobrocky Seatech Ltd., 1977-1978; Littlepage, 1978; Macdonald, 1977) will not be repeated here. However it is necessary to point out that in Alice Arm water temperatures were recorded by the Aanderaa RCM 4 current meter with a specified accuracy of ±0.15° C, but the jump in temperature, 0.5° C, when instruments were exchanged exceeds this specification.

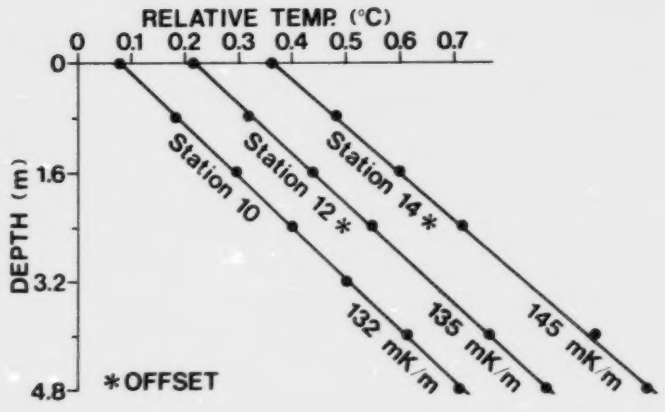

Figure 5. Sediment temperatures observed at three stations in Jervis Inlet. Stations 12 and 14 are successively offset by 0.1° C.

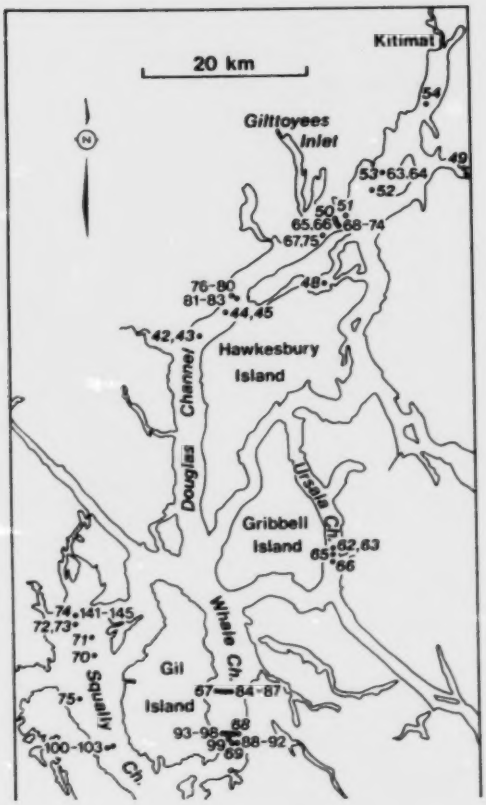

Figure 6. Approximate locations of stations in Douglas Channel System for cruises PGC 77-6 and PGC 78-4.

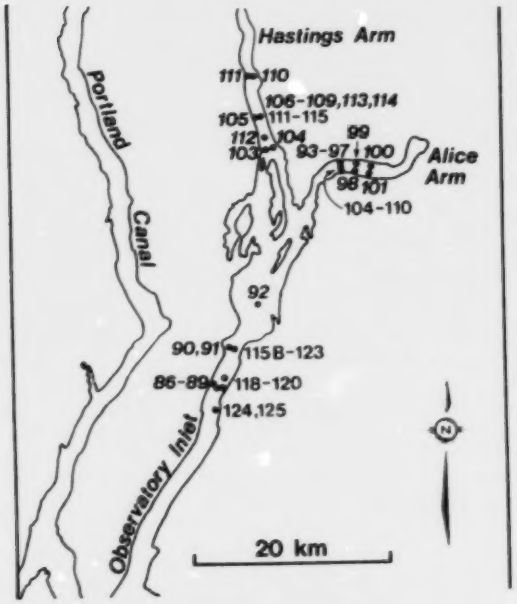

Figure 7. Approximate locations of stations in and near Alice Arm for cruises PGC 77-6, and PGC 78-4.

RESULTS

Water temperature profiles and sediment gradients were measured and cores obtained at stations shown in Figures 6 and 7, and listed in Table 1 for the Kitimat area and in Table 2 for Alice Arm. In this section many examples of temperatures measured in sediments will be presented, and in many cases calculated temperatures will also be shown. The calculated values come from the best fit to the data of either step changes or annual sinusoidal variations in the sediment-water interface temperature. The straight, solid lines on the graphs of temperature vs depth are the best fit to the data of the linear gradient of the model.

ALICE ARM

Pickard (1961) noted that Alice Arm is cooler and less saline than other northern inlets since it has a restricted entrance from Observatory Inlet and rivers provide an ample flow of fresh water. The maximum entrance depth, 55 m, is very small compared to 380 m, the maximum depth of Alice Arm. This condition limits the exchange of deeper, more saline water from Observatory Inlet. Littlepage (1978) and Krauel (1981) have discussed deep water renewal for Alice Arm.

The earliest recorded temperatures of the deeper waters in Alice Arm are 4.30° C at 200 m depth in July, 1951 (Pickard, 1961), and 4.77 and 4.76° C at 350 and 250 m depth, respectively, in May 1966 (Data Reports, 1966). Water temperatures were measured six times during the period of August, 1976, to September, 1977, and continuous recordings of the bottom water temperature were made from August, 1976, to March 1977, and from June to September, 1977 (Dobrocky Seatech Ltd., 1977) (Figure 8). Following these observations, we measured water temperatures and sediment temperatures in October 1977 and May, 1978 (Figure 8 and 9).

The differences between absolute values of temperature measured as discrete measurements and as continual recordings (up to 0.37 K) require a judgement concerning their accuracy. Considering that the sudden increase of 0.5 K observed in the continually recorded temperatures at 360-374 m occurred when an instrument was re-deployed in December, 1976, the temperatures and salinities recorded between December, 1976, and March, 1977, are rejected and the accuracy of all of the other recorded data is left in doubt. The other recorded temperatures, although differing in value by up to 0.37 K, do show variations in time which are in general agreement with the few discrete measurements.

The temperatures recorded in the sediments (Figure 10), especially in May, 1978 (as subsequently shown in Figure 11) are very good quality data, and the thermal conductivity at five different stations is nearly identical: 0.92 W/mk ± 0.7%. Figure 10 shows the temperatures measured by two different probes in October, 1977 as well as the calculated temperatures from a step change of 0.32° C occurring 70 days previously (Aug. 5, 1977) and an annual sinusoidal variation of magnitude 0.29° C.

The data from 6 different stations in May 1978 (Figure 11) have been averaged to give the temperature for each depth, since the thermal conductivity

Table 1. Station parameters for Kitimat Area PGC Cruise 77-6 October 1977.

Stn No.	Coordinates N	Coordinates W	Depth (m)	Date	Time	Type
63	53° 50.95'	128° 47.40'	323	10	1340	Benthos corer
64	53° 50.95'	128° 47.40'	325	10	1426	5 m Bullard
65	53° 47.6 '	128° 52.5 '	374	10	1606	Benthos
66	53° 47.6 '	128° 52.5 '	374	10	1640	5 m Bullard
67	53° 46.89'	128° 54.57'	380	10	1810	Benthos
68	53° 47.5 '	128° 53.7 '	383	10	1856	20' corer & outrigger
69	53° 47.5 '	128° 53.7 '	383	10		5 m Bullard probe
70	53° 47.5 '	128° 53.7 '	383	10	2010	Water temp profile
71	53° 47.6 '	128° 54.0 '	346	10	2120	5 m Bullard
72	53° 47.53'	128° 53.85'	352	10	2240	5 m Bullard
73	53° 47.09'	128° 53.2 '	381	10		5 m Bullard
74	53° 47.23'	128° 53.5 '	390	11	0045	5 m Bullard
75	53° 46.7 '	128° 54.6 '	380	11	0215	5 m Bullard
76	53° 41.8 '	129° 07.0 '	373	11	0615	Benthos
77	53° 41.8 '	129° 07.0 '	385	11	0645	5 m Bullard
78	53° 41.5 '	129° 06.5 '	385	11	0730	5 m Bullard
79	53° 41.3 '	129° 06.3 '	390	11	0825	Benthos
80	53° 41.3 '	129° 06.3 '	390	11	0835	Water profile
81	53° 40.4 '	129° 07.4 '	398	11		5 m Bullard
82	53° 40.4 '	129° 07.4 '	398	11	1102	20 ft. corer w/outrigger
83	53° 40.4 '	129° 07.4 '	398	11	1150	5 m Bullard
84	53° 10.2 '	129° 07.9 '	565	11	1832	20' gravity core & out.
85	53° 10.1 '	129° 09.0 '	562	12	0521	5 m Bullard probe
86	53° 10.1 '	129° 08.3 '	555	12	0640	5 m Bullard
87	53° 10.1 '	129° 07.1 '	555	12	0702	5 m Bullard
88	53° 07.3 '	129° 07 '	545	12	0910	Benthos
89	53° 07.3 '	129° 07 '	545	12	0946	5 m Bullard
90	53° 07.3 '	129° 06.65'	540	12	1032	5 m Bullard
91	53° 07.3 '	129° 06.65'	540	12	1120	Water temp. profile
92	53° 07.3 '	129° 06.65'	540	12	1251	20' corer & outriggers
93	53° 07.9 '	129° 07.5 '	570	12	1502	5 m Bullard
94	53° 07.89'	129° 07.2 '	545	12	1630	5 m Bullard
95	53° 07.9 '	129° 06.9 '	520	12	1710	5 m Bullard
96	53° 07.9 '	129° 06.6 '	508	12	1910	5 m Bullard
97	53° 07.9 '	129° 07.4 '	549	12	2110	20' corer & outriggers
98	53° 07.9 '	129° 07.4 '	549	12	2205	5 m Bullard
99	53° 07.86'	129° 07.73'	565	12	2315	5 m Bullard
100	53° 06.55'	129° 21.8 '	663	13	0123	Benthos corer
101	53° 06.55'	129° 21.8 '	665	13	0220	5 m Bullard
102	53° 06.55'	129° 21.8 '	665	13	0340	Water temp. profile
103	53° 06.4 '	129° 22.4 '	650	13	0417	5 m Bullard
141	53° 16.77'	129° 25.62'	490	17	0942	5 m Bullard
142	53° 16.77'	129° 25.62'	490	17		Water temp. profile
143	53° 16.77'	129° 25.62'	523	17	1115	20' core & outriggers
144	53° 16.79'	129° 26.14'	523	17		5 m Bullard
42	53° 38.7 '	129° 10.6 '	382	21	1155	Tele-probe
43	53° 38.75'	129° 10.62'	382	21	1220	Large core

Table 1. Continued

Stn No.	Coordinates N	Coordinates W	Depth (m)	Date	Time	Type
44	53° 40.3 '	129° 07.4 '	388	21	1351	Tele-probe
45	53° 40.3 '	129° 07.4 '	388	21	1430	Water temp. profile
46	53° 50.2 '	128° 58.1 '	166	21	1857	Tele-probe
48	53° 42.28'	128° 55.97'	229	21/22	2352	Tele-probe
49	53° 50.4 '	128° 36.3 '	198	22	0633	Tele-probe
50	53° 47.45'	128° 53.8 '	368	22	0830	Tele-probe
51	53° 47.6 '	128° 52.5 '	362	22	1008	Tele-probe
52	53° 48.38'	128° 50.0 '	349	22	1117	Tele-probe
53	53° 50.93'	128° 47.4 '	311	22	1215	Tele-probe
54	53° 55.3 '	128° 42.3 '	220	23	0200	Water temp. profile
55	53° 28.29'	128° 19.3 '	485	23	1030	Tele-probe
56	53° 28.29'	128° 19.3 '	487	23	1145	Small core
57	53° 28.97'	128° 20.54'	485	23	1255	Tele-probe
58	53° 28.95'	128° 20.59'	485	23	1400	Small core
59	53° 28.6 '	128° 19.9 '	487	23	1457	Tele-probe
60	53° 27.6 '	128° 14.4 '	459	23	1804	Tele-probe
61	53° 27.6 '	128° 14.4 '	460	24	0321	Tele-probe (repeat)
62	53° 22.13'	128° 53.96'	488	24	1020	Tele-probe
63	53° 22.13'	128° 54.01'	488	24	1200	Small (Benthos) core
64	53° 21.43'	128° 54.22'	494	24	1215	Tele-probe
65	53° 20.31'	128° 54.25'	477	24	1400	Tele-probe
66	53° 20.27'	128° 54.21'	477	24	1510	Small core
67	53° 08.9 '	129° 07.5 '	540	24	1738	Tele-probe
68	53° 07.9 '	129° 07.6 '	529	24	1910	Tele-probe
69	53° 07.2 '	129° 06.6 '	525	24	2000	Tele-probe
70	53° 14.15'	129° 24.0 '	556	24	2333	Tele-probe
71	53° 15.3 '	129° 24.3 '	538	25	0110	Tele-probe
72	53° 16.05'	129° 26.1 '	514	25	0320	Tele-probe
73	53° 16.05'	129° 26.1 '	514	25	0420	Water temp. profile
74	53° 16.8 '	129° 26.3 '	523	25	0540	Tele-probe
75	53° 10.7 '	129° 26.0 '	487	25	0724	Tele-probe

Table 2. Station parameters for Alice Arm.

PGC cruise 77-6, October 1977.

Stn No.	Coordinates N	Coordinates W	Depth (m)	Date	Time	Type
104	55° 27.15'	129° 37.35'	390	14	1330	Benthos Core
105	55° 27.15'	129° 37.35'	390	14	1420	5 m Bullard
106	55° 27.15'	129° 37.35'	390	14	1511	20' core & outriggers
107	55° 27.15'	129° 37.35'	390	14	1535	Water temp. profile
108	55° 27.18'	129° 37.55'	390	14		5 m Bullard
109	55° 27.06'	129° 37.39'	390	14	1725	5 m Bullard
110	55° 27.06'	129° 37.39'	390	14	1822	2 m Bullard
111	55° 30.74'	129° 46.34'	308	14	2135	Water temp. profile
PGC cruise 78-4, May 1978						
93	55° 27.2 '	129° 37.54'	379	27	0220	Tele-probe
94	55° 27.1 '	129° 37.5 '	381	27	0340	Tele-probe
95	55° 27.1 '	129° 37.5 '	381	27	0420	Water temp.
96	55° 27.1 '	129° 37.5 '	381	27	0500	Salinity probe (shallow)
97	55° 27.05'	129° 37.4 '	379	27	0550	Tele-probe
98	55° 27.0 '	129° 36.2 '	379	27	0710	Tele-probe
99	55° 27.14'	129° 36.2 '	379	27	0808	Tele-probe
100	55° 27.3 '	129° 35.72'	375	27	0944	Tele-probe
101	55° 26.96'	129° 35.1 '	373	27	1038	Tele-probe
107	55° 30.7 '	129° 46.65'	307	27	1930	Water temp. profile

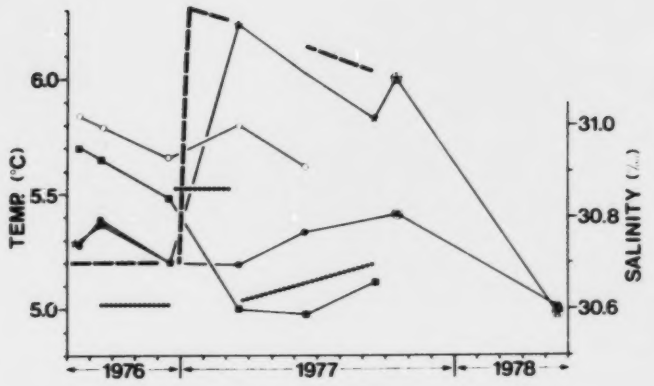

Figure 8. Deep water temperatures in Alice Arm, using our data (circled values with an absolute accuracy of 0.02° C) and data from Dobrocky Seatech Ltd. (1977), including salinity. Temperatures shown by a star are from 200 m depth, and by a dot from 300 m depth. Continuously recorded temperatures from 183 m depth are shown by a dashed line, and from 360-374 m by a series of dots. Squares represent salinities at 200 m depth, and open circles, at 300 m depth.

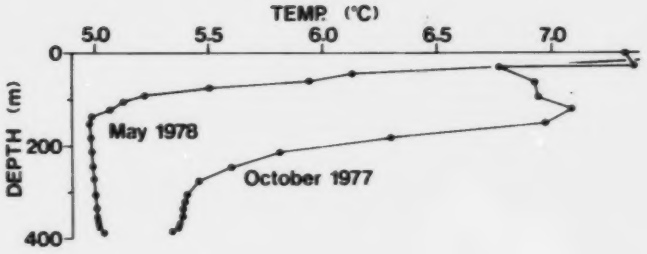

Figure 9. Temperature profiles of the water in Alice Arm in October, 1977, and May, 1978. The deepest measurement is from the top of the sediments, and the thicker line just above this point represents a series of closely spaced measurements.

varies so little, and the individual temperatures are very similar for each depth. Two simple models of bottom water temperatures (Figure 12) were used to fit the data from both cruises (Figures 10 and 11). For the 5 stations at which the thermal conductivity of the sediment was measured, the temperatures were plotted as a function of thermal depth (Figure 13). Thermal depth is the product of depth and thermal resistivity (the inverse of thermal conductivity). This so-called Bullard plot accounts for temperature differences caused by variations in the sediments' thermal conductivity; if the interface temperature were constant with time, then a straight line is expected. Since station 97 differs from the other four stations, it was omitted from the data set which was averaged for modelling purposes.

Sediment temperatures from both October and May (Figure 14) indicate that the top temperature sensor is below the water-sediment interface, as was indicated by the mud line on the instrument. Since the absolute temperature was not recovered from the probes used on the October cruise, the relative temperature between the data from the two cruises was determined for the final models by positioning the deepest sediment temperature measured in October on a straight line approximating the equilibrium gradient. The value of thermal diffusivity used was 2.5×10^{-7} m^2 s^{-1}.

This data can also be fitted by an interface temperature increasing linearly with time (a ramp) commencing 225 days earlier (Figure 14). Any of the three assumed shapes fit the data well, if the times of occurrence and amplitude are adjusted. However some models of the bottom water changes do not produce sediment temperatures resembling those measured. If the ramp model for the October cruise data is continued in time, with a sudden renewal causing a step decrease in temperature sometime between May and October (as shown in Figure 14), the calculated temperatures will not fit the observed sediment temperatures since there is a large positive anomaly in temperature below 1.5 m. In fact any model that allows the high surface temperature of October to persist cannot fit the observations. A better fit is obtained by using two (or more) steps in surface temperature between October and May, or a sinusoidal variation (Figure 12).

The comparison of these models (Figure 12) to the observed temperatures (Figure 8) shows poor agreement. The five individual water temperatures at a depth of 300 m measured before October, 1977, do indicate a quasi-annual component, but with a much reduced amplitude. The maximum bottom water temperatures occur in the early fall and the minima in the early spring, opposite, in sense, to the annual variation seen in the Douglas Channel-Kitimat System. Since the bottom waters in Hastings Arm and upper Observatory Inlet are always warmer and more saline than the Alice Arm waters, any exchange with these waters causes a warming of the bottom waters of Alice Arm.

DOUGLAS CHANNEL-KITIMAT SYSTEM

The data from Alice Arm were considered first since Alice Arm is a single basin, and results should be more easily analyzed for a single basin than for the Douglas Channel-Kitimat system. In May, 1978, water temperatures in Douglas Channel (Figure 15) in the lowest 200 m were nearly 0.5 K warmer than in October, 1977. The temperature below 50 m depth at two stations (70 and 80) 15 km apart is nearly identical in October whereas at a station in May

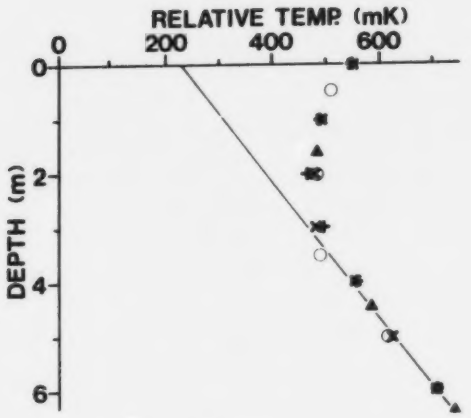

Figure 10. Measured temperatures in the sediments of Alice Arm in October, 1977 (open circles, station 105 and triangles, station 106) and temperatures calculated from the following models of past bottom water temperature variations: (plus) fitted by a single step change occurring 70 days previously (August 5), and (cross) fitted by a sinusoidal annual variation.

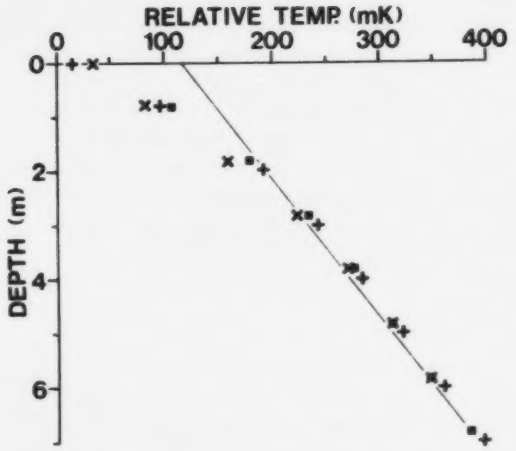

Figure 11. Sediment temperatures in May 1978 in Alice Arm: squares are the average values of measurements of 6 stations, pluses are calculated from a model of the variation of bottom water changes which include the previously determined step change to fit the October Data (Figure 10) and an additional step change, crosses are calculated from the previously determined annual sinusoidal variation, allowing a probe penetration of 0.2 m greater than plotted in May.

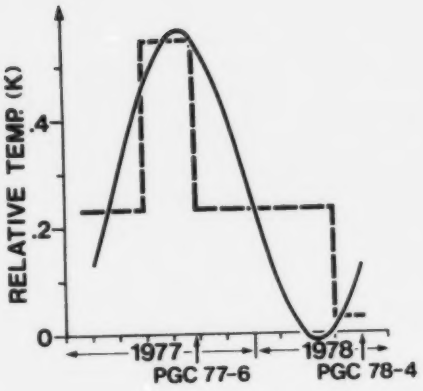

Figure 12. Models of bottom water temperature changes used to produce the calculated sediment temperatures in Figure 11.

(station 45) only 2 km from station 80 the temperature is much warmer. Other measurements of water temperatures made during 1977 and 1978 in this area (Dobrocky, 1977-1978) also demonstrate this large variation with time. A summary of the deepest of water temperatures, including earlier measurements (Pickard, 1961; Data Reports 1963; 1966) and some more recent ones (Macdonald et al., 1978), is presented in Figure 16a. The earlier measurements are omitted from Figure 16b, where all other data are plotted. Although the change at the end of June could be quite abrupt, the seasonal variation in bottom water temperature (Figure 16c) could be well-represented by an annual sinusoidal perturbation.

The four cruises during which the largest variations in bottom water temperatures were measured are the four cruises on which reversing thermometers were used for the measurements. Bottom water temperatures measured with electronic sensors did not vary as much between stations at any one time (Figure 16b); our measurements, for which we claim a relative accuracy of 0.004 K, show a maximum variation of 0.10 K, between Douglas Channel and Squally Channel. Macdonald et al. (1983) have noted that in the winter large volumes of shelf water may be forced into the Kitimat system, and that the temperature of this water varies from year to year. Their data for February, 1977 and 1979 illustrate this for water at intermediate depths, and such a mechanism might cause a variation in bottom water temperatures. The deepest measurements made using reversing thermometers are usually tens of meters above the bottom. The larger temperature variations which they record may indicate that the temperature varies more at that depth than closer to the bottom.

The bottom water temperatures of some basins connected to the Douglas Channel system have changed by larger amounts, and the timing of changes varies as well. The largest observed changes occurred in small, shallow bodies. In Giltoyees Inlet (166 m depth) a temperature decrease of 0.8 K occurred approximately 45 days before the May cruise (6 April). In Kildala Arm (198 m depth) a temperature increase of 0.5 K came approximately 100 days before the October cruise (2 July), and a decrease of 0.4 K, 30 days before the May cruise (22 April).

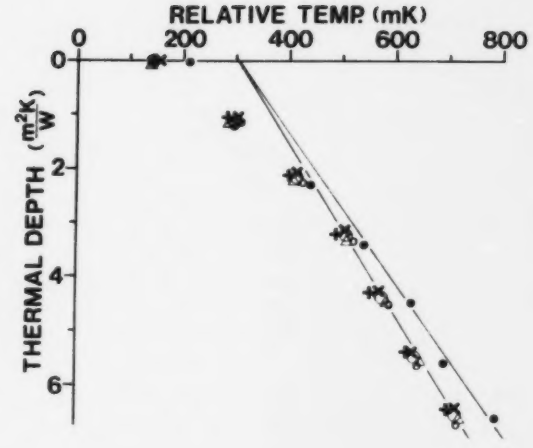

Figure 13. Thermal depth vs measured temperatures, or Bullard plots for 5 stations in Alice Arm, May 1978. Values from the 5 stations are represented by 5 different symbols, and the large open circle is the average temperature at each depth of the four stations best fitting a common curve.

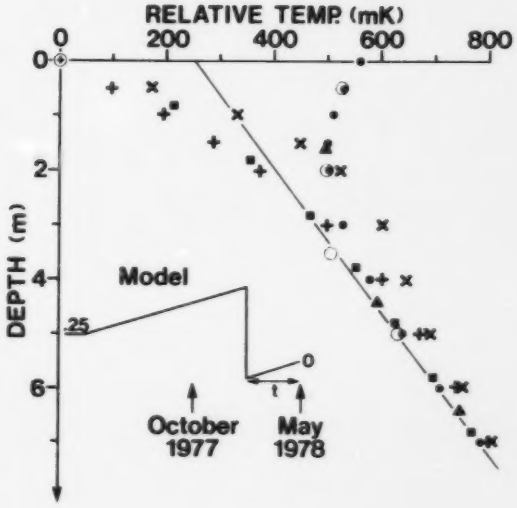

Figure 14. Measured temperatures in the sediments of Alice Arm for October, 1977 (triangles and open circles for two different stations) and for May, 1978 (squares are average values of six stations). Also shown are calculated temperatures (dots) for a ramp fitting the October, 1977 data, and for the May data with a step superimposed on the ramp 35 days (x) and 116 days (+) before the measurements were made in May.

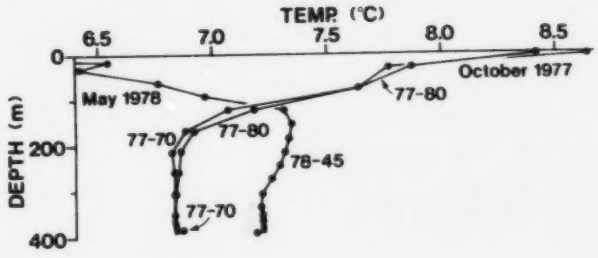

Figure 15. Temperature profiles of the water in Douglas Channel. The sudden change in temperature at the greatest depth of each log represents the sediment temperature when the tip of the probe goes into the soft sediments. The thicker lines just above these points each represent a series of closely spaced measurements.

Since the temperature of the bottom waters in a single basin appears to be only a function of depth at most times, changes in the water sediment boundary temperature should be the same for the whole basin over periods of 10 days or more. It is possible, therefore, to expect the same temperature perturbations to be impressed on the sediments at all stations within a basin, and differences in sediment temperatures between such stations should be caused only by differences in the thermal diffusivity of the sediments.

Squally Channel is considered first since it is a large basin over which the temperature perturbations in the sediments at five stations seem to be similar for each cruise. Before October, 1977, the bottom waters cooled, increasing the gradient near the top of the sediments, whereas just before May, 1978, the water warmed, decreasing the gradient near the sediment-water interface. If single step changes in temperature are fitted to the observations, the best agreement comes from a water temperature cooling by 0.055 to 0.075 K before October, 1977, and an increase of 0.25 to 0.27 K from 30 to 60 days before the next May cruise (PGC 78-4), giving a total change of approximately 0.33 K for the period of a year. The ranges in the amplitudes and times of occurrence include all of the results for this basin.

At three of five stations in Gardner Canal in May, the sediment temperature gradients are quite linear, but at the other two stations the bottom water temperature has increased by 0.29 K approximately 240 days before the cruise (Sept. 20). Echo sounding profiles (3.5 kHz) along the canal (Figure 17) show outcropping bedrock separating a smaller, more shallow basin where the water temperature has changed while the deeper basin has a stable bottom water temperature. Measurements in July, September and December, 1977, and March, 1978, (Dobrocky Seatech Ltd., 1977-78) to depths of 445 m record a change of 0.25 K between July and September, in approximate agreement with the modelled temperatures. However, in May at all five stations the bottom water temperature as measured by the telemetry probe was within 0.01 K of 7.31° C in Gardner Canal; no measurements were made in the previous October.

Several stations were located at the upper end of Douglas Channel on both cruises. In October at 10 of 12 stations the temperature gradient in the sediments was a minimum between 1.5 and 3 m depth, indicative of a similar

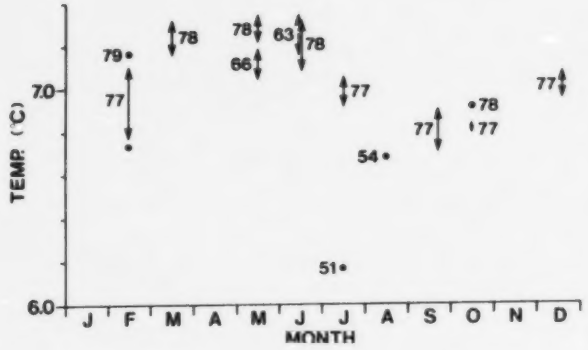

Figure 16a. Near-bottom water temperatures in Douglas Channel System from all known sources of data. The number represents the year in which they were measured.

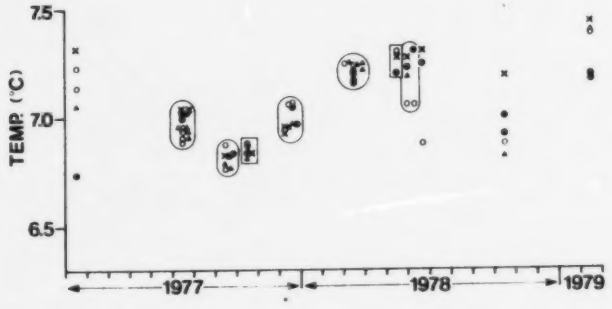

Figure 16b. Near-bottom water temperatures in Douglas Channel System measured by reversing thermometers (unmarked symbols) and by electronic sensors: symbols inside rectangles by our equipment, and symbols inside balloons, by commercial electronic sensors. Data are from Squally Channel (circles), Whale Channel (triangles), Douglas Channel above the sill (dots) and Kitimat Arm (x).

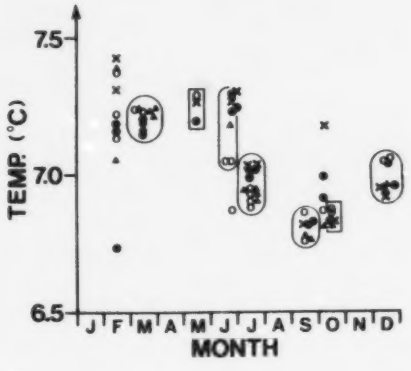

Figure 16c. Bottom water temperatures in Douglas Channel System, as designated in figure 16b, but plotted according to the time of year when measured regardless of which year.

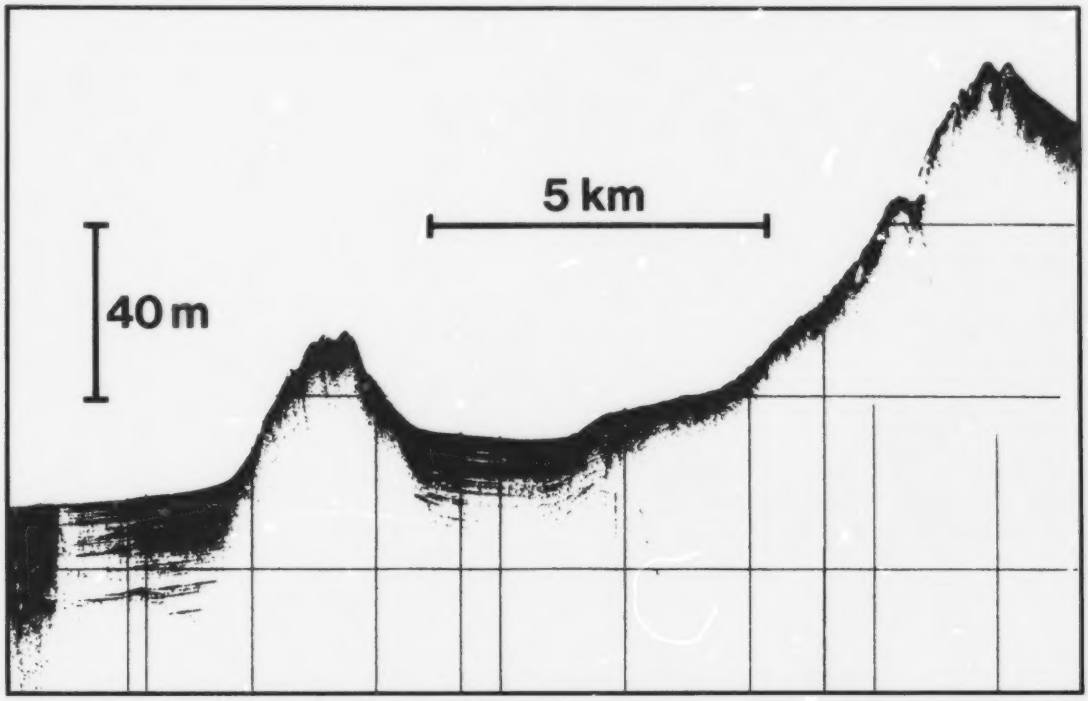

Figure 17. A 3.5 kHz sounder profile along Gardner Canal showing a basin at 457 m depth separated from the deeper basin by bedrock at at depth of 421 m.

change in bottom water temperatures for the entire area. However the magnitude of the gradients averaged over 4.5 m ranged from 10 to 57 mK m^{-1} for these 10 stations. Unfortunately deep cores were not obtained at most stations, but the thermal conductivity measured on shallow cores varies, and in one case the large variation down to a depth of 4.5 m (Figure 18) can account for only a small part of the differences in the temperature gradient.

The temperatures of the sediments measured on May 21, 1978, can be accounted for by an increase in bottom water temperature of 0.26 to 0.29 K occurring 80 to 105 days before (in February). This is in agreement with water temperature profiles measured in December, 1977, and March, 1978 (Fig. 15). The measured temperatures and temperatures calculated from water temperature models are shown in Figure 19 for stations 42 and 53, where the variation in thermal conductivity was very small. The variation in sediment temperature gradients between stations in upper Douglas Channel is largest, as were the differences between bottom water temperatures and near surface sediment temperatures.

INFLUENCE OF BOTTOM WATER TEMPERATURE VARIATION

Using an annual sinusoidal variation or step function (equation 1 or 2) and the amplitudes of temperature variations observed, the changes to the

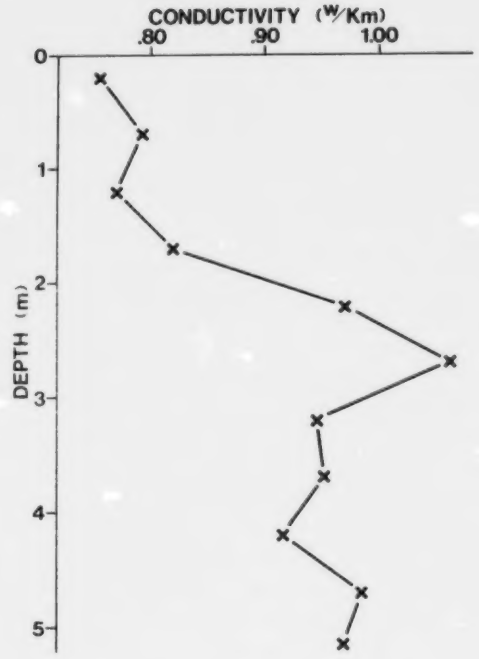

Figure 18. Variation of thermal conductivity measured over the length of a core from station 77-68 in Douglas Channel.

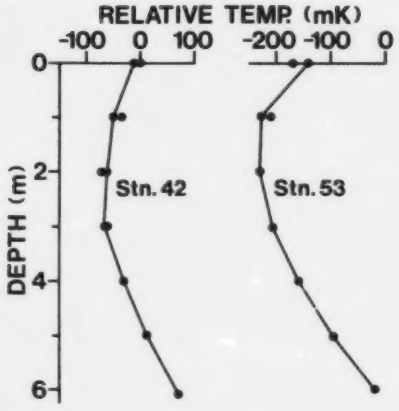

Figure 19. Measured (joined by lines) and calculated sediment temperatures at stations 42 and 53 in Douglas Channel, cruise PGC 78-4.

temperature gradient in the sediments, as well as the uncertainty in the changes, can be calculated. The shorter temperature variations with a period of a year or less are quickly attenuated with depth within the sediments (Fig. 3). For an annual sinusoidal variation in interface temperature, the largest temperature anomaly below 4 m depth is only 8% of the maximum variation at the interface, and the maximum change to the gradient over the depth range of 4 to 6 m is 37 mK m^{-1} for a large interface temperature change of 1 K. Such a large annual variation could be modelled with an accuracy of 10%, making the error in the corrected gradient 3.7 mK m^{-1}, which is less than 10% of the smallest expected gradients (Table 3).

If the average bottom water temperature changes over an interval of years, as can happen (e.g. Pickard 1961; Gade and Edwards 1980), then temperature anomalies in the sediments persist to much greater depths. For example, if the water temperature in 1951 in Douglas Channel (Figure 16a) was 0.8 K cooler than the average temperature now, but only for a period of a year, the effect on the gradient is very small (1 mK m^{-1}). But if the average interface temperature was 0.8 K cooler up until 15 years before the gradients in the sediments were measured, then the effect on the measured temperature gradients is large (50 mK m^{-1}), and does not produce a non-linear gradient for the top 6 m of sediments which would be detected.

CONCLUSIONS

Large changes in the temperature of the bottom waters of Alice Arm and the Douglas Channel - Kitimat System occurred between observations in October, 1977, and May, 1978. Based on observed temperature perturbations in the sediments at the bottom of the fjords, simple models of the past bottom water temperatures were constructed which agree well with the observed temperatures from these two cruises as well as other reliable water temperature measurements.

Over a period of 12 months in 1977, the bottom water temperature in Alice Arm can be approximated by an annual sinusoidal variation with a maximum temperature of 5.5° C in September and a minimum of 5.0° C in March. In the interval mid-1976 to mid-1978 the bottom water temperature in the Douglas Channel - Kitimat system varied approximately sinusoidally with a period of a year. Most of the time the bottom water temperatures in all of the deep, large basins forming this system differed from each other by no more than 0.15 K. The maximum temperature which occurred in April is approximately 7.25° C, and the minimum temperature, in September, is 6.80° C. Some smaller inlets connected to this system had larger variations in bottom water temperatures.

Observations over such a short period of time cannot confirm that bottom water changes occur as annual cycles. The variation in Alice Arm is 180° out of phase with that in the Douglas Channel - Kitimat system. Although mechanisms can explain this (e.g. Muench and Heggie, 1978), more observations are needed. There was no such variation over a period of thirty years in Jervis Inlet (Hyndman, 1976; Lewis et al., in preparation).

Changes in the sediment temperature caused by bottom water changes occurring with periods of a year or less can be modelled and the effects

Table 3. Temperatures and gradients within a semi-infinite solid caused by an annual sinusoidal variation of 1 K applied as the boundary condition.

Diffusivity	Wave No.	Maximum Temperature Change			Maximum Change to Sediment Gradient	
		at 2 m (mK)	at 4 m (mK)	at 6 m (mK)	2-4 m (mK/m)	4-6 m (mK/m)
rock						
1×10^{-6}	.233	640	410	262	135	83
soft sediment						
3×10^{-7}	.576	316	100	32	138	44
2.5×10^{-7}	.631	283	80	23	129	37
2×10^{-7}	.705	244	60	15	117	29

removed to give the equilibrium temperature gradient to an accuracy of about 10% between 4 and 6m below the sediment water interface. However longer term variations or sudden changes in bottom water temperatures which persist for years cannot always be detected, and can affect the temperature gradient in the sediments by large amounts.

ACKNOWLEDGEMENTS

I gratefully acknowledge the many people who assisted in collecting this data. I thank Capt. Marsden and the crew of CSS Vector for their cooperation and skillful navigation, and D. Chisholm and W. Price for their assistance in manuscript preparation. I am indebted to B. Bornhold and R. Macdonald for providing critical comment on the first draft.

REFERENCES

Carslaw, H.S. and J.C. Jaeger. 1959. Conduction of Heat in Solids, Second Edition, Oxford University Press, London.

Data Reports of the Institute of Oceanography, University of British Columbia, Vancouver, B.C.
No. 23. 1963. British Columbia Inlet Cruises
No. 26. 1966. British Columbia and Alaska Inlet and Pacific Cruises
No. 30. 1969. British Columbia Inlet and Pacific Cruises
No. 32. 1970. British Columbia Inlet and Pacific Cruises
No. 34. 1972. British Columbia Inlet Cruises

Dobrocky Seatech Ltd., Annual summary of physical oceanographic measurement in Alice Arm - August 1976 to September 1977. Data Report for J.L. Littlepage, Oceanographic Consultant, Victoria, 111 pp. (1977).

Dobrocky Seatech Ltd., Cruise Reports-Kitimat Oceanographic Study: July, 1977; September, 1977; December, 1977; March, 1978; and June, 1978. (1977-78). For the Institute of Ocean Sciences, Sidney, B.C.

Gade, H.G. and A. Edwards. 1980. Deep Water Renewal in Fjords. In Fjord Oceanography, Freeland, H.J., D.M. Farmer and C.D. Levings (eds.), p. 453-489.

Hyndman, R.D. 1976. Heat flow measurements in the inlets of southwestern British Columbia. J. Geophys. Res., 81, 337-349.

Hyndman, R.D., E.E. Davis and J.A. Wright. 1979. The measurement of marine geothermal heat flow by a multipenetration probe with digital acoustic telemetry and in situ thermal conductivity. Marine Geophysical Research 4, 181-205.

Jaeger, J.C. 1965. Applications of the theoy of heat conduction to geothermal measurements. In Terrestrial Heat Flow, W.H.K. Lee (ed.) Geophysical Monograph Series #8, American Geophysical Union, 7-23.

Krauel, D.P. 1981. Deep water flow and exchange processes in Alice Arm, B.C., Institute of Ocean Sciences Contractor Report Series 81-4 Sidney, B.C.

Lewis, T.J. 1975. A geothermal survey at Lake Dufault, Quebec. Ph.D. Thesis, U. of Western Ontario, London, Ontario.

Littlepage, J.L. 1978. Oceanographic and marine biological surveys Alice Arm and Hastings Arm, British Columbia 1974-1977. Consultants report for Climax Molybdenum Corp. of B.C. Ltd., Terrace 78 pp.

Macdonald, R.W., W.J. Cretney, C.S. Wong and P. Erickson. 1983. Chemical characteristics of water in the Kitimat fjord system. Can. Tech. Rep. Hydrogr. Ocean Sci. 18, 66-87.

Macdonald, R.W., D.M. Macdonald and P.S. Munro. 1978. Oceanographic Data Report, Kitimat Arm, Porpoise Harbour, February, 1977. Pac. Mar. Sci. Rept., 78-24, Institute of Ocean Sciences, Sidney, B.C.

Muench, R.D. and D.T. Heggie. 1978. Deep water exchange in Alaskan sub-arctic fjord, In Estuarine Transport Processes, B. Kjerfrie (ed.) Univ. of South Carolina, pp. 239-267.

Pickard, G.L. 1961. Oceanographic features of inlets in the British Columbia mainland coast. J. Fish. Res. Ed. Canada 18, 907-999.

Ratcliffe, E.H. 1960. The thermal conductivities of ocean sediments. J. Geophys. Res. 65, 1535-1541.

Webster, I. 1980. Kitimat physical oceanographic study 1977-78. Part 3, Estuarine Circulation. Contract Report 80-3, Institute of Ocean Sciences, Sidney, B.C. 81 pp.

LES NOMBREUSES CYCLIQUES SELECTIONNÉES AROMATIQUES D'HYDROCARBURE (NCAH) POUR LES DEPÔTS EN SURFACE, ET LES CENTRES AGES DU KITIMAT ARM - DOUGLAS CHANNEL ET COURS D'EAU ADJOINTS

W.J. Cretney, C.S. Wong and R.W. Macdonald
Institute of Ocean Sciences, Sidney, B.C.

P.E. Erickson and B.R. Fowler
Seakem Oceanography Limited, Sidney, B.C.

RESUME

La concentration des nombreuses cycliques sélectionnées aromatiques d'hydrocarbure (NCAH) dans le dépôt d'échantillon est déterminé de 40 stations d'étude dans tout le Kitimat. La distribution des (NCAH) sur la surface des dépôts au nord de Kitimat Arm est consistants avec le fondeur d'aluminium Alcan, y étant la source. Cette déduction est soutenue par les (NCAH) distribuées dans les centres âgés, qui dénote une augmentation soudaine dans le contenant des (NCAH) correspondant dans la construction et la production prématurée du fondeur. Il y a des évidences équivocales dans les (NCAH) concentrées dans le dépôt des centres éloignés de Kitimat, qui peuvent être élevées du norme historique. Bien que les sources des (NCAH) trouvées dans le dépôt dans les centres lointains - demeure incertain. La calculation basée sur un modèle de plume Gaussian de la transportation atmospherique contaminée indique que le fondeux - aluminium ne peux être exclus comme une source première contributrice. Une considération des facteurs controllant le mouvement de flôt transporte par l'eau des (NCAH) rapport aux particules - suggère que ce mode de transport est improbable à l'importance du procédé par lequelles (NCAH) peuvent être transportées du fondeur aluminium jusqu'aux stations éloignées.

Cretney, W.J., C.S. Wong, R.W. Macdonald, P.E. Erickson and B.R. Fowler. 1983. Polycyclic aromatic hydrocarbons in surface sediments and age-dated cores from Kitimat Arm, Douglas Channel and adjoining waterways, 18, 162-195.

Mot-clés: dépôt a côtes marines, Kitimat, le fondeur d'aluminum, nombreuses cycliques aromatique hydrocarbure, transport

POLYCYCLIC AROMATIC HYDROCARBONS IN SURFACE SEDIMENTS AND AGE-DATED CORES FROM KITIMAT ARM, DOUGLAS CHANNEL AND ADJOINING WATERWAYS.

W.J. Cretney, C.S. Wong and R.W. Macdonald,
Institute of Ocean Sciences, Sidney, B.C.

P.E. Erickson and B.R. Fowler.
Seakem Oceanography Limited, Sidney, B.C.

ABSTRACT

The concentrations of selected polycyclic aromatic hydrocarbons (PAHs) in sediment samples are presented for 40 stations throughout the Kitimat study area. The distribution of PAHs in surface sediments of northern Kitimat Arm is consistent with the Alcan aluminum smelter being the source. This inference is supported by PAH distribution in age-dated cores that show an abrupt increase in PAH content corresponding in time to the construction and early production years of the smelter. There is some equivocal evidence that PAH concentrations in sediments of stations remote from Kitimat may be elevated from the historical norm. Although the sources of the PAHs found in sediments from remote stations remain uncertain, calculations based on a simple Gaussian plume model of atmospheric pollutant transport indicate that the aluminum smelter cannot be excluded as a primary contributing source. Consideration of factors controlling the water-borne movement of PAH bearing particles suggest that this mode of transport is unlikely to be an important process by which PAHs may be transported from the aluminum smelter to remote stations.

Cretney, W.J., C.S. Wong, R.W. Macdonald, P.E. Erickson and B.R. Fowler. 1982. Polycyclic aromatic hydrocarbons in surface sediments and age-dated cores from cores from Kitimat Arm, Douglas Channel and adjoining waterways. Can. Tech. Rep. Hydrogr. Ocean Sci. 18, 162-195.

KEY WORDS: aluminum smelter, coastal marine sediments, Kitimat, polycyclic aromatic hydrocarbons, transport

INTRODUCTION

One of several proposals for transporting Alaskan North Slope crude oil to eastern North America under consideration when this study was conceived would have resulted in the building of an oil tanker port at Kitimat in northern British Columbia (Figure 1) and a pipeline to Edmonton, Alberta, linking there with the continental network. Since specific, detailed knowledge of the environmental state of the marine zone that would be affected was lacking, a variety of on-going or new programs to gather coastal physical and chemical oceanographic data were focussed on Douglas Channel, Kitimat Arm and their adjoining water ways.

Apart from the oil port possibility, the marine approaches to Kitimat were already of particular interest because of the presence of Western Canada's only aluminum smelter (Figure 2) near Kitimat, a town only three decades old and owing its entire existance to the establishment of the smelter in the early 1950's. Studies of Norwegian fjords on which aluminum smelters were located had recently produced evidence that the smelters were a major source of polycylic aromatic hydrocarbons (PAHs) in the local marine environment (Palmork, 1974). Since Kitimat is the only industrial settlement in the area,it represented the first near encroachment of industrial civilization in an otherwise pristine fjord system. Because the aluminum smelter was the only major industry until recently, the Kitimat area promised to afford a place for

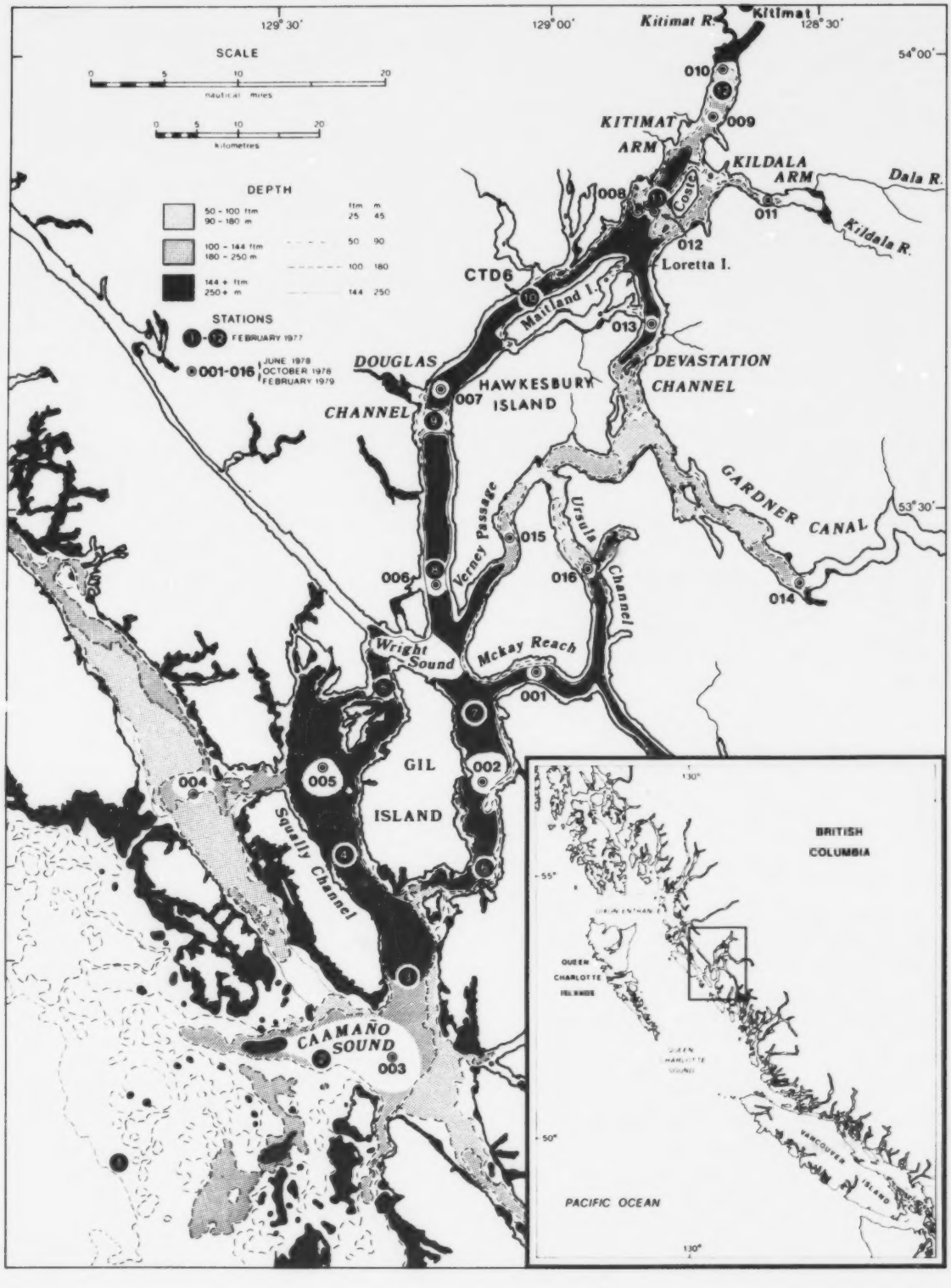

Fig. 1. Kitimat study area and sampling stations in northern British Columbia.

environmental studies relatively uncomplicated by the large manifold of source types and locations of contaminants that usually accompany such studies.

The work described in this paper was concerned mainly with the PAH containing fraction of marine sediment extracts. A principal objective of the work was to delineate the areal and chronological distributions of PAHs in the marine sediments of the region. A further objective was to reconcile the observed distributions with those that might be expected from probable water or air transport modes. In addition, the usefulness of the PAH fraction was to be assessed for the determination of the presence and quantity of petroleum hydrocarbons that might be released during tanker operations.

METHODS

Sampling Stations and Field Methods

Primary oceanographic cruises were carried out, one in each of the months of June and October, 1978, and February, 1979. A full program of hydrocarbon and general oceanographic sampling was carried out at stations 001 to 014, except 012 (Figure 1). Generally only CTD probe casts were made at stations CTD-1 to CTD-10, although a sediment sample was obtained from station CTD-6 during the October cruise. Additional sediment samples were obtained in October at stations 009-1 to 009-5, inclusive, and at stations 010-1 and 010-2, and again in February at stations G1 to G16, inclusive (Figure 2). Sediment core samples were collected at stations 014 and 010 during the June 1978 cruise. The core from station 010 subsequently was found to be unsuitable for determining the PAH geochronology. Other attempts to obtain a suitable core from northern Kitimat Arm also ended unsatisfactorily until three cores were obtained off Emsley Point during a second supplementary cruise conducted in May, 1979.

Sampling Methods

During the three principal cruises a clean-room laboratory module (Wong et al., 1976) was carried aboard the motor vessel "Sea Lion" under charter from Dobrocky Seatech Ltd. to provide a contaminant-free area in which hydrocarbon containing samples could be processed.

Surface sediments were collected with a modified Smith-McIntyre grab sampler (Kahlsico International Corp.) which sampled a surface area of $0.1M^2$. Depth of penetration varied with the type of sediment. Usually, however, the top 10-20 cm of sediment was obtained with a relatively undisturbed surface. A subsample of the upper 5 cm was taken for hydrocarbon analysis from a relatively smooth portion of the grab sample's surface before the samplers jaws were opened to release the sample. To accomplish the subsampling a cleaned aluminum ring, 5 cm in depth and 9 cm in diameter, which had been cut from an aluminum sample can, was pushed into the sediment surface and lifted out together with the sediment core using a broad bladed spatula. The sediment was extruded into a cleaned aluminum can and the lid secured in place with teflon tape. The can was then wrapped in aluminum foil and immediately frozen. Additional subsamples for organic carbon analysis were stored frozen in plastic Whirlpak bags.

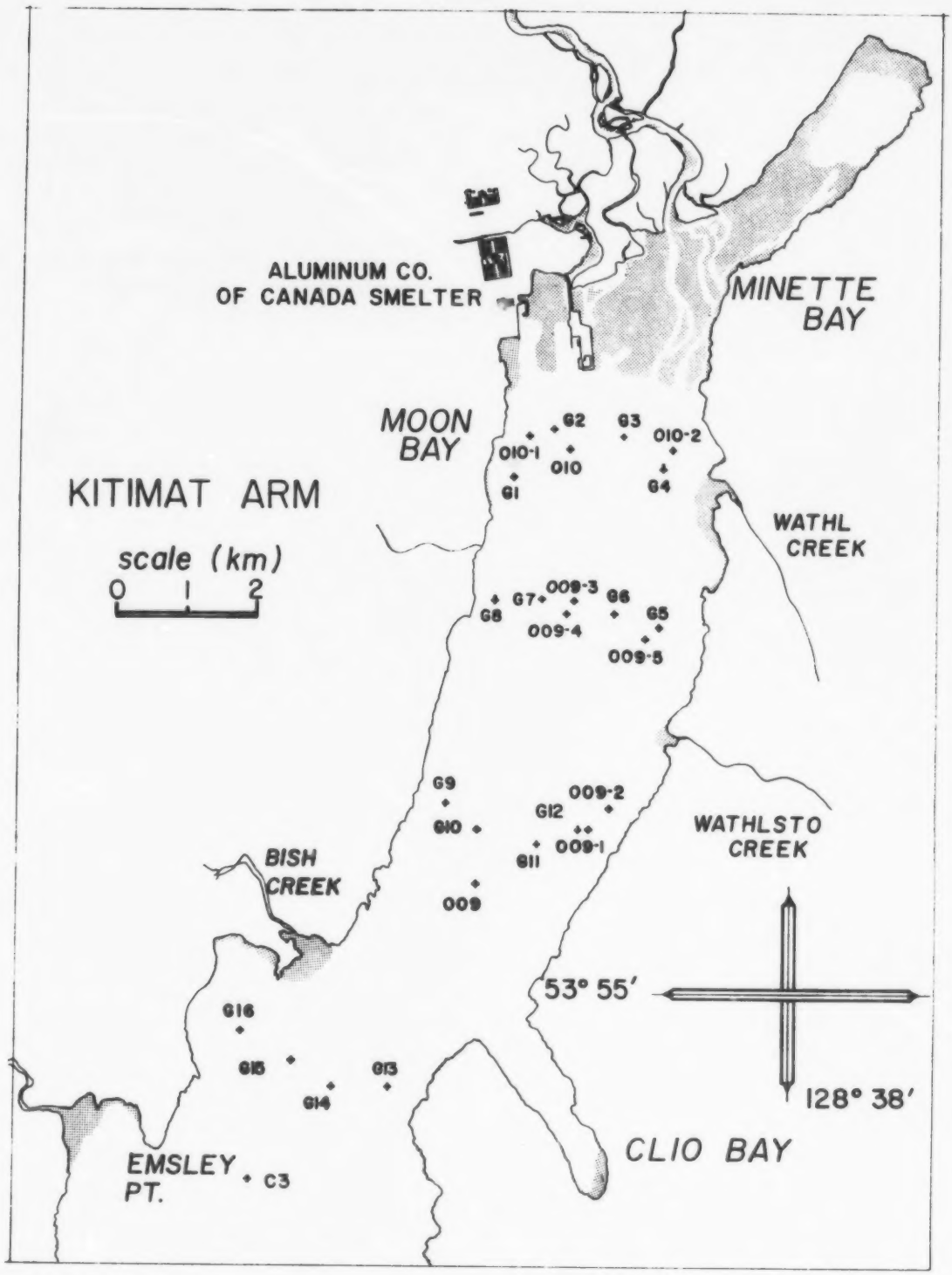

Fig. 2. Site of the Alcan smelter and sampling stations in northern Kitimat Arm.

Cores for ^{210}Pb-dating were obtained by two methods. On principal cruises a Soutar-Bruland, clear vented, slow entry box corer (Young et al., 1973) was used. Subsamples for hydrocarbon analysis were obtained at 3 cm intervals by inserting a syringe-type stainless steel and teflon suction corer through specially machined holes on the side of the box cores that were sealed with metal plugs during deployment and retrieval. The core sediment samples were extruded into cleaned aluminum cans from the suction corer and stored as was done for the grab samples. Samples for organic carbon and ^{210}Pb analyses were collected in a similar manner.

Additional cores were obtained at station C3 using a gravity corer with 10.5 cm internal diameter, clear acrylic, cyclindrical core barrels. Subsamples were obtained by extruding the core in an upright position and slicing off 3 cm thick sections. The central 9 cm core of each section was transferred to a cleaned aluminum can and stored frozen as before. Additional portions from the outside were stored frozen in plastic whirlpak bags for ^{210}Pb and organic carbon analyses.

Laboratory Methods

Materials and equipment were prepared for use as previously described (Cretney et al., 1980a) with some modifications. Following washing with soap and water and immersion overnight in a chromic acid bath, glassware was rinsed with hydrocarbon-free distilled water (Chesler et al., 1976) and baked overnight in an oven at 350°C before use. Aluminum cans were similarly cleaned with omission of the chromic acid immersion. Florisil (60-100 mesh, chromatography grade) was washed thoroughly with distilled water, then methanol and dried for 24 hours at 70°C in a forced-air oven. The Florisil was then calcined at 600°C for 6 hours, allowed to cool under dry, hydrocarbon-free nitrogen gas, and deactivated by equilibration with 5% by weight of hydrocarbon-free water in a sealed flask for a minimum of 48 hours.

Sediment subsamples were obtained from still partially frozen samples in aluminum cans by coring from top to bottom with a cleaned syringe-type suction corer. This procedure provided a vertically integrated subsample with reduced probability of accidentally contaminating an entire sample. The procedure also reduced the likelihood of a microbial alteration resulting from complete thawing, but did not permit total sample homogenization. Sample homogenization prior to freezing in the field was considered too risky because of possible sample contamination.

The extraction, separation, and measurement of selected PAHs were carried out mainly as previously described (Cretney et al. 1980a; 1980b) using for each analysis typically 0.3 µg each of ($^{2}H_{10}$)phenanthrene, ($^{2}H_{10}$)pyrene, ($^{2}H_{12}$)chrysene, ($^{2}H_{12}$)benz(a)anthracene and ($^{2}H_{12}$)perylene as internal standards. Quantification was carried out by the peak height ratio method using a correction factor for the relative response of a given analyte PAH to its deuterated form, if it was used as an internal standard, or its deuterated geometrical isomer. In exception, benzo(b/j/k)fluoranthenes were quantified using the deuterated chrysene/benz(a)anthrancene pair. This exception was made necessary because of the variable recovery of ($^{2}H_{12}$)perylene at the 0.3 µg level due to the unpredictable, sometimes appreciable amount of its chemisorption on Florisil (Cretney et al., 1980a). In order to speed up analyses, two temperature programs were used depending on the boiling points

of the analytes: 150°C for 2 min., then 8°C/min to 250°C or 200°C for 2 min, then 8°C/min to 300°C.

Confirmation of the identity of the analytes was obtained using an INCOS 2300 data system, which was newly acquired toward the end of the study. Confirmation was based on comparison of the relative retention times of analytes with those of the deuterated internal standards and on comparison of analyte mass spectra with those of authentic samples. The relative intensities of mass spectral peaks in the molecular ion cluster of standards and analytes were examined in representative samples to verify the absence of significant interfering signals from coeluting non analyte or standard compounds. In addition, selected extracts were also chromatographed using a flexible fused silica column (25 m, carbowax 20M, Hewlett Packard Corp.) coated with SP2100. The end of this column was pulled down to a narrow constriction using a flame, cut back with a diamond pencil until the pressure drop across the constriction was about 1 atm, and fed directly through the inlet tube to the analyser of the GC/MS/DS system.

Instrumental precision was determined by quadruplicate injection of a single PAH fraction obtained from a sediment homogenate prepared from a large grab sample from station G14. The precision of the method was determined by carrying out the analysis of 4 subsamples (100g) of the same sediment homogenate. The sediment (1.5kg) was homogenized by mixing for 30 minutes with a teflon stirrer attached to a hand held electric drill. Because the homogenization process generated a large amount of fine particulate matter that remained in suspension following aqueous/ethanolic KOH treatment and the usual settling period, the decanted solvent and suspension was filtered through a pre-extracted Whatman GF/A glass fibre filter. The filterables and filter paper were added to the residue for further extraction with refluxing isooctane.

Within-sample variation was estimated through duplicate analyses of vertically integrated subsamples of principal station samples. Within-station variation was estimated through analysis of samples collected at the principal stations in the three main cruises. Since only one sample was collected at each station on each cruise over an eight month period, the variability has an unknown temporal contribution. Assuming an uneventful deposition of sediment between cruises, this contribution should be negligible.

Another four subsamples of the station G14 sediment homogenate were used in an experiment to determine the minimum detectable amount of oil in a representative intermediate PAH level Kitimat Arm sediment using GC/FID and GC/MS based techniques. Aliquots of a solution of Prudhoe Bay crude oil in ethanol/tetrahydrofuran (1:4) were added to the subsamples to give dry weight crude oil concentrations of 9.6 mg/kg, 96 mg/kg, 192 mg/kg, and 480 mg/kg. Individually spiked sediments were rehomogenized with a stainless steel spatula and 50 g subsamples of each were taken for analysis. A procedural blank and an aliquot of the crude oil standard solution were also carried through the entire analytical procedure. Parent PAHs were quantified using the PROMIN system in the usual manner. Other components of the PAH fraction of the oil and oil-spiked sediments were examined using the INCOS 2300 data system operating in the sequential scan mode. Dibenzothiophene and its C_1 and C_2 alkylated derivatives were quantified from the mass fragmentograms.

The extraction efficiency of the method was assessed by re-extracting the residual sediments from the analysis of the samples from station G1 and station 014 (core segment, 30-33 cm). The re-extraction was performed under N_2 gas by the soxhlet method for 7 hours with methylene chloride and then 15 hours with isopropyl alcohol.

^{210}Pb-dating of sediment cores was done using the procedure of Matsumoto and Wong (1977), in which ^{210}Pb was measured by counting the β decay of its ^{210}Bi daughter nuclide in a flow-type counter. The density of the solid phase was determined by pycnometry. Salt corrections were made using the assumption that the salinity of the pore water was the same as that of the overlying bottom water. Sedimentation rates were calculated using the constant rate of supply of ^{210}Pb model (Oldfield et al., 1978).

Organic carbon was determined by the titration method of Gaudette et al. (1974). A standardization blank was processed with each batch of samples.

RESULTS

General Statistical Considerations

Mean instrumental precisions (r.s.d.) of 2.2%, 1.9%, 1.8%, 9.3% and 4.4% for phenanthrene/anthracene, fluoranthene, pyrene, chrysene/triphenylene/benz(a)anthracene, and benzo(b/k)fluoranthenes were determined by replicate injection of a typical PAH containing fraction obtained on work-up of a sediment sample from station G14. The precision of the method was determined by analysis in quadruplicate of a well homogenized sediment sample from the same station. The relative standard deviations were 2.9%, 6.7%, 5.0%, 7.4% and 7.9%, respectively, for the PAHs listed above.

The relationship between the mean PAH concentration and variances of replicate analysis of sediments from several stations was determined using Taylor's power law:

$$\ln s^2 = \ln a + b \ln \bar{x}$$

where s^2 = sample variance, $\bar{x}$ = sample mean, and b is the exponent which determines an appropriate transformation ($z = x^{1-b/2}$ for $b \neq 2$ and $Z = \log x$ for $b = 2$) (Green, 1979) for stabilizing the variance of the samples. The within-sample variance and means were calculated for duplicate analyses of 12 samples, one from each of the stations 003-011, 013, 015, 016 and plotted according to the above expression. The slope, b, of the regression line was 2.08 ($r = 0.77$, $p < 0.005$). Similarly, the within-station sample variances and mean PAH concentrations (calculated from data normalized to organic carbon content) for stations 003, 004, 006, 008, 011, 014, 015 (3 cruises) and 001, 002, 009, 013, 016 (2 cruises) were calculated and regressed against each other. Once again the slope of the regression line was near 2, i.e., 1.93 ($r = 0.89$, $p < 0.001$).

Assuming the existence of a common within-sample coefficient of variation for all stations, its value was estimated from the pooled within-sample variances (Lindgren and McElrath, 1969) of the log transformed PAH concentrations (Eberhardt et al., 1976). The estimate based on all replicate

subsamples was 0.19. The within-station coefficient of variation was estimated as 0.65 in the same way. In excluding the samples obtained from station 013 because the sample collected in October 1979 contained only 0.2% organic carbon, the value reduced to 0.46. The within-station coefficient of variation for the normalized PAH concentrations (exclusive of the June, 1979 samples from stations 001 and 002 for which organic carbon analysis was not done) was determined to be 0.35, which compares with 0.64 determined for the non-normalized PAHs from the same data set. Excluding station 013, the value changed only slightly to 0.34 compared to a change from 0.64 to 0.42 for the unnormalized PAH concentrations in the same data set.

Soxhlet extraction with methylene chloride and isopropyl alcohol of the insoluble residue from the analysis of the sediment sample from station G1 yielded small quantities of initially unextracted PAHs. The additional amount of the PAHs varied from 2-9% of the amounts that were recovered on the first extraction. The percentage recoveries generally increased with increasing molecular weight. Re-extraction of the 30-33 cm core segment from station 14 also yielded additional quantities of PAHs. The percentage recoveries again generally increased with increasing molecular weight, although the range, 10-25%, was larger and the values higher. Because the $C_{14}H_{10}$: $C_{18}H_{12}$ ratio was used as a parameter for characterizing sediment samples from various depths in cores and sites in the study area, the effect of the apparent differential recovery of PAHs from sediments of high and low concentrations was assessed. To take into account the amounts of $C_{14}H_{10}$ and $C_{18}H_{12}$ PAHs as well as internal standards obtained on re-extraction of the sediment sample from station G1, the ratio would have to be decreased by only 1%. A significantly greater decrease of 11% would be required for the station 014 sediment sample.

Minimum Detectable Oil Experiment

Examination of the aromatic fraction from sediment samples obtained from stations G1 and G14 revealed dibenzothiophene was present in an amount less than 10% of the prominant parent PAHs. Since its proportion in the Prudhoe Bay crude oil was relatively high, the incremental change in its concentration in the oil-spiked sediment sample from G14 was readily measureable. As an added bonus, the ethyl- and dimethyldibenzothiophenes having a molecular weight of 212, the same as ($^{2}H_{10}$)phenanthrene, were found to be quantifiable in almost all the sediments analysed by the Promin method. Hence a benchmark for this crude oil marker for the region has also been obtained. Dibenzothiophene was confirmed by comparison of its retention time and mass spectrum with those of an authentic sample. The methyl-, ethyl- and dimethylbenzothiophenes were tentatively identified from their characteristic GC patterns, reasonable retention times relative to dibenzothiophene, and mass spectra.

The concentrations of the dibenzothiophenes in the crude oil spiked sediment samples were found to correlate well with the concentrations of added oil (Figure 3) assuming a precision similar to that which was obtained for PAHs. The correlation appeared to be positive and linear, particularly with respect to dibenzothiophene itself. A single determination only, however, was made at each spike level.

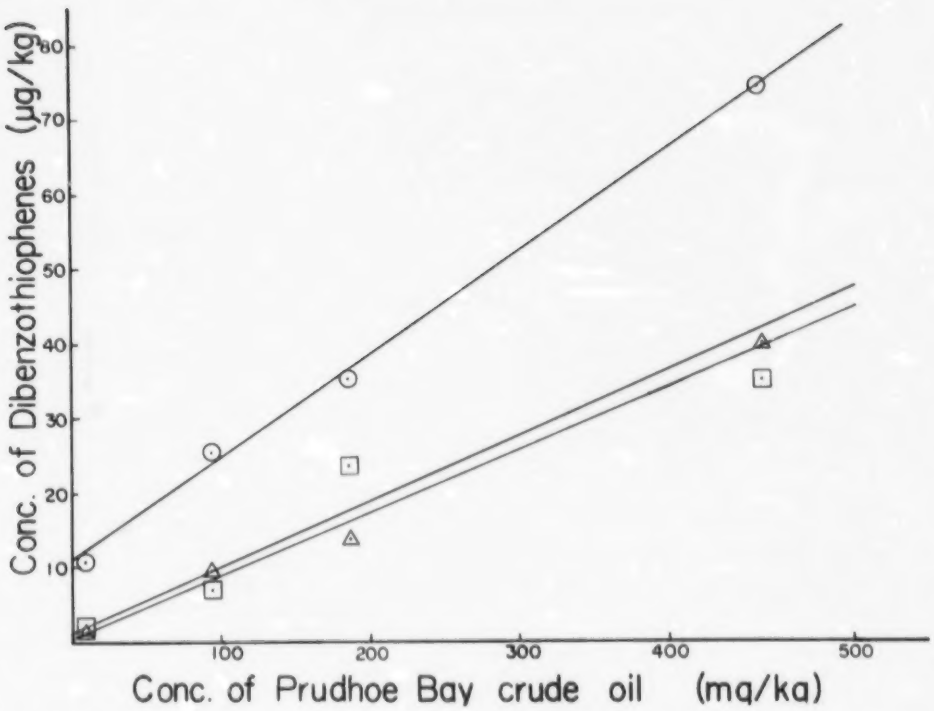

Fig. 3. Plot of dibenzothiophene concentrations against concentration of Prudhoe Bay crude oil added to a sediment sample from station G14. ⊙, dibenzothiophene; △, methyldibenzothiophenes; ⊡, dimethyldibenzothiophenes.

Organic Carbon and Water Content, Particle Size Distribution of Sediments

Sediment samples from the more marine stations generally exhibited higher % organic carbon values (Table 1). Several values in excess of 3.0% were obtained. The sediments with highest % organic carbon also had very high water and fine particle content. Although the relationship among organic carbon content, water content, and particle size distribution was not investigated in detail for the purposes of this paper, they appeared to be correlated.

The northern Kitimat Arm sediments exhibited a narrower range of organic carbon content (Table 2) than sediments from the study area as a whole. Despite the narrow range, 1.0 - 1.8%, there was a link between organic carbon concentration and location in the Arm (Figure 4). The lowest values were obtained for sediments from the centre-east portion of the Arm. The highest values were found in sediments along the east shore, at the entrance to the Arm and in an apparent tongue stretching out from the northwest corner down and part way across channel.

The distributions of organic carbon and water were very uniform along the length of the core obtained off Emsley Point (Table 3). Indeed, the % range of organic carbon was 1.6 - 1.8, with no depth trend discernable. Although only four levels have been analysed, a similar narrow range was observed for the core obtained at station 014.

TABLE 1: Concentration of PAHs and Organic Carbon in Surface Sediments at Primary Stations

Station No.	Cruise No.	$C_{14}H_{10}$[a] (mg/kg)[b]	Fluor., $C_{16}H_{10}$ (mg/kg)	Pyr., $C_{16}H_{10}$ (mg/kg)	$C_{18}H_{12}$[a] (mg/kg)	$C_{20}H_{12}$[a] (mg/kg)	PAH Sum (mg/kg)	Organic Carbon (%)
001	78-01	0.012	0.012	0.011	0.019	0.035	0.088	n.a.[d]
001	78-02	0.032	0.033	0.032	0.052	0.098	0.25	3.6
001	79-01	0.058	0.066	0.063	0.079	0.12	0.39	3.8
002	78-01	0.023	0.023	0.025	0.016	0.039	0.13	n.a.
002	78-02	0.015	0.027	0.026	0.025	0.060	0.15	1.4
002	79-01	0.031	0.024	0.021	0.036	0.060	0.17	2.0
003	78-01	0.041	0.045	0.043	0.028	0.029	0.19	3.2
003[c]	78-02	0.023	0.033	0.029	0.040	0.11	0.24	2.7
003	79-01	0.015	0.016	0.014	0.018	0.063	0.13	2.2
004[c]	78-01	0.0090	0.010	0.015	0.020	0.014	0.068	1.5
004	78-02	0.010	0.0033	0.0046	0.0072	0.015	0.041	0.4
004	79-01	0.0034	0.0033	0.0039	0.0053	0.011	0.027	1.2
005[c,e]	78-01	0.066	0.029	0.043	0.080	0.075	0.29	3.5
006[c]	78-01	0.079	0.13	0.12	0.12	0.24	0.69	2.5
006	78-02	0.050	0.069	0.066	0.074	0.39	0.65	3.5
006	79-01	0.047	0.062	0.058	0.078	0.19	0.44	2.9
007[c]	78-01	0.064	0.088	0.10	0.15	0.28	0.68	1.6
007[e]	79-01	0.025	0.033	0.035	n.d.[f]	n.d.	-	1.6
CTD6[e]	78-02	0.18	0.30	0.30	0.19	0.42	1.4	2.4
008[c]	78-01	0.29	0.52	0.58	0.49	0.87	2.8	1.6
008	78-02	0.13	0.23	0.24	0.23	1.1	1.9	1.7
008	79-01	0.16	0.27	0.27	0.36	0.60	1.7	1.5
009[c]	78-01	0.30	0.46	0.50	0.87	1.5	3.7	1.1
009[e]	78-02	0.26	0.36	0.40	0.70	1.4	3.1	1.5
010	78-01	0.46	0.54	0.64	n.d.	n.d.	-	1.5
010[c,e]	78-02	0.14	0.21	0.20	0.48	0.72	1.8	1.3
011[c]	78-01	0.036	0.087	0.089	0.077	0.14	0.43	2.0
011	78-02	0.050	0.082	0.075	0.12	0.46	0.78	2.2
011	79-01	0.029	0.061	0.056	0.067	0.19	0.40	1.8
013[c]	78-01	0.070	0.14	0.14	0.15	0.33	0.82	2.2
013[e]	78-02	0.0028	0.0047	0.0053	0.0099	0.016	0.039	0.2
014[g]	78-01	0.0099	0.017	0.020	0.033	0.075	0.16	1.6
014	78-02	0.0088	0.017	0.017	0.028	0.10	0.17	1.8
014	79-01	0.0025	0.0021	0.0029	0.0055	0.017	0.030	1.0
015[c]	78-01	0.014	0.031	0.029	0.027	0.036	0.14	0.9
015	78-02	0.0061	0.0090	0.0084	0.022	0.036	0.081	1.2
015[c]	79-01	0.0076	0.014	0.013	0.021	0.052	0.11	1.2
016[e]	78-01	0.041	0.067	0.087	0.049	0.15	0.40	3.4
016	79-01	0.043	0.058	0.051	0.061	0.14	0.35	3.9

[a] $C_{14}H_{10}$, phenanthrene and anthracene; $C_{18}H_{12}$, chrysene, triphenylene and benz(a)anthracene; $C_{20}H_{12}$, benzofluoranthenes; [b] dry weight; [c] arithmetic mean of two determinations; [d] n.a., not analyzed; [e] data for one of more cruises not presented because either no sample was collected or sample was not analyzed; [f] n.d., not determined, usually because of interfering natural products; [g] surface segment (0-3 cm) of core.

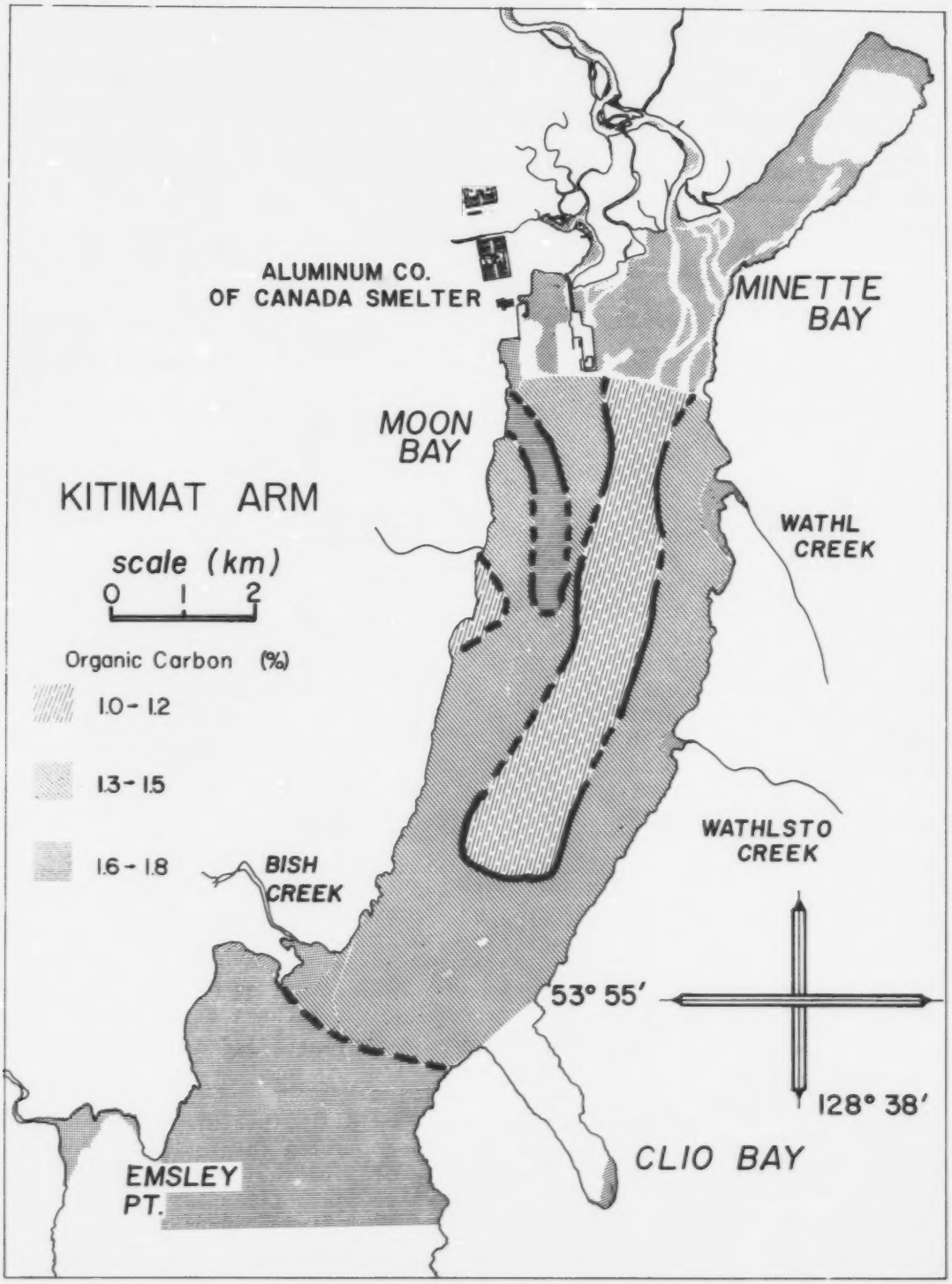

Fig. 4. Organic carbon distribution in sediments of northern Kitimat Arm.

TABLE 2: Concentration of PAHs and Organic Carbon in Surface Sediments at Secondary Stations in North Kitimat Arm

Station No.	Cruise No.	$C_{14}H_{10}$[a] (mg/kg)[b]	Fluor., $C_{16}H_{10}$ (mg/kg)	Pyr., $C_{16}H_{10}$ (mg/kg)	$C_{18}H_{12}$[a] (mg/kg)	$C_{20}H_{12}$[a] (mg/kg)	PAH Sum (mg/kg)	Organic Carbon (%)
009-1	78-02	0.24	0.31	0.33	0.56	1.2	2.6	1.4
009-2	78-02	0.44	0.63	0.59	0.53	0.12	2.3	1.3
009-3	78-02	0.083	0.12	0.13	0.13	0.070	0.53	1.1
009-4	78-02	0.052	0.10	0.099	0.11	0.13	0.49	1.5
009-5	78-02	0.22	0.37	0.35	0.45	0.56	2.0	n.a.[c]
010-1	78-02	0.82	1.2	1.2	1.3	4.0	8.5	1.6
010-2	78-02	0.13	0.22	0.23	0.41	0.61	1.6	1.5
G1	79-01	1.2	1.5	1.6	2.6	3.1	10	1.3
G2	79-01	0.17	0.41	0.41	0.88	1.1	3.0	1.3
G3	79-01	0.018	0.056	0.048	0.074	0.11	0.30	1.1
G4	79-01	0.15	0.17	0.17	0.29	0.35	1.1	1.3
G5	79-01	0.13	0.34	0.33	0.55	1.1	2.4	1.4
G6	79-01	0.17	0.28	0.29	0.36	0.57	1.7	1.1
G7	79-01	0.061	0.091	0.092	0.20	0.14	0.58	1.6
G8	79-01	0.42	0.54	0.57	1.0	1.8	4.4	1.2
G9	79-01	0.50	0.75	0.77	1.0	2.0	5.0	1.3
G10	79-01	0.25	0.20	0.20	0.79	0.60	2.1	1.2
G11	79-01	0.19	0.26	0.27	0.43	0.81	2.0	1.0
G12	79-01	0.17	0.25	0.26	0.42	0.77	1.9	1.3
G13	79-01	0.14	0.19	0.21	0.28	0.52	1.3	1.6
G14	79-01	0.17	0.24	0.24	0.39	0.68	1.7	1.6
G15	79-01	0.25	0.38	0.37	0.55	0.92	2.5	1.8
G16	79-01	0.31	0.49	0.48	0.78	1.3	3.4	1.6

[a] $C_{14}H_{10}$, phenanthrene and anthracene; $C_{18}H_{12}$ chrysene, triphenylene and benz(a)anthracene, $C_{20}H_{12}$, benzofluoranthenes; [b] dry weight; [c] n.a., not analyzed.

Relationship Between PAH Concentrations in Surface Sediments and Organic Carbon Concentrations

Sediments could be somewhat arbitrarily grouped on the basis of their normalized PAH concentrations (Figure 6). Sediments having the lowest concentrations were from stations 001 to 005 and 014 to 016, inclusively. These stations were remotely located from Kitimat in waterways not closely linked with Douglas Channel and Kitimat Arm. The PAH and organic carbon concentrations in the sediments were quite well correlated (Figure 5). Sediments having the highest normalized PAH concentrations were from station 008 and stations located within Kitimat Arm. These sediments showed essentially no correlation between PAH and organic carbon concentrations. The narrow organic carbon concentration

TABLE 3: Concentration of PAHs in Sediment Core from Station C3 off Emsley Point

Depth of Sediment (cm)[a]	$C_{14}H_{10}$[b] (mg/kg)[c]	Fluor., $C_{16}H_{10}$ (mg/kg)	Pyr., $C_{16}H_{10}$ (mg/kg)	$C_{18}H_{12}$[b] (mg/kg)	$C_{20}H_{12}$[b] (mg/kg)	PAH Sum (mg/kg)	Organic Carbon (%)
0-3	0.22	0.30	0.33	0.43	0.71	2.0	1.6
3-6	0.10	0.39	0.43	0.34	0.50	1.8	1.8
6-9	0.021	0.034	0.039	0.054	0.061	0.21	1.7
9-12	0.011	0.011	0.0047	0.0063	0.012	0.044	n.a.[d]
12-15	0.014	0.0025	0.0048	0.0095	0.0084	0.039	1.6
15-18	0.0089	0.0023	0.0043	0.0095	0.0054	0.030	1.8
18-21	0.0098	0.0050	0.0053	0.0077	0.0050	0.033	1.7
21-24	0.012	0.0017	0.0031	0.0055	0.0030	0.025	1.8
27-30	0.014	0.0022	0.0041	0.010	0.0049	0.035	1.7
39-42	0.012	0.0013	0.0029	0.010	0.0087	0.035	1.7
45-48	0.011	0.0020	0.0037	0.0033	0.0039	0.024	1.7
51-54	0.010	0.0007	0.0014	0.0076	0.0042	0.024	1.7
57-60	0.013	0.0018	0.0034	0.0090	0.0042	0.031	1.6
66-69	0.011	0.0026	0.0043	0.0085	0.0040	0.030	1.7
75-78	0.012	0.0016	0.0031	0.0048	0.0042	0.026	1.6

[a] uncorrected for compression; [b] $C_{14}H_{10}$, phenanthrene and anthracene; $C_{18}H_{12}$ chrysene, triphenylene and benz(a)anthracene; $C_{20}H_{12}$, benzofluoranthenes; [c] dry weight; [d] n.a., not analyzed

range and the steep PAH gradient, however, would tend to obscure any micro-scale or smaller scale correlation. The remaining group of sediments could be considered to be transitional, since the sediments' characteristics were intermediate between those of the other two groups. The members of this third group could be geographically distinguished from the other two as well. Although the transitional nature of sediments from just outside Kitimat Arm might be obvious from their location, the transitional nature of those from G3, G7, 009-3 and 009-4 in the arm was deduced from considerations of riverine sedimentary input and estuarine circulation to be presented later.

Distribution of PAHs in ^{210}Pb-Dated Sediment Cores

The core obtained from station C3 off Emsley Point at the southern extention of north Kitimat Arm showed a dramatic decrease in PAH content with increasing depth (Table 3). Dating the core segments used for the hydrocarbon analyses by the ^{210}Pb method provided an estimate of the median year of deposition for some (Figure 7) and evidence that a rapid accumulation of PAHs began sometime in the period 1944-1959. Prior to the postwar accumulation of PAHs, the PAH concentration appeared quite constant for over a century with $\bar{x}_a \pm SD(n) = 0.031 \pm 0.006$ mg/kg(12) or 1.8 ± 0.3 mg/kgC(12), the

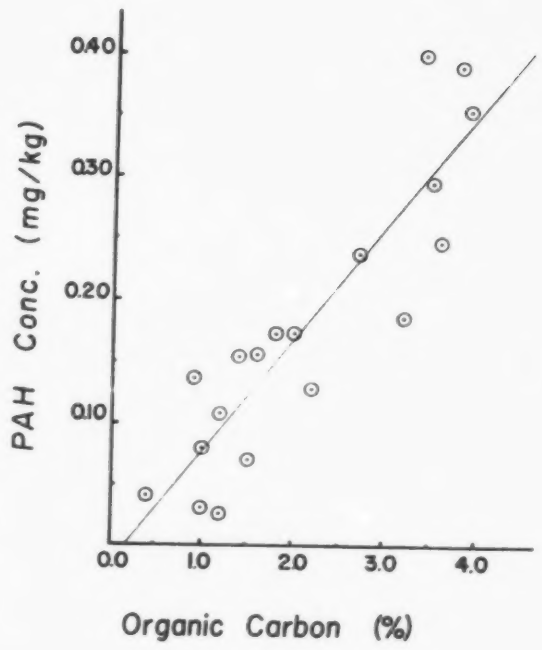

Fig. 5. Plot of PAH conc. against % organic carbon for the remote stations 001-005 and 014-016, inclusive, showing a positive correlation between PAH and organic carbon concentrations ($r=0.80$, $p<0.001$).

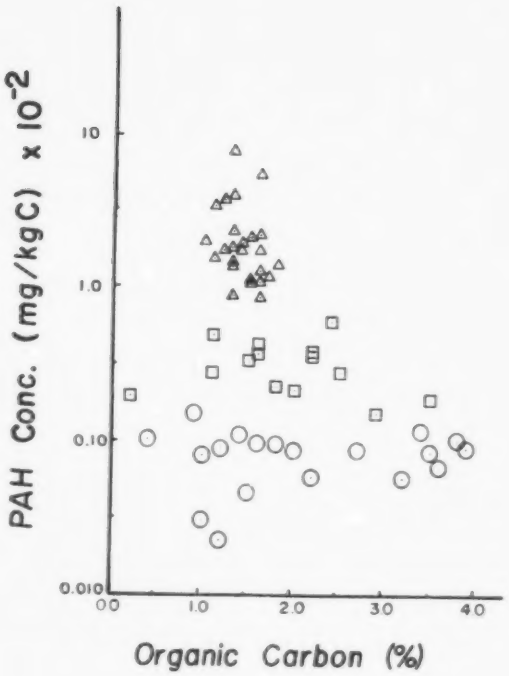

Fig. 6. Plot of normalized PAH conc. against % organic carbon showing how sediments may be grouped into three strata. ⊖, sediments from stations 001-005, and 014-016, inclusive; ▲, sediments from station 8, all Kitimat Arm Stations except G3, G7, 009-3, 009-4; ⊡, sediments from all remaining stations.

latter when the PAH concentrations were normalized with respect to organic carbon. The 12-15 cm segment obtained from the station 014 core and corresponding to the period 1945-1951 produced comparable values of 0.025 mg/kg and 1.8 mg/kgC, respectively, for the unnormalized and normalized PAH concentrations.

A difference in the relative amounts of some PAHs, but not others, was observed between the pre and post mid 20th century sediments. For the station C3 core the ratio of $C_{14}H_{10}$ PAHs to $C_{18}H_{12}$ PAHs was 0.39 ± 0.11 ($\bar{x}_a \pm SD$) for the 3 surface segments and 1.65 ± 0.68 ($n = 12$) for the deeper segments. In the station 014 core the 0-3 cm segment gave a ratio of 0.30 whereas the 12-15 cm segment gave a ratio of 0.98. On the other hand, the ratio of fluoranthene to the benzofluoranthenes for the surface 3 segments (0.59 ± 0.18) was not significantly different from that (0.50 ± 0.18) for the deeper 12 segments.

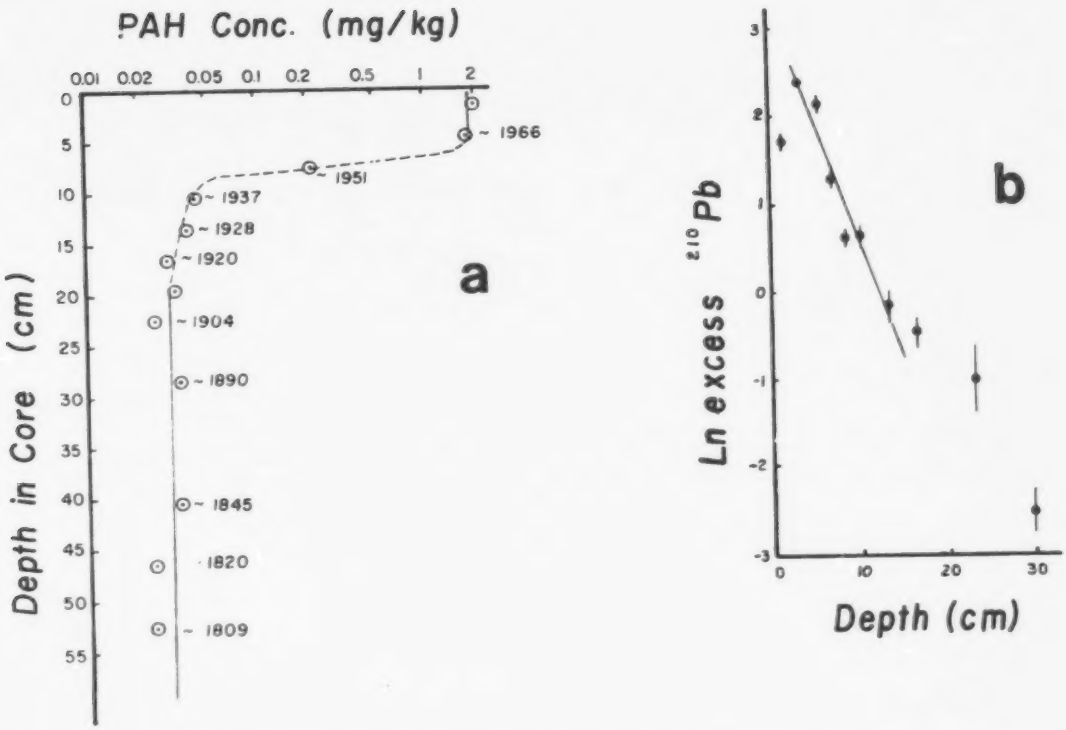

Fig. 7a. Concentration of PAHs in sediment core from station C3 in Kitimat Arm. The depth is uncorrected for compaction.

b. Plot of ln excess ^{210}Pb concentration against depth in same core showing linear range and surface and subsurface anomalies. The depth is corrected for compaction.

Areal Distribution of PAHs in Surface Sediments

The PAH concentrations were found to be highest in surface sediments collected in Kitimat Arm and to generally diminish as a function of distance outside the Arm (Table 1). Thus, in the sequence of stations down Douglas Channel, 008, CTD6, 007, 006, the mean normalized concentrations were 130, 58, 42, and 20 mg/kgC, respectively. The most distant stations sampled, 3 and 4, had the lowest mean normalized concentrations, 7 and 6 mg/kgC, respectively, although even these stations were higher than the apparent historical norm of about 2 mg/kgC.

Within Kitimat Arm a fairly complex distribution of PAHs in surface sediments was observed. For presentation purposes, the surface of the Arm was divided into 4 strata, with each strata corresponding to a unit increment of the ln x scale (Figure 8). The lowest stratum with an arithmetic mean concentration of 0.48 ± 0.12 (SD) mg/kg covered about 6% of the area and encompassed stations G3, G7, 009-3, and 009-4. The next stratum with an arithmetic mean concentration of 1.7 ± 0.3 (SD) mg/kg covered about 47% of the area and encompassed 10 stations in the central part of the Arm. The third stratum with an arithmetic mean concentration of 3.1 ± 1.0 (SD) mg/kg covered about 43% of the area and encompassed 10 stations along both sides of the Arm. The final stratum encompassing only two stations and located on the west

side of the Arm at the Delta front had the highest mean concentration recorded anywhere of 9.3 ± 1.1 (SD) mg/kg. An overall mean concentration of 2.55 ± 0.14(SE) mg/kg was obtained for the Kitimat Arm sediments. It should be observed, however, that the calculation had to be subject to bias both because a within-strata random sampling scheme was not used and the within strata sampling allocation was not appropriate for inventory purposes. Rather a grid pattern was used in which the stations were further separated down inlet than across inlet, since much greater across inlet than down inlet spatial variability was anticipated. For inventory purposes the two strata with the higher concentrations were severely under-sampled compared to the other two. Since the area of northern Kitimat Arm is approximately 41 km^2, the sediment samples were collected from the surface 5 cm, and the density of the sediment was roughly 1.5 g/ml, the total load in the surface sediments was estimated to be about 3.5 X 10^3 kg.

In a manner similar to what was observed with depth in the two cores, the ratio of the $C_{14}H_{10}$ PAHs to the $C_{18}H_{12}$ PAHs generally appeared to increase with distance from Kitimat. Thus, the Kitimat Arm sediments had a mean ratio of 0.44 ± 0.14 (SD, n = 26), whereas the sediments from the 4 remotest stations (002, 003, 004 and 005) taken together gave a ratio of 0.90 ± 0.38 (SD, n = 10). There were notable exceptions among stations of about equal distance, however. Stations 001 and 014 for example had mean ratios of 0.67 ± 0.06 (SD, n = 3) and 0.36 ± 0.09 (SD, n = 3), respectively. Also, stations 015 and 016 had mean ratios of 0.36 ± 0.14 (SD, n = 3) and 0.77 ± 0.10 (SD, n = 2) respectively. Moreover, it is noteworthy that the among station variation for stations 002, 003, 004, 005 was much less than the within-station variations, i.e., SD = 0.06 versus 0.45. Any correspondence with distance of the ratios was, therefore, at best weak . There was no overriding correlation between the ratios and organic carbon content of sediment or concentration of PAHs, either absolute or relative to organic carbon, that would have indicated that the ratio differences were procedural artifacts dependent on one of these factors. To what extent the observed variabilities could be due to analytical imprecision and within-sample variance was assessed by examining the variances in the ratio determined for the duplicate analyses of sediment from the June 1979 sampling of stations 003-011, 013, 015 and 016. The pooled standard deviation was 0.29, most of which was contributed to by the analyses of sediment from stations 005 and 016, particularly the former. The standard deviation, omitting these two stations' samples, was 0.12.

In contrast to what was observed for the ratio discussed above, the ratio of fluoranthene to the benzofluoranthenes did not show a significant difference between Kitimat Arm sediments and sediments from the 4 remote stations. The mean ratios were 0.65±0.99 (SD,n=26) and 0.52±0.41 (SD, n=10). Although stations 001 and 014 were found to have different ratios, i.e., 0.41±0.12 (SD, n=3) and 0.17±0.06 (SD, n=3), respectively, stations 015 and 016 has similar ratios of 0.46±0.35 (SD,n=3) and 0.43±0.03 (SD, n=2), respectively. The among-station variation (SD, = 0.16) for stations 002, 003, 004, and 005 was, as before, less than the within-station variation (SD = 0.82). The pooled within-station standard deviation in the ratios for the June 1979 sediments was 0.27, which, in contrast to what was found for the other ratio, could not be attributed to the results of one or two stations.

Reconstructed ion chromatograms, obtained after replacement of the low resolution packed column with a flexible capillary column, were generated for

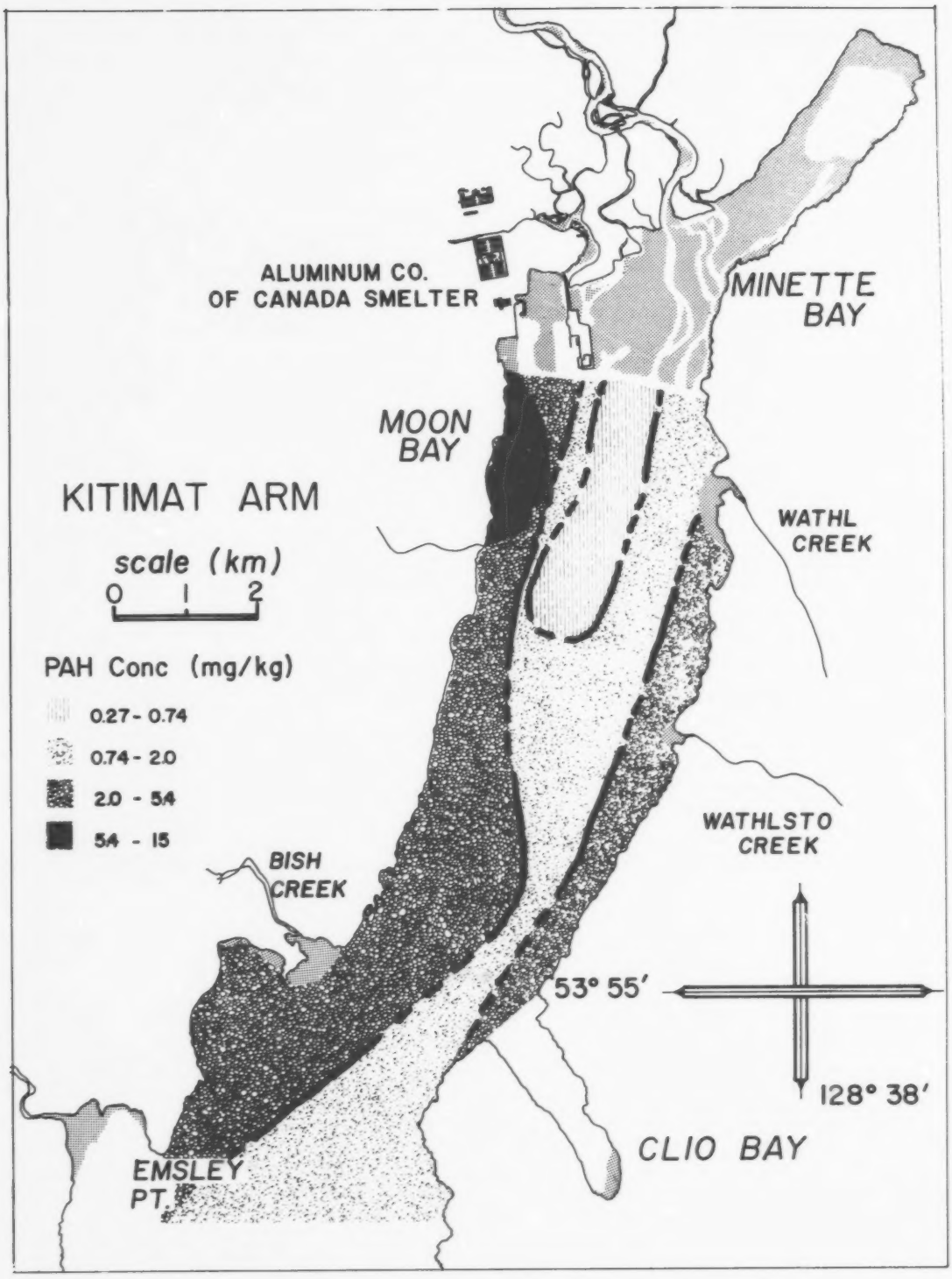

Fig. 8. PAH distribution in sediments of northern Kitimat Arm.

the PAH fraction of sediments from some selected stations. The parent PAHs were found to dominate the alkylated PAHs (eg. Figure 9). Although the benzopyrenes and perylene were not quantified in this study, the relative amounts of these compounds taken as a whole compared to that of the quantified PAHs seemed quite constant at about 1/3 from chromatogram to chromatogram. No attempt was made to determine whether or not there was a diagenetic component of perylene, because of its incomplete resolution from the benzopyrenes on the packed columns used.

DISCUSSION

Detection of Petroleum Contamination in Sediments

When our attention is restricted to the PAH fraction in keeping with the focus of this paper, the parent PAHs, the alkylated PAHs and hetero-atom (N,S,O) containing polyclyclic aromatic compounds present themselves as potentially useful markers for petroleum contamination of sediments. From the results given here, the parent PAHs would have minimal value as markers, particularly within the Kitimat Harbour area. The high benchmark of parent PAHs in much of the study area and the low concentration of parent PAHs in crude oil, either absolute or relative to the alkylated PAHs, would require very high levels of oil contamination indeed before identification and quantification of oil pollution could be made by measurement of parent PAHs. Examination of background sediments and the oil spiked sediments indicates a greater suitability of the alkylated PAHs than the parent PAHs for these purposes.

The dibenzothiophenes, however, may be more suitable indicators of oil pollution in the Kitimat area than the alkylated PAHs for several reasons. The most important reason from a practical standpoint is that the m/z 212 mass fragmentograms, which were obtained for all the sediments for measurement of the molecular ion peak due to ($^2H_{10}$)pyrene added as internal standard, also contain the molecular ion peaks due to the dimethyldibenzothiophenes. For most sample runs the dimethyldibenzothiophenes are quantifiable using the ($^2H_{10}$)pyrene as internal standard, although this has only been carried out in a few instances. In principle, therefore, a dimethyldibenzothiophene benchmark for the region can be achieved from presently available raw data. Another reason is the low concentration of dibenzothiophene relative to the parent PAHs in the two typical Kitimat Arm sediments examined. Thus, less oil is required to cause a significant increase in the concentration of benzothiophene in these sediments. A third more general reason is the practicality of performing the the dibenzothiophene analyses on sediments by gas chromatography using a flame photometric detector in the sulfur mode (Bates and Carpenter, 1979). The dibenzothiophenes will be suitable markers, however, only for oils, such as Prudhoe Bay Crude oil, that contain them in sufficient quantity.

Distribution of PAHs in Age-dated Cores

The PAH record in both age-dated cores indicates that a major influx of PAHs into the sediments began about the middle of this century. The core from station C3 shows a rapid increase in PAH deposition beginning sometime in the 1944-1958 period following a period of over 150 years in which the PAH

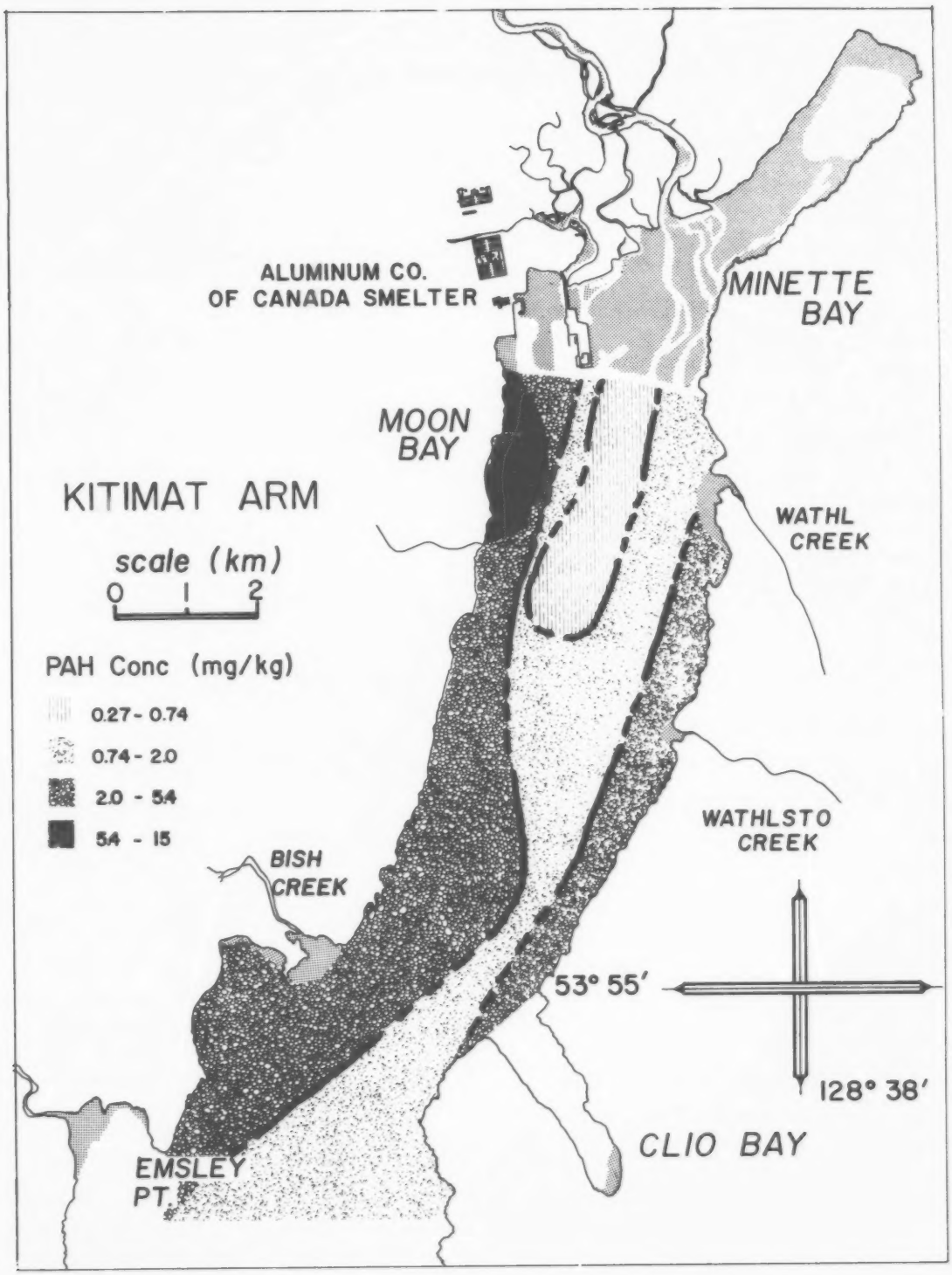

Fig. 8. PAH distribution in sediments of northern Kitimat Arm.

the PAH fraction of sediments from some selected stations. The parent PAHs were found to dominate the alkylated PAHs (eg. Figure 9). Although the benzopyrenes and perylene were not quantified in this study, the relative amounts of these compounds taken as a whole compared to that of the quantified PAHs seemed quite constant at about 1/3 from chromatogram to chromatogram. No attempt was made to determine whether or not there was a diagenetic component of perylene, because of its incomplete resolution from the benzopyrenes on the packed columns used.

DISCUSSION

Detection of Petroleum Contamination in Sediments

When our attention is restricted to the PAH fraction in keeping with the focus of this paper, the parent PAHs, the alkylated PAHs and hetero-atom (N,S,O) containing polyclyclic aromatic compounds present themselves as potentially useful markers for petroleum contamination of sediments. From the results given here, the parent PAHs would have minimal value as markers, particularly within the Kitimat Harbour area. The high benchmark of parent PAHs in much of the study area and the low concentration of parent PAHs in crude oil, either absolute or relative to the alkylated PAHs, would require very high levels of oil contamination indeed before identification and quantification of oil pollution could be made by measurement of parent PAHs. Examination of background sediments and the oil spiked sediments indicates a greater suitability of the alkylated PAHs than the parent PAHs for these purposes.

The dibenzothiophenes, however, may be more suitable indicators of oil pollution in the Kitimat area than the alkylated PAHs for several reasons. The most important reason from a practical standpoint is that the m/z 212 mass fragmentograms, which were obtained for all the sediments for measurement of the molecular ion peak due to ($^2H_{10}$)pyrene added as internal standard, also contain the molecular ion peaks due to the dimethyldibenzothiophenes. For most sample runs the dimethyldibenzothiophenes are quantifiable using the ($^2H_{10}$)pyrene as internal standard, although this has only been carried out in a few instances. In principle, therefore, a dimethyldibenzothiophene benchmark for the region can be achieved from presently available raw data. Another reason is the low concentration of dibenzothiophene relative to the parent PAHs in the two typical Kitimat Arm sediments examined. Thus, less oil is required to cause a significant increase in the concentration of benzothiophene in these sediments. A third more general reason is the practicality of performing the the dibenzothiophene analyses on sediments by gas chromatography using a flame photometric detector in the sulfur mode (Bates and Carpenter, 1979). The dibenzothiophenes will be suitable markers, however, only for oils, such as Prudhoe Bay Crude oil, that contain them in sufficient quantity.

Distribution of PAHs in Age-dated Cores

The PAH record in both age-dated cores indicates that a major influx of PAHs into the sediments began about the middle of this century. The core from station C3 shows a rapid increase in PAH deposition beginning sometime in the 1944-1958 period following a period of over 150 years in which the PAH

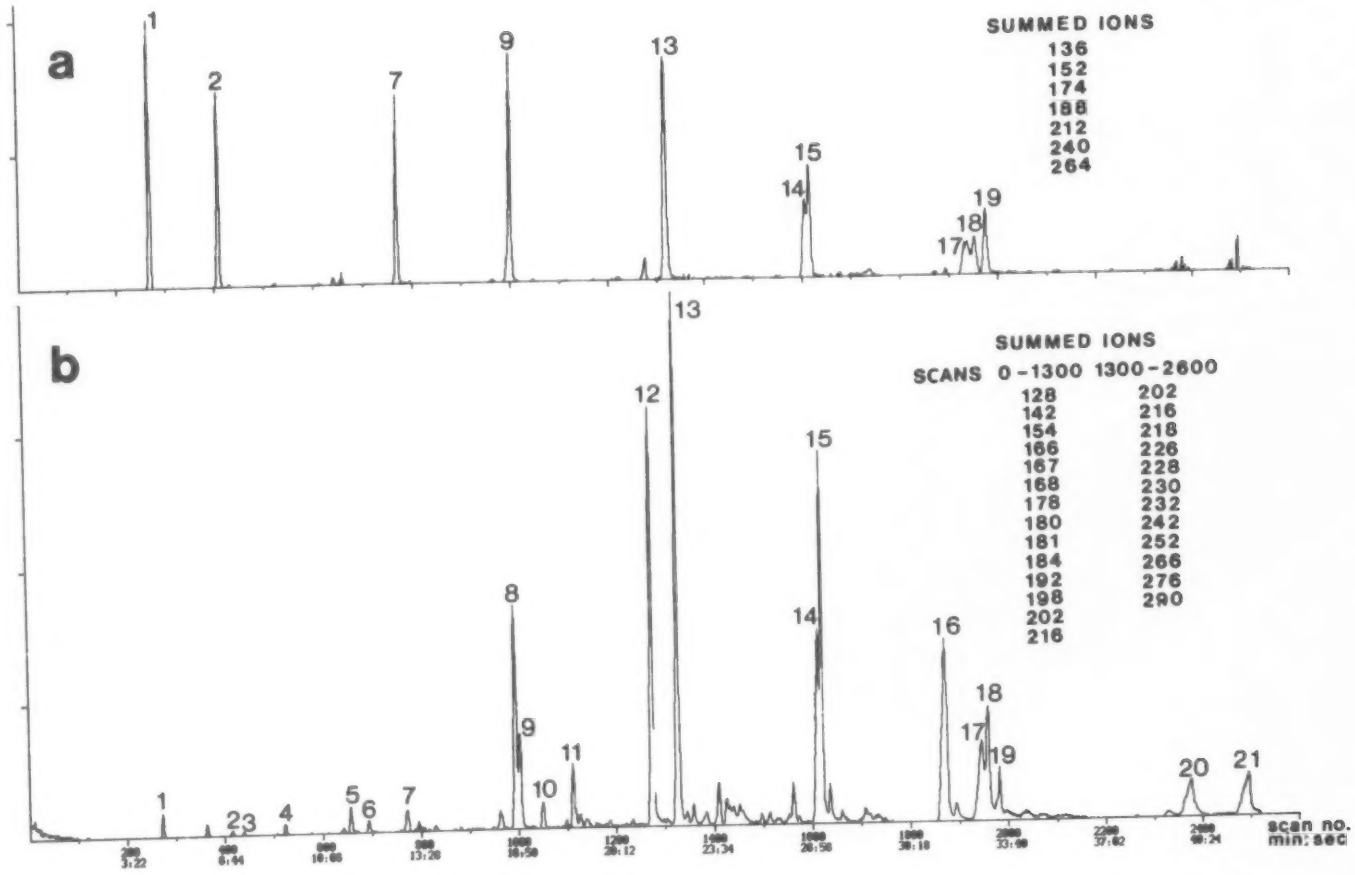

Fig 9. Reconstructed ion chromatograms of the PAH containing fraction from a sediment sample from station G1. The selection of summed ions encompasses all the major PAHs and added standards: (1) naphthalene, (2) 2-methylnaphthalene, (3) 1-methylnaphthalene, (4) biphenyl, (5) acenapthene, (6) dibenzofuran*, (7) fluorene, (8) phenanthrene, (9) anthracene, (10) carbazole*, (11) decafluorotriphenylphosphene, GC/MS standard, (12) fluoranthene, (13) pyrene, (14) benz(a)anthracene, (15) chrysene (+ triphenylene in b), (16) benzo(b/k)fluoranthenes, (17) benzo(e)pyrene, (18) benzo(a)pyrene, (19) perylene, (20) indeno(1,2,3-cd)pyrene*, (21) benzo(ghi)perylene*. * tentative assignment. a) m/z = M^+ for predeuterated PAHs (except for ($^2H_8$, $^1H_2$) fluorene) added as internal standards. b) m/z = M^+, $(M+14)^+$ except for $M+H^+$ = 240 for selected parent analyte PAHs.

deposition rate was fairly constant. The imprecision in determining the time of PAH influx likely derives mainly from the 3 cm length of the analysed segment, which for surface segments corresponds to a deposition period of just over a decade. Although a finer sectioning might have led to a narrower time period, other contributors to the uncertainty of the core data such as bioturbation, slumping, and turbidity flows also limit precision and accuracy in dating cores.

With respect to the core from station C3, there is evidence of at least two events leading to anomalies in the ^{210}Pb depositional record (Figure 7b). The one anomaly occurs at the surface (0-3 cm) and the other at a depth of 15 - 25 cm. The event leading to the surface anomaly would have taken place in about the last dozen years and in the absence of other evidence may be attributable to the massive undersea slide that occurred at the head of the Kitimat Arm in 1975 (Luternauer and Swan 1978; Murty 1979). Further, since the surface 3 cm has a ^{210}Pb excess equivalent to a segment dating from about 1945, it either consists mainly of an overlay of sediment of that age on younger sediment or a mixing together of older and younger sediments. Either occurrence would lead to a depressed PAH concentration at the surface. Thus, the surface segment of the core likely has a lower PAH concentration than it might have had if the slide had not occurred.

The PAH record from the station 014 core supports the estimated beginning of the increased flux of PAHs to the sediments. The sedimentary history of the site appears to be much less eventful than that of station C3, based on the ^{210}Pb record. Consequently, the PAH record for station 014 may be more reliable than the one for station C3, although the record for the latter station unquestionably shows that the increased influx began at some time in the 1946-1958 period. Further, because the rate of deposition is 0.62 cm/y compared to 0.25 cm/y at station C3, each 3 cm segment corresponds to a smaller time period. Although the core was not analysed in detail for PAHs, the surface 3 cm segment, corresponding to the period 1973 - present, shows a 5-6 fold increase in concentration of PAHs over those concentrations in the 12 - 15 cm segment. The deeper segment corresponds in time to the period 1944 - 1952. Insofar as the PAHs in the surface sediments at station 014 are predominately derived from the aluminum smelter at Kitimat, the observed increase in PAHs in sediments can be approximately narrowed to the period 1952 - 1959, which corresponds rather well to the beginning of production of the aluminum smelter at Kitimat and the urbanization of the area with the building of the townsite. The PAH transport problem, on which this analysis depends, will be addressed in a following section.

Areal Distribution of PAHs in Northern Kitimat Arm Surface Sediments.

The overall PAH distribution pattern (Figure 8) in northern Kitimat Arm surface sediments suggests that there is a point source located near the northwest corner of the Arm. The highest concentrations are observed in the northwest corner where the most likely source in the area, the Alcan aluminum smelter, is located. Another possible source, the Kitimat river, can be ruled out. Sites directly south of the main channel of the river show the lowest concentrations of sedimentary PAHs in the Arm. More importantly, while not the subject of this paper, the PAH concentrations in unfiltered river water collected upstream from the aluminum smelter on the main river are much lower than those concentrations found in unfiltered Kitimat Arm water (Cretney et al., in prep.)

The distribution pattern of PAHs in the surface sediments is also consistent with what is known of the estuarine circulation in northern Kitimat Arm (Bell and Kallman, 1976). The salinity distribution for much of the year suggests a two layer estuarine flow system with the major outflow on the west side at least as far south as Bish Creek. The surface riverine water is driven predominately to the west side of the arm by the Coriolis force, entraining saline water as it flows south. Subsurface high salinity ocean water inflows predominately on the east side. A surface eddy in the northwest corner of the arm, which may act as an entrapment zone for PAHs, has been suggested on the basis of the salinity distribution (Bell and Kallman, 1976).

Estuarine circulation may also account in part for the elevated concentrations of PAHs relative on the eastern side to the centre of the arm. If it is assumed that a large anticlockwise gyre forms in northern Kitimat arm, then a means of transport and sedimentation of PAH-laden particulates down the west side, across and then up the east side at the arm can be envisaged. Also some PAH-bearing particulates, after settling through the pycnocline, may be transported north along the east side by the inflowing subsurface high salinity bottom water.

The PAH distribution in sediments may also be explicable in terms of the atmospheric transport of PAH-laden particulates and vapour. PAH fallout in the immediate area of the smelter may be washed off the property to some extent into various creeks entering the western arm of the Kitimat river and thence to the northwest corner of the inlet. Since fluoride emissions predominately affect vegetation on the west side of the valley and arm (Alcan Surveillance Committee, 1979; Bell and Kallman, 1976), PAH emissions which could be expected to be similarly transported, would predominately impact the same areas. PAHs deposited on land to the west side of Kitimat Arm would wash off to the sediments on that side. PAHs transported and deposited across inlet may eventually be washed down to the eastern perimeter sediments, resulting in elevated PAH concentrations there compared to PAH concentrations of the mid channel sediments.

The PAH distribution in the sediments appears also to be consistent with the geomorphology of the benthic sediments. Geologically recent sediments are thickest along the west side of the Arm (Bornhold, 1982). This observation supports the view that the prevailing transport of riverine water and suspended particulates is along the west side. Kitimat Arm has a history of submarine slides, the record of which has been imprinted in the morphology and topography of the bottom sediments (Prior et al., 1982; Murty, 1979; Murty and Brown, 1979; Luternauer and Swan, 1978). A significant slide, which occurred on April 27, 1975 and involved about 2.6×10^{7} m^3 of material (Murty, 1979), covers a 7.5 km^2 area that extends from the delta front over the central portion of the Arm to a distance of about 5 km, as delineated by side scan sonar (Prior et al., 1982). Perhaps as much as 10% of the total slide volume can be attributed to the Moon Bay area south of the Alcan plant, where there was a concomitant land slide. The slide in the Moon Bay area is constricted in a narrow neck between stations G1 and 010-1 of this study. Station 10, though lying to the north of the 1975 slide is located at about the centre of a smaller slide which occurred in 1971 during the building of the Eurocan Terminal. Station G2 appears to lie within an area of irregular hummocks just west of the 1971 slide. The hummocks are undoubtedly dredge spoils as they occur in the vicinity of the Alcan dump site. A similar group of hummocks

appears to be just southeast of station G4. Station G7, 009-4, 009-3 and likely G6 lie within the margin of the 1975 slide.

In view of the extensive slumping and slide activity taking place along the Kitimat River Delta front and elsewhere in the Kitimat Arm, the representativeness of the sediment samples, and PAH concentrations determined, must be assessed cautiously. Station G1 lies shoreward of the 1975 slide constriction in acoustically well stratified sediments (Prior et al., 1982). Assuming a fairly high sedimentation rate (> 1cm/y) this close to the head of the inlet, the 5 cm sample depth may yield mostly post 1975 slide deposit. The sediment sample therefore is probably quite representative of nearshore sediments of the northwest corner of the Arm and should reflect the level of PAHs accumulating since the change over from wet to dry scrubbing of fumes generated at the anode/cryolite bath interface in the mid 1970's (Alcan Surveillance Committee, 1976). Station 010-1 is located within the acoustically amorphous sediments of the Delta front, but just north of the neck of the 1975 slide. The station 010-1 sediment sample may therefore have a somewhat greater possibility of being unrepresentative of the area than the station G1 sediment. If it is assumed that there is a within-station coefficient of variation common to all stations in the study area as indicated in the results section, then the PAH concentrations recorded for these two stations are within one "within-station" standard deviation of each other. Combining the two stations into one stratum seems therefore reasonable.

The sediment sample from station G-2 is believed to be unrepresentative of the sediments in the northwest corner of the inlet. The PAH concentration is below expectation, although by itself this is not grounds for considering it unrepresentative. Rather, this consideration derives from the location of station G-2 within the dredge spoil hummocks of the Alcan dumpsite. Thus, both the period of deposition and the place of origin of any given sediment from the dump zone must necessarily be uncertain. As a result, the within-station variability and between station variability may be higher in the dump zone than outside it, a consequence that would make it unreasonable to assume that an otherwise common regional coefficient of variation would apply in the dump zone.

The sediment samples from the other delta front stations may be considered as representative with the qualification that slumping activity may have exposed or mixed in some pre 1950's sediments. Since the Delta front is accreting and the sedimentation rate along the front may be expected to be very large, the possibility of the samples containing a pre 1950's component seems vanishingly small. Thus, the sediment from G-3, for which the lowest concentration of PAHs in the Arm were determined, most likely reflects the present day riverine input despite its comparatively low concentration of PAHs.

The representativeness of samples from station G-6, G-7, 009-3 and 009-4 may be doubted, since they lie within the longitudinal shear zone of the 1975 slide which is marked by a network of low scarps parallel to the slide axis and smaller scale scarps and cracks traverse to the slide axis (Prior et al., 1982). The possibility, therefore, that some surface sediments were generated by the slide by exposure or mixing in of pre 1950's sediments cannot be excluded. Although the undoubtedly high sedimentation rate in the zone may have covered up much of the slide surface to the sampling depth, there may

have been little deposition on the crest of ridges, for instance.

With regard to the sediment samples collected at the stations outside the delta front and the 1975 slide zone, the acoustically well stratified underlying sediments would indicate that they are well representative for a given area of the present day burden of PAHs in the sediments. Even here some caution must be expressed because of the possible impact of fine sediments transported and deposited outside the immediate zone of the 1975 slide. Consider, for instance, the surface segment of the core obtained at station C-3 that showed an anomalously low ^{210}Pb content, which was more consistent with an age of deposition corresponding to the mid 1940's. At the historical sedimentation rate of 0.25 cm/y only about 1 cm of sediment would have collected between the time of the slide and the time of the sampling. Hence, the bulk of the surface core segment would have consisted of pre slide material, some or all of which may have been deposited as a result of the slide.

In summary, the observed PAH distribution is in accordance with the geomorphology of the region. Unfortunately, the geomorphological record shows that northern Kitimat Arm has particularly unstable sediments and two identifiable dump sites. The representativeness of individual sediment samples must be considered in the light of this record. Assuming that a veneer of post 1975 sediments has accumulated over the bottom of the Arm to the sampling depth, however, the PAH distribution becomes explicable in terms of estuarine circulation and atmospheric transport without regard to the geomorphological record.

Areal Distribution of PAHs in Surface Sediments Outside Northern Kitimat Arm.

The observed distribution of PAHs in the surface sediments is qualitatively consistent with the tidal, wind driven and estuarine circulation in the study area. Since there is a tidal node at the entrance of Devastation Channel south of station 013 (Narayanan, 1981), tidal currents would not be expected to move water-borne PAH-containing particulates into Gardner Canal, Verney Passage or Ursula Channel. Freshwater discharges into Gardner Canal are greater than those into Douglas Channel at all times of the year. Some fraction of the Gardner Canal water is considered to flow north through Devastation Channel into Douglas Channel most of the time (Webster, 1981), forming another barrier to surface water-borne PAH transport. Thus, the observed difference in PAH concentration at sites to the east and west of Hawkesbury Island might be explained in terms of surface flow. The apparent Devastation Channel barrier to water-borne PAH-containing particulates from Kitimat may, however, be breached during strong southerly winds. Water may pile up at the north end of Douglas Channel resulting in a southerly flow through Devastation Channel (Webster, 1981).

A more quantitative analysis of the likelihood of water-borne long range transport of PAHs from Kitimat Arm suggests that most of the PAHs are transported less than 30 km. Comparison of fresh water residence time and particulate residence time in the upper layer (Macdonald 1983) suggests that the bulk of particulates is probably sedimented within this distance. Some fine ($<4\mu m$) unflocculated particles may be transported further and probably account for less than 15% of the particulates supplied by the Kitimat River. Although much of the smelter PAH may initially be borne on particulates in the

less than 4μm range, significant flocculation may occur in response to the increase in salinity (Neff, 1979) in the arm, as has been observed with the riverine suspended particulates (Macdonald, 1983). Aluminum smelter particulates show a tendency to agglomerate (Stenberg and Alsberg, 1981). In addition, ingestion of PAH containing particulates by zooplankton and rapid vertical transport in fecal pellets can be expected to be a significant removal mechanism for water-borne PAHs (Prahl and Carpenter, 1979). Finally, sills form natural barriers to water borne sediments hindering the transport of pollutants between basins (Thompson and Paton, 1976). The waterways in the Kitimat system are transected by a number of sills (Macdonald et al., 1983).

A further point can be considered in assessing the likelihood that water-borne transport governs the PAH distribution in sediments throughout the study area. Lopez-Avila and Hites (1980) propose that a linear relationship between log C_o/C and distance/log P may be generally applicable for the prediction of the sedimentary rate of water-borne organic compounds discharged from a point source, where C is the sediment concentration of the compound and P is its octanol-water partition coefficient. On this basis, the ratio of the $C_{14}H_{10}$ PAHs to the $C_{18}H_{12}$ PAHs or of fluoranthene to the benzofluoranthenes would be expected to decrease exponentially with distance from the head of Kitimat Arm so long as the smelter-derived PAH concentration is significantly in excess of background. No such trend, however, is observable in the data. The ratio of fluoranthene to the benzofluoranthenes remains fairly uniform throughout the study area, without a significant difference between those from Kitimat Harbour and those from the four remotest stations. The ratio of the $C_{14}H_{10}$ PAHs to the $C_{18}H_{12}$ PAHs actually shows an increase with distance, presumably reflecting PAH inputs having a congener distribution differing from that of the aluminum smelter.

In view of the unlikeliness of water-borne, long range transport of PAHs, some attention must be given to the possible impact of air-borne PAHs, particulate or vapour phase or both, from the aluminum smelter. Particulate emissions from the pot room ventilator of the Alcan smelter have been estimated to be $2.0 - 3.3 \times 10^6$ kg/y (Alcan Surveillance Committee, 1979). The weight fraction of PAHs on pot room particulates for this vertical stud Solderberg smelter is likely to be in the range of 1 - 4% (mean 3.3%) (Bjorseth et al., 1981). Thus the Alcan plant may be releasing to the atmosphere $2 - 13 \times 10^4$ kg/y of PAHs on particulates through the pot room ventilators alone, a quantity which may be 20-100% of the amount released as vapour (Bjorseth et al., 1981).

In view of the appreciable release of PAHs to the atmosphere, the potential exists for the contamination of sediments at remote stations by β-mesoscale (25 - 250 km) (Bass, 1981), or longer range atmospheric transport. Some estimate (order of magnitude) may be gained by applying a Gaussian plume model of the mean concentration field due to an elevated point source in which depletion by deposition of particulates (ignoring the complexities of the vapour) is included (Horst, 1977). Important parameters are the wind direction and mean velocity, atmospheric stability, deposition velocity to mean wind velocity ratio and source height and strength.

The wind direction at Kitimat is predominately up and down channel at all times of the year. The winds blow from the NW, N or NE at the Kitimat townsite on the average (1967-1980) 40% of the time; 25% of the time from the

N only (Anon., in press). In the fall and winter months, 56% of the time winds are from the NW, N or NE. The northerly winds, which prevail for extended periods of time (Bell and Kallman, 1976), may transport PAHs down channel to remote marine sites. The mean, frequency weighted, down channel (directly from the N) velocity is 406 cm/s (14.6 km/h), as determined from the 1966-1980 averages.

Surface-based inversions are a common feature of coastal B.C. inlets. In the spring and summer milder Pacific air overrides surface air layers cooled by the cold sea surface with the effect being carried on shore by the prevailing wind. In the winter, inversions are caused by colder Arctic air outflowing along valley bottoms forming a wedge under marine air. At Kitimat in winter surface-based inversions are observed in the early mornings with 40% frequency and in the late afternoons with 65% frequency (Bell and Kallman, 1976). Indeed, surface-based inversions appear to be quite frequent overnight and in the early mornings in all seasons. In January the mean air temperature at Kitimat is about -4°C (Bell and Kallman, 1976), with inlet surface water temperatures about 6-9°C higher (Macdonald et al., in prep.).

Setting aside for the moment the problems of source strength and topology, the likelihood of transport of PAH containing particles from the aluminum plant for distances of about 100 km can be examined. The ratio of concentration-with-deposition to concentration-without-deposition for air-borne material carried down wind at a mean wind speed, $\bar{u}$, and deposition velocity, V_d, in a Gaussian plume under various atmospheric stability conditions and source heights can be computed (Horst, 1977). Assuming a 10 m source height for the pot room ventilators and intermediate Pasquill stabilities (C,D) to high stabilities (E,F) based on the frequent presence of surface-based inversions, Horst's analysis indicates that for $V_d/u \approx 10^{-3}$ materials would be predominately airborne at 100 km, except under Pasquill F stability where the ratio would fall to 20%. The ratio 10^{-3} corresponds to a deposition velocity of about 0.4 m/s for a mean wind speed of 400 cm/s. This deposition velocity from Stoke's law and experiment corresponds to a particle diameter of about 6μm (Windsor and Hites, 1979). Assuming a similarity in the PAH distribution among particle sizes between aluminum smelter pot room particulates (Stenberg and Alsberg, 1981) and coke oven emissions (Bjorseth, 1979) or general atmospheric particulates (Neff, 1979), particulate phase PAHs would appear to be mainly carried on particles in the 1-3μm range. Because the deposition velocity varies as the square of the particle diameter, there is compelling reason to assume that PAH bearing particles can be readily carried even to the remotest sampling sites in the study area.

Although air-borne transport of PAH bearing particulates to the remote areas of the study region appears possible, even likely, there remains question of whether or not enough may be transported to account for the PAH concentrations found in surface sediments in remote sites. Unfortunately, there is insufficient information available to meaningfully model the atmospheric transport of PAH bearing particles throughout the study area. It is perhaps appropriate, nevertheless, to make an engineering estimate of maximum and minimum surface deposition fluxes of PAHs to be expected downwind at a distance equal to the along-channel distance between the head of Kitimat Arm and station 014 from a source in a hypothetical system that retains, where practical, features similar to those of the real one. These fluxes can be

compared with the sedimentary PAH flux determined for the core from station 014.

An engineering estimate can be made of the near surface level concentrations along the axis of a Gaussian plume using the formula (Csanady, 1973):

$$\chi = \frac{q}{\pi u \sigma_y \sigma_z}$$

where χ is the concentration at the distance of interest, σ_y and σ_z are the horizontal and vertical Gaussian plume spread parameters, respectively, and q is the source strength. In this simple dispersion model σ_y and σ_z are estimated from PGT curves. For a distance of 80 km and assumed neutral (Pasquill D) atmospheric conditions, σ_y and σ_z have values 3.3 km and 0.4 km, respectively (from curves reproduced in Csanady, 1973). Thus, the near surface PAH concentration range would be 40-250 ng/m^3 in the hypothetical system in which PAHs on particles are emitted at a rate of 2-13x10^4 kg/y and transported with a wind velocity of 14.6 km/h. If it is assumed further that the wind blows steadily for 25-40% of the year and that at least 75% of the wind is channelled off without affecting the plume spread parameters, the yearly average concentration range would be 2.5-25 ng/m^3 at 80 km for the hypothetical system. Using a range of dry deposition velocities of 0.01-0.5 cm/sec (Gschwend and Hites, 1981) and neglecting any contribution from wet deposition, the calculated flux onto the surface for the hypothetical system would range from 0.8 ng/(cm^{2}y) to 4 x 10^2 ng/(cm^{2}y). From the sedimentary depositional flux of 0.22 g (dry weight)/(cm^{2}y) and the surface PAH concentration, an estimate of the PAH flux at station 014 can be made. For the set of PAHs presumed to be emitted from the Kitimat aluminum smelter by analogy with those studied by Bjorseth et al., (1981), the recent PAH flux is estimated to be 46 ng/(cm^{2}y) of which about 15% could represent the historical background input. The range of flux values for the hypothetical system brackets the values determined for station 014. Given that various processes can result in significant differences between fluxes of PAHs arriving at a water surface and those measured in a sediment core (Gschwend and Hites, 1981), the maximum estimated release rate of PAHs from the aluminum smelter would seem to be more than two orders of magnitude greater than that which could be confidently ignored as making a negligible contribution at 80 km based on an engineering estimate from a simple dispersion model under conditions for which it is applicable.

The simple enginering model fails to take into consideration several important factors that would be expected to govern particle transport in the Kitimat system. A number of contingencies, for example, may severely limit extent of down inlet atmospheric transport of particulates. Wet deposition, although it is generally considered to be less important for organics on fine particles than dry deposition (Eisenreich et al., 1981; Gschwend and Hites, 1981), may be unusually effective in the Kitimat area where rainfall approaches 300 cm/y (Bell and Kallman, 1976). The possibility of extensive photo-oxidation seems unlikely because of the short transport time proposed and the general lack of sunlight in the area. Except for the channelling of the wind, topographical influences of the inlets have been ignored despite the fact that the land surface represents about half the horizontal area of the fjords, which are from 7 - 13 km, ridge to ridge, wide. Across inlet mixing

processes (Pasquill, 1974) may homogeneously distribute the plume across inlet in a relatively few kilometers. Losses through lateral valleys, over ridges (maximum height about 700 m) during periods of ventilation from above and filtering by treed valley sides may rapidly reduce the atmospheric concentration to neglibible levels. Much more knowledge of atmospheric conditions, as well as of the PAH distribution on particles emitted from the smelter, is required before flux calculations would be definitive.

Although the above arguments indicate that station 014, station 006 and more remote stations may show elevated levels of PAHs with respect to the historical norm because of the aluminum smelter, other sources cannot be excluded on the basis of the evidence obtained so far. The distribution of PAHs may very well fit a number of pyrolytic sources. Indeed, the relative amounts of PAHs are similar to those found in sediments elsewhere (Prahl and Carpenter, 1979; Windsor and Hites, 1979; Laflamme and Hites, 1977). An increase in the overall flux of PAHs may have occurred since the middle of the century irrespective of the presence of the aluminum smelter, although the opposite trend appears to have occurred further south in Washington State (Prahl and Carpenter, 1979). The problem with interpreting the observed distributions of PAH in cores, however, is that the distributions may be governed to some extent by *in situ* geochemical processes, which may vary from place to place, giving rise to uncertainty in PAH flux determinations (Farrington et al., 1977).

SUMMARY

The high concentrations of parent PAHs in Kitimat Arm make them unsuitable for the purpose of monitoring crude oil inputs there. The alkylated PAHs and the dibenzothiophenes would seem to be better suited to this purpose.

The distribution of PAHs in age-dated cores is consistent with a sudden large increase in the concentration of PAHs in sediments that corresponds in time with the building and early production years of the aluminum smelter at Kitimat.

The distribution of PAHs in surface sediments of northern Kitimat Arm is consistent with the presence of a point source at the north west corner of the arm where the aluminum smelter is located. Aside from the position of the source of PAHs, the distribution in the northern Kitimat Arm seems to be governed by a combination of estuarine circulation and atmospheric transport processes.

Although the evidence is not unequivocal, there appear to be elevated concentrations of PAHs in sediments compared to the historical norm in all stations of the study area. Further, the general decrease in PAH concentrations with distance observed in Kitimat Arm appears to persist even to the remotest stations of the study area. Water-borne transport seems an unlikely means for moving PAHs such long distances. Given the right conditions, air borne transport could provide a likely mechanism. Although other sources such as local forest fires and global fossil fuel combustion may account for the observed PAHs sediments from the remote sites, a contribution, perhaps major, from the aluminum smelter cannot be ruled out at this time.

ACKNOWLEDGEMENTS

We thank F. McLaughlin, I.O.S. for performing a number of the analyses for PAHs using the capillary GC/MS/DS System. We also thank G. McBean, I.O.S., and M. Kotturi and R. Bennet, Air Studies branch, Ministry of Environment, B.C., for helpful discussions during preparation of the manuscript.

Most of this work was done under contract serial nos. OSS ISB78-00069 (Seakem Oceanography Ltd., Sidney, B.C.).

REFERENCES

Alcan Surveillance Committee. 1979. Environmental Effects of Emissions from the ALCAN Smelter at Kitimat, B.C. Ministry of Environment Report, Province of British Columbia, publ., Victoria, B.C. ix + 151 pp.

Anon. in press. Canadian Climate Normals 1951-1980, Atmospheric Environment Service, Department of the Environment, publ., Downsview, Ont.

Bass, A. 1981. Modeling long range transport and diffusion. pp. 136-158. In: Air Quality Modeling and the Clean Air Act, American Meteorological Society, publ., Boston, Mass, viii + 288 pp.

Bates, T.S. and R. Carpenter. 1979. Organo-sulfur compounds in sediments of the Puget Sound Basin. Geochim. Cosmochim. Acta 43: 1209-1221.

Bell, L.M. and R.J. Kallman. 1976. The Kitimat River Estuary, Environmental Knowledge to 1976. Report of the Estuary Working Group, Department of the Environment, Regional Board, Pacific Region. Special Estuary Series No. 6, Pacific Environment Institute, publ., West Vancouver, B.C. xxviii + 269 pp.

Bjorseth, A. 1979. Determination of polynuclear aromatic hydrocarbons in the working environment, pp. 371-381. In Polynuclear Aromatic Hydrocarbons. Third International Symposium on Chemistry and Biology - Carcinogenesis and Mutagenesis, P.W. Jones and P. Leber, eds. Ann Arbor Science publ., Ann Arbor, Mich. xxvi + 892 pp.

Bjorseth, A., O. Bjorseth and P.E. Fjelstad. 1981. Polycyclic aromatic hydrocarbons in the work atmosphere. Determination of area-specific concentrations and job-specific exposure in a vertical pin Soderberg aluminum plant. Scand. J. Work Environ. Health, 223-232.

Bornhold, B.D. 1982. Sedimentation in Douglas Channel and Kitimat Arm. pp 88-115. In Proceedings of a workshop on the Kitimat marine environment, R.W. Macdonald, ed., Canadian Technical Report of Hydrography and Ocean Sciences No, 18, 88-115.

Chesler, S.N., B.H. Gump, H.S. Hertz, W.E. May, S.M. Dyszel and D.P. Enagonio. 1976. Trace Hydrocarbon Analysis: The National Bureau of Standards Prince William Sound/Northeastern Gulf of Alaska Baseline Study. NBS Technical Note 889. National Bureau of Standards, publ., Caithersburg, Md, v + 66 pp.

Cretney, W.J., R.W. Macdonald, C.S. Wong, P.E. Erickson, and B.R. Fowler. in preparation. Kitimat Hydrocarbon Baseline Study 1978-9. Vol 4. Hydrocarbons in Marine Sediments, Organisms and Water. Canadian Data Report of Hydrography and Ocean Sciences.

Cretney, W.J., P.A. Christensen, B.W. McIntyre and B.R. Fowler. 1980a. Quantification of polycyclic aromatic hydrocarbons in marine environmental samples, pp. 315-336. In: Hydrocarbons and Halogenated Hydrocarbons in the Aquatic Environment, B.K. Afghan and D. Mackay, eds. Vol. 16. Environ. Sci. Res. Ser. Plenum Publishing Corp., publ., New York, N.Y. xiii + 588 pp.

Cretney, W.J., C.S. Wong, D.A. Brown, W.A. Heath, K.A. Thompson and B.R. Fowler 1980b. A statistical correlation between an infiltrative hyalinocytic condition in a marine bivalve mollusk and sediment levels of polycyclic aromatic hydrocarbons. Can.Tech. Rep. Fish. Aquat. Sci. 975: 192-203.

Csanady, G.T. 1973. Turbulent Diffusion in the Environment. D. Reidel Publishing Comp., publ., Dordrecht, Holland, x + 248 pp.

Eberhardt, L.L., R.O. Gilbert, H.L. Hollister and J.M. Thomas. 1976. Sampling for contaminants in ecological systems. Environ. Sci. Technol. 10: 917-925.

Eisenreich, S.J., B.B. Looney and J.D. Thornton. 1981. Airborne organic contaminants in the Great Lakes ecosystem. Environ. Sci. and Technol. 15: 30-38.

Farrington, J.W., N.M. Frew, P.M. Gschwend and B.W. Tripp. 1977. Hydrocrabons in cores of northwestern Atlantic coastal and continental margin sediments. Est Coast. Mar. Sci. 5: 793-808.

Gaudette, H.E., W.R. Flight, L. Toner and D.W. Folger. 1974. An inexpensive titration method for the determination of organic carbon in recent sediments. J. Sed. Petrol. 44: 249-253.

Green, R.H. 1979. Sampling Design and Statistical Methods for Environmental Biologists. John Wiley and Sons Inc., publ., New York, N.Y., xi + 257 pp.

Gschwend, P.M. and R.A. Hites. 1981. Fluxes of polycyclic aromatic hydrocarbons to marine and lacustrine sediments in north eastern United States. Geochim. Cosmochim. Acta 45: 2359-2367.

Horst, T.W. 1977. A surface depletion model for deposition from a Gaussian plume. Atmos. Environ. 11: 41-46.

Laflamme, R.E. and R.A. Hites. 1978. The global distribution of polycylic aromatic hydrocarbons in recent sediments. Geochim. Cosmoschim. Acta. 42: 289-303.

Lopez-Avila, V. and R.A. Hites. 1980. Organic compounds in an industrial wastewater. Their transport into sediments. Environ. Sci. Technol. 14: 1382-1390.

Luternauer, J.L. and D. Swan. 1978. Kitimat submarine slump deposit(s): a preliminary report. Geol. Surv. Can. Paper 78-1A: 327-332.

Macdonald, R.W. 1983. The distribution and dynamics of suspended particles in the Kitimat Fjord system. pp. 116 . In Proceedings of a workshop on the Kitimat marine environment, R.W. Macdonald, ed., Canadian Technical Report of Hydrography and Ocean Sciences No. 18 .

Macdonald R.W., B.D. Bornhold and I Webster. 1983. The Kitimat fjord system: an introduction, pp. 2-13 . In Proceedings of a workshop on the Kitimat marine environment, R.W. Macdonald, ed., Canadian Technical Report of Hydrography and Ocean Sciences No. 18.

Macdonald R.W., W.J. Cretney, C.S. Wong and P.E. Erickson. in preparation. Kitimat Hydrocarbon Baseline Study. Vol. 3. Oceanographic Support Data, Canadian Data Report of Hydrography and Ocean Sciences No., 18, 66-87.

Matsumoto, E., and C.S. Wong. 1977. Heavy metal sedimentation in Saanich Inlet measured with ^{210}Pb technique. J. Geophys. Res. 82: 5477-5482.

Murty, T.S. 1979. Submarine slide-generated water waves in Kitimat Inlet, British Columbia. J. Geophys. Res. 84: 7777-7779.

Murty, T.S., and R.E. Brown. 1979. The Submarine Slide of 27 April, 1975, in Kitimat Inlet and the Water Waves that Accompanied the Slide. Pacific Marine Science Report 79-11, Institute of Ocean Sciences, Patricia Bay, publ., Sidney, B.C., 36 pp.

Narayanan, S. 1980. Kitimat Oceanographic Study 1977-1978. Part 4. Tidal Circulation Model. Contract Report Series 80-3, Institute of Ocean Sciences, Patricia Bay, publ., Sidney, B.C., vii + 62 pp.

Neff, J.M. 1979. Polycyclic Aromatic Hydrocarbons in the Aquatic Environment. Sources, Fates and Biological Effects. Applied Science Publ. Ltd., London, England, xii + 262 pp.

Oldfield, F., P.G. Appleby and R.W. Battarbee. 1978. Alternative ^{210}Pb dating: results from the New Guinea Highlands and Lough Erne. Nature 271: 339-342.

Palmork, K.H. 1974. Polcyclic aromatic hydrocarbons in the marine environment, pp. 99-125. In: The Ninth Nordic Symposium on Water Research. Fjords and Coastal Waters as Recipients. Trondheim, June 27-29, 1973. Special Publication "Nordforsk", The Environment Secretariate (Nor.). Transl. avail. Canada Institute for Scientific and Technical Information, NRC of Canada, Ottawa, Ontario.

Pasquill, F. 1974. Atmospheric Diffusion. The Dispersion of Windborne Materials from Industrial and other Sources, 2nd Edit., Ellis Horwood Ltd., publ., Chichester, England, xi + 429 pp.

Prahl, F.G., and R. Carpenter. 1979. The rate of zooplankton fecal pellets in the sedimentation of polycylic aromatic hydrocarbons in Dabob Bay, Washington. Geochim. Cosmochim. Acta. 43: 1959-1972.

Prior, D.B., B.D. Bornhold, J.W. Coleman and W.R. Bryant. 1982. Morphology of a submarine slide, Kitimat Arm, British Columbia, Geology, 10: 588-592.

Stenberg, U.R., and T.E. Alsberg. 1981. Vacuum sublimation and solvent extraction of polycyclic aromatic compounds adsorbed on carbonaceous materials. Anal. Chem. 53: 2067-2072.

Thompson, J.A.J., and D.W. Paton. 1976. Further studies of mine tailings distribution in Howe Sound, B.C. Fisheries Research Board of Canada. Manuscript Report Series, No. 1383, Pacific Environment Institute, publ., West Vancouver, B.C., 14 pp.

Webster, I. 1980. Kitimat Oceanographic Study 1977-1978. Part 3. Estuarine Circulation. Contract Report Series 80-3 (part 3). Institute of Ocean Sciences, Patricia Bay, publ., Sidney, B.C., viii + 81 pp.

Windsor, I., and R.A. Hites. 1979. Polycyclic aromatic hydrocarbons in Gulf of Maine sediments and Nova Scotia soils. Geochim. Cosmochim. Acta 43: 27-33.

Wong, C.S., W.J. Cretney, J. Piuze, P. Christensen an P.G. Berrang. 1977. Clean laboratory methods to achieve contaminant-free processing and determination of ultra-trace samples in marine environmental studies. pp. 249-258. In: Methods and Standards for Environmental Measurement, Proceedings of the 8th IMR Symposium, National Bureau of Standards Special Publ. 464. National Bureau of Standards, publ., Gaithersburg, MD. xviii + 691 pp.

Young, D.R., J.N. Johnson, A. Soutar and J.D. Isaacs. 1973. Mercury concentrations in dated varved marine sediments collected off southern California. Nature 244: 273-275.

EVALUATION HISTOPATHOLOGIQUE DES PALOURDES DU KITIMAT ARM - DOUGLAS CHANNEL ET ALBERNI INLET, C.B.

D.A. Brown, K.A. Thompson, W.A. Heath and P.E. Erickson
Seakem Oceanography Limited, Sidney, B.C.

W.J. Cretney, and C.S. Wong
Institute of Ocean Sciences, Sidney, B.C.

RÉSUMÉ

Moules (Mytilus edulis) et palourdes (Macoma inconspicua) ont été prisent du Kitimat Arm - Douglas Channel en février et en avril 1979. Elles ont été examinées au microscope pour déterminer si l'on pouvoit trouver des réponses distinctives dans les palourdes de la région du passage contaminé par le niveau des nombreuses cycliques sélectionees d'hydrocarbure (NCAH). En fait de comparaison, l'échantillon de quelques moules à été faite de Alberni Inlet en juillet 1979. Cette entree a des proprietes semblables, mais sans une contamination significante des NCAH. Les palourdes de l'entrée du Kitimat Arm - Douglas Channel étaient en plus piètre condition que celles venant de la direction de l'océan du Douglas Channel, comme tout indiqué par la dégénération des avant-frais (oeufs) reproduisant les follicules; la dégénération du muscle et du tissu digestible épuisement nourissant, et des niveaux éléves des cellules transparentes, granulées et sanglantes. Les élévations morquées en dégré du niveau des cellule vitreuses peuvent être une condition unique des palourdes de l'entrée du Kitimat Arm - Douglas Channel. Dans le cas de quelques palourdes affectées; une grand nombre de cellules transparentes avaient des muscles et des tissus - reproducteur - infiltrés étant ainsi associés à leur destruction. Les moules venant de l'entrée de l'Alberni Inlet étaient en piètre condition comme tout indiquer par la destruction des petits tubes tubulaires et de l'infiltration granulée de ceux-ci. Cette condition peut-être associé avec leur stage de reproduction puisque les moules étaient déjà au stage de reproduction même, et le nombre de granules furent augmenter par l'aide des follicules reproductives. On a donc conclu, que le changement de saison, et l'entrée des deux passages, peuvent être la cause de différence dans la condition du tissu patalogique dans les palourdes - ou dans les peignes. En plus, les facteurs naturels ou contamination peuvent causer une pauvre condition aux palourdes venant de l'entrée de ces passages.

Brown, D.A., K.A. Thompson, W.A. Heath and P.E. Erickson. 1983. Histopathological evaluation of bivalves from Kitimat Arm - Douglas Channel and Alberni Inlet, British Columbia. Can. Tech. Rep. Hydrogr. Ocean. Sci. 18, 196-218.

Mot-clés: Alberni Inlet, histopathology, Kitimat, moules, palourdes, santé

HISTOPATHOLOGICAL EVALUATION OF BIVALVES FROM KITIMAT ARM - DOUGLAS CHANNEL AND ALBERNI INLET, BRITISH COLUMBIA

D.A. Brown, K.A. Thompson, W.A. Heath and P.E. Erickson
Seakem Oceanography Limited, Sidney, B.C.

W.J. Cretney and C.S. Wong
Institute of Ocean Sciences, Sidney, B.C.

ABSTRACT

Mussels (Mytilus edulis) and clams (Macoma inconspicua) were sampled from Kitimat Arm - Douglas Channel in February and April, 1979. These were examined microscopically to determine if distinctive sublethal responses could be found in bivalves from regions of the inlet contaminated by high levels of polycyclic aromatic hydrocarbons (PAHs). As a comparison, mussels were sampled from Alberni Inlet in July, 1979; an inlet of similar properties but without significant PAH contamination. Bivalves from the head of Kitimat Arm - Douglas Channel were in poorer condition than those from the seaward end of Douglas Channel as indicated by degeneration of prespawn reproductive follicles; degeneration of muscle and digestive tissues; nutrient depletion; and elevated levels of hyalinocytic and granulocytic hemocytes. Marked elevations in levels of hyalinocytes may be a condition unique to bivalves from the head of Kitimat Arm - Douglas Channel. In some affected bivalves large numbers of hyalinocytes had infiltrated muscle and reproductive tissues and were associated with their destruction. Mussels from the head of Alberni Inlet were in poor condition as indicated by destruction of digestive tubules and infiltration of these by granulocytes. This condition may be associated with their reproductive stage since mussels were spawning and granulocyte numbers were increased for the resorption of spent reproductive follicles. It was concluded that seasonal changes could account for the differences in distinct histopathological conditons in bivalves from the heads of both inlets. Further, natural factors or contaminants might cause the poorer condition of bivalves towards the heads of these inlets.

Brown, D.A., K.A. Thompson, W.A. Heath and P.E. Erickson. 1983. Histopathological evaluation of bivalves from Kitimat Arm - Douglas Channel and Alberni Inlet, British Columbia. Can. Tech. Rep. Hydrogr. Ocean Sci, 18, 196-218.

Keywords: Alberni Inlet, clams, health, histopathology, Kitimat, mussels

INTRODUCTION

In this study, a histopathological examination of bivalves was conducted as a biological adjunct to the hydrocarbon baseline study of Kitimat Arm - Douglas Channel, British Columbia (Cretney et al, 1983). They found that polycyclic aromatic hydrocarbon (PAH) levels were elevated in the sediments and mussels (Mytilus edulis) of this coastal fjord. These levels were higher along the western side of Kitimat Arm with the highest values (>8 mg kg^{-1} sediment, dry wt.; 2.2 kg^{-1} mussel, wet wt.) occurring in the northwest corner near the Alcan aluminum smelter. This was up to two orders of magnitude higher than levels at control stations near the seaward approaches to Douglas Channel where levels were from 0.04 to 0.48 mg PAH kg^{-1} sediment (dry wt.) and 0.03 to 0.04 mg PAH kg^{-1} mussel (wet wt.). The suspected source of the PAH was

the carbon paste electrodes that are combusted in the smelting of aluminum at a rate of one-half ton of electrode material per ton of aluminum produced (Palmork 1974). PAH levels continued to be highly elevated 21 km downchannel from the suspected source at levels of 2.1 to 3.9 mg kg^{-1} sediment (dry wt.) and 0.3 mg kg^{-1} mussel (wet wt.). PAH levels of 1.7 mg kg^{-1} sediment (dry wt.) and 0.09 mg kg^{-1} mussel (wet wt.) were found 40 km downchannel. Levels greater than 1 mg kg^{-1} sediment (dry wt.) occurred in some samples from as far as 78 km downchannel (Cretney et al, 1983).

In this study, mussels (Mytilus edulis) and clams (Macoma inconspicua) from Kitimat Arm - Douglas Channel were examined microscopically to determine if characteristic sublethal responses could be found in bivalves from regions of the fjord contaminated by high levels of PAH. Mussels were also sampled from Alberni Inlet to provide a comparison of the condition of bivalves from an inlet without a significant source of PAHs but with similar size, urban population and other industries (e.g., pulp and paper, shipping). Bivalves were examined for reproductive development and condition, nutrient store level, digestive tract condition, muscle condition, parasite occurrences, and infiltration of tissues with hemocytes (inflammatory responses).

Histopathological examination is a particularly valuable tool for the toxicologist since it provides an overview of organism health and can be used to detect in situ sublethal responses. However, it must be emphasized that few histopathological changes are pollutant-specific (Bayne et al. 1980) but are, for the most part, a culmination of the effects of all natural and anthropogenic stressors present in the ecosystem.

MATERIALS AND METHODS

Mussels (Mytilus edulis) and clams (Macoma inconspicua) were sampled from stations in Kitimat Arm - Douglas Channel in February and April, 1979 (Fig. 1) and mussels (Mytilus edulis) from Alberni Inlet in July, 1979 (Fig. 2). In both areas, mussels were obtained from rock and natural wood substrate at the mid-tide level during periods of low tide. Mussels of 50 mm length were collected where possible and their lengths recorded. At Kitimat, clams were dug by shovel or hand on mudflats. Approximately 25 organisms were sampled from each station and placed in sea water for 24 h to allow for depuration of stomach contents. These were then shucked and transferred to Helly's fixative (Barszcz and Yevich, 1975) for 16-24 h. Fixed organisms were rinsed in sea water for 16-24 h to remove excess fixative and then stored in 70% ethanol until processed.

Organisms were cut sagittally and 3 mm thick pieces were processed by standard histological techniques. Three slides were produced per animal and stained with Harris' Hematoxylin/Eosin (Bayne et al. 1980). The station(s) farthest downchannel from the suspected pollution source was selected as the control (Station A for mussels, Station F for clams in Kitimat Arm - Douglas Channel; Stations 1 and 2 for Alberni Inlet).

Histopathological conditions were rated on tissue sections prepared from the February, 1979 Kitimat samples using a system where the rater knew the identity of the slides he was rating. For subsequent samples, the rater did not know the identity of the slide he was rating. The mean of the ratings for

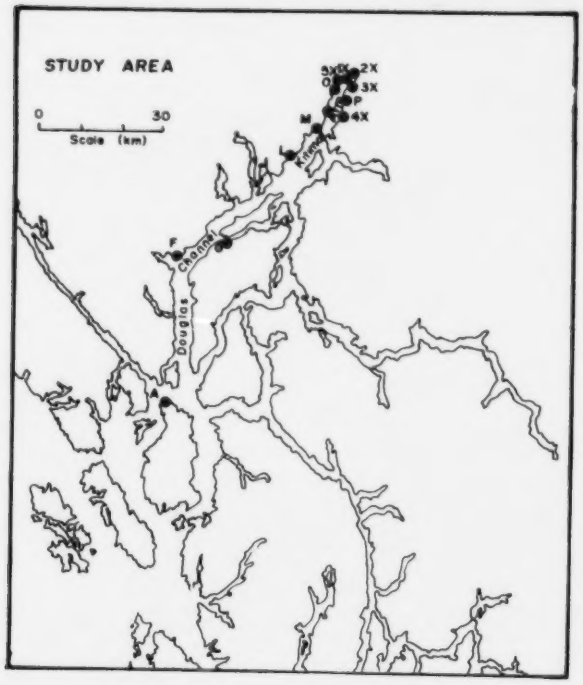

Fig. 1. Inter-tidal bivalve sampling locations in Kitimat Arm - Douglas Channel.

each animal was calculated and the animal assigned to categories which included: good, fair or poor for reproductive and digestive conditions; and low, moderate or high for hemocyte (hyalinocyte and granulocyte) levels. Results were tabulated as the percentage of animals from each station included in each category.

RESULTS

Mytilus edulis Kitimat Arm - Douglas Channel, February, 1979

Mussels from all stations were at the prespawn stage with reproductive follicles full of ripening gametes (Figs. 3-4). Reproductive condition was rated as poor in 44 to 72% of the mussels from the head of the inlet compared with only 16% of the control animals: mussels from Station N were the most severely affected with 72% receiving a poor rating (Table 1). Poor reproductive condition was characterized by the infiltration of reproductive tracts with hemocytes and concomitant poor development or destruction of the reproductive follicles (Figs. 5-7). In some instances hyalinocytes were present within the follicles (Fig. 7). In the most highly affected mussels, the reproductive tracts were almost completely destroyed (Fig. 7).

Nutrient (carbohydrate) store levels in the mantle tissue are indicated by the intensity of pink-red staining with hematoxylin-eosin of the glycogen-filled cells of the connective tissue. These stores were plentiful in most

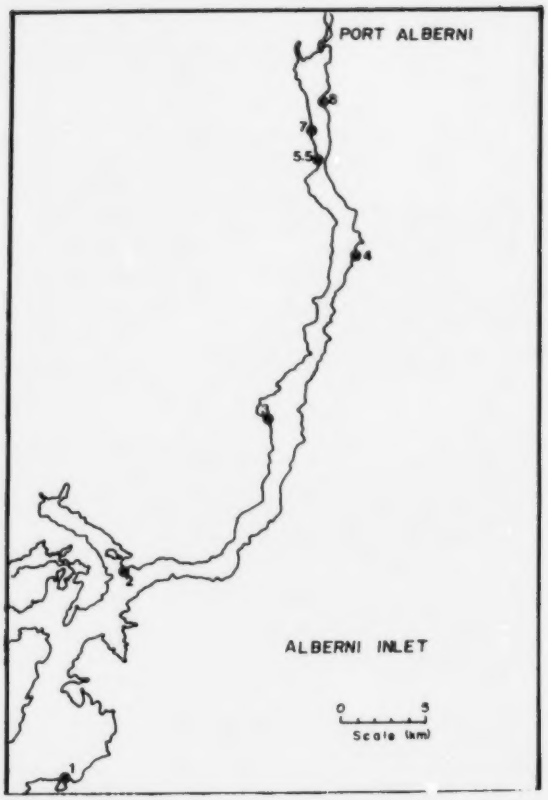

Fig. 2. Inter-tidal mussel sampling locations in Alberni Inlet.

mussels from the control station (Figs. 3-4), but not in those from towards the head of the fjord.

Digestive condition (Fig. 8) was rated as good in 92% of the mussels from control Station A and in 88% of those from station G: it was rated as fair or poor in more than half of the mussels from towards the head of the fjord except for Station P on the east side (Table 1). Poor digestive condition was characterized by the infiltration of digestive tubules with hyalinocytes and/or the destruction of these tubules (Fig. 9). In most cases where digestive condition was rated as poor there was a transformation of epithelial cells of the digestive tubules from columnar/cuboidal types to a squamous cell type (metaplasia) (Fig. 10).

Granulocyte levels were elevated in most mussels from all stations (Table 1), with the elevated levels most severe towards the head of the fjord. Eighty-four percent of the mussels from Station N received a high rating compared with 16% from the control Station A and 28% from Station G.

Hyalinocyte levels were rated as low in 84% of the mussels from the control station and in 80% of the mussels from Station G. Moderate to high levels of hyalinocytes were found in 48 to 96% of the mussels from towards the head of the fjord. The most highly affected mussels were those from Station L where 40% received a moderate rating and 56% a high rating (Table 1). In the most

Table 1. Histopathological condition of Mytilus edulis from Kitimat Arm - Douglas Channel and Alberni Inlet.

Area, Month Station (N)	Reproductive Stage		Reproductive Condition			Digestive Condition			Granulocyte Infiltration			Hyalinocyte Infiltration		
	Prespawn	Spawning	Good	Fair	Poor	Good	Fair	Poor	Low	Moderate	High	Low	Moderate	High
Kitimat, Feb.														
A (25)	100%	0%	20%	64%	16%	92%	8%	0%	20%	64%	16%	84%	16%	0%
G (25)	100	0	8	40	52	88	4	8	8	64	28	80	20	0
L (25)	100	0	12	40	48	40	40	20	4	56	40	4	40	56
M (25)	100	0	8	48	44	40	52	12	0	56	44	24	24	52
N (25)	100	0	0	28	72	16	64	20	0	16	84	36	40	24
O (25)	100	0	12	44	44	24	68	8	4	44	52	52	32	16
P (25)	100	0	4	44	52	64	36	0	0	40	60	48	36	16
Kitimat, Apr.														
A (25)	40	60	8	32	60	64	32	4	8	28	64	79	17	4
F (16)	87	13	13	56	31	38	50	12	6	88	6	62	26	12
N (25)	96	4	4	48	48	4	52	44	4	72	24	8	56	36
O (25)	92	8	0	40	60	8	52	36	0	80	20	4	64	32
3X(24)	100	0	17	33	50	12	46	42	0	71	29	38	29	33
4X(24)	100	0	0	71	29	0	42	58	8	71	21	21	54	25
Kitimat, Jul.														
1 (25)	4	96	20	48	32	32	56	12	24	56	20	96	4	0
2 (25)	20	80	24	52	24	76	24	0	44	48	4	100	0	0
3 (25)	0	100	8	28	64	32	64	4	16	68	16	100	0	0
4 (25)	0	100	0	4	96	24	52	24	0	48	52	100	0	0
5.5(25)	0	100	0	8	92	8	68	24	0	32	68	96	4	0
7 (25)	0	100	0	4	96	12	76	12	0	88	12	100	0	0
8 (25)	0	100	0	28	72	20	68	12	0	84	16	100	0	0

severely affected mussels large numbers of hyalinocytes were present and associated with the almost complete destruction of muscle tissue and reproductive follicles (Figs. 5-7, 9, 12).

Mytilus edulis Kitimat Arm - Douglas Channel, April, 1979

Sixty percent of the mussels from control Station A were spawning or had spawned compared with 13% from Station F, 4% from Station N, 8% from Station O, and none from Stations 3X and 4X. In those mussels that had spawned reproductive condition was rated as poor due to the destruction of remaining unspawned gametes and spent reproductive follicles and their resorption by granulocytes (as in Figs. 14-15). Mussels from the head of the fjord which had not yet spawned received poor ratings and had infiltrative hemocytic conditions similar to those described in mussels from the February, 1979 sampling (Plate A).

Digestive condition was rated as good to fair in 96% and 88% of the mussels from Stations A and F, respectively (Table 1). Poor ratings were given for 36 to 58% of the mussels from near the head of the fjord (Table 1); digestive conditions in these mussels were similar to those described for mussels sampled in February, 1979 (Figs. 8-10).

Granulocyte levels were rated as high in 64% of the mussels from Station A (Table 1); these were apparently active in the resorption of spent reproductive follicles. Granulocyte levels were also elevated in unspawned mussels from towards the head of the fjord but these levels were not as high as in February, 1979 (Table 1).

Hyalinocyte levels were rated as low in 79 and 62% of the mussels from Stations A and F, respectively. Levels were rated as moderate in 29 to 64% and as high in 25 to 36% of the mussels from the head of the fjord (Table 1).

Plate A. Reproductive condition and hyalinocyte levels in Mytilus edulis from Kitimat Arm - Douglas Channel.

Fig. 3. Normal female at prespawn stage; follicles (F) filled with ripening ova (O). Note the nutritive stores (arrows) in the connective tissue cells between the reproductive follicles and the digestive tubules (DT). Bar = 40 µm.

Fig. 4. Normal male at prespawn stage; follicles (F) filled with ripening sperm. Note the nutritive stores (arrows) in the connective tissue cells between the reproductive follicles. M ; muscle tissue. Bar = 40 µm.

Fig. 5. Female mussel in poor reproductive condition with an infiltration by hyalinocytes (H) of the reproductive and digestive tissues. Bar = 40 µm.

Fig. 6. Mussel in poor reproductive condition with an infiltration of high levels of hyalinocytes and destruction of reproductive follicles (arrows), digestive tubules and muscle tissue (M). Bar = 40 µm.

Fig. 7. Female reproductive tract almost completely destroyed; hyalinocytes present within the follicles. Bar = 25 µm.

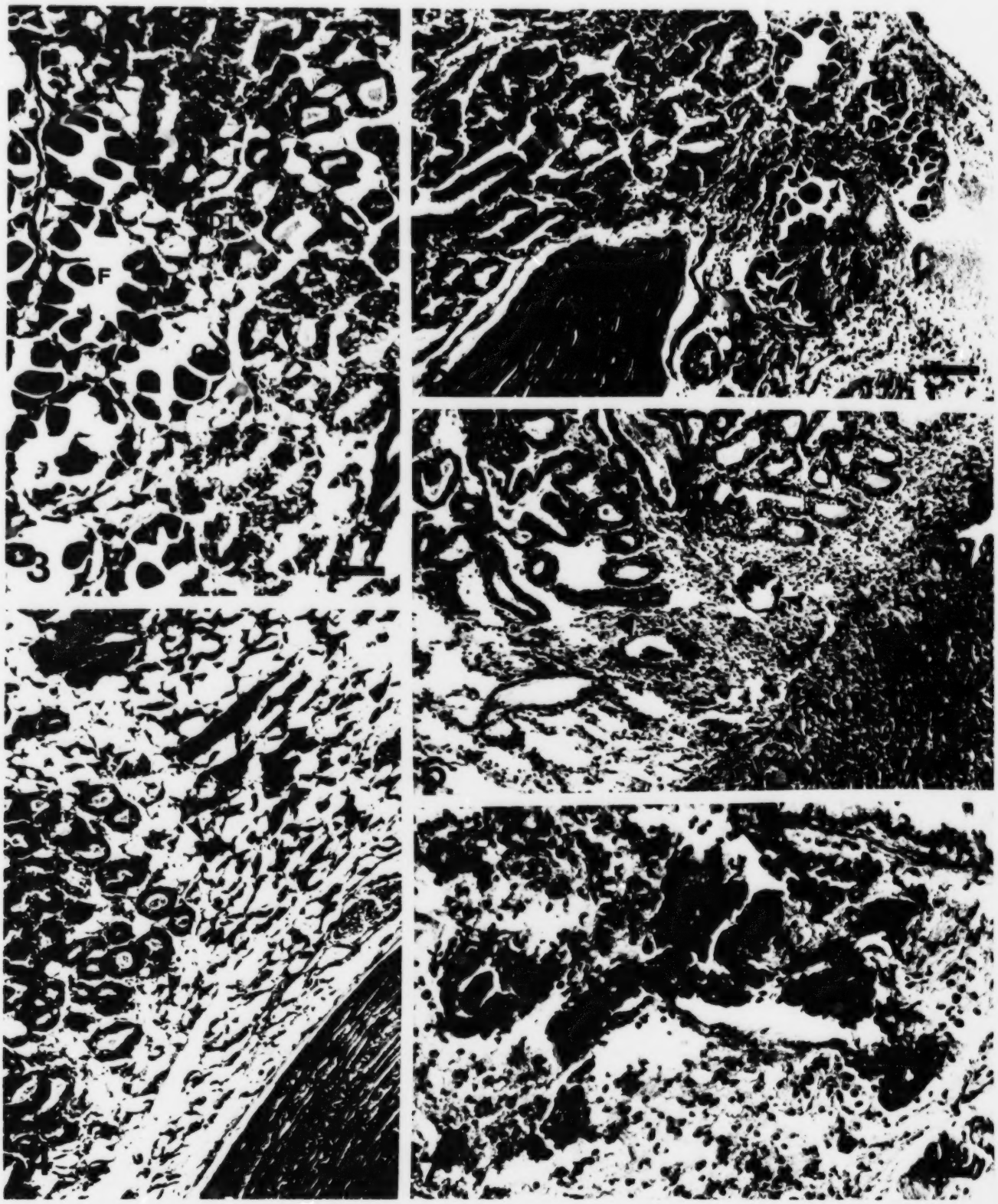
F
93

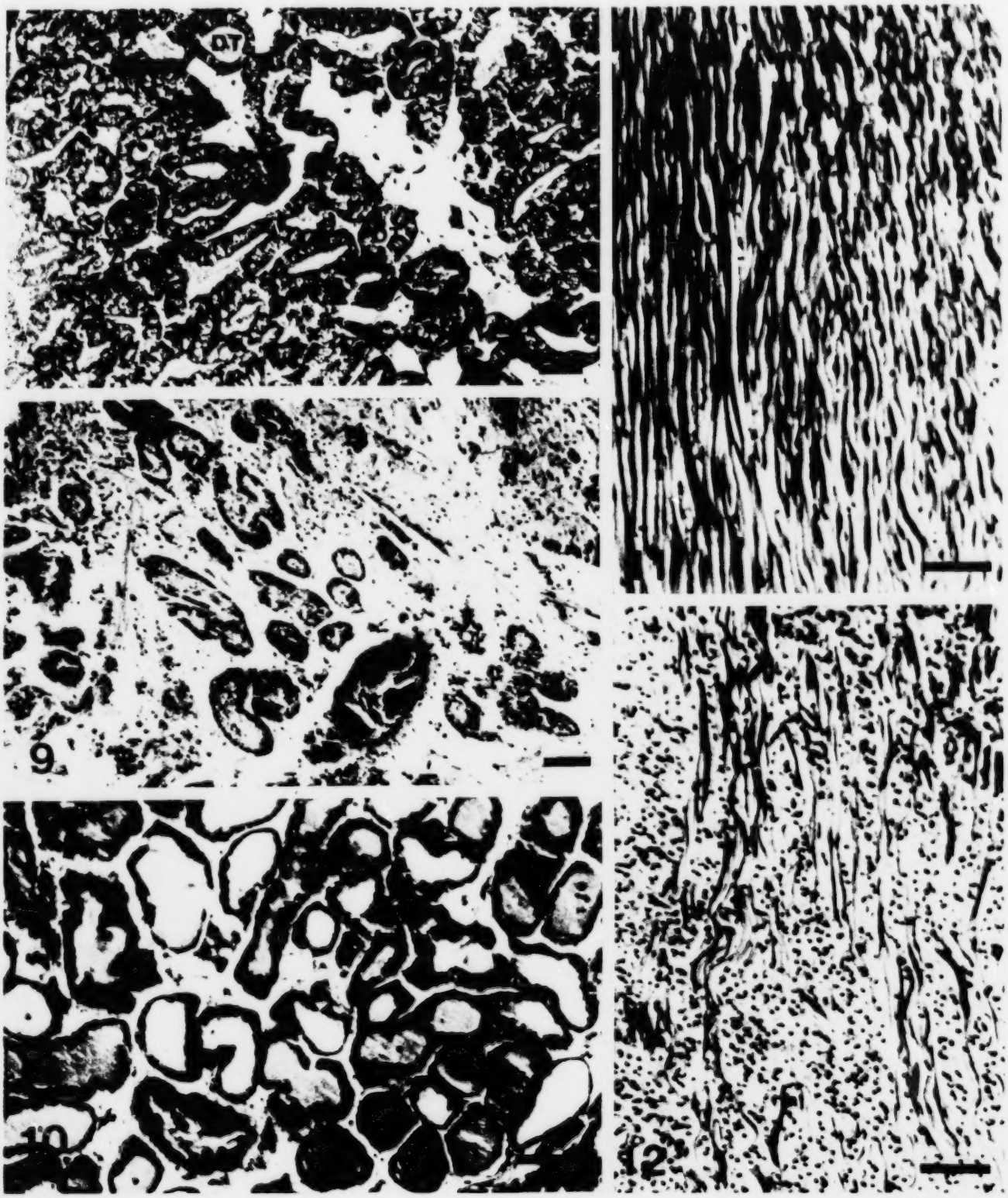
DT
9
10
12

Mytilus edulis Alberni Inlet, July, 1979

Most mussels sampled from Alberni Inlet in July were spawning or had spawned (Table 1: Figs. 13-15). Spawning was completed in more mussels from towards the head of the inlet than at the mouth. In the mussel which had spawned, spent reproductive follicles and unspawned gametes were undergoing resorption by granulocytes (Figs. 14-15). Therefore, reproductive condition was rated as poor in most mussels from the head of the inlet and granulocyte levels were high (Table 1: Figs. 14-16). Nutritive store levels were extremely low in mussels from all stations.

Digestive condition was rated as good to fair in most mussels from all stations (Table 1). When poor digestive condition did occur it was characterized by the infiltration of the connective tissue and digestive tubules by granulocytes (Figs. 16-17), and associated destruction of the digestive epithelium. In some mussels, particularly at Station 5.5, there were hemocytic encapsulations (Fig. 17) - large accumulations of hemocytes, primarily eosinophilic granulocytes encapsulated by fusiform granulocytes - these represent a non-neoplastic inflammatory cellular condition.

Whereas granulocyte levels were rated as moderate or high in most mussels, hyalinocyte levels were rated as low in almost all mussels (Table 1).

Macoma inconspicua Kitimat Arm - Douglas Channel, April, 1979

Macoma inconspicua sampled from Kitimat in April were all at a prespawn state (Table 2: Figs. 18-19). However, those clams from control Station F were more mature reproductively (Fig. 20) than those from Stations 1X, 2X and 5X. Reproductive condition was rated as good in 75% of the clams from control Station F but as poor in 62 to 82% of the clams from the head of the fjord (Table 2).

Digestive condition was rated as good in 64% of the control clams but poor in 31 to 59% of those from the head of the fjord. Both reproductive and digestive degeneration were characterized by the infiltration of these tissues by hemocytes, indicated by elevated levels of granulocyte and hyalinocyte ratings for clams from stations at the head of the inlet (Table 2: Figs. 21-22). The worst tissue destruction was apparent when infiltration was severe and comprised mainly of hyalinocytes (Fig. 22). Hyalinocyte levels were rated

---

Plate B. Digestive and muscle conditions in *Mytilus edulis* from Kitimat Arm - Douglas Channel.

Fig. 8. Normal digestive tubules (DT) with columnar/cuboidal epithelial cells. Bar = 50 µm.

Fig. 9. Poor digestive condition with an infiltration of high levels of hyalinocytes and destruction of digestive tubules. Bar = 50 µm.

Fig.10. Transformation of the columnar/cuboidal epithelial cells of the digestive tubules to the squamous cell type. Bar = 50 µm.

Fig.11. Longitudinal section through normal adductor muscle. Bar = 50 µm.

Fig.12. Longitudinal section of muscle in poor condition. There is an infiltration of high levels of hyalinocytes resulting in almost complete destruction of muscle fibres. Bar = 50 µm.

as low in 100% of M. inconspicua from control Station F, moderate in 17 to 38%, and high in 21 to 45% of those from the head of the inlet.

PHYSICAL CHARACTERISTICS

A comparison of shell lengths of mussels and clams from Kitimat Arm - Douglas Channel, mussels from Alberni Inlet, and a summary of temperature and salinity data for each sampling site are given in Table 3. Bivalves closer to the head of both inlets were smaller. Water temperatures were coldest in Kitimat Arm in February, with a range of 1.7 to 3.3°C. Control Station A was slightly warmer than the other stations. Salinities were relatively constant with a range of 29.8 to 30.5×10^{-3}. In April, temperatures had moderated somewhat and ranged from 3.9 to 4.4°C with the control station slightly cooler than stations near the head. Salinities were slightly lower, in the range of 27.5 to 29×10^{-3}. In Alberni Inlet in July, temperatures were near maximum values for the inlet (18 to 22°C), and were highest near the head. Salinities were very low near the head (0 to 5×10^{-3}), increasing to 20 to 25×10^{-3} at Stations 1 and 2.

DISCUSSION

The results give evidence of histopathological conditions in bivalves which increase in severity along transects from the mouth to the head of both Kitimat Arm - Douglas Channel and Alberni Inlet. Furthermore, mussels decreased in size towards the head of both inlets. Bivalves towards the head of both inlets had histopathological conditions which were unique to those areas. Mussels and clams from the Kitimat area showed marked elevations in hyalinocyte levels; in some cases large numbers of hyalinocytes were present which had infiltrated, and were associated with the destruction of reproductive, digestive and muscle tissues. However, almost all mussels from Alberni Inlet had low hyalinocyte levels. Elevated levels of granulocytes, and some hemocytic encapsulations composed of granulocytes, were found in mussels from the head of Alberni Inlet. Further, in many mussels digestive tubules had been infiltrated with granulocytes and were degenerating. Although

---

Plate C. Condition of Mytilus edulis from Alberni Inlet.

Fig. 13. Normal spawning male; the reproductive follicles are full of ripe sperm (S). DT; digestive tubules. Bar = 50 µm.

Fig. 14. Spawning male undergoing the first stagest of resorption. G; granulocytes. Bar = 50 µm.

Fig. 15. Spent reproductive follicles (F) undergoing resorption by granulocytes. Bar = 50 µm.

Fig. 16. Male mussel in poor condition with an infiltration of high levels of granulocytes resulting in destruction of the reproductive follicles and digestive tubules; note the presence of granulocytes within the connective tissue and in the lumen of the digestive tubules, and destruction of the digestive epithelium. Bar = 50 µm.

Fig. 17. Poor digestive condition with infiltration of digestive tubules by granulocytes; note the large granulocytic encapsulation (GE). Bar = 100 µm.

DT

14

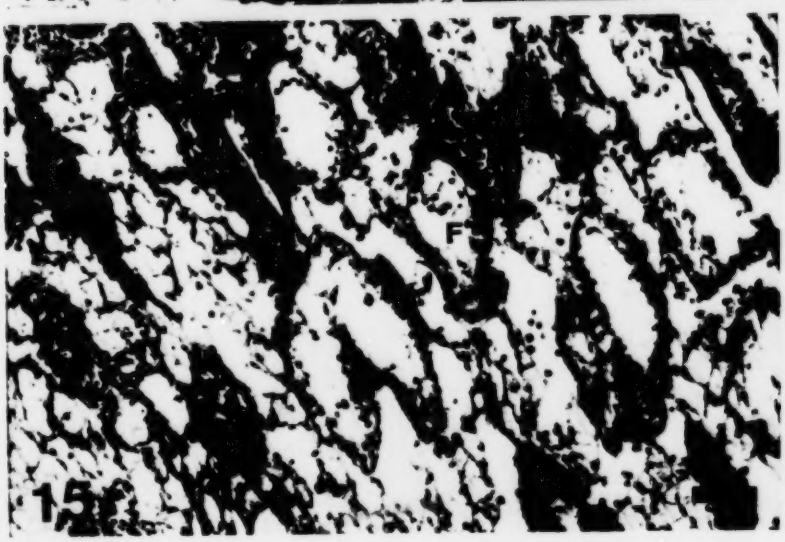
F
15

16

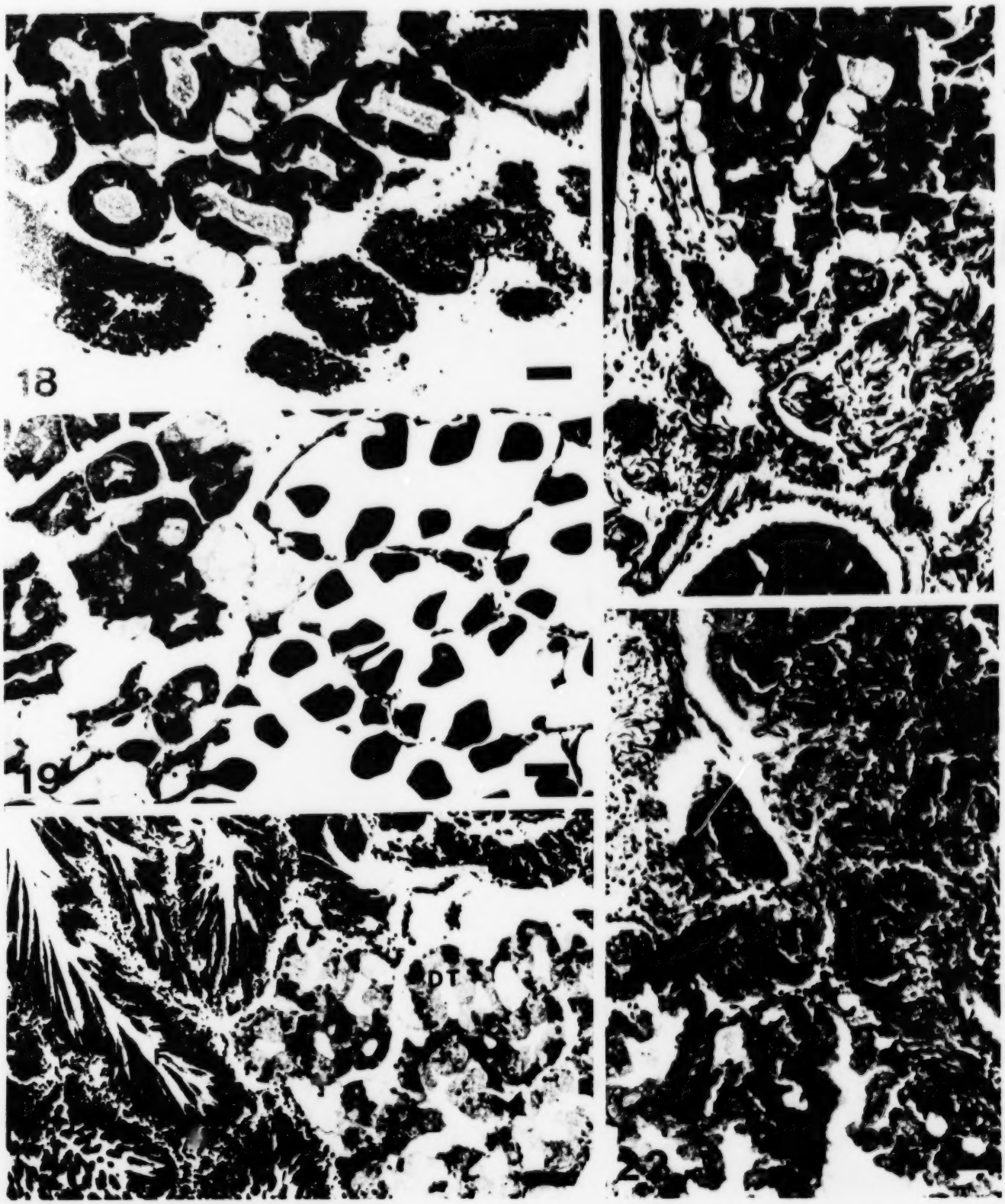
18
19
DT

elevated levels of granulocytes were found in mussels from the Kitimat area, there were no hemocytic encapsulations and a much less marked infiltration of digestive tubules by granulocytes.

Several natural and potential anthropogenic stresses were considered for both areas. As a result of seasonal variation in water properties the two inlets had very different salinity and temperature values. Kitimat Arm - Douglas Channel in February and April received a very low freshwater input with resultant high surface salinities and little change in salinity from the mouth to the head of the fjord. Alberni Inlet in July received a large freshwater discharge as a result of snow melt from the surrounding mountains, resulting in much lower salinities at the head of the inlet. Temperatures were approximately 15°C lower in Kitimat Arm - Douglas Channel in February and April than in Alberni Inlet in July due to winter conditions and the more northerly location of Kitimat. Thus salinity and/or temperature differences might account for the disparity in histopathological conditions in mussels from the two inlets. Temperature gradients from the head to the mouth of each inlet were slight as was the gradient for salinity at Kitimat, but there was a large salinity gradient from the mouth to head of Alberni Inlet in July. Air temperature was not measured but should also be considered an important factor for mussels since they may be exposed for a considerable amount of time during low tide. Mussels near the mouth of Kitimat Arm - Douglas Channel would be subject to temperatures moderated by the influence of the ocean; those near the head would be exposed to much colder air temperatures in winter.

Both inlets receive pulpmill effluent which is biologically treated in aeration lagoons before release, and is usually nonlethal at 100% concentration (D. McLeay, personal communication). However, even the most efficiently treated effluent can cause stress effects in animals (McLeay and Brown, 1979). The potential for pulpmill effluent to cause other sublethal effects is unknown but the effluent may contain carcinogens (e.g., phenolic compounds): leachates from logs may contain similar compounds. In Alberni Inlet detrimental effects of released treated effluent have been well documented in several reports (D. McLeay, personal communication).

In addition to pulpmill effluent, Kitimat Arm receives discharges from the aluminum smelter which include fluorides (Bell and Kallman, 1976). It has been reported that fluoride values for Kitimat Arm surface waters are elevated for several kilometres away from the smelter site (Bell and Kallman, 1976). Since there is no similar influx of fluorides into Alberni Inlet,

---

Plate D. Condition of Macoma inconspicua from Kitimat Arm - Douglas Channel.

Fig. 18. Male clam from the head of the fjord at prespawn stage, in good reproductive and digestive condition. Bar = 50 µm.

Fig. 19. Female clam in good prespawn reproductive and digestive condition. Bar = 50 µm.

Fig. 20. Male clam from Station F in good reproductive and digestive condition. F; follicles: DT; digestive tubules. Bar = 50 µm.

Fig. 21. Male clam in poor reproductive and digestive condition with an infiltration of low levels of hyalinocytes. Bar = 50 µm.

Fig. 22. Clam in poor condition with high levels of hyalinocytes, resulting in severe tissue destruction. Bar = 50 µm.

Table 2. Histopathological condition of Macoma inconspicua from Kitimat Arm - Douglas Channel and Alberni Inlet

Area, Month Station (N)	Reproductive Stage		Reproductive Stage			Digestive Condition			Granulocyte Infiltration			Hyalinocyte Infiltration		
	Prespawn	Spawning	Good	Fair	Poor	Good	Fair	Poor	Low	Moderate	High	Low	Moderate	High
Kitimat, Apr.														
F (12)	100%	0%	75%	17%	8%	64%	36%	0%	75%	25%	0%	100%	0%	0%
1X(29)	100	0	21	17	62	10	59	31	24	62	14	59	20	21
2X(29)	100	0	11	7	82	0	41	59	17	48	35	38	17	45
5X(29)	100	0	24	7	69	7	52	41	14	62	24	34	38	28

Table 3. Shell lengths of mussels and clams and temperatures and salinities of water at time of sampling.

Area, Month, Species Station (N)	Shell Length (mean ± SD) mm	Surface Temperature	Salinity ($\times 10^3$)
Kitimat, February			
Mytilus edulis			
A (25)	63.8 ± 9.0 [a]	3.3	30.5
G (25)	55.8 ± 3.3	1.7	30.6
L (25)	39.8 ± 3.4	2.2	29.8
M (25)	38.7 ± 1.4	2.2	30.4
N (25)	35.6 ± 4.3	2.2	ND
O (25)	31.2 ± 3.3	1.9	29.9
P (25)	33.8 ± 5.0	2.5	29.9
Kitimat, April			
Mytilus edulis			
A (25)	57.0 ± 5.6 [b]	3.9	27.5
F (16)	53.8 ± 5.4	4.4	28.9
N (25)	44.9 ± 3.3	4.4	28.9
O (25)	53.6 ± 3.9	4.4	ND
3X(24)	60.3 ± 4.2	4.4	ND
4X(24)	56.5 ± 4.0	4.4	ND
Alberni, July			
Mytilus edulis			
1 (25)	55.2 ± 3.3 [b]	19.2	25.2
2 (25)	51.9 ± 5.0	18.2	20.9
3 (25)	55.8 ± 6.1	20.2	3.9
4 (25)	54.8 ± 3.5	18.7	9.8
5.5(25)	47.6 ± 2.6	22.3	4.2
7 (25)	48.1 ± 4.1	22.2	2.6
8 (25)	33.9 ± 2.8	21.2	3.0
Kitimat, April			
Macoma inconspicua			
F (12)	13.1 ± 2.2 [a]	4.4	28.9
1X(29)	14.1 ± 1.7	4.4	ND
2X(29)	15.7 ± 2.8	4.4	ND
5X(29)	14.0 ± 2.0	4.4	ND

[a] Measures are of randomly selected organisms.

[b] Measures are of mussels selected as close to 50 mm as possible for histopathological analysis.

ND: not done

their presence in Kitimat Arm could account for different histopathological effects. Polycyclic aromatic hydrocarbon (PAH) levels are increasingly elevated from the mouth to the head of Kitimat Arm and are much higher in Kitimat Arm than in Alberni Inlet. The presence of elevated levels of PAH in Kitimat Arm could also account for the difference in histopathological effects between Kitimat Arm and Alberni Inlet. However, the presence of other undetermined anthropogenic contaminants in these inlets cannot be discounted.

In the following discussion we have considered each biological indice with respect to both natural and potential anthropogenic factors:

(i) Growth Reduction: Although we attempted to sample similar sized mussels from all stations, only smaller mussels were available from the heads of the two inlets. These growth reductions could be caused by reduced availability of food due directly to the effects of pulpmill-associated toxicants on the phytoplankton, or indirectly to a reduction in light available for phytoplankton photosynthesis. Mussels which filterfeed on phytoplankton would therefore experience a reduction in their food source and subsequently in their growth rate. Stockner et al. (1977) have found reduced phytoplankton production in the area of discharge of a pulpmill. In addition, the shading effects of suspended solids introduced with river run-off could reduce productivity by decreasing the availability of light and therefore reducing the nutrient level. Alternatively, reduced mussel size could be due to the effects of a toxicant-related chronic stress on the mussels (Bayne et al. 1980). Determination of whether reduced mussel size is due to natural causes or contaminant input will require measurements of control mussels along transects in pollution-free inlets.

(ii) Nutritive Index: Although not rated, it was clear that mussels from the mouth of Kitimat Arm - Douglas Channel in February and April had high levels of nutrient reserves indicated by the intensity of eosinophilic staining of the carbohydrate-filled cells of the mantle connective tissue surrounding the reproductive follicles. Mussels and clams from the head of Kitimat Arm - Douglas Channel showed distinct depletion of nutrient stores. All mussels sampled from Alberni Inlet in July showed low levels of nutrient stores.

Since the level of nutrient stores is a seasonally variable parameter, it is difficult to explain these results. The fundamental seasonal cycle in bivalves involves reproductive condition. In response to the energy demands of gametogenesis, nutrient reserves are built up in the tissues during periods of nutrient availability. These energy reserves are depleted as they are used for the synthesis of lipids and proteins in the maturation of gametes (Bayne et al. 1980). An interpretation of the results also depends upon a knowledge of food availability throughout the fjords. The nutrient store level differences between prespawn bivalves from downchannel and the head of the fjord indicate that the winter - spring food supply is less at the head than at the mouth and/or, that the stress load is more severe at the head. This stress load could be caused by some natural factor (e.g., temperature) and/or any of the contaminants present in Kitimat Arm. The general stress response in bivalves involves the mobilization of energy reserves to repair

damaged tissues or to synthesize substances used to detoxify contaminants (Bayne et al. 1980) and therefore, nutrient depletion usually indicates a chronic stress response. Since Alberni mussels were all reproductively mature in July, the depletion of the nutritive stores was probably caused by the utilization of their carbohydrate and lipid stores during gametogenesis.

(iii) Reproductive Stage: Both mussels and clams sampled during the April cruise at Kitimat were less reproductively developed at the head of the fjord than at stations closer to the mouth. Mussels sampled in July from Alberni Inlet showed the reverse trend. Previous studies clearly demonstrate that reproductive development is accelerated by warmer temperatures (Seed, 1976). In winter, inlet waters cool below the temperature of open ocean waters while in summer inlet surface waters are warmer than the open ocean (Webster, 1979). Warmer temperatures over several months could account for the accelerated reproductive development of mussels from control stations near the mouth of Douglas Channel and from the head of Alberni Inlet. Alternatively, the differences in reproductive development might be due to contaminants present in Kitimat Arm but not found in Alberni Inlet, since mussels were more reproductively mature at the head of Alberni Inlet than in Kitimat Arm. Mussels sampled from all stations in Kitimat Arm - Douglas Channel in February showed no difference in reproductive development being all at the prespawn stage.

(iv) Reproductive Condition: The reproductive condition of mussels sampled from stations in Kitimat Arm - Douglas Channel in February was poorer at the head of the fjord than at the mouth. The poorer reproductive condition was associated with infiltration of their reproductive tracts by hyalinocytes. It is probable that their poor reproductive condition was due to the presence of natural and/or anthropogenic agent(s) at the head of Kitimat Arm, since all mussels were at a similar prespawn reproductive stage. Mussels sampled in April at control Station A were undergoing resorption which probably accounted for the higher incidence of reproductive tract destruction seen there than at the head of Kitimat Arm. The main difficulty in assessing the effects of environmental factors on reproductive tract condition is in differentiating normal postspawn conditions (i.e., resorption) from abnormal follicular destruction. Therefore, mussels to be compared should be sampled at the same point in their reproductive cycle, preferably at a prespawn time (Bayne et al., 1980). This was evident in mussels sampled from Alberni Inlet in July which were spawning, making interpretation difficult.

In the clams, Macoma inconspicua, there was increasingly more destruction of the reproductive tract going from Control Station F towards the head of the fjord, even though those at the head tended to be less reproductively developed. However, all clams from the April Kitimat sampling were at the prespawn stage thus making the relationship between their reproductive condition and their position along the fjord easier to interpret. As with M. edulis sampled from Kitimat Arm in February, the destruction of the reproductive tract was associated with an hyalinocytic infiltration of the tissues.

(v) Digestive Condition: Most bivalves near the head of Kitimat Arm - Douglas Channel were in poor digestive condition with a large percentage of the digestive epithelial cells having been transformed to the squamous type. In many of these bivalves the destruction of the digestive tract was associated with an infiltration of hyalinocytes into the digestive ducts and tubules similar to that seen in the reproductive tract. The poor digestive condition of mussels sampled from Alberni Inlet was associated with increased numbers of granulocytes as well as the presence of hemocytic encapsulations within the digestive tissues. Granulocyte levels were increased because of resorption.

Since poor digestive condition was common to bivalves from both inlets, its cause(s) could be some natural factor(s) common to both inlets. For instance, it has been reported that several natural stresses including spawning, starvation and elevated temperatures can result in structural alterations in digestive cells (Bayne et al. 1980). In mussels the normal digestive processes are accompanied by a cyclical change in the digestive epithelium from columnar/cuboidal cell types to squamous and then back to the columnar/cuboidal forms (Langton, 1975; Bayne et al., 1980). Therefore, it is normal to observe some portion of the epithelial cells in the squamous stage; however, in polluted environments a much larger proportion of digestive epithelial cells are squamous, and as the pollutant load (degree of stress) increases, the lysosomal stability of the digestive cells decreases. In terms of digestive cell morphology, this phenomenon manifests itself as a loss of synchrony in digestive cell phasing, i.e., there is an increase in the number of cells of the squamous type and in cells which undergo fragmentation. Both intracellular lysosomal digestion of food (Bayne et al. 1976) or accumulation of pollutants in lysosomes (Bayne et al., 1980) cause the release of hydrolytic lysosomal enzymes into the digestive cell cytoplasm. The release of these enzymes may result in the intracellular digestion of structural proteins (e.g., tubulin) causing a collapse in the structural basis of the cell (Moore et al., 1978), and thus producing a squamous cell type or, in more severe cases, total destruction of these cells. Moore et al. (1978) have shown that the PAH, anthracene, can cause severe destruction of digestive epithelial cells and that this is directly attributable to the level of accumulated anthracene in digestive cell lysosomes and the subsequent lysis of these lysosomes and autolysis of digestive cells.

(vi) Hemocytic Infiltration: Increased hemocyte (hyalinocyte or granulocyte) levels were found in bivalves from towards the head of Kitimat Arm - Douglas Channel and Alberni Inlet or in mussels that had spawned. Molluscan hyalinocytes are thought to be immature hemocytes capable of cellular division and granulocytes are fully functional, non-dividing, mature hemocytes (Mix, 1976). Hyalinocyte levels are increased in response to parasites and result in their destruction. Granulocytes have the ability to phagocytize cellular debris and toxicants and transport them for excretion (Lowe and Moore, 1979; Bayne et al., 1980) Granulocyte levels can be elevated after spawning when they function in the resorption of unspawned gametes and postspawn reproductive follicles. In addition, contaminants can be sequestered by granulocytes and stores in their lysosomes (granular structures within the cytoplasm

of the granulocytes) (George et al., 1976; 1978; Bayne et al., 1980). By partitioning the contaminants into lysosomes, the hemocytes remove them from potential sites of toxic action and thereby act to detoxify them. Subsequently, the pollutant-laden hemocytes are discharged from the organisms via the kidneys and other organs (Bayne et al., 1980). If these lysosomes become overloaded with contaminants they will lyse, resulting in the release of hydrolytic enzymes which cause autolysis (Bayne et al., 1980).

In mussels and clams from towards the head of Kitimat Arm - Douglas Channel, hyalinocyte levels were greatly increased even though parasites were seldom seen. Large numbers of hyalinocytes had infiltrated and were associated with damage to reproductive, digestive and muscle tissues. The presence of high levels of hyalinocytes in bivalves, with associated tissue damage, was a condition unique to Kitimat Arm. In the February sample, hyalinocyte levels were rated as high in 56% of the mussels from Station L, 21 km downchannel from the suspected source of PAH contamination; total PAH levels in mussels were 0.3 mg kg^{-1} mussel (wet wt.). At Station 0 at the head of the fjord, PAH levels were 2.2 mg kg^{-1} mussel (wet wt.) but hyalinocyte levels were rated as high in only 16% of the mussels. Therefore, this condition does not seem to be related to high PAH levels. In April hyalinocyte levels were high in 21 to 45% of the clams from the head of Kitimat Arm but low in all clams from the control station; no intermediate stations were sampled.

Granulocyte levels were increased in bivalves from both areas, therefore their presence cannot be considered a unique histopathological condition. However, there were two granulocyte-associated histopathological effects that were unique to mussels from the head of Alberni Inlet: (i) granulocytes had infiltrated digestive tubules and were associated with their damage and (ii) there were hemocytic encapsulations composed mainly of granulocytes. These hemocytic encapsulations act to partition the hemocytes and/or phagocytized materials away from sensitive cellular sites. In addition, they are known to be produced in response to pulp and paper effluent (Lowe and Moore, 1979). Alternatively, since almost all mussels from Alberni Inlet were spawning or had spawned, high levels of granulocytes may have been present for resorption and some may have become encapsulated as part of a natural postspawn process.

Interpretation of the data in terms of cause and effect presents many difficulties. For instance, mussels sampled in July from Alberni Inlet served as a poor comparison for those sampled from Kitimat Arm - Douglas Channel in February and April because (i) they were exposed to different temperatures, salinities, and a variety of other undetermined factors, and (ii) those from Alberni Inlet had spawned so that it was difficult to differentiate histopathological conditions from those associated with normal postspawn resorption.

To determine if histopathological conditions in bivalves from Alberni or Kitimat are unique, and if those in bivalves from alberni are distinct from postspawn changes, it will be necessary to sample both areas at the same time of the year at a prespawn time. Furthermore, it will be necessary to sample mussels from an inlet free from all contaminants to determine if there are histopathological conditions which occur as a result of natural influences at

the head of inlets. These should be sampled frequently for several years so that the range of natural conditions can be established.

Determination of the biological impact of pollutants from histopathological data relies upon correlations between pollutant levels and histopathological changes but these correlations do not show definite cause and effect relationships in a multi-polluted environment. Rather, the histopathological changes are for the most part a culmination of the effects of all pollutants and natural agents present in the ecosystem.

Laboratory studies, exposing organisms to varying concentrations of contaminants, are necessary before cause and effect relationships between histopathological conditions and specific contaminants can be established; but even these may provide insufficient evidence. For example, although it is known that PAHs are associated with the occurrence of neoplasia in bivalves from environmentally contaminated areas (Lowe and Moore, 1978; Mix et al., 1979) it has been proven in one instance, that neoplasia does not occur without the presence of a virus (T.C. Chang, personal communication) and that natural stresses can enhance the ability of the virus to cause neoplasia.

Therefore, to show cause and effect between specific contaminants and biological effects, it will be necessary to develop techniques to show toxicant-specific responses. We can consider histopathology in the context of a hierarchy of biological indices that go from general to the more specific effects of individual contaminants:

(i) Survival or nonsurvival as indicated in species enumeration field surveys and LC 50s. Field surveys do not show cause and effect and neither of these show sublethal effects.

(ii) Changes in physiological processes and cytological conditions which induce sublethal stress are assessed by histopathology, performance studies and stress parameter responses. These show sublethal effects but are not pollutant-specific.

(iii) Effects of contaminants on biochemical sites of toxic action, e.g. enzyme activity can be used to assess the toxic effects of metals. Cause and effect may be established if the site of toxic action is toxicant-specific.

(iv) The loading or overloading of detoxification systems with specific pollutants, e.f., metallothionein with trace metals and lysosomes with hydrocarbons.

Future studies should utilize histopathology to determine the health of organisms and to recognize responses associated with their life-cycle. In addition, to establish cause and effect relationships, these studies should include a determination of the partitioning of specific contaminants between their detoxification systems and their sites of toxic action.

ACKNOWLEDGEMENTS

The authors wish to thank Mrs. Gillian Roe for assistance and encouragement during the preparation of this paper. This research was supported by a grant to Seakem Oceanography Ltd. from the Department of Supply and Services; contracts 1SB78-00069; OSB79-00146.

REFERENCES

Barszcz, C.A. and P.P. Yevich. 1975. The Use of Helly's Fixative for Marine Invertebrate Histopathology. Comp. Path. Bull. 7(3): 4.

Bayne, B.L., R.J. Thompson, and J. Widdows. 1976. Physiology. In B.L. Bayne (ed.) Marine Mussels: Thier Ecology and Physiology. Cambridge University Press, Cambridge.

Bayne, B.L., D.A. Brown, F. Harrison and P.P. Yevich. 1980. Mussel Health, p. 163-235. In E.D. Goldberg (ed.) The International Mussel Watch. U.S. National Academy of Science. 248 pp.

Bell, L.M. and R.J. Kallman. 1976. The Kitimat River Estuary, Environmental Knowledge to 1976. Report of the Estuary Working Group, Department of the Environment, Regional Board Pacific Region. Environment Canada. Special Estuary Series No. 6.

Cretney, W.J., C.S. Wong, R.W. Macdonald, P.E. Erickson and B.R. Fowler. 1983. Polycyclic aromatic hydrocarbons in surface sediments and age dated cores from Kitimat Arm, Douglas Channel and adjoining waterways. Can. Tech. Rep. Hydrogr. Ocean Sci, 18, 162-195.

George, S.G., B.J.S. Pirie, and T.L. Coombs. 1976. The kinetics of accumulation and excretion of ferric hydroxide in Mytilus edulis (L) and its distribution in tissues. J. Exp. Mar. Biol. Ecol. 23: 78-84.

George, S.G., B.J.S. Pirie, A.R. Cheyne, T.L. Coombs, and P.T. Grant. 1978. Detoxication of metals by marine bivalves: An ultrastructural study of the compartmentation of copper and zinc in the oyster Ostrea edulis. Mar. Biol. 45: 147-156.

Langton, R.W. 1975. Synchrony in the digestive diverticula of Mytilus edulis L.J. Mar. Biol. Assoc. U.K. 55: 221-229.

Lowe, D.M., and M.N. Moore. 1978. Cytology and quantitative cytochemistry of a proliferative atypical hemocytic condition in Mytilus edulis (Bivalvia, Mollusca). J. Natl. Cancer Inst. 60(6): 1455-1459.

Lowe, D.M., and M.N. Moore. 1979. The cytology and occurrence of granulocytomas in mussels. Mar. Poll. Bull. 10: 137-141.

McLeay, D.J. and D.J. Brown. 1979. Stress and chronic effects of untreated and treated bleached kraft pulpmill effluent on the biochemistry and stamina of juvenile coho salmon (Oncorhynchus kisutch). J.Fish.Res.Bd. Can. 36: 1049-1059.

Mix, M.C. 1976. A general model for leucocyte cell renewal in bivalve molluscs. Mar. Fish. Rev. 38: 37-41.

Mix, M.C., S.R. Trenholm, and K.I. King. 1979. Benzo(a)pyrene body burdens and the prevalence of cellular proliferative disorders in mussels, Mytilus edulis, from Yaquina Bay, Oregon. In "Pathobiology of Environmental Pollutants - Animal Models and Wildlife as Monitors," NAS Symposium Volume.

Moore, M.N., D.M. Lowe and P.E.M. Fieth. 1978. Lysosomal responses to experimentally injected anthracene in the digestive cells of Mytilus edulis. Mar. Biol. 48: 297-302.

Palmork, K.H. 1974. Polycyclic aromatic hydrocarbons in a marine environment. In The 9th Nordic Symposium on Water Research: Fjords and Coastal Waters as Recipients. Trondheim, 1973: Special Publication: "Nordforsk". The Environment Secretariat, Issue 4: pp. 99-125.

Seed, R. 1976. Ecology, In B.L. Bayne (ed.) Marine Mussels: Their Ecology and Physiology, Cambridge University Press, Cambridge.

Stockner, J.G., D.D. Cliff, and D.B. Buchanan. 1977. Phytoplankton production and distribution in Howe Sound, British Columbia: a coastal marine embayment - fjord under stress. J. Fish. Res. Board Can. 34: 907-1017.

Webster, I. 1983. Kitimat Physical Oceanographic Study. 1977-1978. Part 3. Estuarine circulation, Contract Report Series 80-3, Inst. of Ocean Sciences, Sidney, B.C. 81 pp, 14-33.